‘Impact of surgical and of bronchoscopic lung volume reductions in patients with emphysema and hyperinflation on lung structure, function and inflammation’

Dr Justin L Garner

October 2020

A thesis submitted for the degree of Doctor of Philosophy

Supervisors:
Professor Pallav L Shah (Primary Supervisor)
Dr Omar S Usmani (Secondary Supervisor)

DECLARATIONS

Declaration of Originality

I declare all of the work submitted within this thesis is my own. Those individuals who have kindly assisted me during this endeavour have been duly recognised within the acknowledgements section.

Copyright Declaration

ACKNOWLEDGEMENTS

I would like to express my gratitude to everyone who has helped me during my PhD and made it such an enjoyable and rewarding experience.

I have had the privilege to work with the following individuals: Muscle Laboratory – Dr Will McNulty, Cielito Caneja, Dr Karthi Srikanthan, Dr Eric Tenda, Dr Marli Shen, Dr Arafa Aboelhassan, Dr Chris Orton, Dr Fran Conway, Dr James Tonkin, Dr Bavi Vijaykumar, Dr Adam Lewis, Sara Buttery, Dr Matt Pavitt, Laura Swanton, Dr Keir Phillip, Dr Nick Hopkinson, Professor Michael Polkey; Lung Function – Simon Ward, Suzie Thomas, Jim Robinson, Cara Roberts, Jo Ming, Serena Rhamie, Ann-Marie Jacobs, Ann Sharpe, Angelina Cubuk; Radiology – Trupti Patel, Natalie Gartland, Dr Kshama Wechalekar; Biomedical Research Unit – Najwa Soussi, Anita Abraham, Dingani Mpoko, Richard Mordi, Paul Ryan, Miriam Oliveira, Martyn Biddiscombe, Sally Meah; Research & Development – Patrik Pettersson, Nadia Shabbir, Ira Jakupovic, Winston Banya; Lind ward – Sister Florence Parafina, Ines Meireles, Foon Sing, Hazel Russell, Lorraine Beckett, Catarina Teixeira, Daniela Dzurova, Carol Egbuna, Sara Mamo, Rosemarie Bolla, Andromeda Salih, Paul Cannon, Lesley Weston; Diagnostic Centre, Chelsea & Westminster Hospital – Leeh Faustino, Isaac Mwita, Lilian Anya, Dr John Thornton; Section of Anaesthetics, Pain Medicine and Intensive Care, Chelsea & Westminster Hospital – Dr Sanooj Soni, Dr Marissa Koh, Dr Ying Ying Tan, Faruq Noormohamed, Dr Kieran O'Dea, Dr Michael Wilson.

I am especially grateful to my mentors, Dr Samuel Kemp, Dr Sylvia Verbanck, Dr Omar Usmani, Professor Masao Takata, and Professor Pallav Shah who have been generous with their time, knowledge, and wisdom and have created various opportunities for me. I would also like to thank the Joint Research Committee of Chelsea & Westminster Hospital for kindly awarding me a PhD grant.

Lastly, I pay tribute to my parents who have supported me unwaveringly in all my endeavours and I dedicate this thesis to them.

ABSTRACT

Background – A robust biomarker for predicting and evaluating the response to lung volume reduction (LVR) interventions remains elusive. We investigated the hypothesis that LVR will be accompanied by measurable changes in novel indices of lung structure, function, and inflammation that can be correlated with changes to the conventional clinical parameters and that reliable identifiers of baseline predictors of therapeutic response (minimal clinically important difference, MCID, of at least 10% reduction of residual volume) will be identified.

Methods – 72 consecutive subjects with severe emphysema and hyperinflation scheduled for lung volume reductions were recruited: lung volume reduction surgery (LVRS) – 15; Endobronchial valve (EBV) – 29, Endobronchial coil (EBC) – 28. All underwent detailed clinical phenotyping comprising demographics, symptom scores, computed tomography imaging, exercise capacity and lung function measurements during exacerbation-free periods at baseline and at three months after intervention. Novel techniques including quantitative computed tomography (qCT), impulse oscillometry (IOS) and multiple breath nitrogen washout (MBNW), and microvesicle quantification were employed to assess changes in lung structure, function and inflammation, respectively.

Results – Surgery achieved the greatest lung volume reductions, △residual volume (RV) of -1.26 ± 0.58 litres ($p<0.01$), and more than 90% of recipients met the MCID of ≥10% RV reduction. It was the only intervention to be accompanied by improvements in functional gas trapping on CT, IOS expiratory airways resistance at 5Hz, expiratory and within-breath reactance at 5Hz, and peripheral resonant frequency, attributable to recovery of small airways function.

Valve implantations reduced residual volume by -0.91 ± 0.66 litres ($p<0.01$) and 62% of recipients attained the MCID of ≥10% RV reduction. This was in addition to a smaller reduction in IOS expiratory and within-breath reactance at 5Hz without an accompanying signal in resistance, resonant frequency, or functional gas trapping on CT. Modest improvements to alveolar gas mixing (AME) and small airways function (Sacin) were measured using MBNW in a subset of patients. These data suggest the impact of valves on the peripheral airway compartment was less pronounced than with surgery and

was achieved predominantly by deflation of emphysematous lung tissue and restoration of the mechanical pump.

Coil implantations resulted in modest volume reductions, △residual volume of -0.31 ± 0.60L (p=0.01): Only 35% of subjects achieved the MCID of ≥10% RV reduction. Three-month physiological outcomes were similarly disappointing with improvements limited to CT-intraparenchymal blood vessel volume (perhaps due to greater radial traction exerted by the coils on the surrounding parenchyma) and the area under reactance during expiration (AXex) on IOS. The comparatively minor degree of volume reduction achieved (and the fall in gas transfer) using this technique may explain the relatively small impact on peripheral airways function.

An inflammatory sub-study identified a variety of microvesicle (MV) populations in bronchoalveolar lavage fluid (BALF) and in the plasma of patients with mild to very severe COPD. Of these, polymorphouclear (neutrophil)-derived MVs were found to be substantially increased in BALF and their numbers correlated with airflow limitation, reduced exercise capacity, impaired of quality of life, and the BODE index. BALF neutrophil-derived MVs correlated with BALF neutrophil cell numbers but not with circulating neutrophil MV numbers, implying local alveolar release rather than translocation from the circulation. BALF neutrophil-derived MVs were also shown to be a more robust biomarker of disease severity than BALF neutrophil cell and cytokine levels. In a subset of valve and coil recipients, BALF-neutrophil derived MV levels were evaluated before and after intervention. Mean volume reduction in the coil recipients was exceeded threefold by that of the valve beneficiaries. Unexpectedly there was no statistically significant change in MV numbers at three months in the valve arm. Possible explanations include contamination from more proximal airway sampling / spill over from the ipsilateral lobe(s) or induction of a localised inflammatory response to biofilm formation overlying the nitinol-silicone implants. In contrast, a statistically significant fall in MV numbers was observed in the coil cohort in the absence of clinically meaningful volume reduction. It must however be borne in mind that despite the thin profile of the nitinol endobronchial coil, the surface area of the airway epithelium exposed to sampling is reduced.

There were no identifiable predictors of therapeutic response among the novel indices of lung structure, function, and inflammation analysed.

Conclusions – The degree of lung volume reduction achieved is critical in determining favourable clinical outcomes for patients with severe emphysema and hyperinflation. Similarly, the structural and functional impacts of lung volume reduction on the small airways compartment, the principal site of airflow obstruction, are proportional to the degree of volume reduction achieved (surgery > valves > coils). The impact of these therapies on airways inflammation requires further scrutiny.

qCT and IOS qualify as structural and functional biomarkers, respectively, for evaluating volume reduction – however, their predictive value for therapeutic response is not established from this small dataset. BALF neutrophil-derived MV observations are potentially useful contributors to disease phenotyping alongside lung function tests and qCT imaging – their role as biomarkers for predicting and assessing therapeutic response remains to be seen. Larger randomised controlled trial designs are recommended to further investigate these preliminary findings.

LIST OF FIGURES

LIST OF TABLES

LIST OF ABBREVIATIONS

AATD	Alpha-1-Antitrypsin Deficiency
ANOVA	Analysis of variance
AX	Reactance area
BALF	Bronchoalveolar lavage fluid
BLVR	Bronchoscopic lung volume reduction
BMI	Body mass index
BODE	Body mass index, airflow Obstruction, Dyspnoea, and Exercise capacity
BOLD	Burden of Obstructive Lung Disease
BTS	British Thoracic Society
BSA	Bovine serum albumin
CAO	Coil associated opacity
c	Corrected
CC	Closing capacity
CD	Cluster of differentiation
CDI	Convection-dependent ventilation inhomogeneity
CENT	Central
CEV	Cumulative expired volume
CI	Confidence interval
CLE	Centrilobular emphysema
CMH	Chronic mucus hypersecretion
CO	Carbon monoxide
COPD	Chronic obstructive pulmonary disease
CRP	C reactive protein
Cstat	Static lung compliance
CT	Computed tomography
Curv	Curvilinearity
CV	Closing volume
C_L	Lung compliance
C_{end}	Nitrogen concentration at the end of washout
C_{Start}	Nitrogen concentration at the start of washout
C_W	Chest wall compliance
C°	Celsius
$C_{W\text{-}MAX}$	Chest wall compliance at maximal inspiration
DALY	Disability adjusted life year
DCDI	Diffusion-convection-dependent ventilation inhomogeneity
DH	Dynamic hyperinflation
DICOM	Digital imaging and communications in medicine
DMEM	Dulbecco's Modified Eagle media
$DMSO_4$	Dimethyl sulphate
DS	Destruction score
EbV	MedLung Endobronchial Valve
EBV	Zephyr Endobronchial Valve
ECCS	European Community of Coal and Steel
EELV	End-expiratory lung volume
EFL	Expiratory flow limitation
ELISA	Enzyme-linked immunosorbent assay
EMV	Endobronchial Miyazawa Valve
EMPH	Emphysema
ERV	Expiratory reserve volume

EX/EXP	Expiratory
EXVOL	Exhalation volume
FDA	Food and Drug Administration
Fen	Mean expired N_2 concentration
FETn	End-tidal N_2 concentration
FEV1	Forced Expiratory Volume in 1 second
fGT	Functional Gas Trapping
Fin	Mean inspiratory N_2 concentration
FRC	Functional Residual Capacity
Fres	Resonant frequency
fSAD	Functional small airways disease
FVC	Forced vital capacity
G	G force
G_{AW}	Airways conductance
GBD	Global Burden of Disease
GOLD	Global Initiative for Chronic Obstructive Lung Disease
HCO_3	Bicarbonate
HE	Helium
HIV	Human immunodeficiency virus
HRCT	High resolution computed tomography
HRP	Horseradish peroxidase
HU	Hounsfield Unit
Hz	Hertz
IC	Inspiratory capacity
ICER	Incremental cost-effectiveness ratio
ICS	Inhaled corticosteroid
IN/INSP	Inspiratory
INVOL	Inhalation volume
IQR	Interquartile range
IOS	Impulse oscillometry
IRV	Inspiratory reserve volume
KCO	Carbon monoxide transfer coefficient
kPA	Kilopascal
kVp	Kilovolts peak
L	Litre
LAA	Low attenuation area
LABA	Long-acting beta agonist
LAMA	Long-acting muscarinic antagonist
LCI	Lung clearance index
LRTI	Lower respiratory tract infection
LVR	Lung volume reduction
LVRC	Lung volume reduction coil
LVRS	Lung volume reduction surgery
OCD	Oxygen cost diagram
O_2	Oxygen
MBNW	Multiple breath nitrogen washout
MCID	Minimal clinically important difference
MEF25-75%	Mid-expiratory flow between 25-75% of forced vital capacity
ml	Millilitre
mMRC	Modified Medical Research Council dyspnoea scale
MRC	Medical Research Council dyspnoea scale

MV	Microvesicle
NEJM	New England Journal of Medicine
Neut	Neutrophil
NICE	National Institute for Health and Care Excellence
N_2	Nitrogen
P	Pressure
PA	Pulmonary artery to aorta ratio
P_A	Alveolar pressure
P_{ATM}	Atmospheric pressure
PC	Personal Computer
PCO_2,	Partial pressure for carbon dioxide
Peri	Peripheral
PLE	Panlobular emphysema
PLETH	Plethysmography-derived
PMN	Polymorphonuclear cell
PO_2	Partial pressure for oxygen
PRM	Parametric response mapping
PPP	Platelet poor plasma
PRP	Platelet rich plasma
PSE	Paraseptal emphysema
P_{TLC}	Maximal elastic recoil
qCT	Quantitative computed tomography
R_{AW}	Airways resistance
R	Resistance
RCT	Randomised controlled trial
RV	Residual Volume
RS	Regression slope
S	Normalised alveolar slope per breath
SAE	Serious adverse event
SAP	Small airways physiology
SBNW	Single breath nitrogen washout
S_{acin}	Acinar airway contribution to ventilation inhomogeneity
S_{cond}	Conductive airway contribution to ventilation inhomogeneity
SGRQ	St George's respiratory questionnaire
SH	Static hyperinflation
Sn	Normalised phase III slope
SIII	Gradient of Phase 3 (Alevolar Plateau)
SoC	Standard of care
SVS	Spiration Valve System
TLC	Total lung capacity
TLCO	Transfer factor for carbon monoxide
TLVR	Target lobe volume reduction
TO	Lung Turnover = CEV / FRC
TOT	Total
TP	Transpulmonary pressure
UK	United Kingdom
US/USA	United States (of America)
V	Volume
V'	Expiratory airflow
V'_{MAX}	Maximal expiratory airflow
VA	Alveolar volume

VC	Vital capacity
VDB	Bohr dead space
VDF	Fowler dead space
$V_{[Nitrogen]}$	Total volume of expired nitrogen
V/Q	Ventilation / Perfusion ratio
VT_{EXP}	Tidal volume on expiration
WCC	White cell count
X	Reactance
6MWD	Six-minute walk distance

Table of Contents

CHAPTER 1: Introduction

This chapter presents an overview of chronic obstructive pulmonary disease (COPD) with an emphasis on the emphysematous hyperinflated phenotype. The rationale for lung volume reduction, the approaches – surgical resection and bronchoscopic implantations of endobronchial valves and of coils and what is currently understood of the mechanisms and clinical data supporting their use, are summarised. The impact of volume reductions on lung structure, function and inflammation particularly of the small airways (i.e., those defined as having an internal diameter of < 2mm) is only recently being explored: The tools available are described. The object of this thesis is to examine in greater detail the consequences of these interventions which may for example, help to identify better predictors of response.

Definition of Chronic Obstructive Pulmonary Disease (COPD)

The Global Initiative for Chronic Obstructive Lung Disease (GOLD) was set up in 1997 by the US National Heart, Lung and Blood Institute, National Institutes of Health, USA, and the World Health Organisation to promote awareness of and investment in a then largely neglected but common, disabling disorder. An initial outcome was the redefinition: Chronic obstructive pulmonary disease (COPD) is 'a common, preventable and treatable disease characterised by persistent respiratory symptoms resulting from airflow limitation due to airway and/or alveolar abnormalities usually caused by significant exposure to noxious particles or gases' (GOLD report, 2019[1]). The terminology is thought to better encompass the clinicopathological spectrum as it is now understood.

The airways limitation is driven by a chronic inflammatory process resulting in a combination of small airways disease and parenchymal destruction (emphysema), their relative contributions and evolution peculiar to the individual.

Emphysema is a pathological diagnosis[2] demonstrable with computed tomography[3]: Small airways tethering and intrinsic elastic recoil necessary to maintain the patency of the lumen, are impaired and alveoli are destroyed to be replaced by non-functioning dilated airspaces in the secondary pulmonary lobules, ultimately resulting in hyperinflation[4]. Demonstrable airflow obstruction is fundamental to the GOLD definition[1]. Chronic bronchitis, defined by symptom history of productive cough on most days, for at least 3 months of the year for 2 consecutive years with no objective evidence of obstructed airways, is excluded from the diagnosis of COPD[5].

The History of COPD

More than 300 years have elapsed since the earliest accounts of a disease of the lungs with which we are familiar as emphysema, a term derived from the Greek 'to blow in' or 'inflate', attributed to René Laennec (1781-1826). In 1679, Swiss physician Theophile Bonet described 'voluminous lungs'[6] and a century later, in 1769, Italian anatomist Giovanni Morgagni reported on lungs 'turgid particularly from air'[7]. The Dutch anatomist Frederick Ruysch identified airways obstruction and hyperinflation in the human condition in 1691[8]:

> *'I discovered in a certain part of the lung a multitude of transparent vesicles, expanded with air and so obstructed that I was not able, with a light compression, to evacuate them of the air. I discovered by experiment that breath impelled through the trachea had no further connection with these expanded vesicles, on account of their obstruction. Later, when air was forcibly applied to the trachea, some of the vesicles were ruptured'.*

In 1803, British pathologist Matthew Baillie illustrated the enlarged airspaces of emphysematous lungs in 'The Morbid Anatomy of Some of the Most Important Parts of the Human Body' and highlighted the destructive nature of the disease[9]. The lungs described are thought to have been those of Dr Samuel Johnson, the essayist and lexicographer[10]. Dr James Wilson, performing the autopsy, recorded hyperinflation, loss of elastic recoil and inflammation:

'On opening the cavity of the chest, the lungs did not collapse as they usually do when the air is admitted but remained distended, as if they had lost their power of contracting: the air cells on the surface of the trachea were somewhat inflamed'.

British physician Charles Badham introduced the term catarrh in his 1814 essay on chronic bronchitis[11]. French physician, pathologist and inventor of the stethoscope, René Laennec, correlated his clinical and pathological findings and in 1829 described the association of emphysema and chronic bronchitis in his seminal work, 'A Treatise on the Diseases of the Chest and on Mediate Auscultation'[12]:

'The disease which I designate by this title is very little known and has not hitherto been correctly described by any author. I for a long time thought it very uncommon, because I had observed only a few cases of it: but since I have made use of the stethoscope, I have verified its existence as well on the living as the dead subject and am led to consider it as by no means infrequent…. In opening the chest, it is not unusual to find that the lungs do not collapse, but they fill up the cavity completely on each side of the heart. When experienced, this will appear full of air…. The bronchi of the trachea are often at the same time a good deal filled with mucous fluid'.

Laennec also acutely observed that the peripheral airways were the primary site of airways obstruction in COPD.

In 1952, Gough using large paper-mounted sections of lung, distinguished centrilobular emphysema (focal destruction localised to the proximal respiratory bronchioles of an acinus[1], typically affecting the upper zones, and associated with smoking) from panlobular emphysema (affecting the entire acinus in, predominantly, the lower zones in individuals with alpha-1-antitrypsin deficiency)[13]. In 1957, based on 3-dimensional microscopic reconstructions, McLean hypothesised emphysema was a sequel of inflammation affecting the respiratory bronchioles[14-16] and in 1958, described the

[1] Regional unit of lung supplied by one terminal bronchiole.

accompanying vascular changes[17]. These findings form the classical triad of pathological changes observed in patients with COPD involving the airway, parenchymal and vascular compartments.

The hypothesis that the small airways account for the greatest resistance in normal lungs prevailed until 1963, when Ewald Weibel, a Swiss physician and physiologist, identified the exponentially increasing total cross-sectional area of the dichotomously branching lung towards the periphery[18]. In 1967, Peter Macklem and Jeremiah Mead, Canadian and American physiologists, respectively, conducted seminal experiments using a retrograde catheter positioned in canine airways to partition pulmonary flow resistance [19]. They confirmed that the small airways, defined as those less than 2mm internal diameter and equating to generations 12-23 of Weibel's model[18], offer less than 10% of the total resistance to flow below the larynx[19]. Using this same technique, Macklem, in collaboration with James Hogg and William Thurlbeck, Canadian pathologists, published pioneering research showing that the small airways are the main site of obstruction in excised human lung from individuals with COPD[20]. Furthermore, bronchographic and histologic studies of the post mortem human lungs revealed peripheral resistance was increased because of mucus plugging, narrowing and obliteration of the small airways driven by chronic inflammation[20]. Based on two influential publications in the same issue of the NEJM[21, 22], Mead termed the small airways a 'quiet' zone in which substantial disease must accumulate before being clinically manifest[23].

Epidemiology of COPD

Prevalence

Drawing upon data from the Burden of Obstructive Lung Disease (BOLD) programme[24] and other large epidemiological studies, a global prevalence of 11.7% (95% CI: 8.4 to 15.0%) is estimated[25]. About 3 million deaths attributed to COPD occur annually worldwide[26], and this is predicted to rise to 4.5 million in 2030[27-29].

Morbidity

Proxies for morbidity: physician consultations, emergency department visits and hospitalisations, feature earlier and more frequently in the lives of COPD sufferers[30] than in their peers on account of their respiratory disease and of comorbidities such as cardiovascular disease[31], also a consequence of their lifestyle. This has associated healthcare cost implications[32].

Mortality

COPD is the fourth leading cause of death worldwide[33] and is projected to be the third by 2020[28]. This is in part driven by the ubiquitous habit of smoking, greater longevity, and fewer effective disease-modifying therapies compared to other ailments (e.g. ischaemic heart disease and infections)[1].

Economic impact

In Europe, COPD accounts for approximately 56% (38.6 billion Euros) of respiratory-related healthcare costs[1], much of it related to the frequency of exacerbations. Costs rise exponentially with increasing severity of disease – for example, those associated with hospitalisation and the provision of long-term oxygen equipment. Caring for a disabled relative with COPD may entail stepping back from a career and the consequent loss of two people from the workplace[34, 35] and additional burden on the state.

Social impact

The Global Burden of Disease (GBD) study introduced the Disability Adjusted Life Year (DALY) as a composite measure for the societal impact of a disease[36]. A DALY can be considered as one lost year of 'healthy life'. In 2013, COPD was listed as the fifth highest cause of DALYs worldwide[37].

Aetiology of COPD

The aetiology of COPD is a complex interplay of genetics and environment. Exposure to tobacco smoke is an undisputed important factor[38]; Biomass fuel exposure and air pollution, particularly in developing nations, may also contribute[39]. However, the process is not fully understood. Non-

smokers are not entirely immune and as many as 50% of heavy smokers do not develop the disease[40]. Despite several longitudinal studies spanning over 20 years[41, 42], our understanding of the evolution of the disease is far from complete and we are only starting to build a chronology from the pre-natal period encompassing the entire disease trajectory[43, 44].

Genetics

Alpha-1-antitrypsin deficiency (AATD) is a familiar example; a rare autosomal codominant hereditary condition affecting around 25,000 people in the United Kingdom. These individuals with both copies of the Z allele produce only 10-15% of the protective protease inhibitor and exhibit the severe phenotype of the condition with early onset COPD that progresses more rapidly, especially in those who smoke. Although uncommon, it is a useful model with which to conceptualise the effects of a genetic deficiency on disease pathogenesis.

Familial clustering has been observed among smoking siblings of patients with COPD. Several genes for example, those encoding matrix metalloproteinase 12[45] and glutathione-S-transferase[46], and genetic loci[47], have been implicated in an increased risk of COPD, and their influence merits further evaluation.

Age

Increased life expectancy is bringing with it the additional burden of late onset disease. Senile ‘emphysema’, so-called because the occurrence of enlarged alveolar air spaces is ubiquitous, independent of smoking habits and is considered a normal process of ageing[48]. Alveolar wall destruction and peripheral airways disease of COPD are not features. Oxidative stress is thought to accelerate ageing of the lung via the phosphatidylinositol-4,5-bisphosphate 3-kinase/AKT/mechanistic target of rapamycin signalling pathway[48].

Sex

There is no difference in sexual prevalence but there is data suggesting female smokers tend to have more severe small airways disease than males with a similar smoke exposure[49, 50].

Lung growth and development

A study of 2257 British women aged 60-79 years found a modest positive association between birth weight and adult spirometry suggesting gestational factors may influence lung development and subsequent expression of disease[51]. An individual with a low FEV1 in early adulthood, despite a decline in later life following a normal trajectory in contrast to the classic accelerated pattern leading to COPD, is also recognised as at increased risk of developing the disease[52]. Furthermore, the authors of a prospective study from birth have reported a decline in FEV1 by the age of 43 years in 2172 individuals demonstrating synergistic interactions of smoking, infant respiratory infections and early-life home overcrowding[53].

Particle exposure

Smoking cigarettes is the main risk factor for developing COPD worldwide[38, 54] but pipe smoking[55] and passive inhalation[56] are also recognised risk factors.

Workplace exposures to organic and inorganic dusts are estimated to contribute up to 20% of cases of COPD[57-59]. Indoor biomass exposure to fuels used for cooking and heating presents another at-risk population, especially among females, in the developing nations[60]. The role of outdoor air pollution as a risk factor for COPD is unclear but there is evidence that children from communities with higher levels of air pollution are more likely to suffer from impaired lung function[61], a risk that has been shown may be successfully addressed with implementation of air quality policies[62].

Infections

In 4636 subjects studied as part of the European Community Respiratory Health Survey, respiratory infections in childhood were associated with a 2-fold increased risk of developing COPD[63]. There is evidence that individuals with HIV[64] or Tuberculosis[65] are at increased risk of COPD. Susceptibility to infections also plays a role in COPD exacerbations and decline in lung function[66].

Chronic mucus hypersecretion

Chronic mucus hypersecretion (CMH), the key symptom of chronic bronchitis, is common in smokers and an independent risk factor for developing COPD[54, 67, 68] that may also influence the course of airways disease[69].

Socioeconomic status

Lower socioeconomic status is associated with an increased risk of developing COPD[70]. It remains unclear as to whether this reflects increased particle exposure, lower birthweight, or infections, for example[1].

Pathology of COPD

The nomenclature of the normal anatomy of the human respiratory system adopted in this thesis is summarised. Air acquired through the nasal and oral passages, larynx and trachea is distributed in each lung through a series of at least 23 dichotomously dividing bronchi and bronchioles, the first 14 generations comprising the 'conducting zone', the following, the 'respiratory zone', and ultimately delivered to the interface, at least 75 square meters, of the alveolar-capillary exchange units where exhaust gases are substituted for elimination in the cyclic process of inspiration and expiration[71]. (Figures 1.1 and 1.2).

The small airways, those less than 2mm in internal diameter, are to be found in the 4^{th} to 13^{th} generations[72]: approximately 20% contain cartilage within their walls[73]. They offer little resistance in health (less than 10%) but become the principal site of airways obstruction in COPD[20].

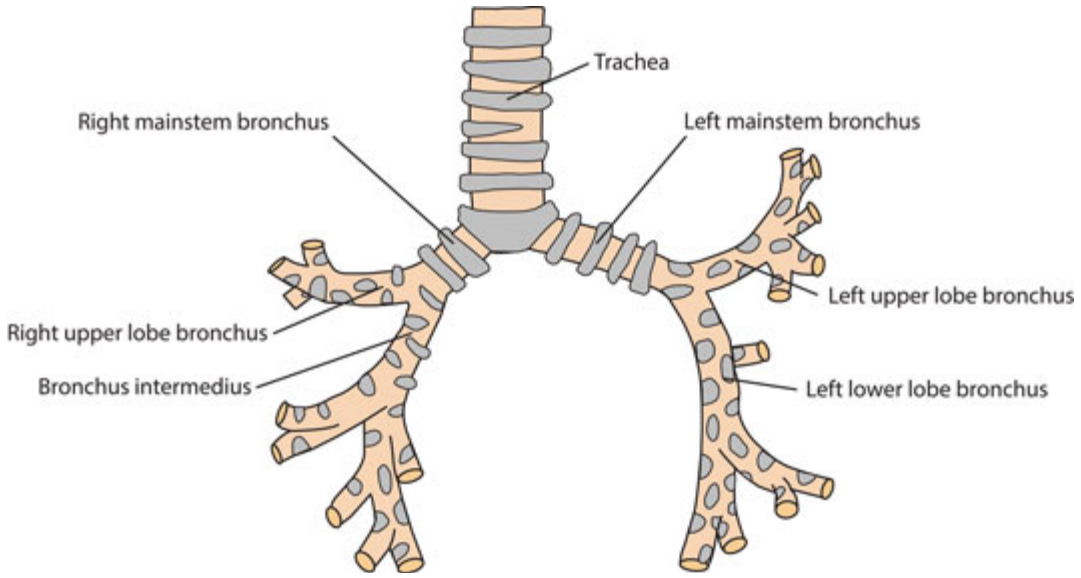

Figure 1.1. The tracheobronchial tree (main divisions).

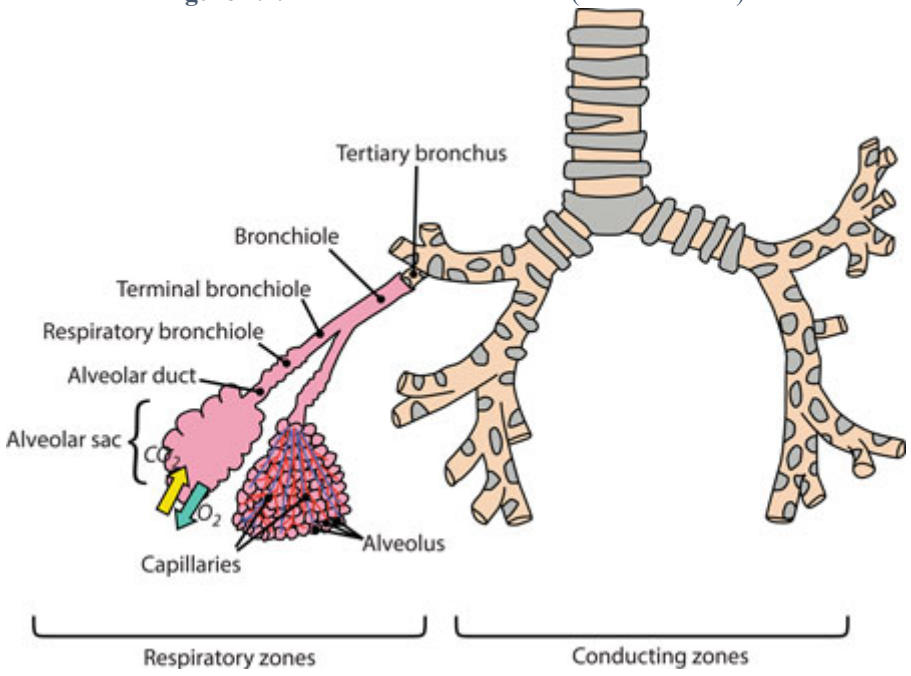

Figure 1.2. Divisions of the bronchial tree into conducting and respiratory zones.

The fundamental unit, likened to a berry, termed the pulmonary acinus (Latin), comprises a terminal bronchiole – the last and the smallest subdivision to have its own complete fibromuscular wall, its progeny of respiratory bronchioles (3 generations), terminating in alveoli, numbering 14,000-20,000, and its accompanying vasculature[74-76]. Other authors adopt a 'primary lobule' as their microscopic fundamental respiratory unit (distal to the highest order respiratory bronchiole) and assign a group of 30 to 50 to make up a secondary lobule[77], the equivalent of 5 to 15 acini[78]. The secondary lobule

is a macroscopic structure, a pyramid defined by fibrous septa 2 to 3cm from apex to base[79, 80]. (Figure 1.3).

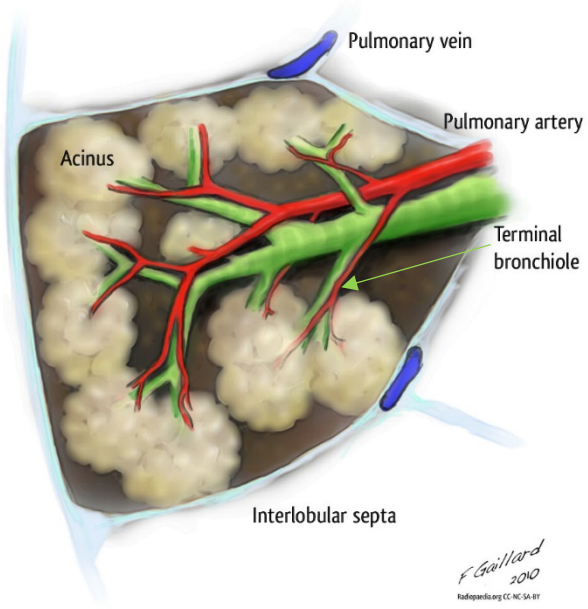

Figure 1.3. Schematic diagram of a secondary pulmonary nodule.
Illustrated by Frank Gaillard of Radiopedia.org, 2010. (Creative Commons attribution 4.0).

The transport of gas from the atmosphere to the alveoli relies on two distinct processes, bulk flow and diffusion. The respiratory muscles generate a pressure gradient along which gas moves in bulk flow from the mouth and nose to the smallest of conducting airways. The exponential increase in airway cross-sectional area results in the transition from bulk flow to diffusion of gas along a concentration gradient (generated by the exchange of oxygen and carbon dioxide) at the union between the conducting and respiratory bronchiole airways, a region of the lung vulnerable to small particle deposition[2] such as that arising from tobacco smoking. Airflow is turbulent in the upper and central airways as defined by a raised Reynolds number[3], becoming increasingly laminar beyond and is described by Poiseuille's equation[4].

[2] Einstein's work on Brownian motion showed that small particles suspended in a diffusing gas settle out first.

[3] The *Reynolds number* is a dimensionless value used to determine whether a fluid (including air) is in turbulent (high) or laminar (low) flow according to the ratio of the inertial and viscous forces.

[4] Poiseuille's equation states resistance *R* to laminar flow of an incompressible fluid having viscosity η through a horizontal tube of uniform radius *r* and length *l* is given by $R = \frac{8\eta l}{\pi r^4}$.

Chronic obstructive pulmonary disease (COPD) is a destructive pathological process affecting a triad of tissues, airways, parenchyma and vasculature[80]. However, it is increasingly appreciated that the origin of the disease is to be found in the inflammatory response of peripheral airways targeted by inhaled noxious particles[20, 81]. Luminal occlusion by mucus, secreted in excess and accumulating due to failure of damaged clearance mechanisms, airways remodelling and loss of radial traction results in air trapping and emphysema[82]. Histological severity correlates with, for example, survival after LVRS, the procedure devised to palliate hyperinflation of emphysema[83].

Airways

Involvement of the small airways is a key pathological feature of COPD recognised in the 19th century. This region of the lung is termed the 'silent zone' and presents a challenging problem[23] - the advent of symptoms and of abnormalities in conventional lung function tests is delayed until substantial injury has accumulated.

Small airways remodelling

The walls of the small airways are thickened at the expense of the lumen by epithelial changes, inflammatory cell infiltration, smooth muscle hyperplasia, excessive collagen deposition, and mucus plugging[84]. (Figure 1.4).

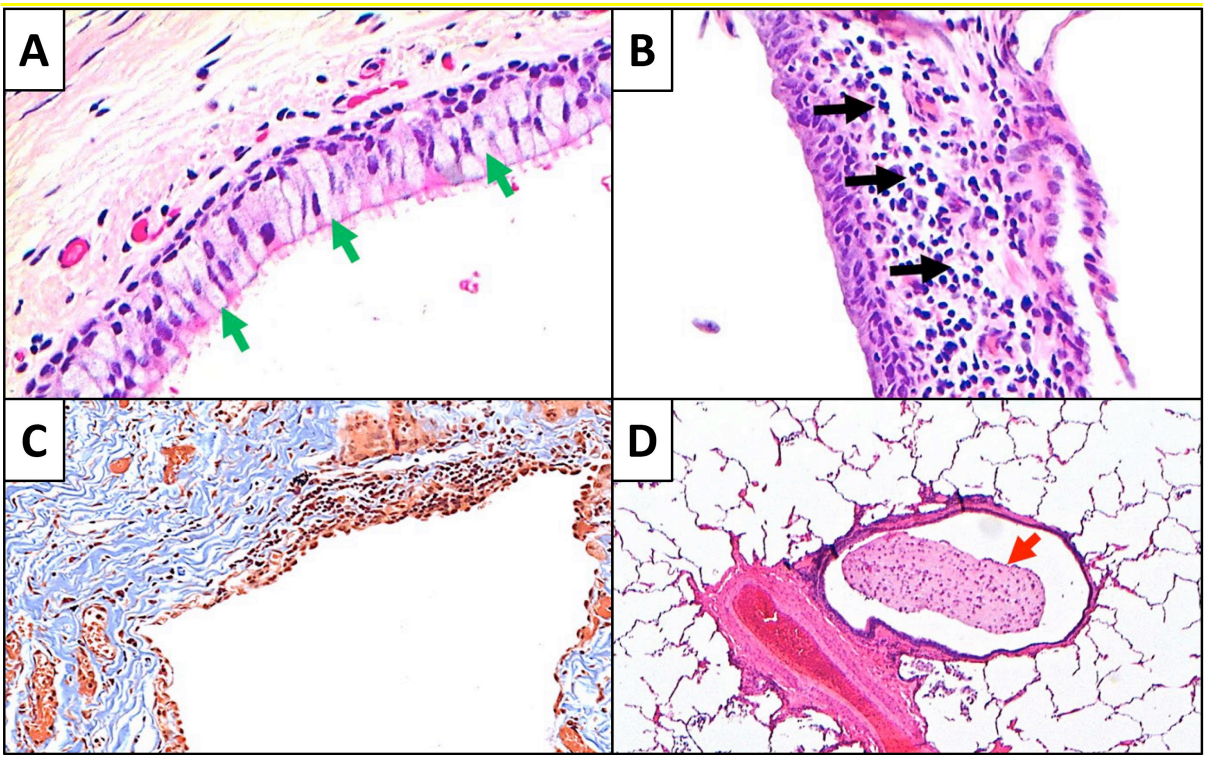

Figure 1.4. Pathology of small airways disease in COPD.
Goblet cell hyperplasia (green arrows) of bronchiolar epithelium stained using haematoxylin and eosin (**A**). Inflammatory cell infiltration (black arrows) of bronchiole wall stained using haematoxylin and eosin (**B**). Excessive collagen deposition (blue bundles) of bronchiole wall stained using Masson's Trichome (**C**). Single bronchiole with intraluminal mucus plug indicated by red arrow (**D**). Adapted from Higham et al[85]. (Creative Commons attribution 4.0).

Epithelial changes include basal cell hyperplasia, goblet cell and squamous metaplasia[85], and persistence of epithelial-mesenchymal transition[5], correlating with peri-bronchial fibrosis and airflow limitation[86]. Dysregulated expression of tight junction proteins compromise the integrity of the epithelial barrier function[87] and together with impaired mucosal immunity, are thought to promote inflammation and progression of airways remodelling in COPD[88].

Inflammatory infiltration of the small airways precedes peri-bronchiolar fibrosis and emphysema[89] and is thought likely to be a feature of the earliest events in the pathogenesis of COPD[20]. The number of small airways containing innate (neutrophils and macrophages) and adaptive (CD4, CD8,

[5] Epithelial-mesenchymal transition (EMT) is a process in which epithelial cells de-differentiate towards mesenchymal cells.

and B cells) immune cells, indicating the extent of inflammation, and the absolute volumes of CD8 cells and B cells, a surrogate for inflammatory activity, are associated with disease severity[84]. Immune cell composition, however, varies according to mural compartment (e.g. epithelial lining or extracellular matrix) and airways analysed and may account for reported differences between studies[85].

Small airways obliteration

Quantitative micro-CT studies of lung explants have demonstrated narrowing and loss of terminal and respiratory bronchioles preceding emphysematous destruction and linearly correlating to COPD disease severity (40% reduction in mild-to-moderate, 80% in severe-to-very severe COPD)[90, 91], emphasising the desirability of early intervention to disrupt the otherwise inexorable disease process.

Parenchyma

Emphysema is defined as 'a condition of the lung characterised by abnormal, permanent enlargement of the air spaces distal to the terminal bronchiole, accompanied by destruction of their walls without obvious fibrosis'[92]. Three subtypes have been determined by their relationship to the acini within the secondary pulmonary lobule: centrilobular (or proximal), paraseptal (or distal), and panlobular. The term 'acinar' is frequently used interchangeably with 'lobular'. (Figure 1.5).

Centrilobular emphysema

Centrilobular emphysema (CLE) is the most common subtype of pulmonary emphysema and involves destruction and enlargement of the first and second-order respiratory bronchioles i.e. the proximal portion of the acinus (sparing the alveoli), the anatomical region favouring small particle deposition such as from cigarette smoke[93]. Radiologically, low-attenuating regions with ill-defined borders are observed in the centre of the secondary pulmonary lobule, preferentially affecting the upper zones of lungs of individuals who have smoked[94].

Panlobular emphysema (PLE)

Uniform destruction and enlargement of the acinus (from respiratory bronchioles to terminal alveoli) is the feature of PLE. Radiologically, the secondary pulmonary lobule exhibits diffusely low attenuation. Basal zone predominance is observed in patients with alpha-1-antitrypsin deficiency[95].

Paraseptal emphysema (PSE)

PSE refers to a peripheral distribution of destruction and enlargement involving the alveolar ducts and sacs, located adjacent to the pleural and interseptal boundaries within the secondary pulmonary lobule. It is asymptomatic and radiologically, typically limited to the dorsal regions of the upper zones[95].

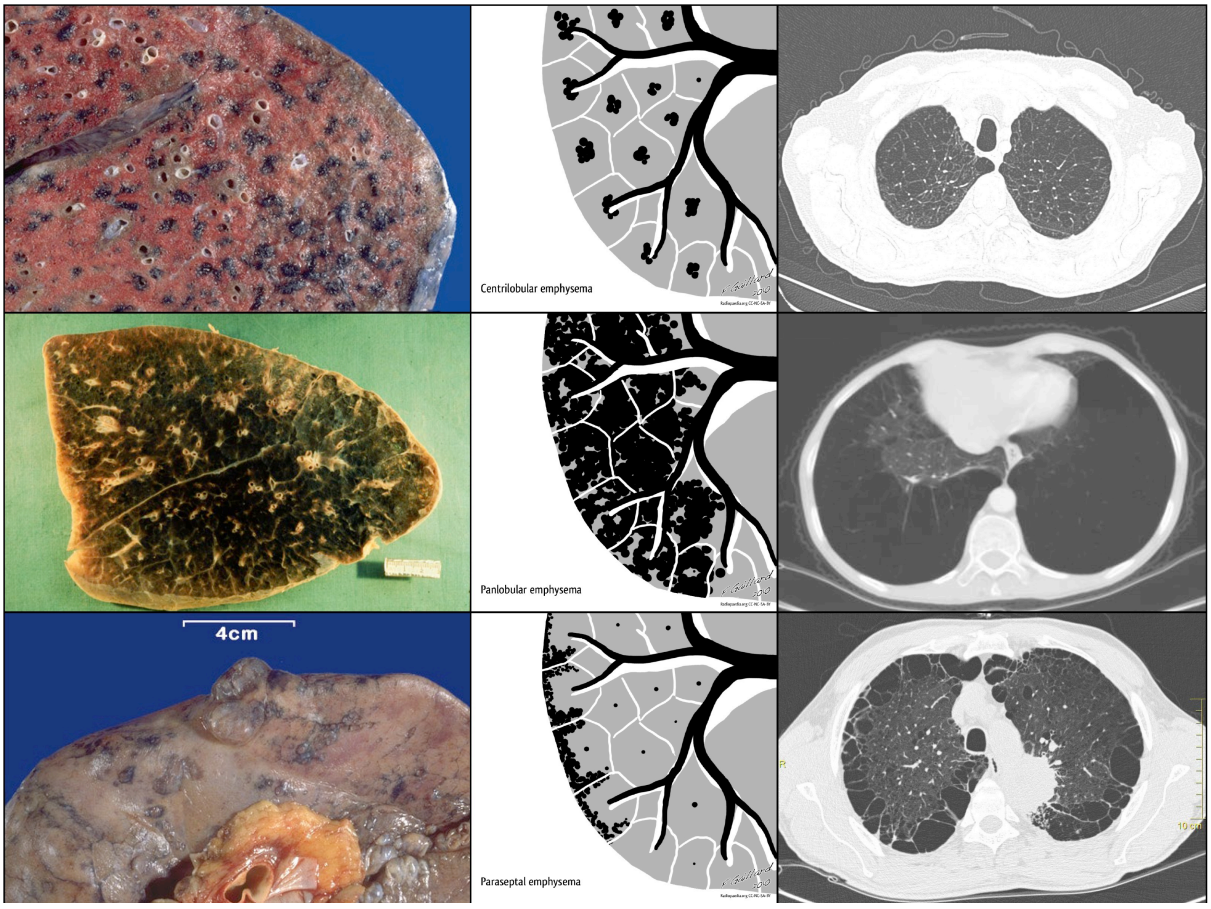

Figure 1.5. Pathological and radiological correlates for emphysema subtypes.
Pathology specimen photos courtesy of The University of Texas (centrilobular and paraseptal emphysema) and Universidad Autónoma de Zacatecas (panlobular emphysema) online resources. Schematic diagrams and CT axial slices by Frank Gaillard of Radiopedia.org, 2010. (Creative Commons attribution 4.0).

Vasculature

Pulmonary hypertension is a common sequel of COPD that predicts survival[96]. Vascular remodelling with thickening of the intima, media and muscularisation of the vessel wall culminates in luminal narrowing and impaired ability to vasodilate[97]: This is in addition to parenchymal destruction and loss of blood vessels[98].

Pathogenesis of COPD

Neutrophilic small airways inflammation

Tobacco smoke is the leading cause of COPD[1] conveying a toxic and carcinogenic mixture of about 5,000 chemicals[99] in particulate form ranging from 0.021 to 1.956 μm[100] that preferentially deposit in the small airways. Inhalation induces an inflammatory response, a complex interplay of immune cells and mediators. Neutrophils are the most abundant of the cells in the vanguard implicated in the pathogenesis of COPD.

Easily identifiable with their multi-lobular nuclei and staining characteristics, in health they account for 70% of circulating white blood cells. They are short-lived, a half-life of six to eight hours, but are replaced at a basal rate of up to 10 x 10^{10} cells per day[101]. Neutrophils exist in three states of readiness, quiescent, primed and activated[6][102]. They are rapidly recruited to threatened sites to initiate the response to invading microorganisms: Phagocytosis, and degranulation releasing disabling proteinases, bactericidal proteins and reactive oxygen species [103]. Excessive or dysregulated neutrophilic activity however leads to host tissue injury and is a frequent feature of airway diseases[104].

[6]Neutrophil activation is a multifaceted process with priming as an intermediary step – a state of enhanced responsiveness to a second stimulus – followed by the acquisition of increased functionality including phagocytosis and degranulation.

Neutrophilic inflammation of small airways is a hallmark of COPD – neutrophil numbers and products, measured in sputum and bronchoalveolar lavage fluid[7], correlate positively with disease severity (FEV1 decline and CT densitometry score)[105-109] and small airways dysfunction[110, 111] and are augmented in COPD exacerbations[112, 113]. The accumulation of airway neutrophils is thought to reflect a combination of heightened recruitment and of retention[114]. Increased pulmonary neutrophilic inflammation is also detectable using non-invasive nuclear imaging modalities[115, 116]. Importantly, the pathological features of COPD can be reproduced using neutrophil products (for example, neutrophil elastase) in animal and *in vitro* studies[117, 118].

The neutrophil may be considered one of the orchestrators of the inflammatory response, a process which however has become dysregulated by a catastrophic breakdown in the 'crosstalk' between a variety of immune cells including macrophages[119], T cells[120], B cells[121], eosinophils[122] and platelets[123], culminating in host tissue injury.

Inflammatory cytokines

IL-1 beta, IL-6, CXCL-8 (formerly IL-8), and TNF-alpha are among the more frequently cited members of a complex pool of inflammatory cytokines mediating these aberrant interactions[124], but investigating / tracking individual components of the inflammatory signalling cascade is bedevilled by the extremes of redundancy built into the system.

Microvesicles

Microvesicles (MVs), until recently disparaged as discarded 'cell dust', are now promoted as biomarkers and as mediators of intra-alveolar inflammation. They are fragments of cell membrane, 0.1 to 2µm in diameter shed by most eukaryotic cells[125]. They have been observed to exert pro-inflammatory effects by virtue of surface expressed proteins and their internal 'cargo'[126]. In COPD, circulating endothelial-derived MVs are elevated[127, 128], peak during acute exacerbations[129],

[7]In health, the macrophage accounts for approximately 85% of the cellular composition of a bronchoalveolar lavage.

and are predictive of rapid decline in FEV1[130]. However, there is a paucity of data on airway-derived microvesicles[131]. It would be of interest to determine the role of neutrophil-derived microvesicles in disease pathogenesis[132].

Development of emphysema

Small airways inflammation is the precursor of emphysema[90]. Putative processes include an imbalance of protease and antiprotease activities[133], accelerated lung aging[134, 135], and reduced diversity of the lung microbiome[136].

Pathophysiology of Hyperinflation

A number of pathophysiological mechanisms are activated resulting in hyperinflation (supra-normal lung volumes)[137], which is recognised as a significant contributory factor to the sufferer's perception of breathlessness on activity[138], exercise limitation[139, 140], and predicts not only the risk and severity of exacerbations[141] but all-cause mortality[142, 143]. This observation has attracted interest in lung volume reduction and the development of techniques targeting the hyperinflation of individuals with predominant emphysema in an attempt at restoring normal respiratory mechanics.

In the emphysematous lung, destruction of the alveolar sac walls results in loss of the passive elastic recoil, which drives expiration at rest and necessitates reinforcement of this phase of breathing with an active forced one[144]. However, loss of radial traction on the small airways renders them susceptible to collapse when subjected to the increased intrathoracic pressure, impeding emptying of the alveoli[145, 146]. Gas entrapment is further encouraged by increased lung compliance[147], and is aggravated by airflow limitation (also from co-existing small airways inflammation[148]) with relatively insufficient expiratory time for lung emptying. The work of breathing is increased throughout the respiratory cycle due to an inspiratory time encroached on by a prolonged active

expiratory phase[147, 149] (Figure 1.6). These pathophysiological changes are examined in pulmonary function testing.

Spirometry parameters including the forced expiratory volume in 1 second (FEV1), forced vital capacity (FVC), FEV1/FVC ratio, and forced expiratory flow at 25-75% of FVC are reduced, indicative of airways obstruction. Dynamic airways compression occurs much earlier at high lung volumes creating a characteristic 'scalloped' appearance of the expiratory flow-volume curve[147].

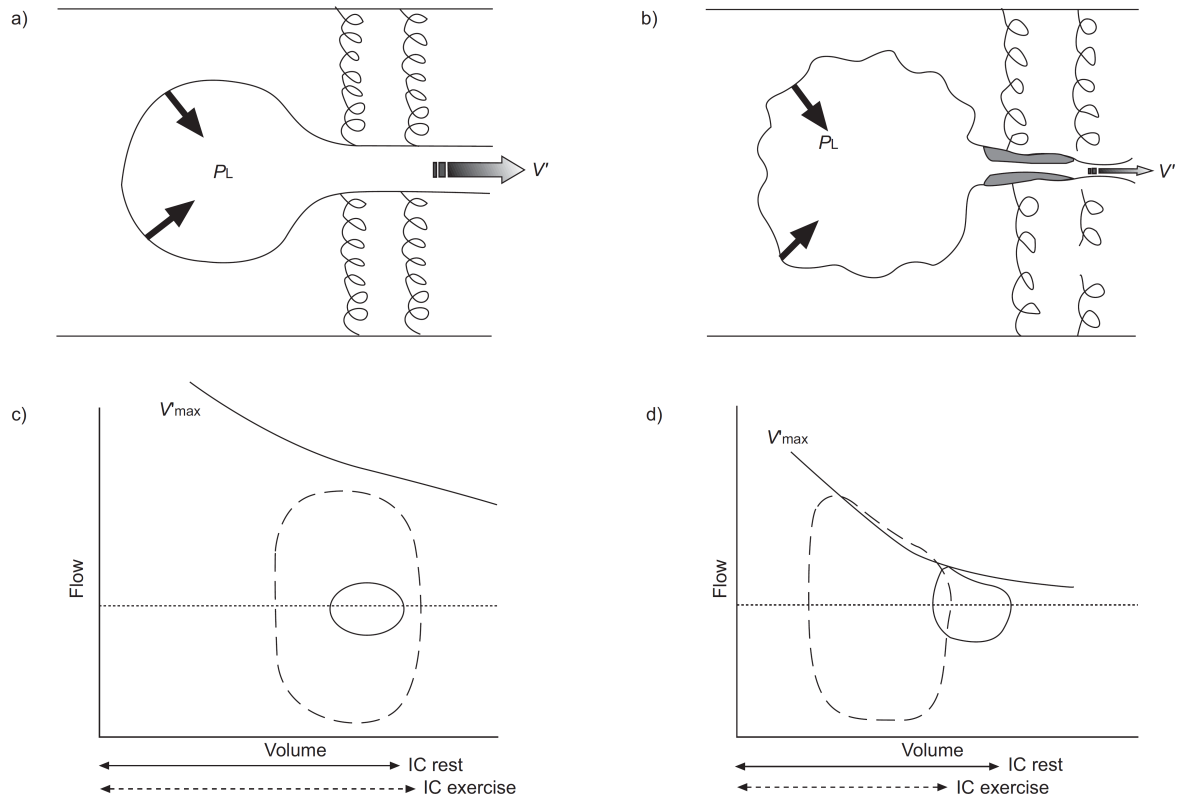

Figure 1.6. The alveolus in health and in COPD.
The alveolus in a) health and in b) COPD with corresponding flow-volume loops, c) and d), respectively. Loss of elastic recoil (P_L) reduces both driving pressure for airflow (V') and airway traction, which aggravated by intrinsic airways narrowing, results in *expiratory flow limitation* (EFL) and *static hyperinflation* (SH). In COPD, maximal expiratory flow (V'_{max}) is attenuated at higher lung volumes by dynamics airways compression, creating the characteristic 'scalloped' flow-volume loop in d). Inspiratory capacity (IC) falls during exercise, termed *dynamic hyperinflation* (DH), elevating end-expiratory lung volume (EELV). Solid curve, tidal breathing at rest; Dashed curve, tidal breathing during exercise. Adapted from O'Donnell DE and Laveneziana P (2006)[149].

Lung volumes may be assessed with whole body plethysmography or helium dilution techniques. In obstructive airways disease, plethysmography is considered more appropriate as the time required for helium equilibration is excessive. In emphysema, total lung capacity (TLC), end-expiratory lung volume (EELV; synonymous with functional residual volume, FRC), and residual volume are typically

increased, termed *static* hyperinflation. The RV/TLC ratio is often greater than 40% and not infrequently exceeds 55%. This in turn exerts a positive end-expiratory intra-pulmonary pressure called auto-PEEP, which must be overcome to create inspiratory flow[147].

During exercise, the situation is aggravated by insufficient expiratory time leading to further gas entrapment, 'breath stacking', and a rise in EELV. This encroaches on inspiratory reserve volume, reducing inspiratory capacity (IC; the volume of air that can be inhaled maximally from EELV or the end of quiet expiration), which can be reliably measured serially to determine the degree of *dynamic* hyperinflation[149] (Figure 1.7). This phenomenon is also observed acutely during COPD exacerbations[150].

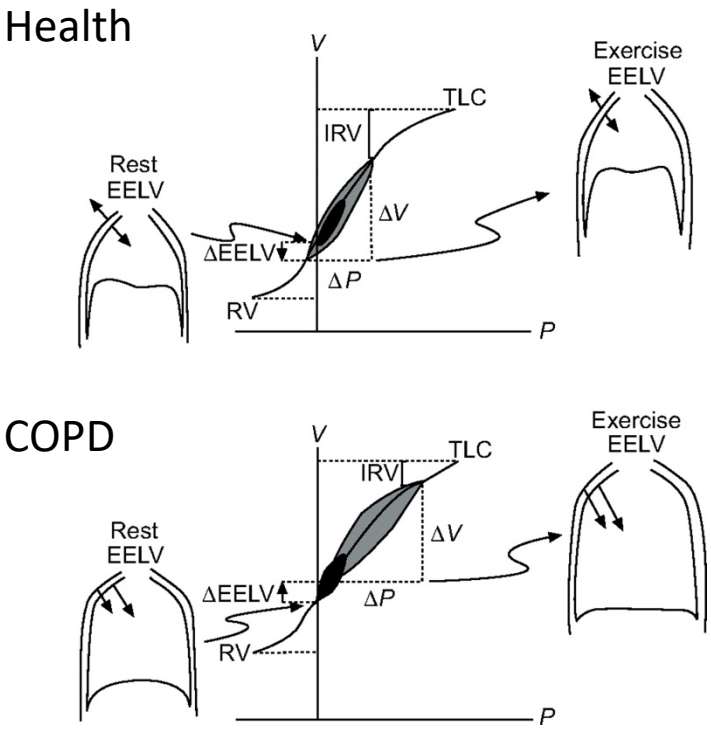

Figure 1.7. Lung pressure-volume relationships at rest and during exercise in health and in COPD.

EELV, End-Expiratory Lung Volume; IRV, Inspiratory Reserve Volume; RV, Residual Volume; TLC, Total Lung Capacity; *Δ*P, change in pressure, *Δ*V, change in volume. Tidal volume at rest (black spindle) and on exercise (grey spindle). Adapted from O'Donnell & Laveneziana (2006)[149].

In emphysema, the pressure-volume curve of the lung has a steeper incline and is displaced upward and to the left, reflecting the higher lung compliance (or reduced elastic recoil), a result of alveolar wall destruction[147]. In contrast to the healthy individual, both chest wall and lung recoil become

inwardly directed at rest and during exercise, when tidal breathing operates closer to TLC on the flatter portion of the curve, leading to increased loading of the inspiratory muscles[149]. Moreover, downward displacement of the diaphragm shortens the muscle fibres and significantly reduces the ability to generate sufficient force to overcome trans-pulmonary pressure and drive inspiratory airflow[151, 152]. The recruitment of accessory muscles is necessitated to overcome the mechanical disadvantage of the system converting the process of exhalation from passive to pathologically active at rest[153]. The inefficient respiratory pump consumes significantly more energy and causes the patient to feel much more breathless[154].

The individual with emphysema has greater physiological dead space due to ventilation (V_A) of poorly perfused (Q) lung units (i.e. regions of lung with high V/Q ratios)[155], demonstrated by topographical differences in radioactive isotope distribution on nuclear medicine scanning. The mismatch in ventilation-perfusion reduces the opportunity for gas exchange and precipitates arterial hypoxaemia[147]. Impaired gas exchange may be investigated with transfer of carbon monoxide. Dynamic hyperinflation during exercise limits ventilation[140].

Physiological basis for lung volume reduction surgery (LVRS)

LVRS as a means of improving the native lung function, was championed by Brantigan and Mueller in the 1950s, postulating improved elastic recoil and airway traction in the remaining lung tissue and restored efficient respiratory muscle mechanics but was met with scepticism. Subjective improvement was noted but physiological data were limited, mortality discouragingly high, and the procedure fell into disfavour[156]. A review in 1996 of surgical treatments of bullae concluded that substantial benefit was to be expected only in symptomatic patients with bullae not less than one third of the volume of the hemithorax[157].

Subsequently, improvements in patient selection and operative techniques developed by Joel Cooper reduced the mortality to single figures and revived interest[158]. Bilateral resections of 20-35% of

each lung in 1218 subjects compared with medical treatment in a randomized study in 2013 demonstrated an improved quality of life, exercise tolerance, and survival at 2 years in those with predominantly upper lobe emphysema and low baseline exercise capacity[159]. At our institution in 2014, 81 patients underwent LVRS: The 90-day survival was 100%[160]. The outcome has been a validation of the pioneers' hypotheses. To these have been added re-inflation of potentially functioning lung compromised by compression and 're-matching' to the thoracic cavity[161]. The physiological effects of LVRS are now summarised.

Lung elastic recoil

An increase in maximal lung elastic recoil at TLC is a consistent outcome of LVRS for both unilateral and bilateral surgery[162-164].

Expiratory flow

Adapting Ohm's law in the field of electricity, expiratory airflow in the lung of the healthy individual at rest is driven by intra-alveolar pressure (P_A - P_{ATM}: P_A, alveolar pressure, generated by the lung's intrinsic elastic recoil; P_{ATM}, atmospheric pressure) and opposed by airways resistance (R_{AW}): $Airflow = P / R_{AW}$. Destruction of the elastic tissues in emphysema reduces elastic recoil (driving pressure) and increases resistance due to early airways collapse during expiration, the consequence of loss of radial traction[137]. A rise in the alveolar pressure and / or fall in airways resistance would be expected to translate to improved airflow. However, in the operated lung, the relationships between lung recoil, airways resistance and expiratory flow are inconsistent, suggesting additional mechanisms[161].

The increases in FEV1, FVC, and lung elastic recoil pressure are rather more impressive than the FEV1/FVC ratio, following LVRS. These observations suggest recruitment of functional lung rather than changes in airways resistance in diseased lung is the more likely explanation[164].

The Fessler-Permutt mathematical model attempts to explain this graphically and shows the improvement in vital capacity (VC) achieved by re-sizing the lungs to match the dimensions of the thoracic cavity, with proportionately greater reduction in RV compared to TLC[165, 166]. (Figure 1.8).

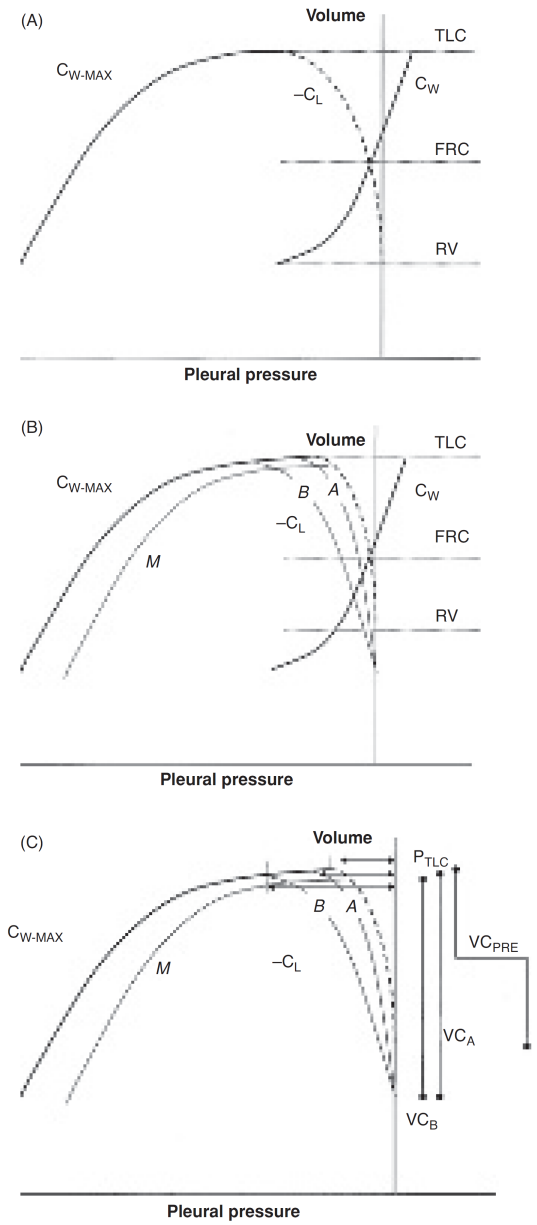

Figure 1.8. Pleural pressure-lung volume relationships

In health (Panel A) and in emphysema (Panels B & C) before and after LVRS. Adapted from reference by Estenne et al (2011)[161]:

Panel (A): This shows the normal pressure-volume relationships of the lung and chest wall. The curves for chest wall compliance (C_W) and lung compliance (C_L) intersect at functional residual capacity (FRC) in the resting state. Also shown are chest wall compliance at maximal inspiration ($C_{W\text{-}MAX}$), total lung capacity (TLC), and residual volume (RV).

Panel (B): Lung compliance (C_L) is displaced upwards in emphysema. Line A represents LVRS in the patient with bullous emphysema where residual volume is addressed, in whom resection would not change lung compliance, Line B illustrates the reduction in lung compliance after resection of diffuse emphysema, Line M reflects the changes to $C_{W\text{-}MAX}$ in the context of post-operative respiratory muscle dysfunction.

Panel (C): The effects of LVRS on maximal elastic recoil (P_{TLC}; double arrowhead) and vital capacity (VC_{PRE} = pre-operative, VC_A=after resection of bullous emphysema, VC_B = after resection of homogeneous emphysema) are shown.

This in turn permits generation of greater elastic recoil pressure at any given lung volume. VC is shown to be the primary determinant of FEV1; improved expiratory flow facilitates lung emptying, leading to reduced static and dynamic hyperinflation[167]. This holds true in patients with high baseline RV/TLC ratios; however, in those less hyperinflated, a higher FEV1/FVC ratio contributed most to an improved post-operative FEV1[168], the reasons for which are speculative and possibly relate to the effects of airway re-tensioning. Line A represents the theoretical effects of LVRS in a patient with bullous disease in whom resection would equate to removal of residual volume and not affect lung compliance and has been modelled on the patient with heterogeneous emphysema. Line B indicates the effects of LVRS in a patient with homogeneous emphysema in whom resection would be anticipated to decrease lung compliance and RV proportionately, resulting in a less pronounced increase in VC. This is offered as a theoretical explanation for why upper zone predominant heterogeneous emphysema patients experience better surgical outcomes[166], though the predicted benefit is small.

This model provides insight into the effects of LVRS on the lung and chest wall relationship and particularly, the frequently observed rise in vital capacity. However, it has a number of limitations as argued by Estenne et al (2011) for example, it assumes FEV1/FVC does not change, it does not take into account the potential contribution of recruited decompressed lung to overall lung compliance, and oversimplifies non-linear pressure-volume relationships which may be modified post-surgery[161]. Nonetheless, it helps to contextualise what is likely to be a complex interplay of factors accounting for the restorative nature of LVRS to expiratory airflow.

Respiratory muscle function

LVRS improves inspiratory muscle function[169-171], notably that of the diaphragm, restoring the pathologically flattened structure toward its normal high domed configuration. The peripheral muscular part in the emphysematous chest is misaligned from the vertical to the horizontal. Inspiratory effort makes little impression in the vertical axis. Instead misdirected inward traction on the lower ribs results in a paradoxical or ‘asynchronous’ movement of the chest wall tending to reduced size of the thoracic cavity[172]. Re-apposition of the muscular diaphragm to the chest wall

corrects its orientation[173]. Reduced elastic loading of the chest wall restores its muscles to their optimal tension/length relationship[174-176]. However, the benefits can be offset by muscle deconditioning following surgery[161].

Gas exchange

Improved gas exchange has been attributed to decompression and restoration of function of relatively preserved lung following surgical resection[177].

Exercise kinetics

LVRS improves maximal oxygen consumption, minute ventilation and dead space-to-tidal volume ratio during exercise. Putative explanations include improved elastic recoil and expiratory airflow, recruitable tidal volume and reduced work of the respiratory muscles[178-180].

Bronchoscopic lung volume reduction (BLVR)

A growing body of research supports the various mechanistic actions thought to underpin LVRS. However, the hazards inherent in surgery in a high-risk population[159, 181, 182] have prompted the parallel development of minimally invasive bronchoscopic lung volume reduction (BLVR) techniques, which it is anticipated will reproduce the benefits of surgery and widen the eligibility for LVR.

Unidirectional valves

Deflation of the emphysematous lung is achieved with one-way valves in the bronchi of the most severely diseased lobe(s) to limit the entry but permit unimpeded expulsion of air and mucus. Typically, three to five are implanted per lobe. They are intended to be permanent but can if necessary be revised or removed. As might be anticipated, absence of collateral interlobar ventilation is an essential requisite in the selection of patients.

Currently four implantable devices have been developed for market: The Zephyr® Endobronchial Valve (EBV) by Pulmonx, the Spiration® Valve System (SVS, formerly known as the Intrabronchial Valve, or

IBV) by Olympus, the MedLung® Endobronchial Valve (EbV), and the Endobronchial Miyazawa Valve (EMV). The EBV and SVS valves are the main contenders - for the purpose of this thesis, we will focus on the EBV. (Figure 1.9). A silicone skin duckbill occludes the airway during inspiration, opens it in expiration, to induce lobar atelectasis. Its self-customising nitinol frame, like an expanding stent, adapts during deployment to its airway.

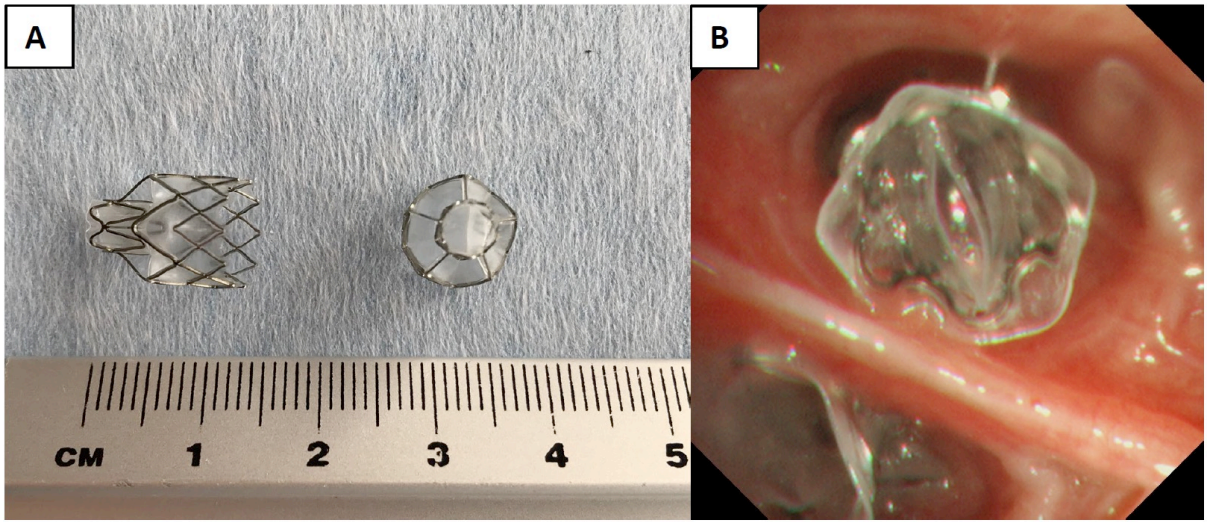

Figure 1.9. Zephyr® Endobronchial Valve

The Endobronchial Valve (EBV) by Pulmonx is available in four sizes: 4.0, 4.0 LP (low profile, to accommodate shorter length airways), 5.0 (A), and 5.0 LP. EBVs implanted in the left lower lobe of a patient with severe emphysema and hyperinflation. The duckbill mechanism is closed during inspiration and open in expiration (B).

Since the first in-human pilot study by Toma et al[183], there have been six published randomised controlled trials evaluating this device, which has now been approved by the United Kingdom's National Institute for Health and Care Excellence (NICE) and the United States' Food and Drug Administration (FDA) as a standard of care for appropriately selected individuals with severe emphysema and hyperinflation. (Tables 1.1 and 1.2).

Clinical evidence

VENT, 2010, a multicentre randomised controlled trial (RCT), the first, compared unilateral lobar EBV treatment to optimised conventional care in patients with severe heterogeneous emphysema (semi-quantitatively assessed using a Likert scale) and hyperinflation[184]. The co-primary efficacy

endpoints were the differences between the changes in FEV1 and in six-minute walk distance (6MWD) in the two groups at six months. The primary safety endpoint was the difference in rates of a composite score of six major complications at 6 months: death, empyema, massive haemoptysis, pneumonia distal to the valves, persistent air leak of more than 7 days duration, and ventilator-dependent respiratory failure for more than 24 hours. The US arm randomised 321 patients in a 2:1 ratio: 220, EBV, and 101, SoC. At six months, EBV treatment resulted in a very small change in residual volume, -1.29%, reflected in modest improvements in FEV1 of 6.8% (95% CI, 2.1 to 11.5; p=0.005), six-minute walk distance of 5.8% (95% CI, 0.5 to 11.2; p=0.04) equivalent to 19.1 meters, and SGRQ total score of -3.4 (95% CI, -6.7 to 0.2; p=0.04). The between-group difference in the composite rate of major complications was 4.9% (95% CI, 1.0 to 8.8), below the pre-specified safety threshold of 30%. Of the EBV group, 16 (7.5%) experienced an implant-related event (expectoration, aspiration, or migration) and 31 (14.1%) underwent valve removal because of adverse events or in response to the subject's request. Important serious adverse events from early (within 90 days) and late windows (3 to 12 months), included pneumonia distal to the valve (0.9% and 3.3%), pneumothorax (4.2% and 1.0%), haemoptysis (5.6% and 6.1%), and exacerbations of COPD requiring hospitalisation (7.9%, EBV, versus 1.1%, SoC (p=0.03) and 10.3%, EBV, versus 9.2%, SoC (p=0.84)). At 12 months, the all cause death rate was 3.7% in the EBV group and 3.5% in the controls (log rank p=0.88). The European arm of 171 patients lacked power to achieve statistical significance[185] – intriguingly, the data suggested benefits not only in heterogeneous but also in homogeneous disease. Post-hoc analyses of the results of USA and of European cohorts demonstrated individuals with CT evidence of fissure integrity (determined by visualisation as 90% or more complete), a surrogate for absent interlobar collateral ventilation, experience much better clinical outcomes[184, 185].

BeLieVeR HIFi, 2015, was a small single centre, double-blind, sham-controlled study of patients with severe heterogeneous emphysema and intact lobar boundaries, a proxy for freedom from collateral ventilation, assessed visually with CT and with the Chartis system employing an inflatable balloon to simulate EBVs in situ and assessing expiratory airflow, but no subject was excluded on the basis of a

failed Chartis test alone[186]. 50 patients were randomised in a 1:1 assignment. The primary endpoint, percentage change in FEV1 at 3 months, was improved by 24.8% for EBV recipients compared with 3.9% for subjects in the sham group (between-group difference of 20.9%; p=0.033). Four patients were collateral ventilation positive on Chartis evaluation and their omission from the analysis improved responder rates to EBV treatment. At 90 days, the most common adverse event was exacerbation of COPD but with similar incidence in both groups: five EBV recipients, however, required hospitalisation compared to three in the control group. Four of the EBV group expectorated a valve (16%), two required valve removal (8%), two developed pneumonia (8%), two, pneumothoraces (8%), and two died from respiratory complications (8%). Combination of efficacy data from the original treatment arm with those in the control group who went on to receive open-label EBV treatment who were confirmed CV negative on Chartis (n=31) demonstrated clinically meaningful improvements across all domains at 3 months: FEV1 +27.3 ± 36.4% (p<0.001), residual volume -0.49 ± 0.76L (p=0.007), 6MWD +32.6 ± 68.7 meters (p=0.01) and SGRQ total score -8.5 ± 20.2 points(p=0.05)[187]. In this series, the incidence of pneumothoraces, considered a marker of procedural effectiveness, was 10.3%, higher than in VENT.

STELVIO, 2015, was a single centre, RCT of patients without collateral ventilation confirmed using the Chartis system[188]. 68 patients with heterogeneous and homogeneous emphysema (visually assessed on CT) were randomised in a 1:1 assignment. The co-primary endpoints, improvements in FEV1, FVC and 6MWD at six months, were significantly greater in the EBV group compared to controls: FEV1 20.9% versus 3.1%, FVC 18.3% versus 4.0%, and 19.6 meters versus -3.6 meters (all $p < 0.01$), respectively. This was accompanied by clinically meaningful improvement in RV of -856 ml, target lobar volume reduction (TLVR) of 1366 ml and SGRQ of -14.7 points. The effects tended to be larger in those with heterogeneous emphysema. No valves were expectorated but seven patients underwent removal on account of adverse events (21%). The trial protocol permitted a repeat bronchoscopy to replace valves that had for example migrated and this was undertaken in 4 (12%). Over six months,

there were 22 respiratory-related SAEs in the EBV group (three in the SoC arm): six pneumothoraces (18%), four COPD exacerbations (12%), one pneumonia distal to the valve (3%), and one death (3%).

For these results to be generalisable, larger studies have been undertaken. TRANSFORM, 2017, was a multicentre 2:1 RCT of patients with heterogeneous emphysema (defined as ≥10% difference in destruction scores between target and adjoining lobe) and no collateral ventilation[189]. Target lobe occlusion and volume reduction were assessed with HRCT at 45 days. Valve revision was undertaken if occlusion was incomplete or TLVR <50%. The primary endpoint was the achievement of ≥12% improvement in FEV1 over that of the SoC group at 3 months. 97 patients were randomised to EBV (n=65) and SoC (n=32). 55.4% of EBV versus 6.5% of SoC subjects reached the primary endpoint ($p<0.001$), an achievement durable to 6 months and accompanied by clinically meaningful benefits in RV -670ml, 6MWD +78.7 and SGRQ total score -6.5 favouring the EBV arm. One subject expectorated a valve and seven underwent permanent valve removal. Over 6 months, there were 44 respiratory-related SAEs in 31 EBV subjects (47.7%) compared to four events in three (9.4%) SoC subjects, the majority occurring ≤30 days of the procedure. These included COPD exacerbation (48.8%, EBV, versus 36.1%, SoC), pneumothorax (30.3% EBV), dyspnoea (32.4% versus 3.1%), and pneumonia (12.1% versus 3.1%). One patient died from an in-hospital cardiac arrest complicating pneumothorax.

LIBERATE, 2018, was a large multicentre 2:1 RCT to evaluate the effectiveness and safety of the EBV in patients with heterogeneous emphysema (defined as ≥15% difference in destruction scores between target and adjoining lobe) and no collateral ventilation (in Chartis tests) out to 12 months[190]. The innovative trial design incorporated pre- and post-procedure pulmonary rehabilitation to ensure any treatment gains were capitalised on and maintained, in addition to a revision procedure at day 45 in the event of <50% TLVR or incomplete lobar occlusion. The controls also underwent repeated pulmonary rehabilitation. The primary endpoint was the achievement of ≥15% improvement in FEV1 at 12 months. 190 patients were randomised to EBV (n=128) or SoC (n=62). At 12 months, 47.7% of EBV versus 16.8% of SoC subjects achieved primary endpoint with a

between group difference of 31.0% (95% CI, 18.0 to 43.9%; p<0.001). There were significantly more EBV responders than SOC for secondary outcomes including: RV ≥-310ml (61.6% versus 22.4%), 6MWD ≥25m (41.8% versus 19.6%), and SGRQ total score ≥-4 points (56.2% versus 30.2%). Importantly, 79.1% of EBV recipients achieved the MCID for TLVR at 45 days and 84.2% at 12 months (mean TLVR of 1.14L), corresponding to a mean RV reduction of 0.5L and confirming the principal mechanical action of valves. The LIBERATE trial also confirmed the suitability of EBVs for both upper and lower lobe disease with 45.9% upper lobe treated subjects and 57.1% lower lobe treated subjects achieving a ≥15% improvement in FEV1. Two of the EBV subjects expectorated a valve and 28 secondary procedures involving valve removal and/or replacement were required for adverse events. During the treatment period (≤45 days), 35.2% of EBV subjects compared to 4.8% of SoC subjects experienced respiratory-related SAEs, the majority pneumothoraces (26.6%, EBV) and COPD exacerbation (7.8% versus 4.8%). In the longer term (>46 days to 12 months), 33.6% of EBV recipients and 30.6% of SoC subjects experienced one or more respiratory SAEs. Interestingly, there was a lower frequency of SAEs (COPD exacerbations, pneumonias, and respiratory failure) in the EBV compared with the SoC group (23.0% versus 30.6%, 5.7% versus 8.1%, and 0.8% versus 3.2%, respectively), and although none of these differences reached statistical significance, it suggested the potential beneficial impact of this treatment on other important clinical outcomes. At 12 months, there were 5 deaths in the EBV group (3 pneumothoraces, 1 COPD exacerbation and 1 respiratory failure) and 1 death in the control group (cardiac arrhythmia).

The distribution of emphysema in patients enrolled in early clinical studies of the EBV was reported to be predominantly heterogeneous, although the definition varied across studies. Post-hoc analyses of the European cohort of VENT and of STELVIO comparing the outcomes of their patients with homogeneous disease with those whose emphysema was heterogeneous suggested a lesser benefit. A prospective multicentre RCT, IMPACT, 2016, set out to formally test the safety and efficacy of valves in subjects with homogeneous emphysema[191]. Consensus on the distinction lacking, the authors defined their homogeneous subjects as those in whom the difference between the emphysematous

destruction scores for the target lobe and its ipsilateral companion was <15% and the difference between right and left lungs' perfusion scintigraphy, <20%. Collateral ventilation was excluded with Chartis. The primary endpoint was the change in FEV1 at 3months. 93 subjects were randomised to EBV (n=43) and SoC arms (n=50). At 3 months, FEV1 improved by 13.7 ± 28.2% in the EBV group and fell by -3.2 ± 13.0% in the SoC group (mean between group difference, 17.0%; p=0.0002). This was accompanied by an RV reduction of 0.42L in the EBV arm. There were significantly more responders in the EBV group compared to SoC for secondary outcomes including reduction in RV ≥-430ml (44.2% versus 18.0%; p=0.006), improvement in 6MWD ≥26m (50% versus 14%; p=0.0002) and SGRQ ≥-4 points (56.8% versus 25%; p=0.003). One participant expectorated a valve and five required removal / replacement of 1 or more valves. Over 3 months, respiratory-related SAEs occurred in 44.2% of the EBV group and in 12% of the SoC group including pneumothorax (25.6%, EBV) and COPD exacerbation requiring hospitalisation (16.3% versus 12.0%). One death from nosocomial pneumonia occurred in the SOC group.

Focusing on four of the RCTs using the Chartis system for trial inclusion, Hartman et al estimated between-group differences in FEV1 of 17-29%, RV of -522 to -831mls, 6MWD of 39-79m and SGRQ of -6.5 to -14.7 points in favour of the EBV over a 12-month period[192]. However, 19-35% of patients required a second bronchoscopy for revision or replacement of valves. There was an 18-34% risk of pneumothorax, most occurring within 72 hours[193, 194], illustrating the importance of in-hospital surveillance for this complication over at least 3 days post-procedure[195]. (Figure 1.10). Intercostal drainage sufficed in the majority of cases – however a persistent air leak may require one or more valves to be (temporarily) removed and the reader is directed to dedicated guidelines[196]. Pneumothorax, often considered a sign of technical success, does not appear to affect long term outcomes including survival[197].

Longer term data are limited. In a series of 256 patients whose absent CV was determined radiologically or using Chartis, 3-years responder rates for improved FEV1 > 100ml, reduced RV >-430ml and increased 6MWD > 26m were relatively high at 10%, 79% and 53%, respectively[198].

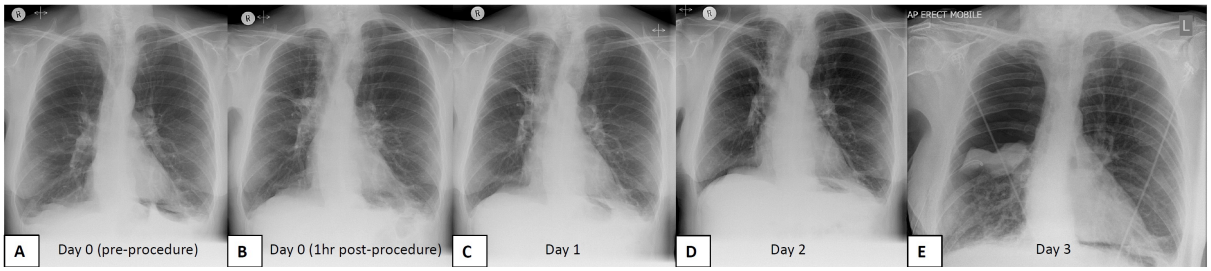

Figure 1.10. Endobronchial valve implantation and pneumothorax.

Right upper lobe endobronchial valve (EBV) implantation resulting in progressive lobar atelectasis and pneumothorax on day three post-procedure. Pre-procedure chest x-ray demonstrating hyperinflated lungs (A). Progressive volume reduction after insertion of three EBVs (B-D). Large pneumothorax complicating complete right upper lobe atelectasis necessitating insertion of a drain(E). *hr* = hour. Procedures performed by JLG.

EBV treatment has a favourable incremental cost-effectiveness ratio (ICER) of approximately $43,000 per QALY at 5 years and $23,000 per QALY at 10 years[199, 200]. In line with this, the LIBERATE trial suggested reduced healthcare burden with a lower frequency of COPD exacerbations requiring hospitalisation in the longer term[190]. A significant survival benefit has also been shown in those who achieve EBV-induced lobar atelectasis: 5-year survival of 65.3% (43.9%, no atelectasis; p=0.009) among 449 patients[197], and even out to 10-years in a small retrospective cohort of 19 patients[201].

RCT data supporting use of the EBV is robust. Chartis evaluation under general anaesthesia appears superior to that under sedation[202].

	VENT (US)	BELIEVER	STELVIO	TRANSFORM	LIBERATE	IMPACT
Device	EBV	EBV	EBV	EBV	EBV	EBV
Age, years	65	63	58	65	64	64
FEV1, %	30	32	29	30	28	28
RV, %	216	232	216	250	225	277
6MWD, meters	334	338	372	282	311	308
SGRQ, points	–	69†	59	64	55	63
Emphysema distribution	Hetero/Homo	Hetero/Homo	Hetero/Homo	Hetero	Hetero	Homo

FEV1, Forced Expiratory Volume in 1 second; Hetero, Heterogeneous; Homo, Homogeneous; RV, Residual Volume; SGRQ, St George's Respiratory Questionnaire; US, United States; 6MWD, Six-minute walk distance. †SGRQ-C questionnaire used.

Note - demographics pertain to treated group only.

Table 1.1. Baseline characteristics of the unidirectional valve RCTs.

Study	Device	Patients treated, *n*	Follow-up, months	ΔFEV1, ml	ΔRV, ml	Δ6MWD, meters	ΔSGRQ, points
VENT	EBV	220	12	60*	–	19*	-3.4*
BELIEVER	EBV	25	3	160	-370	33	-5.1†
STELVIO	EBV	34	6	191	-831	106	-14.7
TRANSFORM	EBV	65	6	230	-670	79	-6.5
LIBERATE	EBV	128	12	106	-522	39	-7.1
IMPACT	EBV	43	3	120	-480	40	-9.6

FEV1, Forced Expiratory Volume in 1 second; ml, millilitre; RV, Residual Volume; SGRQ, St George's Respiratory Questionnaire; 6MWD, Six-minute walk distance.

Δ between-group difference (i.e. intervention minus control) used. †SGRQ-C questionnaire used. *6-month data shown.

Table 1.2. Results of the unidirectional valve RCTs.

Endobronchial coils

Lung volume reduction coils (LVRCs) were introduced in 2008, an alternative to EBVs, particularly in the treatment of patients with hyperinflated emphysema complicated by collateral ventilation, a contraindication for valves[203]. Made of memory-shape nitinol they are inserted into the subsegmental airways in an extended configuration, and released from their introducer, assume a pre-determined form of a two-turn coil pulling in the surrounding tissues. (Figure 1.11). Typically, about a dozen coils are implanted in each lobe in a fan-shaped distribution within the middle third of the lung[204]. Symmetrical emplacement of coils in the contralateral lung is delayed 4 to 8 weeks to minimise risk of bilateral pneumothoraces. In addition to the mechanical effects of volume reduction, endobronchial coils are speculated to work by increasing elastic recoil and re-tensioning the airway network facilitating expiratory flow and gas emptying[205]. There have been three RCTs to date. (Tables 1.3 and 1.4).

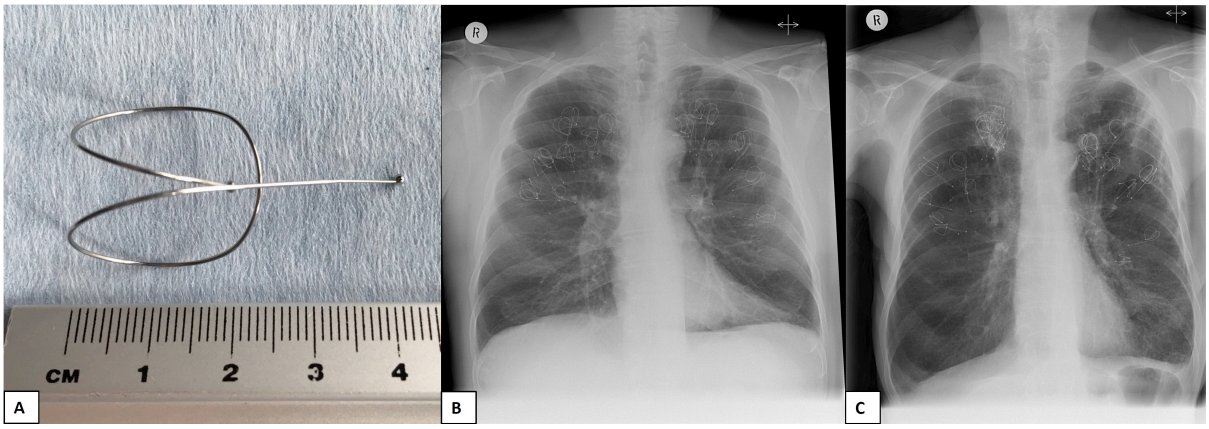

Figure 1.11. Lung volume reduction coil (LVRC) by PneumRx®, BTG.

Available in three sizes: 100mm, 125mm and 150mm (A). Bilateral sequential coil implantation to upper lobes (B). Bilateral sequential coil implantation to upper lobes with coil-associated opacity (C). Procedures performed by JLG, SVK, and PLS.

	RESET	REVOLENS	RENEW
Age, years	62	62	63
FEV1, %	27	26	26
RV, %	236	271	246
6MWD, meters	294	300	312
SGRQ, points	65	61	60
Emphysema distribution	Hetero/Homo	Hetero/Homo	Hetero/Homo

FEV1, Forced Expiratory Volume in 1 second; Hetero, Heterogeneous; Homo, Homogeneous; RV, Residual Volume; SGRQ, St George's Respiratory Questionnaire; 6MWD, Six-minute walk distance.

Note - demographics pertain to treated group only.

Table 1.3. Baseline characteristics of the endobronchial coil RCTs.

Study	Patients treated, *n*	Follow-up, months	ΔFEV1, ml	ΔRV, ml	Δ6MWD, meters	ΔSGRQ, points
RESET	23	3	–	-310	64	-8.4
REVOLENS	50	12	80	-360	21	-10.6
RENEW	158	12	70	-310	14.6	-8.9

FEV1, Forced Expiratory Volume in 1 second; ml, millilitre; RV, Residual Volume; SGRQ, St George's Respiratory Questionnaire; 6MWD, Six-minute walk distance. Δ between-group difference (i.e. intervention minus control) used.

Table 1.4. Results of the endobronchial coil RCTs.

Clinical evidence

RESET, 2013, following on from the promising results of several small single centre studies [203, 206], was a multicentre RCT of 47 patients with severe emphysema (heterogeneous and homogeneous determined using a semiquantitative visual assessment) and hyperinflation comparing LVRC therapy (n=23) to SoC (n=24)[207]. LVRCs were implanted in one or two lobes in each lung in sequential

procedures. At 90 days the changes in the SGRQ scores for the coil recipients was -8.11, the SoC +0.25. The between group difference, the primary endpoint, -8.36 (p=0.04) exceeded the MCID. This was accompanied by clinically meaningful improvements in RV -0.51 (-0.20, SoC; p=0.03) and FEV1 +14.19% (+3.57%; p=0.03) favouring the coil group. In the early post-operative period of each treatment (<30 days), six SAEs were reported in the LVRC group (two pneumothoraces, two exacerbations, and two lower respiratory tract infections, LRTIs) compared to one in the SoC group (COPD exacerbation). From days 30 to 90, three SAEs occurred in each arm (exacerbations and LRTIs). The benefits were also experienced by subjects who crossed over and received open label treatment with an acceptable safety profile and durability to 12 months[208].

REVOLENS, 2016, was a RCT of 100 patients with severe emphysema (heterogeneous and homogeneous using a semiquantitative visual assessment) and hyperinflation comparing LVRC therapy (n=50) to SoC (n=50)[209]. Recruitment was extended to patients with greater disability than those in RESET for example, 6MWD <140 meters, DLCO <20%, and α-1 antitrypsin deficiency and set a higher MCID for the primary endpoint. LVRCs were implanted in one lobe of each lung in staggered procedures. The primary endpoint was an improvement in 6MWD of ≥54m at 6 months and was achieved by 18 LVRC (36%) and 9 SoC (18%) patients (p=0.03). At 12 months, clinically meaningful reductions in RV (-0.52, LVRC, versus -0.15 SoC; p=0.01) and SGRQ (-11.1, LVRC, versus +2.3, SoC; p<0.001) were observed, though not in 6MWD. The latter may have been affected by performing the six-minute walk test (6MWT) on room air – approximately 60% of patients at baseline were requiring home oxygen. Important respiratory SAEs included COPD exacerbation (26%, LVRC, versus 22%, SoC; p=0.64), pneumonia (18%, LVRC, versus 4%, SoC; p=0.03), and pneumothorax (6%, LVRC, versus 2%, SoC; p=0.62). Death rates were similar (8%, LVRC, versus 6%, SoC; p=0.99). 2-year follow-up confirms durable benefits in volume reduction, quality of life, and safety profile[210].

RENEW, 2016, is the largest multicentre, randomised controlled, assessor-blinded, study of 315 patients with severe emphysema (heterogeneous and homogeneous using a semiquantitative visual

assessment) and hyperinflation comparing bilobar coil implantation (n=158) to SoC (n-157)[211]. LVRCs were implanted in one lobe of each lung in sequential operations. During the trial recruitment was extended to patients whose hyperinflation, an RV of 175%, was short of the initial 225% threshold. The 12-month primary endpoints were change from baseline in 6MWD and the proportion of patients experiencing at least 1 of 7 prespecified major complications (death, pneumothorax requiring chest tube drainage >7 days, haemoptysis requiring inpatient intervention, COPD exacerbation requiring hospitalisation, chest infection requiring hospitalisation, respiratory failure requiring ventilatory support, and second bronchoscopy to remove one or more coils for a device-related adverse event). At 12-months, modest improvements in 6MWD (10.3 meters, LVRC, versus -7.6 meters, SoC; p=0.02), RV (-410ml, LVRC, versus -100ml, SoC; p=0.001) and FEV1 (3.8%, LVRC, versus -2.5%, SoC; p<0.001) favouring LVRCs were observed. Reduction in SGRQ total score, however, was clinically meaningful in LVRC recipients (-8.1, LVRC, versus 0.8, SoC; p<0.001). Post-hoc analysis identified a subgroup of patients who were super-hyperinflated (RV ≥225%) with heterogeneous emphysema experiencing superior clinical outcomes (6MWD of +29.1m, FEV1 of +12.3%, and SGRQ of -10.1 points). Additional predictors of response include fewer than 4 co-morbidities, target lobe emphysema score >20% low attenuation area (LAA) and absence of airway disease[212], and the development of coil-associated opacity (CAO), a non-infectious localised inflammatory response to the implanted device(s). (figure 11). In fact, more than a third of patients initially suspected of developing pneumonia were reclassified as CAO[211]. Major complications arising in 34.8% of LVRC recipients compared to 19.1% of SoC (p=0.002) were mainly increased frequency of lower respiratory tract infections (18.7%, LVRC, versus 4.5%, SoC; p<0.001). Other serious adverse events included pneumonia (20%, LVRC, versus 4.5%, SoC; p<0.001) and pneumothorax (9.7%, LVRC, versus 0.6%, SoC; p<0.001). Death rates were similar (6.5%, LVRC, versus 5.1%, SoC; p=0.64).

Comparison of the three studies must be approached with caution. Recruitment criteria and targets were not identical, and coils of different sizes were used. Nevertheless, the data are generally

supportive of a role for coils in significantly hyperinflated individuals (RV>200%), inclusive of the homogeneous and heterogeneous emphysematous subtypes with and without collateral ventilation.

Health economic analysis from the REVOLENS trial estimated the 12-month cost of LVRC treatment at $53,151 with a 3-year modelled incremental cost-effectiveness ratio (ICER) of €300,000 / QALY[209]. Longer term data are limited. Three-year survival of 84% has been reported for participants in pilot studies[213]. In accord with a recent meta-analysis[214], we have observed a substantial 5-year survival benefit for patients enrolled in RESET who achieved ≥10% reduction in RV at 3 months after completion of treatment[215].

Patient selection is crucial given the expense, complexity, and irreversible nature of this intervention. Non-invasive quantitative CT analysis looks promising for this purpose[216].

Evaluating the impact of lung volume reduction on lung structure, function, and inflammation

There is a paucity of data on the effects of volume reduction (LVR) on lung morphology, function and inflammation, particularly pertaining to the small airways, which are of interest since they are believed to be the initial site of disease pathogenesis. The tools and techniques currently available for exploring these domains in greater depth are reviewed below.

Lung structure

Computed tomography (CT)

CT imaging permits non-invasive evaluation of the structure of the lung, which can be isolated into airway, parenchyma and vascular compartments, the regions of interest that are affected pathologically[80].

Airways

The tracheobronchial tree can be segmented to the level of the small airways with an internal diameter of 2mm, the limit of resolution. However, a surrogate index of changes in the smaller airways is derived by comparing density thresholds of voxels[8] in images made in inspiration and in expiration (see below).

Parenchyma

In addition to calculation of lobar volumes, the lung fields can be examined for 1) the parenchymal destruction of emphysema (on inspiration) and 2) air trapping (on expiration), a proxy for airflow limitation.

The sum of areas of low attenuation (≤ -950 Hounsfield units[9]) on the slices made in inspiration, expressed as a percentage of the whole ($\%LAA_{-950insp}$), correlates well with pathological emphysema[217, 218]: That in expiration (≤ -856 Hounsfield units[10], $\%LAA_{-856exp}$) with obstruction of conductive airways measured with conventional spirometry[219].

The attenuation in air trapping images however does not distinguish and exclude attenuation due to emphysema. Capture of the contribution made by the small airways alone, those less than 2mm internal diameter, is subject to the limitations of the current systems' spatial resolution and the increased radiation dose requirement. A solution is to be found in co-registering CT density maps made in inspiration and in expiration in a system termed *parametric response mapping* (PRM)[220].

PRM identifies three families of voxels representing normal lung (voxels above -950insp and -856exp), emphysema (PRM^{emph}; voxels below -950insp and -856exp) and functional small airways disease (PRM^{fSAD}; voxels above -950insp and below -856exp). (Figure 1.12).

Bhatt et al in a study of 1508 current and former smokers, GOLD stages 1 to 4, showed that PRM^{fSAD} detected in patients with normal spirometry, at 5 year follow-up was associated with a decline in FEV1,

[8] Voxel, a portmanteau of 'volume' and 'pixel', represents a discrete unit of a three-dimensional matrix.

[9] The Hounsfield Unit (HU), named after the Nobel prize-winning British physicist Godfrey Hounsfield, is a measurement of radiodensity: Water has a value of zero, air -1000 HU, and bone +1000 HU.

[10] -856 HU is the mean attenuation of normally inflated lung (≈6ml per gram), which is higher on expiration.

that the rate of decline was greatest in mild to moderate disease and suggested the findings may precede the development of emphysema[95]. Labaki et al in a similar study of 725 participants GOLD stages 0 to 4 were in agreement[221] and aligned with Hogg's micro-CT findings[222]. Pompe et al observed PRM^{fSAD} correlates with a number of relevant clinical and functional outcome measures, notably pack years, BMI, dyspnoea score, lung function (spirometry, plethysmography, gas transfer) and six-minute walk distance[223].

Occhipinti et al reported the relative contributions of emphysematous and of non-emphysematous gas trapping determined by co-registration can also be accurately derived by calculating the density threshold differences of inspiratory and expiratory phase CT scans (r = 0.99) according to the following equation[224]:

$$\%fGT = [\%LAA_{-856exp} - (\%LAA_{-950insp} - 6\%)],$$

where %fGT is the percentage of functional gas trapping pertaining to the small airways (equivalent to PRM^{fSAD}). This offer a reliable alternative to PRM analysis which can be achieved at no additional cost using readily measurable density thresholds.

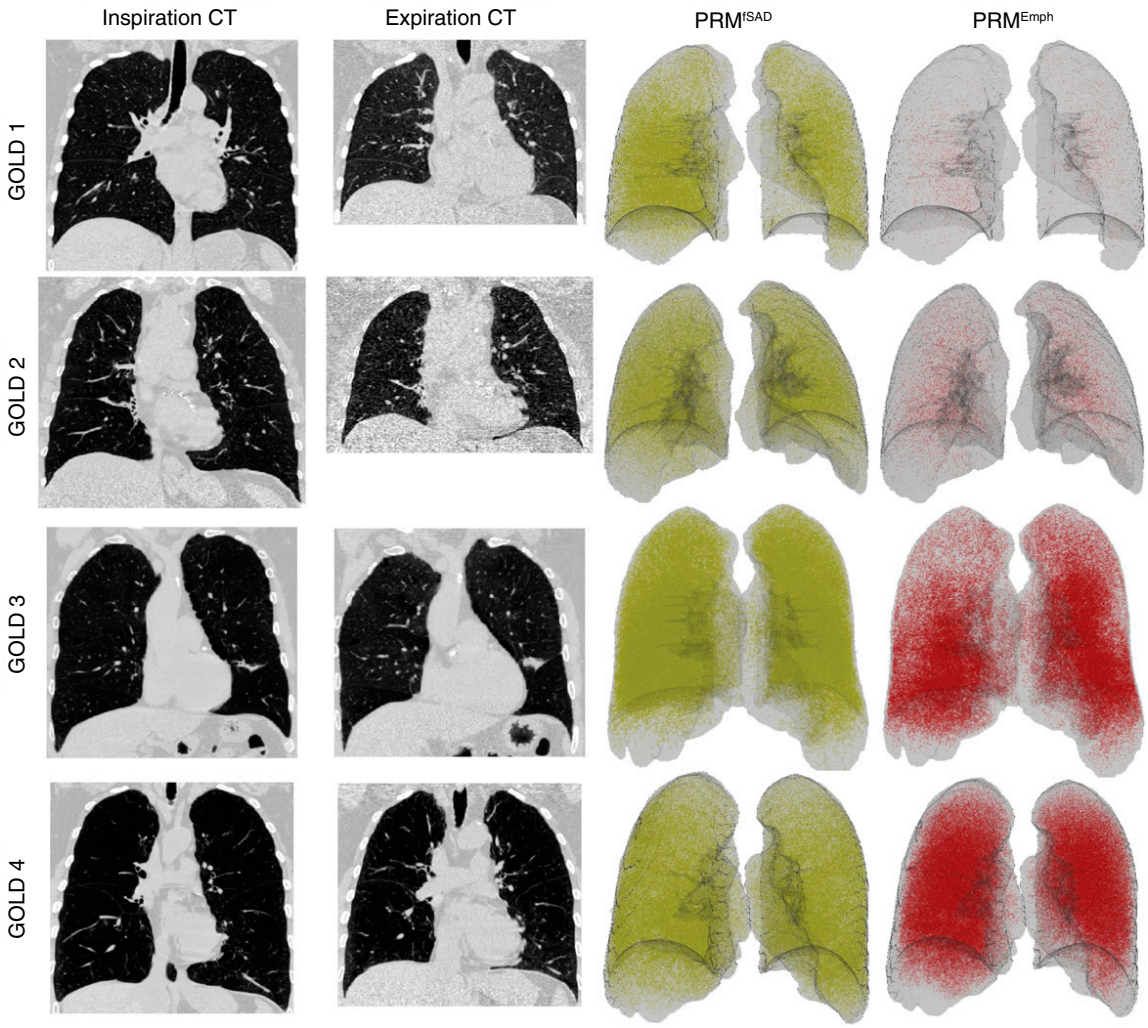

	PRM Normal (%)	PRM Functional Small Airways Disease (%)	PRM Emphysema (%)
GOLD 1	78.8	18.5	0.8
GOLD 2	44.9	41.6	7.0
GOLD 3	28.8	40.8	25.1
GOLD 4	21.8	26.9	43.2

Figure 1.12. Parametric Response Mapping (PRM) images of COPD.

Graded from GOLD Stage 1 to 4. Inspiratory and expiratory computed tomography (CT) images, respectively, are shown on the left. PRM emphysema (PRM^{emph}) voxels in red and PRM functional small airways (PRM^{fSAD}) voxels in yellow are shown on the right. Greater colour intensity indicates more voxels classified in each category. Adapted from[95].

Vasculature

The pulmonary artery to aorta ratio can be measured as a surrogate measure for pulmonary hypertension[225]. Intra-pulmonary vasculature can also be segmented to the level of the small vessels (defined as those with an internal diameter of 2mm)[226].

Lung function

Spirometry

A widely used objective and reproducible method of assessing the severity and monitoring the progress of airflow limitation. The volume of air forcibly exhaled from maximal inspiration (forced vital capacity, FVC) and the volume expelled during the first second of the manoeuvre (forced expiratory volume in 1 second, FEV1) yield a ratio (FEV1/FVC). Measurements are compared to reference ranges for example, the European Community of Coal and Steel (ECCS), based on race, age, sex, and height[227].

It is crucially dependant on patient cooperation, particularly challenging for the hyperinflated, necessitating an experienced operator to ensure validity[228]. FEV1 correlates poorly to quality of life[229, 230] and exercise capacity [231], but is helpful monitoring progress and establishing prognosis in COPD. It is however, an insensitive tool for examining small airways disease[232-234] which, in health, contribute only 25% of the total airways resistance[235]. Pathology of the small airways is the principal cause of obstruction of COPD and precedes the development of emphysema[236]. A considerable burden of disease is accrued before a significant effect on spirometry is likely to be observed[20]. The maximum mid-expiratory flow between 25% and 75% of FVC (MEF25-75%) is considered more sensitive for small airways disease than FEV1[237, 238], particularly when corrected for FVC (MEF25-75%/FVC)[239]. Computer quantification of the inflection point or ‘angle of collapse’ on the expiratory flow loop has also been shown to correlate better to the presence of emphysema than FEV1[240].

Body plethysmography

Body plethysmography accurately measures lung volumes with higher values of functional residual capacity (FRC), residual volume (RV) and total lung capacity (TLC) indicative of hyperinflation[4], a crude surrogate for the presence of small airways disease.

Body plethysmography can also be used to determine airways resistance (R_{AW}) and its reciprocal, airways conductance (G_{AW}). Specific values, sR_{AW} and sG_{AW}, are derived from the figures corrected for thoracic gas volume[241]. Though more sensitive than FEV1, they too fail to distinguish sites of obstruction[241].

Gas transfer

Gas transfer is a test of the integrity of the alveolar-capillary interface and correlates with the severity of tissue destruction in emphysema[242]. A lower baseline value is associated with more rapid progression of emphysema and lung function decline[243].

Gas exchange

Gas exchange is impaired with the development of hypoxaemia and hypercapnia that is compounded by the ventilatory mechanical constraints of hyperinflation[244].

Impulse oscillometry

Impedance oscillometry, introduced in 1956[245], is a non-invasive test which, independent of patient effort, utilizes the fluctuating pressure/flow responses to sound waves imposed on tidal flow to extract information on airways mechanics especially those of the smaller airways. It is a modification of the original forced oscillation technique which examined individual wave frequencies sequentially. The less time consuming impulse method uses a mix of frequencies from 5 to 30Hz emitted from a loudspeaker in a single burst[246]. Low frequency waves (5 Hertz, Hz) penetrate the lungs, reach and are reflected from the alveoli, and inform on the entire airway. High frequency transmissions (20 Hertz) are reflected from the large airways: Beyond, they are damped. The performance of the small airways can be deduced. A Fourier transformation mathematical device is used in the analysis of the reflected waveforms and the flow responses to determine impedance, the sum of resistance (R) and of reactance (X)[247]. Total airways resistance is measured at 5Hz, large airways at 20Hz. Small airways resistance is inferred (R5-R20). Resistance (strictly impedance) becomes *frequency dependent* with a pronounced increase in the lower range, which is characteristic of small airways obstruction[246].

Reactance (X) is a composite of airway elasticity (capacitance) and inertia of the airway column, and at low frequency (5Hz), yields important information about the small airways which have a high capacitance. Small airways obstruction increases the reactance (which at low frequency, X5, is numerically negative) as impulses are unable to pass the obstruction and the less compliant overall are the airways (this is conceptually distinct from the compliance of the lung parenchyma, which is increased in emphysema)[246].

The resonant frequency, Fres, when reactance equals zero (i.e. capacitance and inertial forces are equal and opposite), is higher in obstructive airways disease. The reactance area (AX) corresponds to the integrated area between 5Hz and Fres and is an index of small airways obstruction[246].

IOS findings in COPD correlate well with those of traditional/conventional diagnostics[248, 249] but IOS is more sensitive to the changes of early disease[250]. Both R5 and R5-R20 are higher in COPD and correlate with increasing GOLD stage classification[251-253]. R5-20 significantly correlates with symptom scores [251, 254] and FEV1[253]. Fres progressively increases and X5 decreases across the disease spectrum [251, 253] and within-breath analysis shows expiration generates a more negative reactance[255, 256]. Both Fres and reactance increase with airflow obstruction and hyperinflation in COPD[246]. X5 may be more discriminatory than resistance parameters in diagnosing COPD[248] and relates well to health status[254]. Furthermore, IOS can be used to evaluate inhaled drug efficacy[257, 258] and monitor recovery from an exacerbation[150].

Inert gas washout

Washout tests employ an inert gas, resident or inhaled (e.g. nitrogen, 4% sulphur hexafluoride, or helium), to explore the anatomy, for example large and small airways, and pathology of the lungs. The more commonly used include single and multiple-breath nitrogen washout tests.

Single breath nitrogen washout (SBNW) was devised by Fowler in 1948 attempting to measure the ‘dead space’, and has evolved into a sophisticated means of identifying ventilation inhomogeneity and location of disease processes[259]. An inhalation of 100% oxygen from RV to TLC brings about a distribution of varied dilutions of the residual nitrogen in the airways, determined by anatomical

location and by pathology, and which influences the exhalant from TLC to RV. Four successive phases are identified in the course of exhalation, expressed in a quasi-sigmoid relationship of nitrogen concentration to expiratory volumes: Phase 1 = exhalation of dead space gas containing negligible nitrogen; Phase 2 = bronchial phase with mixing of dead space and alveolar gas resulting in a rapid rise in expired nitrogen; Phase 3 = alveolar plateau of expired nitrogen rises less steeply due to heterogeneity in ventilation, the gradient of which (SIII) increases in obstructive lung disease; Phase 4 = fast rising phase in which peripheral airway closure redirects gas from the upper zones (containing higher concentrations of nitrogen) resulting in a more rapid rise in expired nitrogen[260, 261]. The expired volume during phase 4 is termed the closing volume (CV), which when added to the RV, gives the closing capacity (CC = CV + RV), the volume remaining in the lungs when the peripheral airways begin to close, and increases in obstructive airways disease. (Figure 1.13).

Using SBNW, SIII correlates significantly with dyspnoea scores, lung function (including FEV1 and diffusion capacity), extent of emphysema and airway neutrophilic inflammation [262-264].

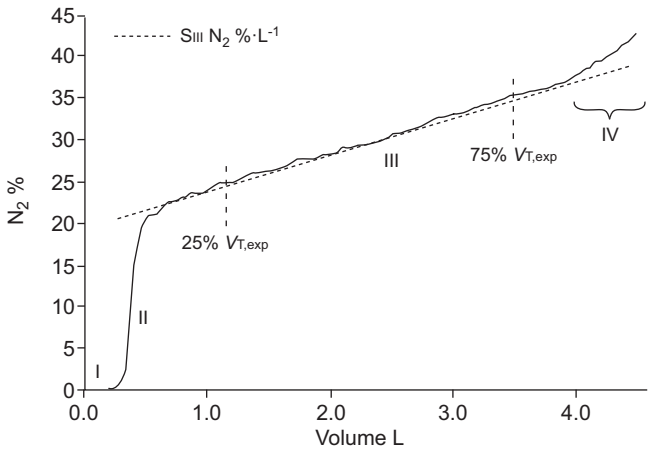

Figure 1.13. A normal single breath nitrogen washout (SBNW) trace.

SIII N_2, slope of alveolar plateau of expired nitrogen (phase 3). $V_{T,exp}$, tidal volume on expiration. Adapted from [261].

Multiple breath nitrogen washout (MBNW), devised by Becklake in 1952[265], involves tidal breathing of 100% oxygen at a fixed volume (typically 1 litre in adults) and rate and recording the number of breaths or turnovers required to reduce the expired end-tidal nitrogen to a 1 in 40 dilution (i.e. from

the atmospheric 80% to approximately 2%) for three successive runs[260, 261]. This seemingly arbitrary threshold is historically determined by the sensitivity of the early analogue analysers and continues to be used[266], though modern analysers will also report a 1 in 16 dilution (5% threshold) cut-off. The resulting washout trace can be used to derive several indices relating to the efficiency of gas mixing termed *ventilation heterogeneity or inhomogeneity*.

The most commonly measured parameter, the lung clearance index (LCI), is calculated by dividing the cumulative expired volume (CEV) by functional residual capacity (FRC):

$$LCI = CEV / FRC.$$

FRC in turn can be determined by dividing the total volume of exhaled nitrogen by the difference in nitrogen concentration between the first and last breaths of the washout:

$$FRC = V_{[Nitrogen]} / C_{start} – C_{end}).$$

Impairment of gas mixing can be estimated by calculating SIII for each breath to derive the relative contributions of the conductive (S_{cond}) and acinar (S_{acin}) airways[267], reflecting convection-dependent (CDI) and diffusion-convection-dependent (DCDI) mechanisms of ventilation inhomogeneity, respectively, an advantage over SBNW.

Using MBNW, S_{cond} and S_{acin} are both elevated in patients with COPD[268]. S_{cond} correlates to FEV1 and specific airways conductance[269], while S_{acin} relates to diffusion capacity[268], lung volumes[270], and CT extent of emphysema[271]. Furthermore, S_{acin} is weakly correlated to impulse oscillometry-derived resistance and reactance[270]. Ventilation inhomogeneity has also been shown to improve in response to Aclidinium[272].

Lung inflammation

It is widely accepted that neutrophilic small airways inflammation underlies the pathogenesis of COPD. In a small non-randomised study of 54 patients with severe emphysema and hyperinflation, LVRS compared to standard of care was shown to decrease inflammatory circulating mediators and this was correlated with the reduction in RV[273], an observation suggesting a mechanistic link between inflammation and mechanical stress[274]. To investigate this phenomenon across different lung volume reduction techniques, candidate biomarkers pertinent to COPD pathogenesis, notably IL-1 beta, IL-6, CXCL-8 (formerly IL-8), and TNF-alpha[275], are measured using enzyme-linked immunosorbent assay (ELISA)[276]. Microvesicles have recently also been identified as biomarkers and mediators of intra-alveolar inflammation in pulmonary disease[126] and are evaluated in parallel. Microvesicles (MVs) stained for cell surface markers pertaining to neutrophil, macrophage, monocyte, platelet, endothelial and epithelial lineages that have been implicated in the development of COPD[277], are quantified using flow cytometry. Paired blood and bronchoalveolar lavage samples are obtained at baseline and three months following intervention and analysed for cytokine and microvesicle content to explore the relationships between systemic and alveolar compartments, respectively.

The biomarker challenge in COPD

A biomarker is defined as “a characteristic that is measured as an indicator of normal biological processes, pathogenic processes or responses to an exposure or intervention”[278]. To date, a robust biomarker for predicting and evaluating the response to lung volume reduction (LVR) interventions remains elusive[279]. Blood and airway-based biomarkers may shed light on the underlying COPD disease process and reveal additional exploitable therapeutic targets for modulating the ongoing inflammation beyond what is currently a very limited and relatively ineffective armamentarium[280].

In this thesis, a variety of novel metrics covering the spectrum of lung morphology, physiology, and inflammation will be evaluated before and after lung volume reduction.

A reduction in residual volume of 10% or greater is used as the outcome measure for a successful procedure and for responder analysis[214]. Such a threshold is tailored to the individual and permits comparison between disparate techniques.

A three month follow-up timepoint is chosen based on precedent, lung volume reduction studies indicating this as ideal for evaluating therapeutic response and for determining the need for additional intervention[195, 281].

Aims

The aims of this thesis are two-fold:

- To explore and compare the influences of lung volume reduction surgery, endobronchial valves and endobronchial coils, on lung structure and function in patients with emphysema and hyperinflation and to identify novel biomarkers to predict and evaluate therapeutic response.
- To evaluate the airway microenvironment: inflammatory cytokine and microvesicle levels, pre- and post-lung volume reduction as possible predictive biomarkers of disease severity and of therapeutic response.

Hypotheses

The hypotheses of this thesis are:

- The response to lung volume reduction achieved by surgical and by bronchoscopic interventions in patients with emphysema and hyperinflation involves changes in small airways structure, function, and inflammation.
- Novel indices of small airways structure, function, and inflammation can be used to predict and evaluate therapeutic response to lung volume reduction procedures.

CHAPTER 2: Methods

This chapter details the measurements made at baseline and 3-months to evaluate the changes in lung structure, function and inflammation in COPD patients after surgical and bronchoscopic lung volume reduction procedures.

Symptom scores

Breathlessness (or dyspnoea) is a complex subjective sensation that is challenging to quantify. Validated techniques based on history using structured questionnaires include the modified MRC scale recording the limitations imposed on activities of daily living and the St George's Respiratory Questionnaire which collects information on health-related quality of life. All questionnaires are conducted by Dr Justin Leo Garner (JLG).

Modified Medical Research Council Scale

The Medical Research Council (MRC) scale is a five point questionnaire[282] adapted in 1988 from the MRC scale devised at the Pneumoconiosis Research Unit in Cardiff in the 1950s to grade disability of coalminers[283, 284]. (Table 2.1).

Grade	Symptom severity
0	Breathlessness only with strenuous exercise
1	Breathlessness when hurrying on level ground or walking up a slight hill
2	Walks slower than people of the same age because of breathlessness, or has to stop for breath
3	Stops for breath after walking 100 yards (91 meters) or after a few minutes on level ground
4	Too breathlessness to leave house or breathless when dressing

Table 2.1. The modified Medical Research Council (mMRC) dyspnoea scale.

The validation studies by Mahler[282] and Hajiro[285] and subsequent research[286] have confirmed moderate correlations between the mMRC and other dyspnoea scores (for example, the baseline dyspnoea index, BDI, and the oxygen cost diagram, OCD). Correlations with health-related quality of

life[287], morbidity[287, 288] and mortality[289] of COPD patients are good, less consistently with lung function and exercise capacity[286]. Since 2011, the Global Initiative for Obstructive Lung Disease (GOLD) guidelines recommend combining the mMRC with the patient's exacerbation rate and FEV1 percent predicted in order to guide therapy[290].

The mMRC scale can be self-administered or conducted by an interviewer, with high inter-rater agreement, within minutes and employs terms that relate to everyday activities and that can be easily understood by patients[291]. It provides a simple means of categorising patients in terms of the disability associated with breathlessness due to COPD[292] and is designed to establish baseline functional impairment[291]. It is relatively insensitive to change[293] but despite this, is often applied serially in interventional studies to measure therapeutic response. A minimum clinically important difference (MCID) of ≥1 is considered meaningful[294].

St George's Respiratory Questionnaire

The St George's Respiratory Questionnaire (SGRQ) is a standardized 50-item instrument developed in 1991 to measure quality of life in patients with airways obstruction, to facilitate comparison of patient populations, and to quantify changes after therapy[295, 296]. Scores are calculated for three domains: Symptoms (frequency and severity), Activities (that cause or are limited by breathlessness), and Impacts (psycho-social disturbance resulting from airways disease), that are combined to generate a total score. Scores range from 0 to 100, with higher scores indicating more severe limitation, and are calculated using either an algorithmic spreadsheet or stand-alone digital application. Studies have confirmed the SGRQ as a valid measure of impaired health in chronic airways diseases which is repeatable and sensitive[296]. Furthermore, it has significant correlations to other measures of disease activity (mMRC scale, lung function, and exercise capacity using 6MWD)[296]. COPD treatments that significantly improve quality of life have been shown to produce a MCID of at least 4 points[297-299]. The SGRQ can either be self-administered or completed by an interviewer.

Evaluation of lung structure

Computed tomography

A Somatom Sensation 64 computed tomography scanner (Siemens, Erlangen, Germany) is used to acquire high resolution radiographic images of thin slices (1mm) of the lungs at maximal inspiration (corresponding to total lung capacity, TLC, measured using body plethysmography) and in expiration (corresponding to residual volume, RV). Subjects are scanned supine from lung apices to bases employing a peak voltage of 120 kilo volts peak (kVp) and tube current modulation range of 30 to 140 mA. Images are reconstructed using a high spatial frequency B40F kernel to axial, coronal and sagittal formats. Isolation of selected structures ranked by radiographic density using the Hounslow Unit scale is achieved with dedicated in-house software (see LungSeg Toolbox).

To minimise radiation exposure, pre-enrolment CT scans performed by a referring centre and adopting a similar imaging protocol are not repeated in a small number of patients. All other CT scans are performed by the Royal Brompton Hospital radiology department.

LungSeg Toolbox

The LungSeg Toolbox software package developed in the Hamlyn Centre (Imperial College London) in collaboration with the Royal Brompton Hospital[216] operates in MATLAB (by MathWorks), a multi-paradigm computing environment, and analyses CT acquired DICOM images. The user interface displays images in three planes (axial, coronal, and sagittal). Image optimisation employs gaussian smoothing for noise reduction and histogram equalisation for contrast enhancement. A variety of functions enables interrogation of the structure of the lung (Figure 2.1):

- Segmentation of large airways (≥2mm internal diameter) and calculation of airway volume.
- Segmentation of right and left lungs and calculation of lung volumes.
- Semi-automated marking of fissures, labelling of lobes and calculation of lobar volumes.
- Characterisation of parenchyma at -950 HU on inspiration and -856 HU on expiration.
- Extraction of intra-pulmonary vessels and calculation of vessel volume.

- Measurement of pulmonary artery to aorta ratio.

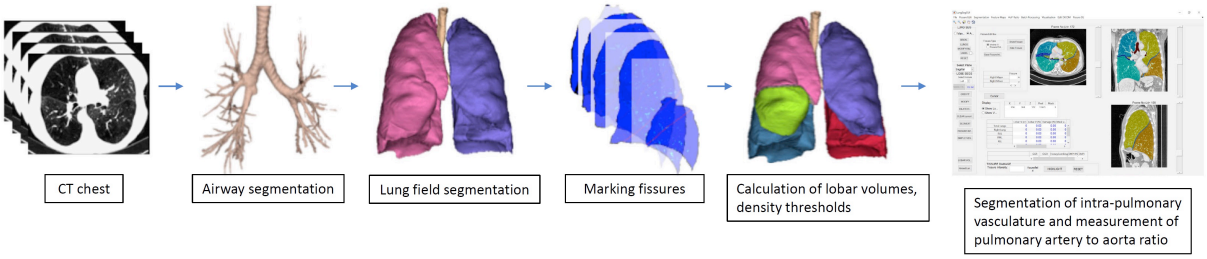

Figure 2.1. LungSeg Toolbox processing workflow schematic.

1) Large conducting airway (≥2mm internal diameter) segmentation using an adaptive region growing method; 2) Segmentation of left and right lungs using a threshold-based region growing method; 3) Semi-automated marking of fissure boundaries (right major oblique, right minor horizontal, and left major oblique), which are interpolated into smooth 3D fissure surfaces; 4) Labelling of individual lobes (right upper lobe, RUL, right middle lobe, RML, right lower lobe, RLL, left upper lobe, LUL, and left lower lobe, LLL) using connected component analysis – lobar volumes are measured and parenchymal density scores (%) calculated using a choice of thresholds including –950 (inspiration) and –856 (expiration) HU; 5) Extraction of pulmonary vessels from the segmented lung volumes based on their higher density value; 6) Measurement of the pulmonary artery to aorta ratio. (There is the option for manual correction at each of the above steps to address issues caused by individual anatomical variability).

The relative contributions of emphysematous and of non-emphysematous gas trapping are determined by calculating the density threshold differences of inspiratory and expiratory phase CT scans according to the following equation[224]:

$$\%fGT = [\%LAA_{-856exp} - (\%LAA_{-950insp} - 6\%)],$$

where %fGT is the percentage of functional gas trapping (non-emphysematous pertaining to the small airways), $\%LAA_{856exp}$ is the percentage lung volume occupied by low attenuation areas ≤ -856 HU on expiratory CT, and $\%LAA_{-950insp}$ is the percentage lung volume occupied by low attenuation areas ≤ -950 HU on inspiratory CT.

All LungSeg analyses are undertaken by JLG.

Evaluation of lung function

Routine lung function

The Jaeger Master Lab (Cardinal Health, Hoechberg, Germany) comprises two pieces of equipment, a constant volume body plethysmograph (MasterScreen™ Body) and single breath gas transfer unit (MasterScreen™ PFT). (Figure 2.2). Each has an integral pneumotachograph accessed with FreeFlow™

mouthpiece (Carefusion, UK) and single-use bacterial filter, to perform spirometry. Prior to use, both machines are calibrated for ambient conditions (temperature in °C, relative humidity in %, and barometric pressure in kPA) and for flow-volume using a 3-litre syringe. Anthropometric measurements including age, height, and weight are input to allow comparison to the European Community for Steel and Coal (ECSC) reference values. All measurements are made post-inhalation of 400mcg of salbutamol and at least three reproducible readouts are recorded[300] by the Royal Brompton Hospital lung function department.

Figure 2.2. Whole body plethysmograph (left) and Single breath gas transfer unit (right).

Body plethysmography

The constant volume plethysmograph is used to estimate airways resistance and the components of lung volume.

The patient is seated in an air-tight box, with an occlusive nasal clip breathing into a mouthpiece connected through a pneumotachograph, (a flow transducer), to the atmosphere outside the box[301]. Pressure changes are recorded at the mouthpiece and in the plethysmograph box. Volume changes in the box are deduced from the pressure measurements. (In a closed system changes in pressure (P) and volume (V) of a gas, at constant temperature, are reciprocal: $P_1V_1 = P_2V_2$. Boyle's Law). Following a period of tidal breathing, the patient is instructed to pant gently at a frequency of 30-35 breaths per minute with hands pressed firmly against the cheeks to record airways resistance (R_{AW})

and its reciprocal, airways conductance (G_{AW}) in kPA/L/s. At the end of the last tidal exhalation, a shutter closes for 2 seconds to measure functional residual capacity (FRC). When the shutter reopens, the patient is instructed to inhale up to total lung capacity (TLC), exhale to residual volume (RV), and to return to tidal breathing. The components of lung volume are calculated and expressed in litres (L) and percent predicted (%). (Figure 2.3).

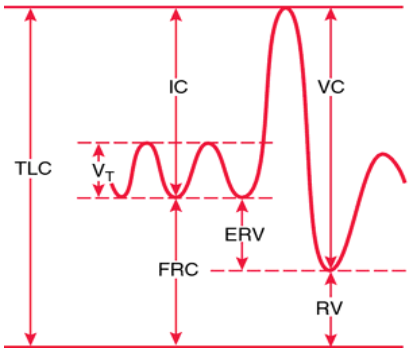

Figure 2.3. Subdivisions of lung volumes.

ERV, Expiratory Reserve Volume. FRC, Functional Residual Volume. IC, Inspiratory Capacity. RV, Residual Volume. TLC, Total Lung Capacity. VC, Vital Capacity. V_T, Tidal Volume.

Gas transfer – single breath technique

A single breath gas transfer measurement is used to assess the effectiveness of pulmonary gas exchange, using carbon monoxide (CO) as a substitute for oxygen (O_2). Helium (HE) is a non-transferable marker. The changes in the proportions of the gases are determined in the mid-flow sample of the immediately following expiration.

Following a brief period of quiet breathing into a mouthpiece connecting to the atmosphere through a valve box the patient is instructed to inhale to TLC and then exhale gently to RV. At the start of the next inspiration the valve is triggered to allow the patient access to a gas mixture (0.28% carbon monoxide, 9.0% helium, and 19.0% oxygen; British Oxygen Company, UK). At TLC the breath is held for 10 seconds before exhalation and mid-flow sampling for analysis. Gas transfer (TLCO), alveolar volume (VA) and specific gas transfer (KCO) are computed, taking into account ambient atmospheric conditions and the patients' capillary haemoglobin concentration. TLCO and KCO are expressed in mmol/min/kPa and as a percentage of predicted (%), VA in litres (L) and percent predicted (%)[302].

(The rebreathing technique is considered more appropriate for patients with vital capacity (VC) less than 1300mls).

Spirometry

After a period of tidal breathing, the patient is instructed to inhale to TLC, then perform a maximal forced exhalation to RV, and finally a fast-maximal inhalation up to TLC. FEV1, FVC, FEV1/FVC, and MEF25-75% can be calculated in litres (L) and percent predicted (%)[303].

Capillary blood gas (CBG)

An earlobe is massaged with warm water swabs to encourage blood flow and cleansed with an alcohol street. A small incision is made with a disposable blade (Swann-Morton No.15). Blood is collected in a pre-heparinised 230µl capillary tube and analysed on blood gas machine (ABL90 FLEX PLUS, Radiometer, UK) for pH, PCO_2 (kPA), PO_2 (kPA), and HCO_3 (mEq/L) and on HemoCue for haemoglobin.

Small airways physiology

Impulse oscillometry

Oscillometry quantifies impedance to airflow, distinguishing the contributions of small and large airways, and picking up the early abnormalities of COPD undetected with conventional spirometry. Rapidly alternating pressure waves are imposed on tidal flow introducing another element to resistance – reactance. The opposition to airflow offered by reactance, (expressed in the same units as resistance), is dependent on the frequency of the wave form. So also, is the penetration into the lungs. Low frequency waves reach the alveoli. High frequency waves are damped before reaching the peripheral airways. The mix of frequencies used in impulse oscillometry enables the impedances contributed by the small airways and by the large airways to be determined.

Setup and calibration

The Impulse Oscillometry System (Cardinal Health, Hoechberg, Germany) comprises a loudspeaker imposing bursts of mixed frequency pressure waves on to a patient's tidal ventilation monitored by pressure and flow transducers and a computer producing readouts of respiratory resistance (kPA/L/s)

at 5Hz and at 20Hz, reactance (kPa/L/s) at 5Hz, reactance area for whole breath (AX), and resonant frequency (1/L). (Figure 2.4).

Prior to use, the machine is calibrated for ambient conditions (temperature in °C, relative humidity in %, and barometric pressure in mmHg), flow-volume using a 3-litre syringe, and resistance using a reference impedance device (resistance should measure 0.20 kPA between 5 – 35Hz). Importantly, the screen cap on the Y-adapter (terminal resistance) is open for the volume calibration and closed during impedance calibration. A single-use bacterial filter with re-useable FreeFlow™ mouthpiece (Carefusion, UK) is attached to the pneumotachograph. Anthropometric measurements including age, height, and weight are input. All test measurements are made post-bronchodilation using 400mcg of salbutamol and at least three reproducible readouts are recorded[246] by JLG.

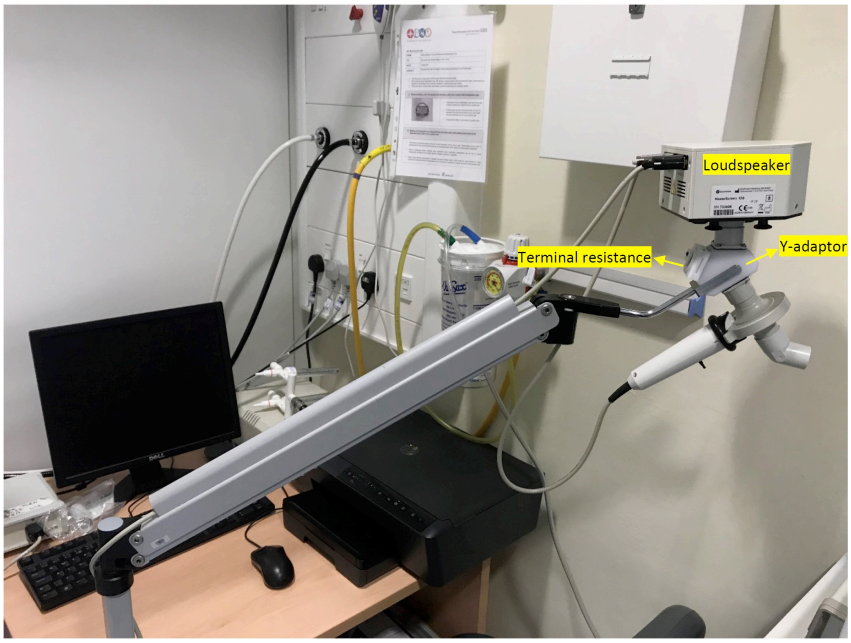

Figure 2.4. The Impulse Oscillometry System (Cardinal Health, Hoechberg, Germany).

Performing test

The patient should be seated upright with legs uncrossed and feet firmly placed on the floor to relax the respiratory muscles. The patient is instructed to come onto the mouthpiece ensuring the tongue is placed under the depressor and the flange sits between the gums and lips. With nose clip applied,

the patient supports their cheeks during the tests (to minimise absorption of sound waves by unsupported tissues) and breathes normally for 30-60 seconds.

Analysis

At the end of each run, the result is checked and adjusted for artefacts (for example, swallowing) by separating tidal breathing from resistance at 5Hz and selecting the representative portions of the trace. At least three reproducible readouts are recorded and averaged.

Multiple breath nitrogen washout (MBNW)

Setup and calibration

A bespoke assembly comprising a 400-litre 'bag-in-box' system with pneumatic valves is used, a replica construction based on a prototype built in Belgium[304][11]. A non-rebreathing valve separates inhaled (IN) from exhaled (EX) air, each in dedicated 150 litre Douglas bags. Air breathing occurs through valves 1 and 4 and oxygen breathing via valves 1 and 2. The dead space volume is 50mls. Volume and pressure changes in the box or bags are recorded by the integrated Fleisch-type pneumotachograph, 5. Nitrogen (N_2) concentration at the mouthpiece is monitored continually with a built-in needle-valve probe connected to a nitrogen analyser, 6 (P. K. Morgan, Kent, UK). Volume, pressure and N_2 concentration signals are processed using a dedicated Labview program (National Instruments, Austin, TX) which also controls the valves and provides visual feedback of inspiratory volume achieved on a personal computer (PC) screen to the patient. (Figures 2.5 and 2.6).

[11]There is concern regarding use of commercial machinery which has been reported to substantially over-read FRC by up to 30% compared to body plethysmography.

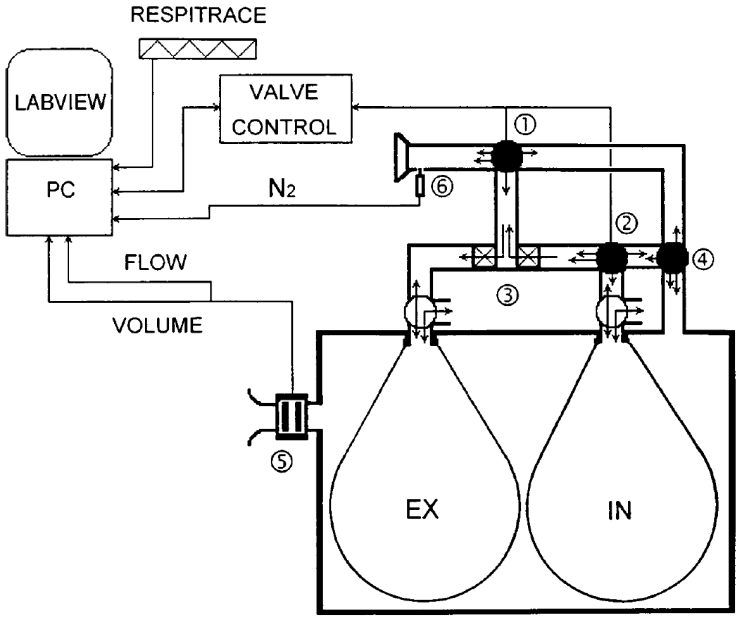

Figure 2.5. Schematic representation of the experimental setup used for MBNW. EX, Expiratory; IN, Inspiratory; PC, Personal computer[304]. (see text for details).

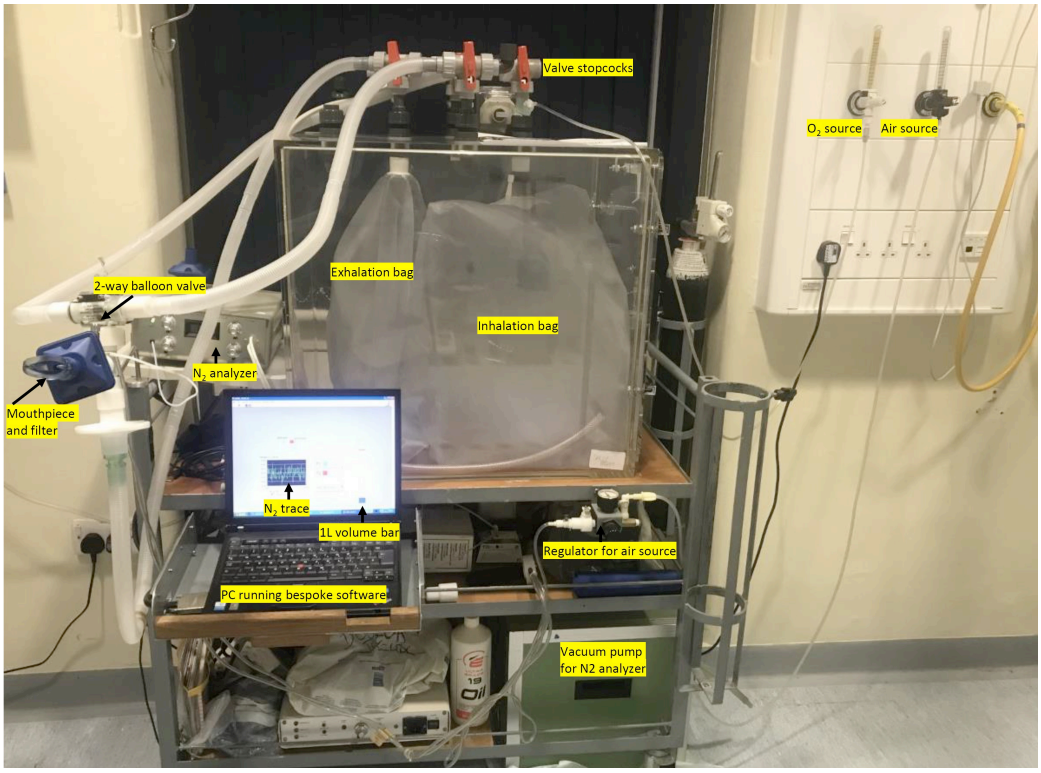

Figure 2.6. Photo of the experimental setup used for MBNW.

Prior to use, the machine is calibrated to ensure the nitrogen analyser reads between 70-80%, approximating atmospheric conditions and for flow-volume using a 1-litre syringe. The 1 litre syringe is also used to simulate a patient tidal breathing in order to generate a test washout curve – this is to

ensure there is no leak in the system causing a drift in the trace or inability to achieve a drop in N_2 concentration to < 2% (1 in 40 dilution).

Performing test

The subject sits comfortably with nose clip applied and comes onto the TRU-FIT™ mouthpiece attached to the pneumotachograph via an interposed Vitalograph disposable bacterial filter. The MBNW test requires a regular breathing pattern with a tidal volume of 1 litre.

After a period of tidal breathing of air (via the box), the patient is switched to the inspiratory (IN) bag containing 100% oxygen during an exhalation (to minimise gas mixing) using a two-way inflatable balloon system (Hans Rudolph, USA). The subject is instructed to restrict tidal breathing to 1 litre excursions guided by a graphical representation of his/her effort on a PC screen. The number of tidal breaths of 1 litre required to achieve a 1 in 40 dilution (approximating 2% above baseline) is termed the lung clearance index (LCI). The interval between tests is 10 minutes. Three tests are performed by each subject post-bronchodilation using 400mcg of salbutamol under the supervision of JLG. Each test records a diminishing N_2 concentration trace. (Figure 2.7).

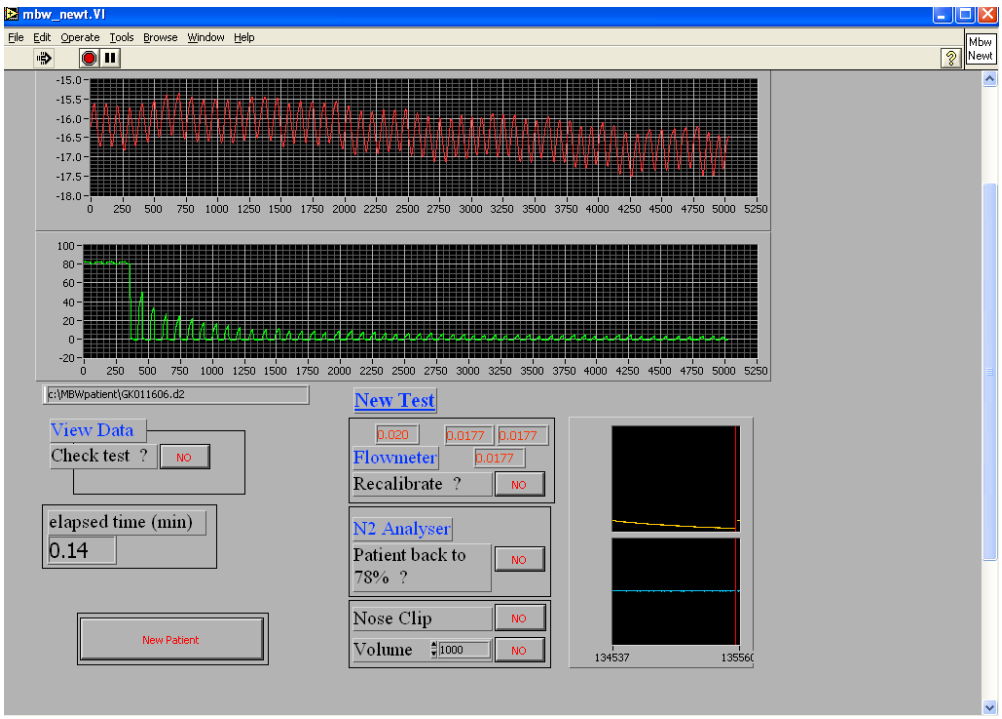

Figure 2.7. Example MBNW trace obtained from a patient with emphysema and hyperinflation. Tidal breathing is indicated in red and diminishing nitrogen concentration in green.

Analysis

A 'washout curve' is generated by plotting a semilogarithmic graph of the log of the mean expired N_2 concentration of each breath expressed as a percentage of the starting N_2 concentration, log [N_2], against lung turnover, TO (defined as the cumulative expired volume divided by FRC). (Figure 2.8A). TO is used rather than number of breaths as it permits comparison of patients with different lung volumes and dilutions. To determine the relative contributions of the conductive (S_{cond}) and acinar (S_{acin}) airways to assess ventilation inhomogeneity, the alveolar slope of each breath (the equivalent of a single breath N_2 washout trace) is determined by linear regression of N_2 concentration versus expired volume (0.65 to 1 litre) in the alveolar phase III, which is then divided by mean expired N_2 concentration to derive a normalised alveolar slope (S). S is then plotted as a function of TO. (Figure 2.8B). S_{cond} is derived by linear regression of the normalised alveolar slope (S) between TO 1.5 to 6.0 (i.e., that portion contributed by the conducting airways) to give the gradient per unit TO. S_{acin} is derived by subtracting S_{cond} from the slope of the first breath and multiplying by the TO of that breath.

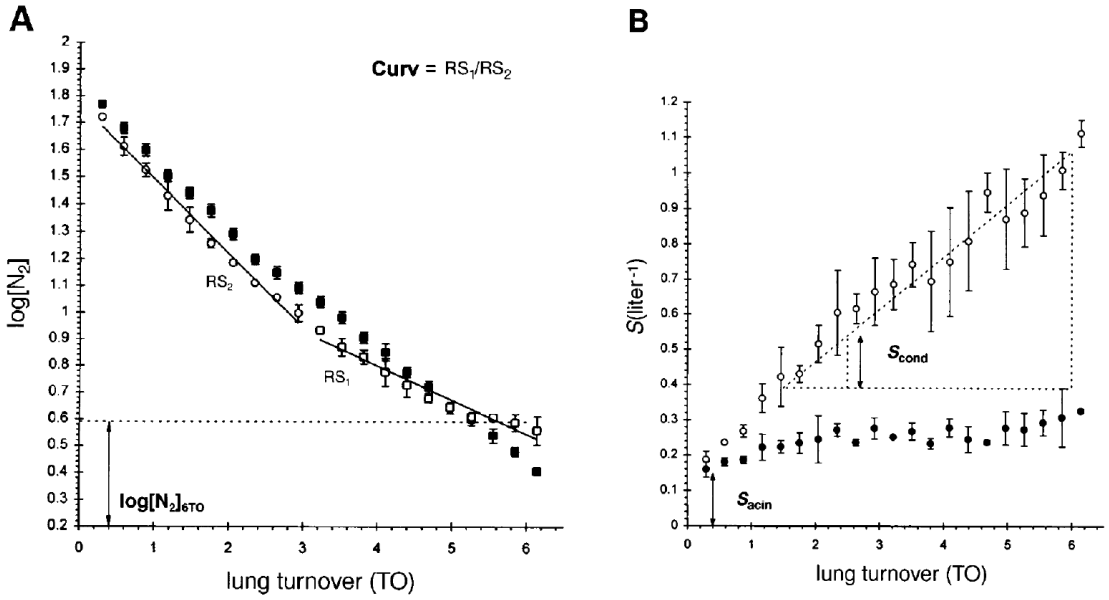

Figure 2.8. Example multiple breath nitrogen washout tracings (MBNW).

MBNW recordings from a patient at baseline (solid symbols) and after undergoing a provocation test (open symbols). (**A**) 'Nitrogen (N_2) washout curve' generated by plotting the logarithm of the mean expired N_2 concentration of each breath expressed as a percentage of the starting N_2 concentration against lung turnover (TO). The Curvilinearity (Curv) is the ratio of the regression slopes, RS_1/RS_2. (**B**) The normalised alveolar slope of each breath (S) plotted as a function of TO from which two indices of ventilation inhomogeneity can be derived, S_{cond} and S_{acin}. Adapted from [304].

Data are analysed by JLG using a bespoke programme coded by Sylvia Verbanck in Turbo Pascal (a software development system) and running in DOSBox (a DOS-emulator). Each test file is individually uploaded and undergoes a series of manual steps as illustrated in Figure 2.9. Corrections are first made for any drift in tidal breathing followed by setting of the delay time (i.e. the interval between N_2 sampling at the mouth and reaching the analyser, is typically set at 5 seconds). Next, N_2 concentration is selected whilst breathing air and then for each subsequent breath at end-inspiration. Phase III slopes are then drawn for each exhaled breath. An output file is generated containing the following parameters: TO – lung turnover, VDF = Fowler dead space, VDB = Bohr dead space, Sn = normalised phase III slope, FRC = functional residual capacity, FETn = end-tidal N_2 concentration, Fen = mean expired N_2 concentration, INVOL = inhalation volume, EXVOL = exhalation volume, and Fin = mean inspiratory N_2 concentration. The output file data for each test run (usually three) are copied into a customised excel template, coded by Sylvia Verbanck, for generating graphs of: 1) Fen vs TO to determine LCI and 2) Sn vs TO (TO set at 1.5 to 6.0) to derive S_{cond} and S_{acin} indices (/L).

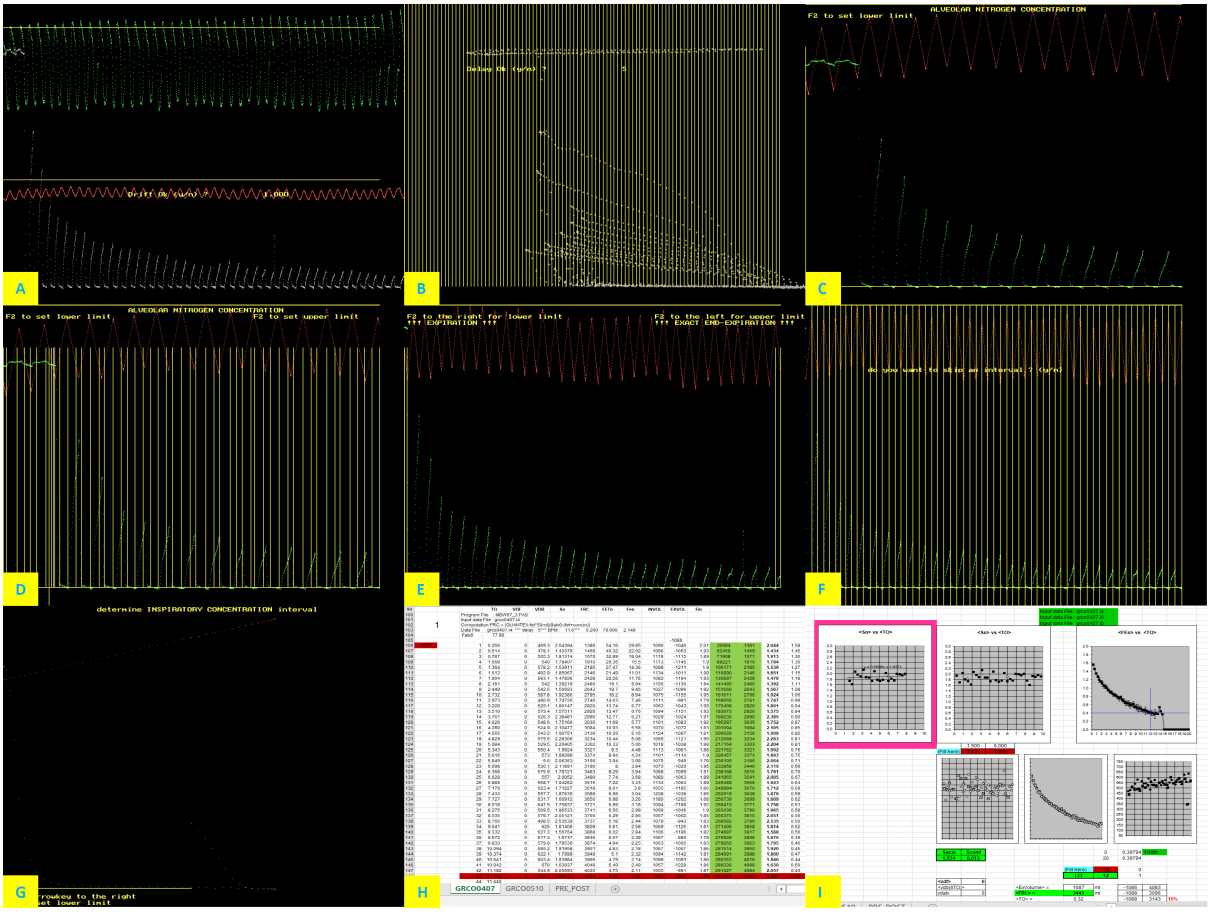

Figure 2.9. Workflow for MBNW analysis.

An experimental software platform devised by Sylvia Verbanck is used[304]. Adjustments are made for drift in tidal volume (A) and delay in N_2 sensing (B). N_2 concentration is selected whilst breathing air (C) and then for each subsequent breath at end-inspiration (D-E). Phase III slopes are drawn for each exhaled breath (G). An output file is generated and copied into a customised excel template for analysis (H) and plotting of graphs to derive the lung clearance index (LCI) and ventilation inhomogeneity indices for the conducting (S_{cond}) and acinar airways (S_{acin}).

Lung compliance.

Lung compliance is an index of lung volume responsiveness to changes in transpulmonary pressure and is expressed as l/cm H_20. The relationship is not linear: A point selected from the end 500mls of the expiratory curve is considered representative. Volume changes are computed from the output of a pneumotachograph, a flow transducer, at the mouth. Transpulmonary pressures are derived from intra-pleural pressure recordings obtained with an oesophageal balloon manometer and alveolar pressures measured at the mouthpiece during intervals when flow is briefly interrupted with a shutter[305].

Transpulmonary pressure (TP) in expiration = intrapleural pressure – alveolar pressure

The balloon catheter, lightly coated with Instillagel sterile lubricant, is fed through the subject's nose to the lower third of the oesophagus. Correct placement is facilitated by graduations on the catheter and application of Zaplatel's formula:

Distance from nares (cm) = height (cm)/ 5 + 9.

Fine adjustment is made if artefacts originating from the heart or from the stomach are detected. The balloon is emptied with a Valsalva manoeuvre, re-inflated to 0.5ml and the catheter connected to a pressure transducer. The subject with nose clipped breathes into a mouthpiece connected to a Jaeger plethysmograph and after establishment of tidal breathing inhales to TLC followed by a relaxed expiration to RV. Repeated brief interruptions of flow by a volume-controlled shutter – at 100 to 200ml intervals – are made during recordings of the expiratory phase. Reproducibility is confirmed with at least three runs supervised by the Royal Brompton Hospital lung function department and JLG.

Exercise capacity

Six-minute walk test

This test records the distance a patient walks as quickly as possible in six minutes, without encouragement during the walk. It is self-paced and stopping and resting does not invalidate the test. Supplemental oxygen is permitted but must be used with the same delivery setting in subsequent tests for valid comparison. It provides a snapshot of functional status, is reproducible and is used to re-evaluate after a medical intervention, particularly in patients with moderate to severe lung disease [306]. Exercise testing is conducted by JLG.

Evaluation of lung inflammation

Inflammatory markers, cytokines, and microvesicles, circulating and bronchoalveolar, are examined before and after lung reduction procedures. The techniques employed are described:

Venous blood drawn with a vacutainer into two 4ml heparinised bottles is decanted into a 15ml Falcon centrifuge tube and spun at 200g for 10 minutes at 4˚C. An aliquot of the platelet-rich supernatant is aspirated for microvesicle analysis and the remainder spun again, at 4,500g for 20 minutes at 4°C. The second supernatant, platelet-depleted, is analysed for cytokines. Both samples are stored in cryotubes at -80 degrees °C. (Figure 2.10).

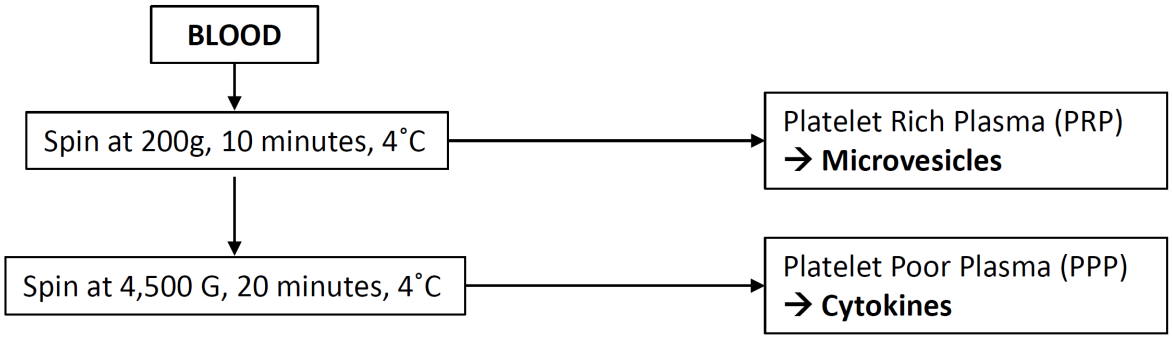

Figure 2.10. Venous blood preparation.

Venous blood is differentially centrifuged to obtain fractions for microvesicle and for cytokine analyses.

Material for bronchoalveolar examination is obtained with a lavage during bronchoscopy (BAL) conducted under sedation or general anaesthesia in accordance with BTS guidelines[307]. 50mls of normal saline is instilled into the target lobe and the entrained bronchoalveolar debris aspirated with a syringe. The constituents are recovered in a series of centrifuge operations at 4°C. The first at 200g for 5 minutes yields a pellet of cells which is resuspended in Dulbecco's Modified Eagle Media (DMEM) and Dimethyl Sulphate ($DMSO_4$) for analysis. The supernatant is filtered through a 100µm strainer and centrifuged again at 200g for 5 minutes at 4°C. An aliquot is removed for microvesicle assessment. The remainder undergoes a third spin at 21,000g for 30 minutes: The resulting supernatant contains the cytokines. The yields are stored in cryotubes at -80°C. (Figure 2.11).

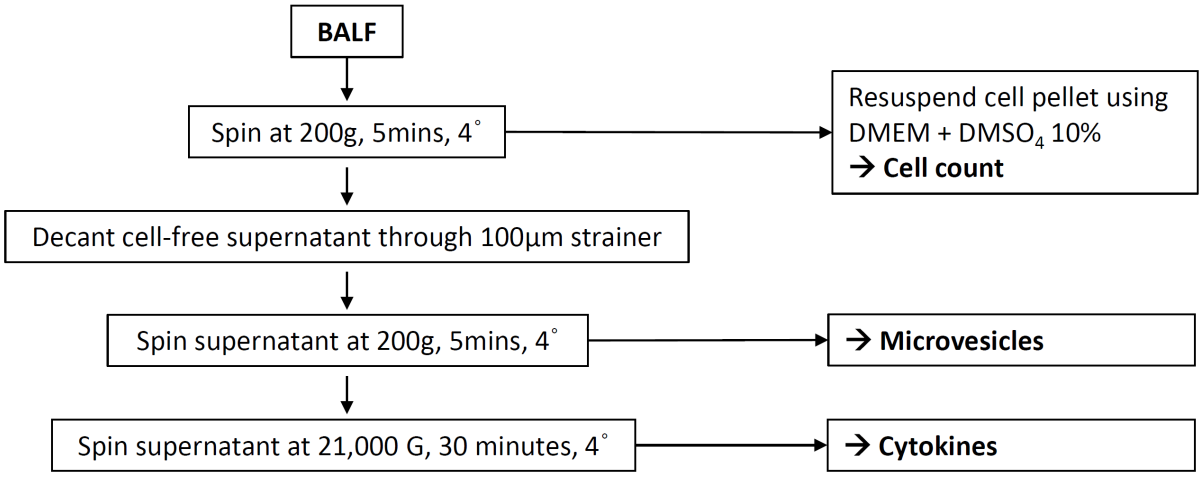

Figure 2.11. Bronchoalveolar lavage fluid (BALF) preparation.
BALF is differentially centrifuged to obtain fractions for cell count, microvesicle and cytokine analyses. DMEM, Dulbecco's Modified Eagle Media; $DMSO_4$, Dimethyl Sulphate.

Microvesicle analysis

Microvesicles (MVs) express surface proteins that can be targeted with fluorophore-conjugated monoclonal antibodies (Biolegend and eBioscience, San Diego, CA) to determine cell origin. PRP and BALF samples containing microvesicles are thawed and incubated with fluorophore-conjugated antibody combinations (Table 2.2):

CELL SURFACE MARKER	CELL ORIGIN
CD45 + CD66b	Neutrophil
CD66b + CD11b	Neutrophil
CD45 + CD14	Monocyte
CD206 + CD71	Macrophage
CD324 + CD31	Platelet
CD42b + CD31	Platelet
CD326 + T1α	Epithelial
CD146 + CD62E	Endothelial
CD146 + CD31	Endothelial
CD144 + CD62E	Endothelial
CD144 + CD31	Endothelial

Table 2.2. Cell surface markers to identify the cellular origin of the microvesicle populations.
CD, cluster of differentiation. CD11b, integrin family member; CD14, co-receptor for the detection of bacterial lipopolysaccharide; CD31, platelet endothelial cell adhesion molecule (PECAM-1); CD42b, platelet surface membrane glycoprotein (Glycoprotein 1b); CD45, leucocyte common antigen; CD62E, endothelial cell adhesion molecule (E-Selectin); CD66b, carcinoembryonic antigen-related cell adhesion molecule 8 (CECAM 8); CD71 transferrin receptor; CD144, vascular endothelial cadherin (VE-Cadherin); CD146, melanoma cell adhesion molecule (MCAM); CD206, mannose receptor; CD324, epithelial cadherin (E-Cadherin); T1α, alveolar type 1 epithelial cell surface marker.

A Cyan flow cytometer (Beckman Coulter, High Wycombe, UK) with side scatter threshold of 0.03% and gating for events under 1µm is used to identify MVs as those staining positive for the above cell surface markers and which are sensitive to 0.1% triton X-100 detergent (which solubilizes the lipid bilayer membrane) to validate the population. FlowJo software (Tree Star, Ashland, OR) is used to analyse the data. Flow cytometry and data analysis are undertaken by JLG and Dr Sanooj Soni (SS).

Cytokine analysis

A sandwich enzyme-linked immunosorbent assay (ELISA, R&D Systems®) is used to measure IL-1β, IL-6, IL-8, and TNF-α levels in PPP and BALF samples.

A 96-well microplate prepared with coating of 50µl of capture antibody is stood overnight at 4°C, washed with buffer (0.05% Tween 20 in phosphate buffered saline), blocked with 300µl of 1% bovine serum albumin (BSA) for 1 hour at room temperature, and washed again. 50µl standards (reconstituted in BSA at concentrations specified by the manufacturer's protocol) and 50µL samples are added in duplicate to the wells and incubated for 2 hours at room temperature. The wash is

repeated and 50µl of biotinylated detection antibody (diluted in BSA) added to each well for 2 hours at room temperature. The microplate is washed and 50µL of the working dilution of streptavidin-HRP (R&D, Abingdon, UK) added to each well and stood in darkness for 20 minutes. The plate is washed again and 50µl of substrate solution (3,3', 5,5'-Tetramethylbenzidine, Sigma) added to each well for a further 20 minutes in the dark. 50µl of stop solution (2M Sulphuric Acid) is added to terminate the substrate reaction. The plate is placed in the reader and the optical density of each well read at a wavelength of 450nm. Results are expressed in picograms (pg). Cytokine measurements are performed by JLG, SS, and Dr Marissa Koh (MK).

Statistical analysis

Categorical data are presented as percentages (%) and comparisons made using the Chi-squared or Fisher's exact test for two or more categorical variables. Parametric continuous data are presented as mean ± SD or 95% confidence intervals and non-parametric continuous data as median (interquartile range, IQR). Comparisons of two matched groups are made using a paired t test or the Wilcoxon test for parametric and non-parametric distributions, respectively; two unmatched groups, an unpaired t test or Mann-Whitney test; three matched groups, repeated measures ANOVA or Friedman test; and three unmatched groups, a one-way ANOVA or Kruskal-Wallis test (Tukey's and Dunn's tests applied, respectively, for multiple comparisons). Quantifying the association between two variables is measured using Pearson or Spearman correlations for parametric and non-parametric distributions, respectively. The strength of the correlation for the absolute value of *r* is described as follows: 0.00–0.19, 'very weak'; 0.20 – 0.39, 'weak'; 0.40 – 0.59, 'moderate'; 0.60–0.79, 'strong'; 0.80–1.0', 'very strong'. Binary logistic regression is undertaken to determine predictors of response, defined as a reduction in residual volume of ≥10%. All tests are 2 tailed and significance set at $p < 0.05$. Statistical analysis is performed using SPSS version 24.0 (IBM, Chicago, IL, USA) and presented using GraphPad Prism version 8 (San Diego, CA).

CHAPTER 3: Impact of Lung Volume Reduction on Lung Structure

This chapter evaluates the radiological changes observed in lung structures after volume reductions achieved with each of the three validated procedures, surgical excision and deflation with endobronchial valves and with coils.

Abstract

Background – In pursuit of a robust biomarker to predict the response to lung volume reduction (LVR) interventions, we investigated the hypothesis that lung volume reduction will be accompanied by measurable radiological changes in the structure of the airways, parenchyma, and vasculature that can be correlated with changes to the conventional clinical parameters and that reliable radiological baseline predictors of therapeutic response (reduction of residual volume of at least 10%) will be identified.

Methods – 72 consecutive subjects with severe emphysema and hyperinflation scheduled for lung volume reductions were recruited: Unilateral LVRS – 15; Endobronchial valve – 29, Endobronchial coil – 28. All underwent detailed clinical phenotyping comprising demographic, symptom score, lung function, exercise capacity and CT-imaging measurements during exacerbation-free periods at baseline and at three months after intervention. Inspiratory and expiratory CT images were analysed using an in-house software platform, LungSeg, to interrogate lung structures: airways, parenchymal, and vasculatur compartments.

Results – Surgery achieved the greatest degree of lung volume reduction (LVR), △CT-total lung $volume_{insp}$ of -873.8 ± 428.3mls and was the only intervention to be accompanied by improvements in both total and functional gas trapping (fGT), inferring improvement in peripheral airways function. EBV implantation accomplished a △CT-total lung $volume_{insp}$ of -577.0 ± 769.3mls and reduction in total

gas trapping without an accompanying signal in fGT suggesting the benefits observed related predominantly to deflation of emphysematous lung. EBC implantation resulted in modest volume reduction, △CT-total lung volume$_{insp}$ of -140.6 ± 298.8mls, and 3-month physiological outcomes were similarly disappointing – interestingly, CT-intraparenchymal blood vessel volume was significantly increased post-intervention perhaps due to greater radial traction exerted by the coils on the surrounding parenchyma. There were no radiological predictors of volume reduction identified for any of the interventional arms.

Conclusions – Chest computed tomography (CT) is a readily accessible and non-invasive means of examining lung structures and their responses to intervention *in vivo*. Volume reduction is crucial and is the key driver of benefit which is manifest proportionally as improvements in total and in functional gas trapping, an index showing promise as an objective measure of interventional outcome. However, a radiological biomarker to reliably predict therapeutic response could not be established from this small dataset.

Introduction

The hyperinflated lungs of advanced COPD are the consequence of irreversible expiratory airflow limitation caused by a combination of small airways disease and parenchymal destruction[1]. To the burden of resistance to airflow is added the constraints imposed on the mechanism of the respiratory pump[308]. Surgical excision and bronchoscopic deflation of diseased lung tissue are radical solutions with proven benefit[214]. Volume reduction has been the principal focus of attention optimising the interventions. Little is known of the impact on the morphology of the airways, the parenchyma, and the vasculature.

Chest computed tomography (CT) is a readily accessible and non-invasive means of examining *in vivo* these structures and their responses to intervention, which to date have been largely focused on lobar volume change[309]. A robust biomarker, a dependable predictor of outcome to guide selection of patient and of procedure, is lacking[279] and an easily acquired and interpreted radiological metric would be welcome.

Airway compartment

The normal responsiveness of airways to inspiratory effort is attenuated early in the course of COPD, an observation attributed to the fixed hyperinflated state and to a reduction of the radially disposed alveolar attachments to bronchioles[310-312]. Petty et al studying excised human lungs with and without emphysema showed FEV1 to be positively correlated with the numbers of alveolar attachments to small bronchioles (those less than 2mm internal diameter), inversely with fibrosis of the airways[313]. Diaz et al employed CT imaging to stage emphysematous lungs and to quantify the distensibility of large to medium calibre airways in response to inspiration, correlating the two and found an inverse association[314]: longitudinal stretching of bronchioles unsupported by radial traction has been suggested as a mechanism[315]. Tanabe et al developed a novel CT biomarker, airway volume percent (AWV%) index, measuring the ratio of right upper and middle lobe airway tree volumes to total right lung volume, and showing that a disproportionately small airway tree volume

is associated with worsening of airflow obstruction and gas trapping[316]. The resolution of CT does not as yet permit visualisation of the small airways *in vivo*[94]. Micro-CT investigation of airways less than 2mm in internal diameter is confined to excised lung[317]. Instead, a surrogate index quantifying their contribution to non-emphysematous gas trapping, termed functional gas trapping (fGT), can be derived using an algorithm comparing low attenuation areas of different thresholds in inspiration (-950 Hounsfield units, HU) and expiration (-856 HU)[224]. fGT has been shown to be strongly correlated with functional small airways disease (fSAD) determined with parametric response mapping (PRM). PRM, in turn, has been shown to accurately differentiate COPD disease phenotypes and is strongly associated with the severity of disease[220, 223].

Parenchymal compartment

Distinction of emphysema on CT by the fraction (expressed as a percentage) of voxels below -950 HU (%LAA-950) has been verified with histological observations[217, 218] as well as with physiological parameters of disease, including FEV1, lung volumes, gas transfer and desaturation on six-minute walk testing[219, 318].

Vascular compartment

Remodelled vascular tissues complete the triad of pathological structures observed in emphysema[80]. A CT measured pulmonary artery to aorta ratio is superior to echocardiography for diagnosing resting pulmonary hypertension in severe COPD[225] and is associated with severe exacerbations[319]. Reduction in small pulmonary vessel cross-sectional area also correlated with the severity of pulmonary hypertension in severe emphysema[98].

Study objective

To investigate the hypothesis that lung volume reduction will be accompanied by measurable radiological changes in the structure of the airways, parenchyma, and vasculature that can be correlated with the conventional clinical parameters and that reliable radiological baseline predictors of therapeutic response (reduction of residual volume of at least 10%), will be identified.

Methods

Ethics

This study was undertaken in accordance with the Declaration of Helsinki and is based on CT imaging data acquired prospectively from two observational trials performed at the Royal Brompton Hospital:

1) Changes in Small Airways Physiology following bronchoscopic treatments for Obstructive Airways Disease, SAP-OAD (REC reference 14/SC/0193, IRAS 145030) – enrolled patients undergoing LVRS, endobronchial valve and endobronchial coil (registry) implantations.
2) Identifying REsponders and Exploring Mechanisms of ACTION of the Endobronchial Coil Treatment for Emphysema, REACTION (REC reference 16/LO/0933, IRAS 179313, NCT02179125) – enrolled patients undergoing endobronchial coil implantations.

Written informed consent was obtained from all patients.

Study subjects

72 consecutive subjects scheduled for lung volume reductions were recruited: Unilateral LVRS – 15; Endobronchial valve – 29, Endobronchial coil – 28. All underwent detailed clinical phenotyping comprising demographic, symptom score, lung function, and exercise capacity measurements during exacerbation-free periods from 4th July 2016 to 13th August 2019.

Symptom scores

The modified Medical Research Council (mMRC) dyspnea scale[282] was used to evaluate disability associated with breathlessness due to COPD[292]. A minimum clinically important difference (MCID) of 1 was considered meaningful[294].

The St George's Respiratory Questionnaire (SGRQ) was used to measure quality of life[295, 296]. Scores were calculated for three domains: Symptoms (frequency and severity), Activities (that cause or are limited by breathlessness), and Impacts (psycho-social disturbance resulting from airways

disease), that were combined to generate a total score. Scores range from 0 to 100, with higher scores indicating more severe limitation. An MCID of -4 was considered clinically meaningful[298].

Computed tomography

A Somatom Sensation 64 computed tomography scanner (Siemens, Erlangen, Germany) was used to acquire high resolution radiographic images of thin slices (1mm) of the lungs at maximal inspiration (corresponding to total lung capacity, TLC, measured using body plethysmography) and in maximal expiration (corresponding to residual volume, RV). Supine subjects were scanned from lung apices to bases employing a peak voltage of 120 kilo volts (kVp) and tube current modulation range of 30 to 140 mA. Images were reconstructed using a high spatial frequency B40F kernel to axial, coronal and sagittal formats. Isolation of selected structures ranked by radiographic density using the Hounslow Unit (HU) scale was achieved with dedicated in-house software (see LungSeg Toolbox). (To minimise radiation exposure, pre-enrolment CT scans performed by a referring centre and adopting a similar imaging protocol were not repeated in a small number of patients).

The LungSeg Toolbox, a validated software package developed in the Hamlyn Centre (Imperial College, London) in collaboration with the Royal Brompton Hospital[216], operates in MATLAB (by MathWorks), a multi-paradigm computing environment, and analyses CT-acquired DICOM images. The user interface displays images in three planes (axial, coronal, and sagittal). Image optimization employs gaussian smoothing for noise reduction and histogram equalization for contrast enhancement. A variety of functions enable interrogation of the structure of the lung:

- Segmentation and calculation of total lung volume on full inspiration and expiration.
- Characterisation of parenchyma at -950 HU on inspiration and -856 HU on expiration.
- Extraction and calculation of intra-parenchymal vessel volume.
- Measurement of pulmonary artery to aorta ratio.

Routine lung function and exercise capacity

The Jaeger Master Lab (Cardinal Health, Hoechberg, Germany) comprises two pieces of equipment, a constant volume body plethysmograph (MasterScreen™ Body) and a single breath gas transfer unit (MasterScreen™ PFT). Each has an integral pneumotachograph accessed with FreeFlow™ mouthpiece (Carefusion, UK) and single-use bacterial filter, to perform spirometry. Prior to use, both machines were calibrated for ambient conditions (temperature in °C, relative humidity in %, and barometric pressure in kPA) and for flow-volume using a 3-litre syringe. Anthropometric measurements including age, height, and weight were input to allow comparison with the European Community for Steel and Coal (ECSC) reference values. All measurements were made post-inhalation of 400mcg of salbutamol and at least three reproducible readouts were recorded[300]. An earlobe capillary blood sample was analysed on an ABL90 FLEX PLUS (Radiometer, UK) for pH, PCO_2 (kPA), PO_2 (kPA), and HCO_3 (mEq/L) and on HemoCue for haemoglobin. Six-minute walk test was performed to evaluate exercise capacity according to ATS guidelines[320].

Statistics

Categorical data are presented as percentages (%) and comparisons made using the Chi-squared or Fisher's exact test for two or more categorical variables. Parametric continuous data are presented as mean ± SD or 95% confidence intervals and non-parametric continuous data as median (interquartile range, IQR). Comparisons of two matched groups were made using a paired t test or the Wilcoxon test for parametric and non-parametric distributions, respectively; two unmatched groups, an unpaired t test or Mann-Whitney test; three matched groups, repeated measures ANOVA or Friedman test; and three unmatched groups, a one-way ANOVA or Kruskal-Wallis test (Tukey's and Dunn's tests applied, respectively, for multiple comparisons). Quantifying the association between two variables was measured using Pearson or Spearman correlations for parametric and non-parametric distributions, respectively. The strength of the correlation for the absolute value of *r* was described as follows: 0.00–0.19, 'very weak'; 0.20 – 0.39, 'weak'; 0.40 – 0.59, 'moderate'; 0.60–0.79, 'strong'; 0.80–1.0', 'very

strong'. Binary logistic regression was undertaken to determine predictors of response, defined as a reduction in residual volume of ≥10%. All tests were 2 tailed and significance was set at $p < 0.05$. Statistical analysis was performed using SPSS version 24.0 (IBM, Chicago, IL, USA) and presented using GraphPad Prism version 8 (San Diego, CA).

Results

The three cohorts were well matched (Table 3.1) and were treated as a single unit pre-intervention to establish baseline correlations of CT-acquired lung volumes with the equivalent plethysmography-derived values as a preliminary verification and validation.

We then focus on individual therapies and their impact on lung structure comparing clinical characteristics at baseline and at 3 months, delta correlations with the pre-specified CT metrics, and evaluating for radiological predictors of a ≥10% RV reduction to identify potential mechanisms of action. Finally, the cohorts are compared to clarify differences between techniques.

		Combined cohort	LVRS	Valve	Coil	Group comparison
Demographics						*p-value*
Number		72	15	29	28	
Age, years		64.32 ± 9.74	58.47 ± 12.13	64.86 ± 8.75	66.89 ± 8.21	0.05
Gender (male), %:		52.78	60.00	58.62	42.86	0.40†
BMI, kg/m^2		24.02 ± 3.93	23.10 ± 3.40	24.63 ± 4.34	23.88 ± 3.77	0.44
Active co-morbidities		2 (1, 3)	1 (0, 2)	2 (1, 3)	2 (1, 3)	0.35‡
Pack years		42.50 (32.00, 52.88)	33.75 (25.00, 48.00)	45.00 (32.50, 53.00)	42.00 (33.38, 53.00)	0.49‡
Exacerbations (last year)		2, (0,3)	2 (0, 3)	1 (0, 3)	2 (0, 3)	0.90‡
GOLD grade, %	II	3	13	0	0	0.80‡
	III	36	27	43	36	
	IV	61	60	57	64	
Heterogeneous, %		46.97	53.84	46.43	44.00	0.84†
Baseline medications						
LABA, %		94.44	86.67	93.10	100.00	0.18†
LAMA, %		95.83	86.67	96.55	100.00	0.11†
ICS, %		91.67	100	89.66	89.29	0.42†
Oxygen, %		25.00	33.33	72.41	17.86	0.49†
Symptoms						
mMRC		3 (2, 3)	3 (2, 3)	3 (2, 3)	3 (2, 3)	0.80‡
SGRQ	*total*	56.56 ± 14.61	57.41 ± 10.94	59.98 ± 18.47	52.57 ± 10.78	0.16
	symptoms	53.46 ± 19.83	57.90 ± 18.63	52.79 ± 21.88	51.78 ± 18.54	0.62
	impacts	43.19 ± 18.84	43.98 ± 12.27	48.83 ± 24.35	36.93 ± 12.84	0.74
	activity	81.05 ± 13.88	80.28 ± 16.12	82.62 ± 15.02	79.84 ± 11.54	0.06
Lung function						
FEV_1, L		0.79 ± 0.28	0.93 ± 0.41	0.79 ± 0.23	0.71 ± 0.22	0.06
FEV_1, %		29.89 ± 8.69	31.64 ± 11.85	29.28 ± 7.80	29.56 ± 7.73	0.68
FVC, L		3.00 ± 0.85	3.20 ± 1.01	3.06 ± 0.65	2.83 ± 0.93	0.35
FVC, %		90.18 ± 15.78	87.54 ± 19.57	89.57 ± 12.42	92.21 ± 16.85	0.64
FEV1/FVC, %		25.86 ± 6.19	28.78 ± 8.03	24.94 ± 4.99	25.22 ± 5.90	0.12
MEF25-75%, L/s		0.21 ± 0.11	0.28 ± 0.20	0.20 ± 0.06	0.19 ± 0.05	**0.04**
RV, L		5.22 ± 1.19	5.51 ± 1.71	5.15 ± 0.96	5.14 ± 1.10	0.58
RV, %		236.30 ± 43.59	253.10 ± 59.90	231.00 ± 41.93	232.70 ± 33.35	0.24
TLC, L		8.27 ± 1.66	8.71 ± 2.09	8.29 ± 1.20	8.01 ± 1.81	0.42
TLC, %		141.00 ± 13.41	140.50 ± 18.77	139.90 ± 12.57	142.30 ± 11.11	0.79
RV/TLC		63.17 ± 7.16	62.79 ± 10.89	62.12 ± 6.32	64.46 ± 5.39	0.46
IC		1.98 ± 0.58	2.01 ± 0.64	2.06 ± 0.55	1.90 ± 0.58	0.59

	Combined cohort	LVRS	Valve	Coil	Group comparison
R_{aw}, kPA/L/s	1.03 ± 0.56	0.88 ± 0.44	1.05 ± 0.54	1.09 ± 0.64	0.50
G_{aw}, kPA/L/s	0.25 ± 0.14	0.27 ± 0.20	0.27 ± 0.15	0.23 ± 0.08	0.45
TLCOc, mmol/min/kPA	2.82 ± 0.96	3.13 ± 1.01	2.83 ± 0.98	2.62 ± 0.88	0.30
TLCOc, %	33.58 ± 9.34	33.93 ± 7.94	33.85 ± 10.31	33.03 ± 9.26	0.94
KCOc, mmol/min/kPA	0.63 ± 0.17	0.68 ± 0.14	0.63 ± 0.18	0.60 ± 0.17	0.39
KCOc, %	42.51 ± 11.24	44.33 ± 9.46	43.28 ± 12.75	40.47 ± 10.37	0.54
pH	7.44 ± 0.03	7.44 ± 0.02	7.44 ± 0.02	7.44 ± 0.03	0.75
PCO_2	5.04 ± 0.64	4.94 ± 0.54	5.05 ± 0.61	5.08 ± 0.73	0.81
PO_2	9.32 ± 1.25	9.76 ± 1.14	9.04 ± 1.04	9.35 ± 1.44	0.22
HCO_3	25.02 ± 2.63	24.34 ± 2.34	25.29 ± 2.68	25.10 ± 2.75	0.55
Static compliance, L/cm H_20	3.46 ± 2.80	3.10 ± 1.56	3.76 ± 2.88	3.30 ± 2.97	0.76
Exercise capacity					
6MWD, meters	333.90 ± 106.80	343.70 ± 107.60	324.00 ± 114.10	338.90 ± 101.50	0.81
CT metrics					
Total Lung Vol_{insp}, ml	6830 ± 1519	7401 ± 2146	6948 ± 1086	6432 ± 1500	0.23
Total Lung Vol_{exp}, ml	5422 ± 1399	5915 ± 1828	5649 ± 1003	5072 ± 1437	0.22
Total Lung DS, % (-950insp)	39 (32, 42)	41 (39, 47)	41 (34, 42)	33 (26, 39)	**<0.01**‡
Total Lung DS, % (-856exp)	76 (70, 79)	77 (74, 84)	74 (65, 80)	76 (70, 78)	0.28‡
fGT, %	44 (41, 48)	42 (39, 46)	43 (37, 45)	46 (42, 53)	**0.02**‡
Total Lung Vessel Vol, ml	183 (149, 220)	188 (165, 245)	199 (170, 227)	151 (117, 183)	**<0.01**‡
PA ratio	0.81 (0.73, 0.88)	0.79 (0.70, 0.92)	0.85 (0.78, 0.88)	0.78 (0.71, 0.83)	0.15‡
Mortality Score					
BODE Index	5 (4, 7)	5 (4, 6)	6 (4, 7)	5 (4, 7)	0.83
Inflammatory marker					
White cell count, 10^9/L	8.19 ± 2.14	8.33 ± 2.18	7.84 ± 2.01	8.48 ± 2.27	0.52
Fibrinogen, mg/dL	3.59 ± 0.66	3.30 ± 0.26	3.45 ± 0.73	3.76 ± 0.62	0.14
C-reactive protein, mg/dL	4.15 ± 6.06	2.64 ± 2.06	3.60 ± 4.98	5.39 ± 7.91	0.33

Categorical data are presented as a frequency (%) and compared using a Chi-square test† (nominal) or Kruskal-Wallis test‡ (ordinal). Parametric continuous data are presented as mean ± SD and compared using a one-way ANOVA unless otherwise stated. Non-parametric continuous data are presented as median (IQR) and compared using a Kruskal-Wallis test‡. BMI, Body Mass Index; BODE index = Body mass index, airflow Obstruction, Dyspnoea, and Exercise capacity; c, corrected for haemoglobin concentration; DS, Destruction Score; FEV_1, Forced Expiratory Volume in 1 second; FVC, Forced Vital Capacity; HCO_3, Bicarbonate; G_{aw}, airways conductance; IC, Inspiratory Capacity; K_{CO}, carbon monoxide diffusing capacity per unit alveolar volume; LVRS, lung volume reduction surgery; mMRC, modified Medical Research Council dyspnoea scale; PCO_2, Partial pressure for carbon dioxide; PO_2, Partial pressure for oxygen; R_{aw}, airways resistance; RV, Residual Volume; SGRQ, St George's Respiratory Questionnaire; TLC, Total Lung Capacity; TL_{CO}, Transfer factor for carbon monoxide; Vol, Volume; 6MWD, Six-Minute Walk Distance.

Table 3.1. Baseline characteristics of patients.

Combined cohort

CT-total lung volume$_{insp}$ was very strongly correlated with TLC$_{pleth}$ (r=0.96; p<0.01) and CT-total lung volume$_{exp}$ strongly correlated with RV$_{pleth}$ (r=0.74; p<0.01), confirming quality management and substantiating a previous report using the LungSeg software platform[216]. (Figure 3.1).

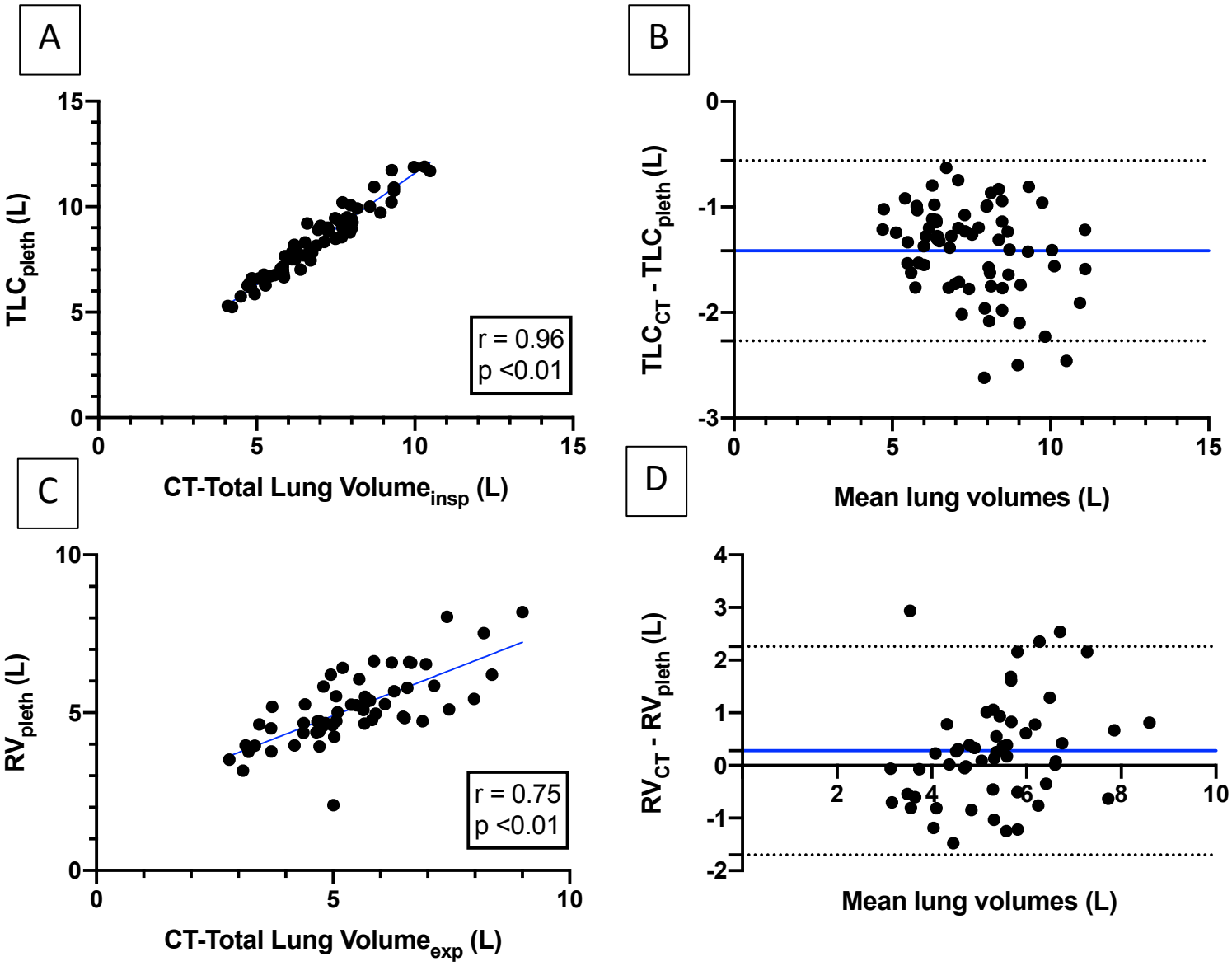

Figure 3.1. Relationships between CT-acquired and plethysmography-derived lung volumes.

TLC$_{CT}$ and TLC$_{pleth}$ correlation (**A**) and Bland-Altman (**B**) plots. RV$_{CT}$ and RV$_{pleth}$ correlation (**C**) and Bland-Altman (**D**) plots.

Lung volume reduction surgery (LVRS)

Baseline characteristics

15 patients were enrolled: mean age 58.5 ± 12.1 years, 60% male, 34 pack year smoking history, and two exacerbations in the preceding 12 months. 13% were classified as GOLD grade II, 27% III and 60% IV. Questionnaires recorded a mMRC of 3 (2, 3) and SGRQ-total of 57.4 ± 10.9 points. The cohort demonstrated severe airflow obstruction, FEV1 31.6 ± 11.9%, and hyperinflation, RV 253.1 ± 59.9%. Lung function, exercise capacity and quantitative CT (qCT) parameters are detailed in Table 3.1.

Changes in characteristics at 3-months

At 3-months, a reduction in mMRC of 1 (p<0.01) and in SGRQ-total of 17.57 points (<0.01) was observed. Improvements in FEV1 of +8.59% (p<0.01), FEV1/FVC of +5.26% (p=0.03), RV of -59.39% (p<0.01), TLC of -16.87% (p<0.01), RV/TLC of -7.93% (p<0.01), $G_{AW\text{-}total}$ of +0.17 kPA/L/s (p<0.01), 6MWD of +45.29 meters (p=0.02), and BODE index of -2 (p<0.01) were measured. qCT revealed decreases in total lung volume of -873.8 ± 428.3 (p<0.01), total gas trapping of 8% (p<0.01), and fGT of 6% (p<0.01). (Table 3.2).

CT-metric delta correlations

Focusing on those qCT metrics that were significantly changed at 3 months: Δ**CT-lung volume$_{INSP}$** was negatively related to ΔpH (r=-0.68; p=0.02); Δ**CT-856HU** was positively correlated with ΔmMRC (r=0.75; p=0.02) and negatively related to airways conductance (r=-0.85; p<0.01). (Figure 3.2 and Appendix B: Table S3.1).

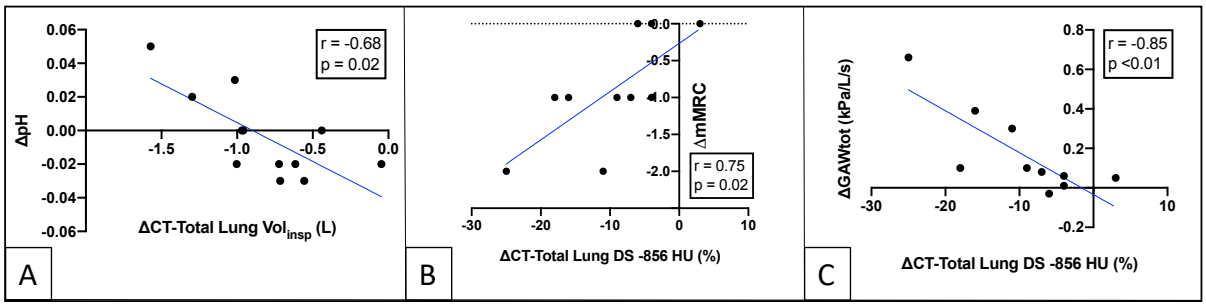

Figure 3.2. Delta correlations – surgery cohort.

CT-total lung volume$_{insp}$ with pH (**A**); CT-total lung density score at -856HU with mMRC (**B**) and with GAW$_{tot}$ (**C**).

Predictors of volume reduction

14 of 15 subjects (93%) achieved a ≥10% RV reduction (Table 3.3): binomial logistic regression using a two-component CT-metric model did not identify any baseline predictors. Input of additional variables was not possible owing to small numbers.

Overall impact of LVRS on lung structure

At 3 months, CT-total lung volume was reduced by a mean of 873.8mls ($p<0.01$) and accompanied by statistically significant reductions in total and functional gas trapping. The reduction in total gas trapping was inversely correlated with airways conductance. These findings suggest improved peripheral airways function as a consequence of architectural change following surgical resection of emphysematous tissue.

		LVRS difference	*p-value*	Valve difference	*p-value*	Coil difference	*p-value*	Group comparison *p-value*
Symptoms								
∆mMRC		-1	**<0.01**†	-1	**<0.01**†	0	**0.01**†	0.18‡
∆SGRQ	*Total score*	-17.57 ± 12.82 (95% CI: -24.67, -10.47)	**<0.01**	-9.41 ± 15.60 (95% CI: -15.34, -3.48)	**<0.01**	-5.82 ± 16.54 (95% CI: -12.50, 0.86)	0.08	0.07
	Symptoms	-17.80 ± 18.12 (95% CI: -27.83, -7.77)	**<0.01**	-1.17 ± 25.05 (95% CI: -10.70, 8.36)	0.80	0.55 ± 22.79 (95% CI: -8.65, 9.76)	0.90	0.09
	Activity	-15.61 ± 18.71 (95% CI: -25.97, -5.25)	**<0.01**	-10.26 ± 16.65 (95% CI: -16.59, -3.92)	**<0.01**	-8.41 ± 14.69 (95% CI: -14.34, -2.47)	**<0.01**	0.40
	Impacts	-18.32 ± 14.19 (95% CI: -26.18, -10.46)	**<0.01**	-11.18 ± 17.47 (95% CI: -17.82, -4.53)	**<0.01**	-6.08 ± 19.69 (95% CI: -14.03, 1.88)	0.13	0.11
Lung function								
∆FEV_1, L		0.26 ± 0.24 (95% CI: 0.13, 0.39)	**<0.01**	0.19 ± 0.20 (95% CI: 0.11, 0.26)	**<0.01**	0.04 ± 0.14 (95% CI: -0.02, 0.10)	0.19	**<0.01**
∆FEV_1, %		8.59 ± 7.17 (95% CI: 4.62, 12.56)	**<0.01**	7.59 ± 7.20 (95% CI: 4.80, 10.38	**<0.01**	1.85 ± 6.02 (95% CI: -0.58, 4.29)	0.13	**<0.01**
∆FVC, L		0.19 ± 0.43 (95% CI -0.05, 0.43)	0.10	0.33 ± 0.52 (95% CI: 0.12, 0.53)	**<0.01**	0.09 ± 0.35 (95% CI: -0.05, 0.24)	0.18	0.17
∆FVC, %		6.09 ± 13.02 (95% CI: -1.12, 13.30)	0.09	11.74 ± 15.23 (95% CI: 5.84, 17.65)	**<0.01**	2.62 ± 12.46 (95% CI: -2.41, 7.65)	0.29	0.06
∆FEV1/FVC, %		5.26 ± 8.56 (95% CI: 0.52, 10.00)	**0.03**	3.03 ± 3.79 (95% CI: 1.56, 4.50)	**<0.01**	0.38 ± 4.07 (95% CI: -1.27, 2.02)	0.64	**0.02**
∆MEF25-75%, L/s		0.15 ± 0.28 (95% CI: -0.01, 0.30)	0.06	0.05 ± 0.07 (95% CI: 0.02, 0.09)	**<0.01**	0.02 ± 0.08 (95% CI: -0.01, 0.06)	0.17	0.05
∆RV, L		-1.26 ± 0.58 (95% CI: -1.58, -0.94)	**<0.01**	-0.91 ± 0.66 (95% CI: -1.17, -0.66)	**<0.01**	-0.31 ± 0.60 (95% CI: -0.55, -0.07)	**0.01**	**<0.01**
∆RV, %		-59.39 ± 25.39 (95% CI: -73.46, -45.33)	**<0.01**	-40.66 ± 28.33 (95% CI: -51.43, -29.88)	**<0.01**	-15.12 ± 29.26 (95% CI: -26.94, -3.30)	**0.01**	**<0.01**
∆TLC, L		-1.02 ± 0.36 (95% CI: -1.22, -0.82)	**<0.01**	-0.61 ± 0.48 (95% CI: -0.80, 0.43)	**<0.01**	-0.18 ± 0.40 (95% CI: -0.34, -0.02)	**0.03**	**<0.01**
∆TLC, %		-16.87 ± 7.09 (95% CI: -20.80, -12.95)	**<0.01**	-9.81 ± 6.95 (95% CI: -12.45, -7.16	**<0.01**	-3.67 ± 9.26 (95% CI: -7.41, 0.07)	0.05	**<0.01**
∆RV/TLC		-7.93 ± 5.15 (95% CI: -10.78, -5.08)	**<0.01**	-7.04 ± 6.99 (95% CI: -9.70, -4.38)	**<0.01**	-2.58 ± 5.53 (95% CI: -482, -0.35)	**0.03**	**<0.01**
∆IC		0.13 ± 0.27	0.07	0.16 ± 0.40	0.05	-0.00 ± 0.28	0.99	0.20

	LVRS difference	*p-value*	Valve difference	*p-value*	Coil difference	*p-value*	Group comparison *p-value*
	(95% CI: -0.01, 0.28)		(95% CI: -0.00, 0.31)		(95% CI: -0.11, 0.11)		
∆R_{aw}, kPA/L/s	-0.17 ± 0.37	0.09	-0.19 ± 0.46	**0.04**	-0.04 ± 0.41	0.61	0.41
	(95% CI: -0.38, 0.03)		(95% CI: -0.37, -0.01)		(95% CI: -0.21, 0.12)		
∆G_{aw}, kPA/L/s	0.17 ± 0.19	**<0.01**	0.03 ± 0.10	0.18	0.02 ± 0.10	0.25	**<0.01**
	(95% CI: 0.06, 0.27)		(95% CI: -0.01, 0.06)		(95% CI: -0.02, 0.06)		
∆TLCOc, mmol/min/kPA	0.28 ± 0.65	0.13	0.17 ± 0.49	0.09	-0.18 ± 0.39	0.06	**<0.01**
	(95% CI: -0.09, 0.66)		(95% CI: -0.03, 0.36)		(95% CI: -0.37, 0.01)		
∆TLCOc, %	3.07 ± 6.53	0.10	2.22 ± 5.71	0.05	-1.98 ± 4.94	0.10	**0.03**
	(95% CI: -0.70, 6.84)		(95% CI: -0.04, 4.48		(95% CI: -436, 0.40)		
∆KCOc, mmol/min/kPA	0.02 ± 0.16	0.67	0.00 ± 0.07	0.89	-0.06 ± 0.08	**<0.01**	**<0.01**
	(95% CI: -0.07, 0.11)		(95% CI: -0.02, 0.03)		(95% CI: -0.10, -0.02)		
∆KCOc, %	1.04 ± 8.86	0.67	0.78 ± 4.89	0.41	-3.67 ± 4.71	**<0.01**	**0.03**
	(95% CI: -4.08, 6.15)		(95% CI: -1.16, 2.72		(95% CI: -5.94, -1.40)		
∆pH	0.00 ± 0.03	0.92	-0.00 ± 0.03	0.94	0.00 ± 0.04	0.92	0.99
	(95% CI: -0.02, 0.02)		(95% CI: -0.01, 0.01)		(95% CI: -0.02, 0.01)		
∆PCO_2	-0.13 ± 0.48	0.34	-0.15 ± 0.44	0.09	0.16 ± 0.50	0.13	0.05
	(95% CI: -0.40, 0.15)		(95% CI: -0.33, 0.02)		(95% CI: -0.05, 0.36)		
∆PO_2	0.44 ± 1.12	0.16	-0.27 ± 0.91	0.15	-0.44 ± 1.25	0.09	0.05
	(95% CI: -0.21, 1.09)		(95% CI: -0.63, 0.10)		(95% CI: -0.96, 0.07)		
∆HCO_3	-0.52 ± 2.54	0.46	-0.92 ± 1.52	**0.04**	0.94 ± 1.80	**0.02**	**<0.01**
	(95% CI: -1.99, 0.95)		(95% CI: -1.54, -0.31)		(95% CI: 0.20, 1.68)		
∆Static compliance, L/cm H_20	1.91 ± 1.66	0.18	0.01 ± 3.01	0.99	0.28 ± 3.33	0.71	0.49
	(95% CI: -2.22, 6.04)		(95% CI: -1.40, 1.42)		(95% CI: -1.28, 1.83)		
Exercise capacity							
∆6MWD, m	45.29 ± 63.19	**0.02**	44.28 ± 63.06	**<0.01**	4.04 ± 43.16	0.64	**0.02**
	(95% CI: 8.80, 81.77)		(95% CI: 20.29, 68.26)		(95% CI: -13.39, 21.47)		
CT metrics							
∆Total Lung Vol_{insp}, ml	-873.80 ± 428.3	**<0.01**	-577.00 ± 769.30	**<0.01**	-140.60 ± 298.80	**0.02**	**<0.01**
	(95% CI: -1133, -615)		(95% CI: -875, 279)		(95% CI: -261, -20)		
∆Total Lung Vol_{exp}, ml	-1297.00 ± 981.10	**<0.01**	-576.10 ± 529.40	**<0.01**	-34.60 ± 909.90	0.85	**<0.01**
	(95% CI: -1998, -595)		(95% CI: -848, -304)		(95% CI: -410, 341)		
∆Total Lung DS, % (-950insp)	-2.00	0.15†	-1.00	0.21†	-1.00	0.79†	0.35‡
∆Total Lung DS, % (-856exp)	-8.00	**<0.01**†	-5.61	**0.04**†	-1.00	0.89†	**<0.01**‡

	LVRS difference	*p-value*	Valve difference	*p-value*	Coil difference	*p-value*	Group comparison *p-value*
∆ fGT, %	-6.00	**<0.01**†	-4.61	0.10†	0.00	0.94†	**0.02**‡
∆Total Lung Vessel Vol, ml	-3.00	0.64†	6.00	0.09†	16.50	**<0.01**†	**<0.01**‡
∆PA ratio	0.01	0.85†	0.01	0.20†	0.02	0.38†	0.81‡
Mortality Score							
∆BODE Index	-2.00	**<0.01**†	-1.00	**<0.01**†	-0.50	**<0.01**†	**0.02**‡
Inflammatory marker							
∆WCC, 10^9/L	-0.96 ± 1.54 (95% CI: -1.86, -0.07)	0.04	0.32 ± 1.86 (95% CI: -0.43, 1.07)	0.39	-0.42 ± 2.01 (95% CI: -1.24, 0.39)	0.29	0.10
∆Fibrinogen, mg/dL	-0.08 ± 0.61 (95% CI: -1.04, 0.89)	0.82	-0.06 ± 0.51 (95% CI: -0.30, 0.19)	0.63	-0.05 ± 0.62 (95% CI: -0.31, 0.21)	0.69	0.93
∆CRP, mg/dL	3.50 ± 9.48 (95% CI: -1.97, 9.97)	0.19	7.22 ± 29.48 (95% CI: -5.53, 19.97	0.25	2.73 ± 23.98 (95% CI: -6.96, 12.42)	0.57	0.13

Paired categorical (ordinal) and non-parametric continuous data are compared using a Wilcoxon signed-rank test†, presented as a median of differences, and between three groups using a Kruskal-Wallis test‡. Paired parametric continuous data are compared using a t-test, presented as mean ± SD (95% CI), and between three groups using a one-way ANOVA unless otherwise stated. BMI, Body Mass Index; BODE index = Body mass index, airflow Obstruction, Dyspnoea, and Exercise capacity; c, corrected for haemoglobin concentration; DS, Destruction Score; FEV_1, Forced Expiratory Volume in 1 second; FVC, Forced Vital Capacity; HCO3, Bicarbonate; G_{aw}, airways conductance; IC, Inspiratory Capacity; K_{CO}, carbon monoxide diffusing capacity per unit alveolar volume; LVRS, lung volume reduction surgery; mMRC, modified Medical Research Council dyspnoea scale; PCO_2, Partial pressure for carbon dioxide; PO_2, Partial pressure for oxygen; R_{aw}, airways resistance; RV, Residual Volume; SGRQ, St George's Respiratory Questionnaire; TLC, Total Lung Capacity; TL_{CO}, Transfer factor for carbon monoxide; Vol, Volume; 6MWD, Six-Minute Walk Distance.

Table 3.2. Changes in clinical characteristics over 3-months.

		LVRS responder	LVRS non-responder	*p-value*
Demographics			*p-value*	
Number		14	1	
Age, years		59.86 ± 11.28	39	
Gender (male), %:		57.14	100	
BMI, kg/m^2		23.21 ± 3.51	21.70	
Active co-morbidities		2 (1, 2)	0	
Pack years		36.38 (25.75, 49.25)	23.75	
Exacerbations (last year)		2 (0, 3)	2	
GOLD grade, %	II	7	100	
	III	29	0	
	IV	64	0	
Heterogeneous, %		50	100	
Baseline medications				
LABA, %		93.00	0	
LAMA, %		86.00	100	
ICS, %		100	100	
Oxygen, %		35.71	0	
Symptoms				
mMRC		3 (2, 3)	2	
SGRQ	*total*	58.13 ± 10.97	47.32	
	symptoms	60.94 ± 15.00	15.43	
	impacts	43.62 ± 12.65	49.01	
	activity	81.77 ± 15.62	59.46	
Lung function				
FEV_1, L		0.83 ± 0.19	2.25	
FEV_1, %		29.46 ± 8.66	62.10	
FVC, L		3.10 ± 0.96	4.69	
FVC, %		86.20 ± 19.58	106.30	
FEV1/FVC, %		27.45 ± 6.40	47.35	
MEF25-75%, L/s		0.23 ± 0.06	0.98	
FRC, L		7.06 ± 1.86	4.39	
FRC, %		215.50 ± 33.41	142.30	
RV, L		5.75 ± 1.47	2.07	
RV, %		262.80 ± 48.37	117.10	
TLC, L		8.85 ± 2.09	6.82	
TLC, %		142.90 ± 16.79	106.10	
RV/TLC		65.11 ± 6.36	30.27	
IC		1.98 ± 0.65	2.43	
R_{aw}, kPA/L/s		0.78 ± 0.32	0.24	
G_{aw}, kPA/L/s		0.26 ± 0.09	1.13	
TLCOc, mmol/min/kPA		3.10 ± 1.05	3.48	
TLCOc, %		34.15 ± 8.22	31.10	
KCOc, mmol/min/kPA		0.69 ± 0.14	0.55	
KCOc, %		45.50 ± 8.73	29.10	
pH		7.44 ± 0.02	7.42	
PCO_2		5.01 ± 0.50	4.11	
PO_2		9.83 ± 1.16	8.86	
HCO_3		24.70 ± 2.00	19.70	
Static compliance, L/cm H_20		3.10 ± 1.56		

	LVRS responder	LVRS non-responder	*p-value*
Exercise capacity			
6MWD, meters	335.90 ± 107.10	453.00	
CT metrics			
Total Lung Vol_{insp}, ml	7531 ± 2187	5842	
Total Lung Vol_{exp}, ml	6016 ± 1909	5008	
Total Lung DS, % (-950insp)	41.0 (38.5, 43.8)	50.0	
Total Lung DS, % (-856exp)	77.0 (73.0, 84.0)	74.0	
fGT, %	42.0 (40.5, 46.5)	30.0	
Total Lung Vessel Vol, ml	187.0 (162.0, 234.5)	254.0	
PA ratio	0.81 ± 0.12	0.83	
Mortality Score			
BODE Index	5 (4, 6)	2	
Inflammatory marker			
White cell count, 10^9/L	8.24 ± 2.24	9.50	
Fibrinogen, mg/dL	3.30 ± 0.29	3.30	
C-reactive protein, mg/dL	2.46 ± 2.03	5.00	

Categorical data are presented as a frequency (%). Parametric continuous data are presented as mean ± SD. Non-parametric continuous data are presented as median (IQR). BMI, Body Mass Index; BODE index = Body mass index, airflow Obstruction, Dyspnoea, and Exercise capacity; c, corrected for haemoglobin concentration; DS, Destruction Score; FEV_1, Forced Expiratory Volume in 1 second; FVC, Forced Vital Capacity; HCO3, Bicarbonate; G_{aw}, airways conductance; IC, Inspiratory Capacity; K_{CO}, carbon monoxide diffusing capacity per unit alveolar volume; LVRS, lung volume reduction surgery; mMRC, modified Medical Research Council dyspnoea scale; PCO_2, Partial pressure for carbon dioxide; PO_2, Partial pressure for oxygen; R_{aw}, airways resistance; RV, Residual Volume; SGRQ, St George's Respiratory Questionnaire; TLC, Total Lung Capacity; TL_{CO}, Transfer factor for carbon monoxide; Vol, Volume; 6MWD, Six-Minute Walk Distance.

Table 3.3. Baseline characteristics of responders versus non-responders – surgery cohort.

[Responders were defined as those individuals who achieved RV reduction of ≥10% at 3 months].

Endobronchial valve (EBV)

Baseline characteristics

29 patients were enrolled: mean age 64.9 ± 8.8 years, 59% male, 45 pack year smoking history, and one exacerbation in the preceding 12 months. 43% were classified as GOLD grade III, 57% IV. Questionnaires recorded a mMRC of 3 (2, 3) and mean SGRQ-total of 59.98 ± 18.47 points. The cohort demonstrated severe airflow obstruction, FEV1 29.3 ± 7.8%, and hyperinflation, RV 231.0 ± 41.9%. Lung function, exercise capacity and quantitative CT parameters are detailed in Table 3.1.

Changes in characteristics at 3-months

At 3-months, a reduction in mMRC of 1 ($p<0.01$) and in SGRQ-total of 9.41 points (<0.01) was observed. Improvements in FEV1 of +7.59% ($p<0.01$), FEV1/FVC of +3.03% ($p<0.01$), $MEF_{25-75\%}$ of 0.05 ($P<0.01$), RV of -40.66% ($p<0.01$), TLC of -9.81% ($p<0.01$), RV/TLC of -7.04% ($p<0.01$), $R_{AW\text{-}total}$ of -0.19 kPA/L/s ($p=0.04$), HCO_3 of -0.92 ($p=0.04$), 6MWD of +44.28 meters ($p<0.01$), and BODE index of -1 ($p<0.01$) were recorded. qCT revealed decreases in total lung volume of 577.0 ± 769.3mls ($p<0.01$) and total gas trapping of 5.61% ($p=0.04$). (Table 3.2).

CT-metric delta correlations

Focusing on those qCT metrics that were significantly changed at 3 months: Δ**CT-lung volume$_{INSP}$** was negatively related to ΔMEF25-75% ($r=-0.49$; $p=0.03$) and positively correlated with ΔTLC ($r=0.40$; $p=0.03$); Δ**CT-lung volume$_{EXP}$** was negatively related to 6MWD ($r=-0.48$; $p=0.04$); Δ**CT-density score at -856 HU** was negatively related to Δgas transfer ($r=-0.56$; $p=0.02$) and Δ6MWD ($r=-0.55$; $p=0.02$). (Figure 3.3 and Appendix B: Table S3.2).

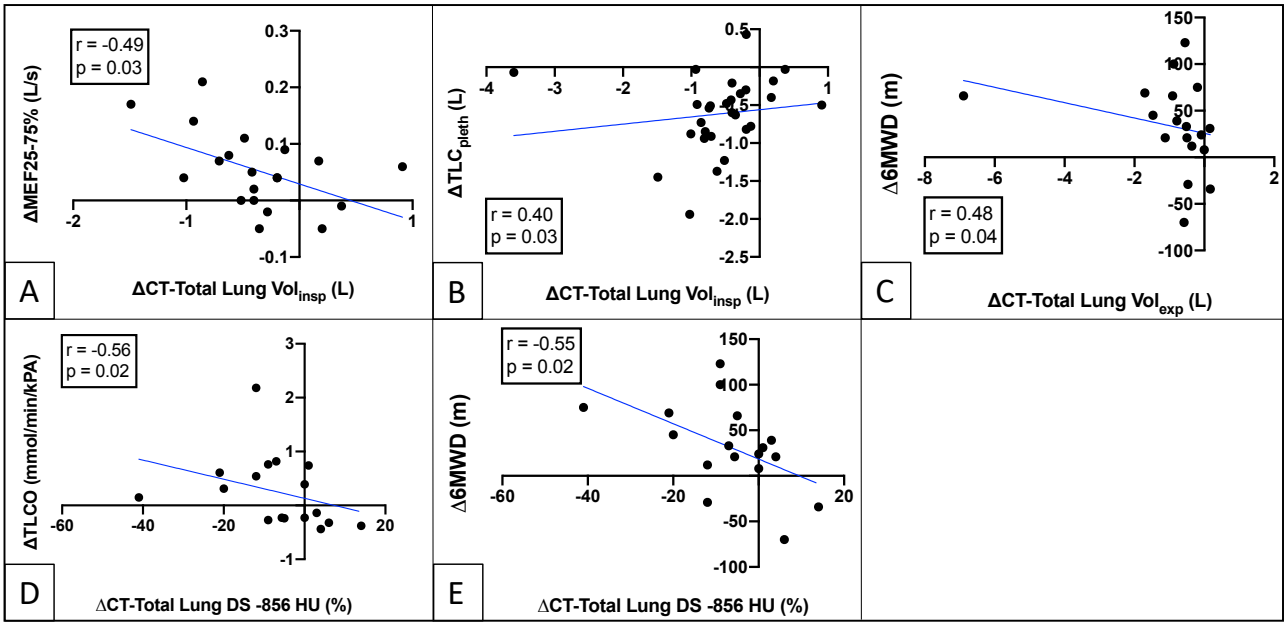

Figure 3.3. Delta correlations – valve cohort.

CT-total lung volume$_{insp}$ with MEF25-75% (**A**) and TLC$_{pleth}$ (**B**); CT-total lung volume$_{exp}$ with 6MWD (**C**); CT-total lung density score at -856 HU with TLCO (**D**) and 6MWD (**E**).

Predictors of volume reduction

18 of 29 subjects (62%) achieved a ≥10% reduction in RV. Responders were characterised at baseline by a lower gas transfer (p=0.02) and higher emphysema destruction scores (p=0.04). (Table 3.4). Binomial logistic regression did not identify any baseline predictors of a ≥10% reduction in RV.

Overall impact of EBV implantation on lung structure

At 3 months, CT-total lung volume$_{insp}$ was reduced by a mean of 577mls (p<0.01) and accompanied by modest decreases in CT-total gas trapping (p=0.04), which was negatively correlated with gas transfer and 6MWD. There was no discernible impact on CT-functional gas trapping, CT-emphysema destruction score or CT-vessel metrics. Collectively, these changes suggest a reduction in emphysematous gas trapping from deflation of diseased lung.

		Valve responder	Valve non-responder	*p-value*	Coil responder	Coil non-responder	*p-value*
Demographics						*p-value*	
Number		18	11		9	17	
Age, years		65.33 ± 8.10	64.09 ± 10.09	0.73	65.89 ± 12.62	67.00 ± 5.58	0.81
Gender (male), %:		61.11	54.54	1.00†	44.44	35.29	0.65†
BMI, kg/m^2		23.99 ± 4.04	25.69 ± 4.79	0.34	24.06 ± 3.94	24.31 ± 3.63	0.88
Active co-morbidities		2 (1, 3)	3 (1, 3)	0.39‡	1 (1, 2)	2 (1, 3)	0.45‡
Pack years		44.50 (30.50, 53.25)	46.00 (32.00, 54.00)	0.40‡	39.00 (15.30, 53.00)	42.00 (37.50, 54.75)	0.18‡
Exacerbations (last year)		3 (0, 3)	1 (1, 1)	0.15‡	1 (1, 2)	2 (0, 3)	0.50‡
GOLD grade, %	II	0	0	0.70‡	0	0	0.05‡
	III	39	50		66.67	23.53	
	IV	61	50		33.33	76.47	
Heterogeneous, %		52.94	36.36	0.39†	28.57	47.06	0.28†
Baseline medications							
LABA, %		94.44	90.91	1.00†	100.00	100.00	1.00†
LAMA, %		94.44	100.00	1.00†	100.00	100.00	1.00†
ICS, %		88.89	90.91	1.00†	88.89	88.24	0.96†
Oxygen, %		22.22	36.36	0.43†	11.11	17.65	0.66†
Symptoms							
mMRC		3 (2, 3)	2 (2, 3)	0.36‡	2 (2, 3)	3 (2, 3)	0.68‡
SGRQ	*total*	60.81 ± 21.08	58.61 ± 14.02	0.74	50.55 ± 11.14	51.91 ± 9.86	0.76
	symptoms	49.91 ± 23.32	57.50 ± 19.40	0.35	57.97 ± 19.90	49.01 ± 18.21	0.28
	impacts	51.00 ± 27.53	45.28 ± 18.71	0.51	34.29 ± 10.35	35.61 ± 12.13	0.77
	activity	82.91 ± 15.31	82.14 ± 15.24	0.90	74.44 ± 15.12	81.53 ± 8.11	0.22
Lung function							
FEV_1, L		0.76 ± 0.23	0.86 ± 0.24	0.28	0.83 ± 0.28	0.67 ± 0.17	0.13
FEV_1, %		28.18 ± 7.90	31.25 ± 7.61	0.33	35.27 ± 8.79	27.58 ± 5.46	**0.04**
FVC, L		2.97 ± 0.57	3.23 ± 0.77	0.37	2.77 ± 0.74	2.88 ± 1.05	0.75
FVC, %		88.01 ± 11.44	92.39 ± 14.20	0.42	92.98 ± 13.47	94.33 ± 17.48	0.83
FEV1/FVC, %		24.62 ± 5.78	25.52 ± 3.30	0.61	28.88 ± 5.50	23.58 ± 5.54	**0.03**
MEF25-75%, L/s		0.20 ± 0.06	0.22 ± 0.08	0.58	0.22 ± 0.06	0.17 ± 0.04	**0.02**
FRC, L		6.44 ± 0.96	6.02 ± 1.12	0.31	5.72 ± 1.21	6.09 ± 1.40	0.50
FRC, %		201.90 ± 26.07	190.4 ± 20.55	0.20	189.30 ± 18.18	202.40 ± 29.31	0.17
RV, L		5.35 ± 0.94	4.84 ± 0.97	0.18	4.98 ± 1.00	5.01 ± 1.04	0.95

	Valve responder	Valve non-responder	*p-value*	Coil responder	Coil non-responder	*p-value*
RV, %	238.80 ± 46.24	218.10 ± 31.56	0.16	232.20 ± 33.85	228.70 ± 33.00	0.80
TLC, L	8.36 ± 1.08	8.16 ± 1.43	0.69	7.73 ± 1.62	7.93 ± 1.88	0.78
TLC, %	141.10 ± 13.24	138.00 ± 11.74	0.52	141.30 ± 7.08	142.00 ± 13.16	0.86
RV/TLC	63.85 ± 6.18	59.30 ± 5.72	0.06	64.66 ± 3.89	63.74 ± 6.06	0.64
IC	1.98 ± 0.58	2.19 ± 0.49	0.32	2.02 ± 0.60	1.84 ± 0.62	0.48
R_{aw}, kPA/L/s	0.94 ± 0.44	0.78 ± 0.35	0.29	0.73 ± 0.24	0.96 ± 0.46	0.10
G_{aw}, kPA/L/s	0.24 ± 0.15	0.27 ± 0.11	0.52	0.33 ± 0.11	0.24 ± 0.08	0.07
TLCOc, mmol/min/kPA	2.48 ± 0.74	3.45 ± 1.09	**0.03**	2.71 ± 1.17	2.61 ± 0.71	0.81
TLCOc, %	30.17 ± 8.24	40.47 ±10.73	**0.02**	35.09 ± 10.82	32.33 ± 8.31	0.53
KCOc, mmol/min/kPA	0.58 ± 0.13	0.73 ± 0.23	0.06	0.66 ± 0.15	0.57 ± 0.19	0.22
KCOc, %	39.61 ±9.99	49.89 ± 14.96	0.07	45.34 ± 9.41	37.13 ± 10.07	0.07
pH	7.44 ± 0.03	7.45 ± 0.02	0.09	7.45 ± 0.03	7.44 ± 0.03	0.56
PCO_2	5.11 ± 0.61	4.94 ± 0.62	0.51	4.69 ± 0.56	5.28 ± 0.78	**0.04**
PO_2	8.99 ± 1.06	9.14 ± 1.06	0.74	9.54 ± 0.80	9.24 ± 1.73	0.56
HCO_3	25.36 ± 2.53	25.14 ± 3.10	0.86	23.68 ± 2.45	25.98 ± 2.77	**0.04**
Static compliance, L/cm H_20	3.88 ± 3.27	3.59 ± 2.44	0.82	3.01 ± 2.05	3.59 ± 3.49	0.92
Exercise capacity						
6MWD, meters	300.00 ± 114.60	363.40 ± 106.70	0.15	340.30 ± 107.30	341.90 ± 93.48	0.97
CT metrics						
Total Lung Vol_{insp}, ml	7020 ± 963	6837 ± 1296	0.69	6239 ± 1400	6504 ± 1623	0.67
Total Lung Vol_{exp}, ml	5570 ± 927	5767 ± 1163	0.69	4845 ± 1165	5185 ± 1622	0.55
Total Lung DS, % (-950insp)	42.0 (35.5, 42.0)	35.0 (29.0, 41.0)	**0.04**‡	39.0 (21.5, 42.0)	31.0 (24.5, 38.5)	0.26‡
Total Lung DS, % (-856exp)	77.0 (65.0, 81.0)	71.0 (62.3, 76.3)	0.26‡	77.0 (67.0, 78.5)	74.0 (69.5, 78.5)	0.80‡
fGT, %	43.0 (37.0, 46.0)	42.5 (36.3, 44.8)	0.79‡	44.0 (41.0, 52.5)	46.0 (42.5, 53.5)	0.59‡
Total Lung Vessel Vol, ml	194.0 (163.0, 224.5)	206.0 (188.0, 228.0)	0.65‡	149.0 (114.5, 201.5)	160.0 (130.5, 190.0)	0.45‡
PA ratio	0.85 (0.81, 0.88)	0.84 (0.72, 0.88)	0.55‡	0.74 (0.71, 0.80)	0.79 (0.73, 0.91)	0.19‡
Mortality Score						
BODE Index	6 (5, 7)	5 (4, 6)	0.10‡	4 (4, 7)	5 (5, 7)	0.30‡
Inflammatory marker						
White cell count, 10^9/L	8.32 ± 2.04	7.08 ± 1.80	0.10	7.99 ± 1.50	8.59 ± 2.05	0.40
Fibrinogen, mg/dL	3.42 ± 0.36	3.49 ± 1.11	0.86	3.39 ± 0.53	3.94 ± 0.60	**0.03**
C-reactive protein, mg/dL	3.07 ± 3.08	4.40 ± 7.07	0.59	3.22 ± 3.15	6.94 ± 9.69	0.16

Categorical data are presented as a frequency (%) and compared using a Fisher's exact test † (nominal) or Mann-Whitney test‡ (ordinal). Parametric continuous data are presented as mean ± SD and compared using an independent t-test unless otherwise stated. Non-parametric continuous data are presented as median (IQR) and compared using a Mann-Whitney test‡. BMI, Body Mass Index; BODE index = Body mass index, airflow Obstruction, Dyspnoea, and Exercise capacity; c, corrected for

	Valve responder	Valve non-responder	*p-value*	Coil responder	Coil non-responder	*p-value*

haemoglobin concentration; DS, Destruction Score; FEV_1, Forced Expiratory Volume in 1 second; FVC, Forced Vital Capacity; HCO3, Bicarbonate; G_{aw}, airways conductance; IC, Inspiratory Capacity; K_{CO}, carbon monoxide diffusing capacity per unit alveolar volume; mMRC, modified Medical Research Council dyspnoea scale; PCO_2, Partial pressure for carbon dioxide; PO_2, Partial pressure for oxygen; R_{aw}, airways resistance; RV, Residual Volume; SGRQ, St George's Respiratory Questionnaire; TLC, Total Lung Capacity; TL_{CO}, Transfer factor for carbon monoxide; Vol, Volume; 6MWD, Six-Minute Walk Distance.

Table 3.4. Baseline characteristics of responders versus non-responders – valve & coil cohorts.

[Responders were defined as those individuals who achieved RV reduction of ≥10% at 3 months].

Endobronchial coil (EBC)

Baseline characteristics

28 patients were enrolled: mean age 66.9 ± 8.2 years, 43% male, 42 pack year smoking history, and two exacerbations in the preceding 12 months. 36% were classified as GOLD grade III, 64% IV. Questionnaires recorded a mMRC of 3 (2, 3) and SGRQ-total of 52.6 ± 10.8 points. The cohort demonstrated severe airflow obstruction, FEV1 29.6 ± 7.7%, and hyperinflation, RV 232.7 ± 33.4%. Lung function, exercise capacity and quantitative CT parameters are detailed in Table 3.1.

Changes in characteristics at 3-months

At 3-months, a reduction in SGRQ-activity of 8.41 points (<0.01) was observed. Improvements in RV of -15.12% (p=0.01), RV/TLC of -2.58% (p=0.03), KCO of -3.67% (p<0.01), HCO_3 of +0.94 (p=0.02), and BODE index of -0.5 (p<0.01) were recorded. qCT measured a median increase in total lung vessel volume of 16.5mls (p<0.01). (Table 3.2).

CT-metric delta correlations

Focusing on those qCT metrics that were significantly changed at 3 months: there were no relevant delta correlations. (Appendix B: Table S3.3).

Predictors of volume reduction

9 of 26 subjects achieved a ≥10% reduction in RV. Responders were characterised by higher baseline FEV1% (p=0.04), MEF25-75% (p=0.02), and lower pCO_2, HCO_3, and fibrinogen levels. (Table 3.4). Binomial logistic regression did not identify any baseline predictors of a ≥10% reduction in RV.

Overall impact of EBC implantation on lung structure

At 3 months, a small but statistically significant reduction in mean CT-total lung $volume_{insp}$ of -140.6mls (p=0.02) was measured and accompanied by an increase in CT-total vessel volume (p<0.01). No impact on emphysema destruction score, gas trapping or PA ratio was observed. The comparative lack of volume reduction achieved using this technique may explain the fewer correlations.

Group comparisons

Baseline characteristics

There were no significant differences between surgery and valve cohorts (Tables 3.1 and 3.6).

The surgery cohort had higher baseline values compared to the coil cohort for $MEF_{25-75\%}$ (0.28 versus 0.19 L/s; p=0.03), total lung emphysema score (41 versus 33%; p<0.01), and vessel volume (188 versus 151mls; p=0.01).

The valve cohort had lower baseline fGT (42 versus 46%; p=0.03) but higher vessel volume (188 versus 151mls; p<0.01) compared to the coil cohort.

Changes in characteristics at 3-months

The surgery cohort achieved greater mean improvements compared to the valve cohort in TLC% (-7.07; p=0.02) and $G_{AW\text{-}total}$ (+0.14; p<0.01). (Tables 3.2 and 3.7).

The surgery cohort achieved greater mean improvements compared to the coil cohort in SGRQ-symptoms (-18.35; p=0.04), FEV1% (+6.73; p<0.01), FEV1/FVC (+4.88; p=0.02), $MEF_{25-75\%}$ (+0.12; p=0.04), RV% (-44.27; p<0.01), TLC% (-13.20; p<0.01), $G_{AW\text{-}total}$ (+0.03; p<0.01), TLCO (+0.73; p<0.01), BODE index (-17.32; p=0.02), CT-total lung $volume_{insp}$ (-733.2mls; p<0.01), CT-air trapping (-18.26%; p<0.01), and CT-vessel volume (-19.53mls; p<0.01).

The valve cohort achieved greater mean improvements compared to the coil cohort in FEV1% (+5.74; p<0.01), RV% (-25.54; p<0.01), TLC% (-6.13; p=0.02), RV/TLC (-4.46; p=0.02), TLCO% (+5.22; p=0.03), KCO% (+4.45; p=0.04), HCO_3 (-1.86; p<0.01), 6MWD (+40.24 meters; p=0.03), and CT-total lung $volume_{insp}$ (-436.4mls; p<0.01).

		Group *p-value*	LVRS versus Valve difference	*p-value*	LVRS versus Coil difference	*p-value*	Valve versus Coil difference	*p-value*
Demographics								
Age, years		0.05	-6.40 (95% CI: -16.58, 3.79)	0.22	-8.43 (95% CI: -18.56, 1.71)	0.07	-2.03 (95% CI: -8.17, 4.11)	0.75
Gender (male), %		0.40†						
BMI, kg/m^2		0.44	-1.53 (95% CI: -4.85, 1.80)	0.50	-0.78 (95% CI: -3.96, 2.40)	0.87	0.75 (95% CI: -2.19, 3.69)	0.86
Active co-morbidities		0.35‡	-8.93	0.50	-3.69	1.00	5.24	1.00
Pack years		0.49‡	-7.72	0.74	-6.49	1.00	1.23	1.00
Exacerbations		0.90‡	-1.73	1.00	-3.01	1.00	-1.28	1.00
GOLD grade, %		0.80‡	-0.88	1.00	-3.35	1.00	-2.64	1.00
Heterogeneous, %		0.84†						
Baseline medications								
LABA, %		0.18†						
LAMA, %		0.11†						
ICS, %		0.42†						
Oxygen, %		0.49†						
Symptoms								
mMRC		0.80‡	0.18	1.00	3.16	1.00	2.98	1.00
SGRQ	*Total Score*	0.16	-2.57 (95% CI: -13.56, 8.42)	0.84	4.84 (95% CI: -6.22, 15.90)	0.55	7.42 (95% CI: -1.74, 16.57)	0.14
	Symptoms	0.62	5.11 (95% CI: -10.11, 20.33)	0.70	6.12 (95% CI: -9.19, 21.43)	0.61	1.01 (95% CI: -11.67, 13.68)	0.98
	Activity	0.74	-2.34 (95% CI: -13.01, 8.34)	0.86	0.44 (95% CI: -10.30, 11.18)	0.99	2.78 (95% CI: -6.12, 11.67)	0.74
	Impacts	0.06	-4.86 (95% CI: -18.82, 9.10)	0.68	7.05 (95% CI: -7.00, 21.09)	0.46	11.90 (95% CI: 0.28, 23.53)	**0.04**
Lung function								
FEV_1, L		0.06	0.13 (95% CI: -0.07, 0.34)	0.28	0.21 (95% CI: 0.00, 0.42)	0.05	0.08 (95% CI: -0.10, 0.25)	0.54
FEV_1, %		0.68	2.37 (95% CI: -4.35, 9.08)	0.68	2.08 (95% CI: -4.64, 8.80)	0.74	-0.28 (95% CI: -5.89, 5.33)	0.99
FVC, L		0.35	0.14 (95% CI -0.51, 0.79)	0.86	0.38 (95% CI: -0.28, 1.03)	0.36	0.23 (95% CI: -0.31, 0.78)	0.56
FVC, %		0.64	-2.03 (95% CI: -14.22, 10.16)	0.92	-4.67 (95% CI: -16.87, 7.52)	0.63	-2.64 (95% CI: -12.83, 7.54)	0.81
FEV1/FVC, %		0.12	3.84 (95% CI: -0.82, 8.50)	0.13	3.56 (95% CI: -1.10, 8.22)	0.17	-0.28 (95% CI: -4.17, 3.62)	0.98
MEF25-75%, L/s		**0.04**	0.07 (95% CI: -0.02, 0.16)	0.15	0.09 (95% CI: 0.01, 0.17)	**0.03**	0.02 (95% CI: -0.06, 0.10)	0.83
RV, L		0.58	0.35 (95% CI: -0.56, 1.27)	0.62	0.37 (95% CI: -0.55, 1.29)	0.60	0.02 (95% CI: -0.74, 0.78)	1.00
RV, %		0.24	22.13 (95% CI: -10.88, 55.13)	0.25	20.39 (95% CI: -12.81, 53.60)	0.31	-1.74 (95% CI: -29.23, 25.76)	0.99
TLC, L		0.42	0.43 (95% CI: -0.83, 1.69)	0.70	0.71 (95% CI: -0.57, 1.98)	0.38	0.28 (95% CI: -0.77, 1.33)	0.80
TLC, %		0.79	0.53 (95% CI: -9.80, 10.86)	0.99	-1.88 (95% CI: -12.27, 8.52)	0.90	-2.40 (95% CI: -11.01, 6.20)	0.78
RV/TLC		0.46	0.66 (95% CI: -4.81, 6.14)	0.95	-1.67 (95% CI: -7.18, 3.83)	0.75	-2.34 (95% CI: -6.90, 2.23)	0.44
IC		0.59	-0.05 (95% CI: -0.50, 0.40)	0.96	0.11 (95% CI: -0.34, 0.55)	0.84	0.16 (95% CI: -0.22, 0.53)	0.57
R_{aw}, kPA/L/s		0.50	-0.17 (95% CI: -0.60, 0.26)	0.60	-0.21 (95% CI: -0.64, 0.23)	0.49	-0.03 (95% CI: -0.39, 0.33)	0.98

	Group *p-value*	LVRS versus Valve difference	*p-value*	LVRS versus Coil difference	*p-value*	Valve versus Coil difference	*p-value*
G_{aw}, kPA/L/s	0.45	-0.00 (95% CI: -0.11, 0.11)	1.00	0.04 (95% CI: -0.07, 0.15)	0.63	0.05 (95% CI: -0.05, 0.14)	0.46
TLCOc, mmol/min/kPA	0.30	0.30 (95% CI: -0.45, 1.05)	0.60	0.51 (95% CI: -0.27, 1.28)	0.26	0.21 (95% CI: -0.44, 0.85)	0.72
TLCOc, %	0.94	0.08 (95% CI: -7.38, 7.53)	1.00	0.90 (95% CI: -6.82, 8.62)	0.96	0.82 (95% CI: -5.58, 7.23)	0.95
KCOc, mmol/min/kPA	0.39	0.04 (95% CI: -0.09, 0.18)	0.71	0.08 (95% CI: -0.06, 0.22)	0.36	0.04 (95% CI: -0.08, 0.15)	0.75
KCOc, %	0.54	1.05 (95% CI: -7.84, 9.94)	0.96	3.86 (95% CI: -5.34, 13.06)	0.58	2.81 (95% CI: -4.83, 10.45)	0.65
pH	0.75	-0.01 (95% CI: -0.03, 0.02)	0.76	-0.00 (95% CI: -0.02, 0.02)	0.96	0.00 (95% CI: -0.01, 0.02)	0.85
PCO_2	0.81	-0.11 (95% CI: -0.62, 0.41)	0.87	-0.14 (95% CI: -0.64, 0.37)	0.80	-0.03 (95% CI: -0.45, 0.40)	0.99
PO_2	0.22	0.72 (95% CI: -0.26, 1.70)	0.19	0.41 (95% CI: -0.56, 1.38)	0.57	-0.31 (95% CI: -1.12, 0.50)	0.63
HCO_3	0.55	-0.95 (95% CI: -3.05, 1.16)	0.53	-0.76 (95% CI: -2.84, 1.32)	0.66	0.19 (95% CI: -1.54, 1.92)	0.96
Static compliance, L/cm H_20	0.76	-0.65 (95% CI: -3.59, 2.28)	0.86	-0.20 ((95% CI: -3.06, 2.67)	1.00	0.45 (95% CI: -1.89, 2.80)	0.93
Exercise capacity							
6MWD, m	0.81	19.70 (95% CI: -62.56, 102.0)	0.83	4.81 (95% CI: -77.95, 87.56)	0.99	-14.89 (95% CI: -83.42, 53.63)	0.86
CT metrics							
Total Lung Vol_{insp}, ml	0.23	453.0 (95% CI: -1448, 2354)	0.85	969.3 (95% CI: 981.6, 2920)	0.40	516.3 (95% CI: -457.4, 1490)	0.38
Total Lung Vol_{exp}, ml	0.22	266.2 (95% CI: -1674, 2206)	0.96	842.7 (95% CI: -1135, 2820)	0.49	576.5 (95% CI: -403.9, 1557)	0.30
Total Lung DS, % (-950insp)	**<0.01**‡	9.01	0.52	22.34	**<0.01**	13.33	0.04
Total Lung DS, % (-856exp)	0.28‡	9.42	0.41	8.82	0.43	-0.60	1.00
fGT, %	**0.02**‡	1.70	1.00	-11.15	0.19	-12.85	**0.03**
Total Lung Ves Vol, ml	**<0.01**‡	2.18	1.00	19.24	**0.01**	17.06	**<0.01**
PA ratio	0.15‡	-6.91	0.89	3.30	1.00	10.21	0.17
Mortality Score							
BODE Index	0.83‡	-3.73	1.00	-1.34	1.00	2.39	1.00
Inflammatory marker							
WCC, 10^9/L	0.52	0.49 (95% CI: -1.20, 2.18)	0.76	-0.15 (95% CI: -1.84, 1.53)	0.97	-0.64 (95% CI: -2.03, 0.73)	0.50
Fibrinogen, mg/dL	0.14	-0.15 (95% CI: -0.92, 0.62)	0.89	-0.46 (95% CI: -1.22, 0.30)	0.31	-0.32 (95% CI: -0.76, 0.13)	0.21
CRP, mg/dL	0.33	-0.96 (95% CI: -5.80, 3.88)	0.88	-2.75 (95% CI: -7.50, 2.00)	0.35	-1.79 (95% CI: -5.78, 2.20)	0.53

Group comparisons of categorial data are made using a Chi-square test† (nominal) or Kruskal-Wallis test‡ (ordinal). Parametric continuous data are compared using a one-way ANOVA unless otherwise stated: Tukey's multiple comparisons test is presented as mean difference (95% confidence interval, CI). Non-parametric continuous data are compared using a Kruskal-Wallis test‡: Dunn's multiple comparisons test is presented as mean rank difference. BMI, Body Mass Index; BODE index = Body mass index, airflow Obstruction, Dyspnoea, and Exercise capacity; c, corrected for haemoglobin concentration; DS, Destruction Score; FEV_1, Forced Expiratory Volume in 1 second; FVC, Forced Vital Capacity; HCO3, Bicarbonate; G_{aw}, airways conductance; IC, Inspiratory Capacity; K_{CO}, carbon monoxide diffusing capacity per unit alveolar volume; LVRS, lung volume reduction surgery; mMRC, modified Medical Research Council dyspnoea scale; PCO_2, Partial pressure for carbon dioxide; PO_2, Partial pressure for oxygen; R_{aw}, airways resistance; RV, Residual Volume; SGRQ, St George's Respiratory Questionnaire; TLC, Total Lung Capacity; TL_{CO}, Transfer factor for carbon monoxide; Vol, Volume; 6MWD, Six-Minute Walk Distance.

Table 3.5. Group comparisons at baseline.

	Group *p-value*	LVRS versus Valve difference	*p-value*	LVRS versus Coil difference	*p-value*	Valve versus Coil difference	*p-value*
Symptoms							
∆mMRC	0.18‡	-7.93	0.57	-11.35	0.20	-3.42	1.00
∆SGRQ *Total Score*	0.07	-8.11 (95% CI: -19.87, 3.64)	0.23	-11.70 (95% CI: -23.69, 0.28)	0.06	-3.59 (95% CI: -13.57, 6.39)	0.67
Symptoms	0.09	-16.62 (95% CI: -34.08, 0.83)	0.07	-18.35 (95% CI: -36.15, -0.55)	**0.04**	-1.73 (95% CI: -16.55, 13.10)	0.96
Activity	0.40	-5.35 (95% CI: -17.86, 7.16)	0.56	-7.20 (95% CI: -19.96, 5.56)	0.37	-1.85 (95% CI: -12.48, 8.78)	0.91
Impacts	0.11	-7.14 (95% CI: -20.66, 6.37)	0.42	-12.25 (95% CI: -26.02, 1.53)	0.09	-5.10 (95% CI: -16.58, 6.38)	0.54
Lung function							
∆FEV_1, L	**<0.01**	0.07 (95% CI: -0.07, 0.22)	0.44	0.22 (95% CI: 0.07, 0.37)	**<0.01**	0.15 (95% CI: 0.02, 0.27)	**0.02**
∆FEV_1, %	**<0.01**	0.99 (95% CI: -4.20, 6.19)	0.89	6.73 (95% CI:1.47, 12.00)	**<0.01**	5.74 (95% CI: 1.32, 10.16)	**<0.01**
∆FVC, L	0.17	-0.13 (95% CI -0.47, 0.21)	0.62	0.10 (95% CI: -0.25, 0.44)	0.78	0.23 (95% CI: -0.06, 0.52)	0.15
∆FVC, %	0.06	-5.66 (95% CI: -16.22, 4.91)	0.41	3.47 (95% CI: -7.24, 14.17)	0.72	9.12 (95% CI: 0.13, 18.12)	0.05
∆FEV1/FVC, %	**0.02**	2.23 (95% CI: -1.81, 6.26)	0.39	4.88 (95% CI: 0.79, 8.97)	**0.02**	2.66 (95% CI: -0.78, 6.09)	0.16
∆MEF25-75%, L/s	0.05	0.09 (95% CI: -0.03, 0.22)	0.18	0.12 (95% CI: 0.00, 0.25)	**0.04**	0.03 (95% CI: -0.08, 0.14)	0.78
∆RV, L	**<0.01**	-0.35 (95% CI: -0.82, 0.13)	0.19	-0.95 (95% CI: -1.44, -0.47)	**<0.01**	-0.61 (95% CI: -1.01, -0.20)	**<0.01**
∆RV, %	**<0.01**	-18.73 (95% CI: -40.15, 2.69)	0.10	-44.27 (95% CI: -66.11, -22.43)	**<0.01**	-25.54 (95% CI: -43.72, -7.35)	**<0.01**
∆TLC, L	**<0.01**	-0.41 (95% CI: -0.73, -0.08)	**0.01**	-0.84 (95% CI: -1.17, 0.51)	**<0.01**	-0.44 (95% CI: -0.71, -0.16)	**<0.01**
∆TLC, %	**<0.01**	-7.07 (95% CI: -13.10, -1.03)	**0.02**	-13.20 (95% CI: -19.36, -7.05)	**<0.01**	-6.13 (95% CI: -11.26, -1.01)	**0.02**
∆RV/TLC	**<0.01**	-0.89 (95% CI: -5.55, 3.77)	0.89	-5.35 (95% CI: -10.10, -0.60)	**0.02**	-4.46 (95% CI: -8.42, -0.50)	**0.02**
∆IC	0.20	-0.02 (95% CI: -0.28, 0.23)	0.97	0.13 (95% CI: -0.12, 0.39)	0.43	0.16 (95% CI: -0.06, 0.37)	0.20
∆R_{aw}, kPA/L/s	0.41	0.01 (95% CI: -0.31, 0.34)	0.99	-0.13 (95% CI: -0.46, 0.20)	0.60	-0.15 (95% CI: -0.43, 0.13)	0.41
∆G_{aw}, kPA/L/s	**<0.01**	0.14 (95% CI: 0.05, 0.24)	**<0.01**	0.03 ± 0.10 (95% CI: -0.01, 0.06)	**<0.01**	0.00 (95% CI: -0.08, 0.08)	1.00
∆TLCOc, mmol/min/kPA	**<0.01**	0.04 (95% CI: -0.50, 0.58)	0.98	0.73 (95% CI: 0.16, 1.29)	**<0.01**	0.69 (95% CI: 0.21, 1.16)	**<0.01**
∆TLCOc, %	**0.03**	-0.16 (95% CI: -5.45, 5.13)	1.00	5.05 (95% CI: -0.64, 10.74)	0.09	5.22 (95% CI: 0.41, 10.02)	**0.03**
∆KCOc, mmol/min/kPA	**<0.01**	0.02 (95% CI: -0.09, 0.13)	0.93	0.14 (95% CI: 0.03, 0.25)	0.01	0.13 (95% CI: 0.03, 0.22)	**<0.01**
∆KCOc, %	**0.03**	0.25 (95% CI: -4.49, 5.00)	0.99	4.70 (95% CI: -0.37, 9.78)	0.07	4.45 (95% CI: 0.14, 8.76)	**0.04**
∆pH	0.99	0.00 (95% CI: -0.03, 0.03)	0.99	-0.00 (95% CI: -0.03, 0.03)	1.00	-0.00 (95% CI: -0.03, 0.02)	0.99
∆PCO_2	0.05	0.03 (95% CI: -0.35, 0.40)	0.98	-0.29 (95% CI: -0.66, 0.09)	0.18	-0.31 (95% CI: -0.63, 0.00)	0.06
∆PO_2	0.05	0.71 (95% CI: -0.16, 1.58)	0.13	0.88 (95% CI: 0.01, 1.76)	0.05	0.18 (95% CI: -0.56, 0.91)	0.83
∆HCO_3	**<0.01**	0.40 (95% CI: -1.10, 1.90)	0.80	-1.46 (95% CI: -2.97, 0.05)	0.06	-1.86 (95% CI: -3.13, -0.60)	**<0.01**
∆Cstat, L/cm H_20	0.49	1.90 (95% CI: -2.79, 6.59)	0.59	1.63 (95% CI: -3.06, 6.32)	0.68	-0.27 (95% CI: -2.66, 2.13)	0.96
Exercise capacity							
∆6MWD, m	**0.02**	1.01 (95% CI: -42.99, 45.01)	1.00	41.25 (95% CI: -3.57, 86.06)	0.08	40.24 (95% CI: 3.72, 76.75)	**0.03**
CT metrics							
∆Total Lung Vol_{insp}, ml	**<0.01**	-296.7 (95% CI: -818.8, 225.3)	0.32	-733.2 (95% CI: -1124, -342.5)	**<0.01**	-436.4 (95% CI: -873.7, 0.85)	**0.03**

	Group *p-value*	LVRS versus Valve difference	*p-value*	LVRS versus Coil difference	*p-value*	Valve versus Coil difference	*p-value*
∆Total Lung Vol_{exp}, ml	**<0.01**	-369.7 (95% CI: -1746, 1007)	0.83	-1262.0 (95% CI: -2338, -185.6)	**<0.01**	-892.2 (95% CI: -2072, 287.9)	0.11
∆Total Lung DS, % (-950insp)	0.35‡	-7.76	0.70	-9.29	0.47	-1.53	1.00
∆Total Lung DS, % (-856exp)	**<0.01‡**	-8.08	0.57	-18.26	**<0.01**	-10.18	0.10
∆ fGT, %	0.02‡	-6.00	0.99	-14.73	0.03	-8.72	0.21
∆Total Lung Ves Vol, ml	**<0.01‡**	-9.18	0.48	-19.53	**<0.01**	-10.35	0.14
∆PA ratio	0.81‡	-4.07	1.00	-1.96	1.00	2.11	1.00
Mortality Score							
∆BODE Index	**0.02‡**	-7.25	0.74	-17.32	**0.02**	-10.07	0.16
Inflammatory marker							
∆WCC, 10^9/L	0.10	-1.28 (95% CI: -2.77, 0.20)	0.10	-0.54 (95% CI: -2.02, 0.94)	0.66	0.74 (95% CI: -0.50, 1.98)	0.33
∆Fibrinogen, mg/dL	0.93	-0.19 (95% CI: -1.42, 1.05)	0.93	-0.18 (95% CI: -1.40, 1.04)	0.93	0.00 (95% CI: -0.68, 0.68)	0.93
∆CRP, mg/dL	0.13	2.21 (95% CI: -4.48, 8.91)	0.71	5.41 (95% CI: -1.17, 11.99)	0.13	3.20 (95% CI: -2.66, 9.06)	0.39

Parametric continuous data are compared using a one-way ANOVA unless otherwise stated: Tukey's multiple comparisons test is presented as mean difference (95% confidence interval, CI). Non-parametric continuous data are compared using a Kruskal-Wallis test‡: Dunn's multiple comparisons test is presented as mean rank difference. BMI, Body Mass Index; BODE index = Body mass index, airflow Obstruction, Dyspnoea, and Exercise capacity; c, corrected for haemoglobin concentration; Cstat, static compliance; DS, Destruction Score; FEV_1, Forced Expiratory Volume in 1 second; FVC, Forced Vital Capacity; HCO3, Bicarbonate; G_{aw}, airways conductance; IC, Inspiratory Capacity; K_{CO}, carbon monoxide diffusing capacity per unit alveolar volume; LVRS, lung volume reduction surgery; mMRC, modified Medical Research Council dyspnoea scale; PCO_2, Partial pressure for carbon dioxide; PO_2, Partial pressure for oxygen; R_{aw}, airways resistance; RV, Residual Volume; SGRQ, St George's Respiratory Questionnaire; TLC, Total Lung Capacity; TL_{CO}, Transfer factor for carbon monoxide; Vol, Volume; 6MWD, Six-Minute Walk Distance.

Table 3.6. Group comparisons at 3-months.

Discussion

The diagnosis and classification of COPD are based on spirometry and the clinical expression of the disease. It yields no analysis of the pathologies and the contributions of the anatomical components of the lungs. However, awareness of the complexity of the pathological process under the microscope and the advent of sophisticated techniques investigating structure and function are promoting understanding of the course of the disease and identification of sub-phenotypes[321, 322] distinguished by pathological processes affecting the airway, parenchymal and vascular structures and their interplay which has been termed the interdependence of the respiratory system[323]. qCT is a recent addition to the armamentarium enabling non-invasive investigation of structure. Each component can be thought of as an elastic structure whose properties influences the others with physiological and pathophysiological consequences. For example, in the individual with emphysema and hyperinflation, the loss of parenchymal structures responsible for passive elastic recoil in the lung during expiration impacts on the alveoli diminishing the transmural pressure or drive and on the small bronchioles resulting in a reduced calibre and increased resistance. The spatial heterogeneity of the disease gives rise to a complex uncoupling of these compartments contributing to airway dysfunction, impairment of gas exchange, and pulmonary hypertension. For the population studied, we will now discuss each of the compartments pathologically affected by COPD, as characterised using CT, and the impact of lung volume reduction on these individually.

Lung volume

Baseline CT-derived lung volumes of the three cohorts, defined by the prospective interventions, but combined for this purpose, correlated strongly with those obtained with whole body plethysmography, consistent with a previous report employing the LungSeg software platform[216]. A baseline total lung capacity of 141% and residual volume of 236% are commensurate with severe hyperinflation[159]. The changes in CT-derived lung volumes paralleled those of TLC_{pleth} and RV_{pleth} with surgery having the most profound impact, followed by valves and coils. CT-acquired lung volume

measurements appear to be reliable surrogates for plethysmography-derived values and could be used as radiological endpoints in lung volume reduction studies.

Emphysema score

The relationship between quantitative CT acquired emphysema score and histological severity has been shown to be consistent, particularly when a density mask of -950HU is applied[324-328]. Shroeder et al who studied 4062 subjects with a spectrum of COPD from GOLD grade I to IV showed that qCT measurements of inspiratory low attenuation areas at -950 HU were moderately correlated with spirometric impairment[219]. In contrast Washko et al analysed CT images obtained from 1094 patients enrolled in the National Emphysema Treatment Trial and found emphysematous lung destruction was a weak predictor of lung function and mechanics in individuals with severe emphysema[329]. However, the authors of the latter study suggested this might be an artefact of the homogeneity of their population who principally had severe emphysema and airflow limitation. Additionally, lung densitometry corrected for lung volume has been found a use in the follow-up of drug evaluation studies on pulmonary emphysema[330].

In our study, emphysema CT scores at -950HU corresponded to severe disease burden[219] and were not modified by lung volume reduction in the homogenous diseased lungs, nor, perhaps unexpectedly, in the heterogeneous diseased. However, interpretation of density is complicated by the mix of potentially conflicting contributions of volume depletion on resurrected lung and the homogeneity/heterogeneity of surrounding tissues.

Gas trapping

A density mask of -856 HU applied to an end-expiratory CT permits distinction and quantification of emphysematous and non-emphysematous gas trapping[219]. The latter, a feature of small airways disease, termed functional gas trapping (fGT) can be identified by registering inspiratory and expiratory images either as a part of a parametric response map[220] or mathematical algorithm[224].

Shroeder et al in 2013, examining more than 4000 CT scans made in expiration of individuals who were smokers, with and without chronic obstructive pulmonary disease (COPD), correlated total gas trapping with physiological measures of airway obstruction and their estimations of FEV1 compared favourably with those of spirometry[219]. In our study, baseline CT-total gas trapping was consistent with severe disease. Surgery and endobronchial valve emplacement were seen to reduce the burden of total gas trapping to a similar degree.

Small airways disease is now known to be a major component of early COPD but because of the large capacity is clinically reticent at this time[148]. Bhatt et al have shown that the contribution of small airways disease to decline in FEV1 is proportionately greatest in those individuals with mild-to-moderate COPD[95]. In our study, baseline levels of fGT were consistent with severe small airways disease burden[224]. The impact of lung volume reduction on fGT was evident with surgery alone, and whilst this may be seen only with substantial tissue resection, the absence of a signal in patients who achieved similar physiological outcomes using endobronchial valves suggests that deflation or removal of emphysematous tissue is the principal driver of benefit improving chest wall asynchrony[172] and diaphragmatic movement[176].

Vasculature

The reference range for CT-total intrapulmonary vessel volume has not been established in the literature for individuals with severe COPD. Sealant-based bronchoscopic lung volume reduction has been shown to enhance the intraparenchymal pulmonary vasculature and the volume of the lung distant from the targeted sites in patients with severe emphysema and hyperinflation[331]. In our study, a response in CT-intraparenchymal vessel volume was observed only in endobronchial coil recipients, the cohort in whom the least amount of volume reduction was achieved.

A CT pulmonary artery to aorta (CT-PA) ratio of greater than 1 outperforms echocardiography for diagnosing resting pulmonary hypertension in individuals with severe COPD[225]. In our population, the median PA ratio was 0.81. Interestingly, no effects of lung volume reduction were observed on CT-PA ratio, and whilst this may reflect the highly selected population of patients enrolled, is

supported by physiological studies performed 6 months after LVRS[332]. Unfortunately, transthoracic echocardiography was performed in a minority limiting the conclusions that can be drawn but one possible explanation is that the effects of lung volume reduction may be further downstream i.e., blood vessels smaller than 2mm in internal diameter. Howell et al who demonstrated in the excised lungs of dogs the existence of two vascular compartments, one consisting of relatively large vessels that increases in volume in response to inflation (corresponding to CT-vessel volume), and the other comprising smaller vessels that decreases in volume (for which we do not have a radiological correlate)[333]. They further hypothesised that the blood vessels are subject to the same elastic tractional forces as the bronchioles. Another possibility is that in individuals with severe emphysema and hyperinflation, large vessel remodelling may take longer than the duration of the follow-up period or that CT-PA may not be sensitive enough to haemodynamic change, as has been observed in a small cohort of six individuals with severe emphysema and established pulmonary hypertension who underwent bronchoscopic lung volume reduction[334].

Impact of individual lung volume reduction therapies

Surgery achieved the greatest degree of lung volume reduction and more than 90% of recipients attained the MCID of at least 10% reduction in RV. It was the only intervention to be accompanied by improvements in both total and functional gas trapping inferring improvement in small airways function. Emphysema with hyperinflation is the end-stage of the COPD spectrum with substantial loss of terminal bronchioles, destruction of the elastic scaffold maintaining patency of airways and facilitating passive recoil, and compromised tissue with functional potential[335]. The mechanically disadvantaged ventilatory pump is disencumbered by volume reduction, resurrecting functionally preserved tissue, and re-tensioning the remaining airway network[335]. This is conceptually attractive to explain the radiological impact of surgery on the small airways network, the principal site of airflow obstruction in COPD[20].

Valve implantation accomplished a reduction in total gas trapping without an accompanying signal in functional gas trapping suggesting the benefits observed related predominantly to deflation of

emphysematous lung tissue and relief of the mechanical pump, although diaphragmatic and chest wall function were not formally assessed in this study. The ultimate objective of surgery and of valve implantation is the same – and the three-month physiological outcomes were not overly dissimilar to surgery. One might speculate that the two techniques impact lung structure via different mechanisms, but a greater than two-fold reduction in CT-total lung $volume_{EXP}$ with surgery is a convincing alternative explanation. Indeed, only 62% of EBV recipients attained the MCID of ≥10% RV reduction. Coil implantation resulted in modest volume reduction, rather less than in previous trials such as RESET[207], and may be consequence of a more infirm cohort, burden of airway sampling using bronchoalveolar lavage (two lobes versus one), or employment of smaller size coils with less tensioning effects. Only 35% of subjects achieved the MCID of ≥10% RV reduction and 3-month physiological outcomes were disappointing. Interestingly, CT-intraparenchymal blood vessel volume was significantly increased post-intervention perhaps due to greater radial traction exerted by the coils on the surrounding parenchyma.

The role of quantitative CT as a biomarker for lung volume reduction

Volume reduction is undoubtedly the crucial objective[214] and the majority of studies have adopted CT-acquired measurements as the means of assessment [281, 335] not attempting to differentiate the contributions of the individual compartments, parenchymal, airway and vascular. In this study we have availed ourselves of the opportunity to do so with qCT which may contribute to understanding the disparity in outcomes of the techniques. To facilitate comparison, a reduction of at least 10% of RV has been adopted as the MCID – a percentage threshold was considered better tailored to the individual.

The greater lung volume reduction achieved in surgical patients included a contribution from the small airways compartment, which was not detected in those treated with valves or with coils. Endobronchial coil implantation made a modest impact with physiological volume reduction but not on radiological indices. qCT succeeds as a potential biomarker for confirming volume reduction and for evaluating the impact on the individual structural compartments – however, its predictive value

for therapeutic response is not established from this small dataset. We also anticipate the opportunity of greater insights as the resolution of CT is improved.

Limitations

The study was small and comprised individuals mostly with severe emphysema and hyperinflation. Volume reduction was not universally achieved, particularly with endobronchial coils. The relative homogeneity of lung function within a cohort of selected individuals with severe airflow obstruction and hyperinflation limits extrapolation of the data and requires further validation in more heterogeneous populations exhibiting a spectrum of disease severity to establish robust qCT reference ranges.

Patient cooperation acquiring images for qCT is critical demanding intensive coaching by the imaging technician, but in such a physiologically compromised cohort challenging to achieve. Madani et al illustrated the importance of breathing technique and showed a submaximal inspiration induced underestimation of pulmonary emphysema[336]. These effects can be minimised by a factor of two using volume correction[330], which was not undertaken in this study. Furthermore, differences in reconstruction algorithm can strongly affect density mask results[337, 338] and the variation in protocols for a small group of individuals who had undergone CT imaging prior to referral to our specialist centre may have impacted on the results[339]. Current software platforms including LungSeg are unable to reliably distinguish emphysema subtypes such as centrilobular, paraseptal and panlobular patterns, and though scans are visually vetted by a thoracic radiologist, inclusion of patterns other than centrilobular may alter the behaviour of the lung to volume reduction therapies. Additionally, CT-total airway volume could not be reliably measured using the current version of LungSeg and had to be abandoned as a potential surrogate for spirometric-derived measures. Lastly, the global impact of lung volume reduction on lung structure was surveyed, and by doing so may have missed regional influences – however, an overall picture is arguably more valuable and relatable to the interdependence of the tri-compartment model of the lung.

Conclusions

In conclusion, CT quantitative imaging analysis is likely to prove complementary to disease phenotyping defined by lung function. Acknowledging the conflict of image resolution and radiation exposure, CT chest imaging is a widely available, safe, and cost-effective modality with which to characterise COPD and for assessing interventional outcomes, but further research in larger trials is needed to fully validate its potential as a predictive biomarker of therapeutic response.

CHAPTER 4: Impact of Lung Volume Reduction on Lung Function

This chapter evaluates the changes observed in large and small airways function after volume reductions achieved with each of the three validated procedures, surgical excision and deflation with endobronchial valves and with coils.

Abstract

Background – In the continued quest for a dependable biomarker to predict the response to lung volume reduction (LVR) procedures, we investigated the hypothesis that lung volume reduction will be accompanied by measurable changes in novel indices of small airways function that can be correlated with changes to the conventional clinical parameters and that reliable identifiers of baseline predictors of therapeutic response (reduction of residual volume of at least 10%) may be identified.

Methods – 72 consecutive subjects with severe emphysema and hyperinflation scheduled for lung volume reductions were recruited: Unilateral LVRS – 15; Endobronchial valve – 29, Endobronchial coil – 28. All underwent detailed clinical phenotyping comprising demographic, symptom score, CT-imaging, exercise capacity and lung function measurements during exacerbation-free periods at baseline and at three months after intervention. Small airways physiology (SAP) was evaluated using impulse oscillometry (IOS) and multiple breath nitrogen washout (MBNW) modalities.

Results – Surgery achieved the greatest lung volume reduction (LVR), $\triangle$residual volume of -1.26 ± 0.58 litres ($p<0.01$) and was the only intervention to be accompanied by improvements in IOS expiratory airways resistance at 5Hz, expiratory and within-breath reactance at 5 Hz, and peripheral resonant frequency. Together with decreases in total and functional gas trapping on computed tomography

(CT), these findings suggest improved peripheral airways function as a consequence of surgical resection of emphysematous tissue.

Valve implantations accomplished a △residual volume of -0.91 ± 0.66 litres ($p<0.01$) and a smaller reduction in IOS expiratory and within-breath reactance at 5Hz without an accompanying signal in resistance, resonant frequency, or functional gas trapping on CT. Modest improvements to alveolar gas mixing (AME) and small airways function (S_{acin}) were measured using MBNW in a subset of patients. The impact of valves on the peripheral airway compartment was less pronounced than with surgery and was predominantly due to deflation of emphysematous lung tissue and relief of the mechanical pump.

Coil implantations resulted in modest volume reduction, △ residual volume of -0.31 ± 0.60L ($p=0.01$), and 3-month physiological outcomes were similarly disappointing with IOS detected improvement limited to the area under reactance during expiration (AX_{ex}). The comparatively minor volume reduction achieved and the fall in gas transfer using this technique may explain the relatively small impact on peripheral airways function.

There were no SAP predictors of volume reduction identified for any of the interventional arms.

Conclusions – IOS and MBNW have furnished insight into the impact of lung volume reduction on large and small airways function, the latter proportionally affected by increasing degrees of volume reduction achieved. IOS is likely to prove complementary to disease phenotyping using conventional lung function measures and is a safe, well-tolerated, and quick to perform non-invasive test with which to characterise COPD both as a biomarker of disease severity and as an objective endpoint for assessing interventional outcomes. However, its predictive value for therapeutic response is not established from this small dataset and further research in larger trials is needed.

Introduction

The small airways, those less than 2mm in internal diameter, offer little resistance to airflow in health (less than 10%), but targeted by inhaled noxious particles, in time become the principal site of obstruction to airflow in COPD[20, 81]. This region of the lung is termed the 'silent zone' and presents a challenging problem[23] - the advent of symptoms and of abnormalities in conventional lung function tests is delayed until substantial injury has accumulated. Quantitative micro-CT studies of lung explants have demonstrated narrowing and loss of terminal and respiratory bronchioles preceding emphysematous destruction and linearly correlating with COPD disease severity according to GOLD spirometry criteria (40% reduction in mild-to-moderate, 80% in severe-to-very severe COPD)[90, 91].

As the disease progresses, a number of pathophysiological mechanisms conspire to inflate the lungs to supra-normal lung volumes[137], recognised as a contributory factor to the sufferer's perception of breathlessness on activity[138], exercise limitation[139, 140], and predicts not only the risk and severity of exacerbations[141] but all-cause mortality[142, 143]. This observation has attracted interest in lung volume reduction (LVR) and the development of techniques targeting the hyperinflation of individuals with predominant emphysema in an attempt at restoring normal respiratory mechanics. However, the hazards inherent in surgery in a high-risk population[159, 181, 182] have prompted the parallel development of minimally invasive bronchoscopic lung volume reduction (BLVR) techniques including the implantation of endobronchial valves (EBVs) and of endobronchial coils (EBCs)[281, 335]. Volume reduction is the key driver of benefit[214]. There is, however, a paucity of data on the effects of volume reduction on the function of the small airways, which are of interest since they are believed to be the initial site of disease pathogenesis[236].

Impulse oscillometry (IOS) and multiple breath nitrogen washout (MBNW) are welcome additions to the investigative armamentarium, enabling the regional contributions to airways resistance to be distinguished, facilitating study of the small airways. IOS findings in COPD correlate well with those of

traditional/conventional diagnostics[248, 249]. Both R5 and R5-R20 are higher in COPD and correlate with increasing GOLD stage classification[251-253]. R5-20 significantly correlates with symptom scores [251, 254] and FEV1[253]. The resonant frequency (Fres) progressively increases and X5 decreases across the disease spectrum [251, 253] and within-breath analysis shows expiration generates a more negative reactance[255, 256]. Both Fres and reactance increase with airflow obstruction and hyperinflation in COPD[246]. X5 may be more discriminatory than resistance parameters in diagnosing COPD[248] and relates well to health status[254]. Furthermore, IOS can be used to evaluate inhaled drug efficacy[257, 258] and monitor recovery from an exacerbation[150]. Using (MBNW), S_{cond} and S_{acin} are both elevated in patients with COPD[268]. S_{cond} correlates to FEV1 and specific airways conductance[269], while S_{acin} relates to diffusion capacity[268], lung volumes[270], and CT extent of emphysema[271]. Furthermore, S_{acin} is weakly correlated to impulse oscillometry-derived resistance and reactance[270]. Ventilation inhomogeneity has also been shown to improve in response to Aclidinium[272].

Study objective

The objective of this study was to investigate the hypothesis that lung volume reduction will be accompanied by measurable changes in small airways function that can be correlated with the conventional clinical parameters and that reliable baseline predictors of therapeutic response (reduction of residual volume of at least 10%[206]), will be identified.

Methods

Ethics

This study was undertaken in accordance with the Declaration of Helsinki and is based on lung function data acquired prospectively from two observational trials performed at the Royal Brompton Hospital:

3) Changes in Small Airways Physiology following bronchoscopic treatments for Obstructive Airways Disease, SAP-OAD (REC reference 14/SC/0193, IRAS 145030) – enrolled patients undergoing LVRS, endobronchial valve and endobronchial coil (registry) implantations.
4) Identifying REsponders and Exploring Mechanisms of ACTION of the Endobronchial Coil Treatment for Emphysema, REACTION (REC reference 16/LO/0933, IRAS 179313, NCT02179125) – enrolled patients undergoing endobronchial coil implantations.

Written informed consent was obtained from all patients.

Study subjects

72 consecutive subjects scheduled for lung volume reductions were recruited: Unilateral LVRS – 15; Endobronchial valve – 29, Endobronchial coil – 28. All underwent detailed clinical phenotyping comprising demographic, symptom score, computed tomography (CT) imaging, lung function, and exercise capacity measurements during exacerbation-free periods from 4th July 2016 to 13th August 2019.

Symptom scores

The modified Medical Research Council (mMRC) dyspnea scale[282] was used to evaluate disability associated with breathlessness due to COPD[292]. A minimum clinically important difference (MCID) of 1 was considered meaningful[294].

The St George's Respiratory Questionnaire (SGRQ) is a 50-item multidimensional instrument to measure quality of life in patients with airways obstruction and to quantify changes after therapy[295, 296]. Scores were calculated for three domains: Symptoms (frequency and severity), Activities (that cause or are limited by breathlessness), and Impacts (psycho-social disturbance resulting from airways disease), that were combined to generate a total score. Scores range from 0 to 100, with higher scores indicating more severe limitation. An MCID of -4 was considered clinically meaningful[298].

Computed tomography

A Somatom Sensation 64 computed tomography scanner (Siemens, Erlangen, Germany) was used to acquire high resolution radiographic images of thin slices (1mm) of the lungs at maximal inspiration (corresponding to total lung capacity, TLC, measured using body plethysmography) and in maximal expiration (corresponding to residual volume, RV). Supine subjects were scanned from lung apices to bases employing a peak voltage of 120 kilo volts (kVp) and tube current modulation range of 30 to 140 mA. Images were reconstructed using a high spatial frequency B40F kernel to axial, coronal and sagittal formats. Isolation of selected structures ranked by radiographic density using the Hounslow Unit (HU) scale was achieved with dedicated in-house software (see LungSeg Toolbox). (To minimise radiation exposure, pre-enrolment CT scans performed by a referring centre and adopting a similar imaging protocol were not repeated in a small number of patients).

The LungSeg Toolbox, a validated software package developed in the Hamlyn Centre (Imperial College, London) in collaboration with the Royal Brompton Hospital[216], operates in MATLAB (by MathWorks), a multi-paradigm computing environment, and analyses CT-acquired DICOM images. The user interface displays images in three planes (axial, coronal, and sagittal). Images optimised with gaussian smoothing for reducing 'noise' and histogram equalization for contrast enhancement. A variety of functions enable interrogation of the structure of the lung:

- Segmentation and calculation of total lung volume on full inspiration and expiration.
- Characterisation of parenchyma at -950 HU on inspiration and -856 HU on expiration.
- Extraction and calculation of intra-parenchymal vessel volume.
- Measurement of pulmonary artery to aorta ratio.

Routine lung function and exercise capacity

The Jaeger Master Lab (Cardinal Health, Hoechberg, Germany) comprises two pieces of equipment, a constant volume body plethysmograph (MasterScreen™ Body) and a single breath gas transfer unit (MasterScreen™ PFT). Each has an integral pneumotachograph accessed with FreeFlow™ mouthpiece

(Carefusion, UK) and single-use bacterial filter, to perform spirometry. They were calibrated to correct for deviations of ambient temperature (°C), humidity (%) and barometric pressure (kPA) from standardised conditions and for flow-volume using a 3-litre syringe. Anthropometric measurements including age, height, and weight were input to allow comparison with the European Community for Steel and Coal (ECSC) reference values. All measurements were made post-inhalation of 400mcg of salbutamol and at least three reproducible readouts were recorded[300]. An earlobe capillary blood sample was analysed on an ABL90 FLEX PLUS (Radiometer, UK) for pH, PCO_2 (kPA), PO_2 (kPA), and HCO_3 (mEq/L) and on HemoCue for haemoglobin. Six-minute walk test was performed to evaluate exercise capacity according to ATS guidelines[320].

Small airways physiology

Impulse Oscillometry System (IOS)

The IOS (Cardinal Health, Hoechberg, Germany) comprises a loudspeaker imposing bursts of mixed frequency pressure waves on to a patient's tidal ventilation monitored by pressure and flow transducers and a computer producing readouts at 5Hz and at 20Hz of respiratory resistance (R), reactance (X) at 5Hz, the area of reactance (AX), and resonant frequency (Fres).

Prior to use, the machine was calibrated for ambient conditions (temperature in °C, relative humidity in %, and barometric pressure in mmHg), flow-volume using a 3-litre syringe, and resistance using a reference impedance device (resistance should measure 0.20 kPA between 5 – 35Hz).

The patient seated upright with legs uncrossed and feet firmly placed on the floor to relax the respiratory muscles was instructed to come onto the mouthpiece ensuring the tongue was placed under the depressor and the flange located between the gums and lips and with nose clip applied and cheeks supported (to minimise absorption of sound waves) breathe normally for 30-60 seconds. At the end of each run, the result was checked and adjusted for artefacts (for example, swallowing) by separating tidal breathing from resistance at 5Hz and selecting the representative portions of the

trace. All test measurements were made post-bronchodilation using 400mcg of salbutamol. At least three reproducible readouts were recorded[246].

Multiple breath nitrogen washout (MBNW)

A bespoke assembly, a 400-litre 'bag-in-box' system with pneumatic valves was used, a replica construction based on a prototype built in Belgium[304]. A non-return valve connects the mouthpiece to a pair of 150 litre Douglas bags enclosed in a box, one delivering O_2 during inspiration and the other collecting expired air. Volume and pressure changes in the box or bags are recorded by an integrated Fleisch-type pneumotachograph, 5. Nitrogen (N_2) concentration at the mouthpiece is monitored continually with a built-in needle-valve probe connected to a nitrogen analyser, 6 (P. K. Morgan, Kent, UK). Volume, pressure and N_2 concentration signals are processed using a dedicated Labview program (National Instruments, Austin, TX) which also controls the valves and provides visual feedback of inspiratory volume achieved on a personal computer (PC) screen to the patient.

Prior to use, the machine was calibrated to ensure the nitrogen analyser read between 70-80%, approximating atmospheric conditions and for flow-volume using a 1-litre syringe. The 1 litre syringe was also used to simulate a patient's tidal breathing, generating a test washout curve – to confirm there was no leak in the system.

The subject with nose clip applied came onto the TRU-FIT™ mouthpiece attached to the pneumotachograph via an interposed Vitalograph disposable bacterial filter.

After a period of quiet breathing through the box, the patient was switched to the O_2 bag during an exhalation to minimise gas mixing (using a two-way inflatable balloon system: Hans Rudolph, USA) and instructed to restrict tidal breathing to 1 litre excursions guided by a graphical representation of his/her effort on a PC screen. The number of tidal breaths of 1 litre required to achieve a 1 in 40 dilution (approximating 2% above baseline) is termed the lung clearance index (LCI). The tests were

repeated at 10-minute intervals and three in all performed by each subject post-bronchodilation using 400mcg of salbutamol.

A 'washout curve' was generated plotting a semilogarithmic graph of the log of the mean expired N_2 concentration of each breath expressed as a percentage of the initial N_2 concentration, log [N_2], against lung turnover, TO (defined as the cumulative expired volume divided by FRC). TO was used rather than number of breaths as it permits comparison of patients with different lung volumes and dilutions. To determine the relative contributions of the conductive (S_{cond}) and acinar (S_{acin}) airways and assess ventilation inhomogeneity, the alveolar slope of each breath (the equivalent of a single breath N_2 washout trace) was determined by linear regression of N_2 concentration versus expired volume (0.65 to 1 litre) in the alveolar phase III, which was then divided by mean expired N_2 concentration to derive a normalised alveolar slope (S). S was then plotted as a function of TO. S_{cond} was derived by linear regression of the normalised alveolar slope (S) between TO 1.5 to 6.0 (i.e. that portion contributed by the conducting airways) to give the gradient per unit TO. S_{acin} was derived by subtracting S_{cond} from the slope of the first breath and multiplying by the TO of that breath.

Data were analysed using a bespoke programme coded by Sylvia Verbanck in Turbo Pascal (a software development system) and running in DOSBox (a DOS-emulator). Each test file was individually uploaded and underwent a series of manual steps. Corrections were first made for any drift in tidal breathing followed by setting of the delay time (i.e. the interval between N_2 sampling at the mouth and reaching the analyser, was set at 5 seconds). Next, N_2 concentration was selected whilst breathing air and then for each subsequent breath at end-inspiration. Phase III slopes were then drawn for each exhaled breath. An output file was generated containing the following parameters: TO – lung turnover, VDF = Fowler dead space, VDB = Bohr dead space, Sn = normalised phase III slope, FRC = functional residual capacity, FETn = end-tidal N_2 concentration, Fen = mean expired N_2 concentration, INVOL = inhalation volume, EXVOL = exhalation volume, and Fin = mean inspiratory N_2 concentration. The output file data for each test run (usually three) were copied into a customised excel template, coded

by Sylvia Verbanck, for generating graphs of: 1) Fen vs TO to determine LCI and; 2) Sn vs TO (TO set at 1.5 to 6.0) to derive S_{cond} and S_{acin} indices (/L).

Statistics

Categorical data are presented as percentages (%) and comparisons made using the Chi-squared or Fisher's exact test for two or more categorical variables. Parametric continuous data are presented as mean ± SD or 95% confidence intervals and non-parametric continuous data as median (interquartile range, IQR). Comparisons of two matched groups were made using a paired t test or the Wilcoxon test for parametric and non-parametric distributions, respectively; two unmatched groups, an unpaired t test or Mann-Whitney test; three matched groups, repeated measures ANOVA or Friedman test; and three unmatched groups, a one-way ANOVA or Kruskal-Wallis test (Tukey's and Dunn's tests applied, respectively, for multiple comparisons). Quantifying the association between two variables was measured using Pearson or Spearman correlations for parametric and non-parametric distributions, respectively. The strength of the correlation for the absolute value of *r* was described as follows: 0.00–0.19, 'very weak'; 0.20 – 0.39, 'weak'; 0.40 – 0.59, 'moderate'; 0.60–0.79, 'strong'; 0.80–1.0', 'very strong'. Binary logistic regression was undertaken to determine predictors of response, defined as a reduction in residual volume of ≥10%. All tests were 2 tailed and significance was set at $p < 0.05$. Statistical analysis was performed using SPSS version 24.0 (IBM, Chicago, IL, USA) and presented using GraphPad Prism version 8 (San Diego, CA).

Results

We first focus on individual therapies and their impact on small airways function comparing clinical characteristics at baseline and at 3 months, delta correlations with the pre-specified small airways metrics, and evaluating for baseline predictors of a ≥10% RV reduction to identify potential mechanisms of action. The cohorts are then compared to clarify differences between techniques.

Impulse oscillometry

Lung volume reduction surgery (LVRS)

Baseline characteristics

15 patients were enrolled: mean age 58.5 ± 12.1 years, 60% male, 34 pack year smoking history, and two exacerbations in the preceding 12 months. 13% were classified as GOLD grade II, 27% III and 60% IV. Questionnaires recorded a mMRC of 3 (2, 3) and SGRQ-total of 57.4 ± 10.9 points. The cohort demonstrated severe airflow obstruction, FEV1 31.6 ± 11.9%, and hyperinflation, RV 253.1 ± 59.9%. Lung function, exercise capacity and quantitative CT (qCT) parameters are detailed in Table 4.1.

Changes in characteristics at 3-months

At 3-months, reductions in mMRC of -1 ($p<0.01$), SGRQ-total of -17.57 points (<0.01) and BODE index of -2 ($p<0.01$) were observed. qCT revealed decreases in total lung volume of -873.8 ± 428.3 ($p<0.01$), total gas trapping of 8% ($p<0.01$), and fGT of 6% ($p<0.01$).

Functional improvements were measured in FEV1 of +8.59% ($p<0.01$), FEV1/FVC of +5.26% ($p=0.03$), RV of -59.39% ($p<0.01$), TLC of -16.87% ($p<0.01$), RV/TLC of -7.93% ($p<0.01$), $G_{AW\text{-}total}$ of +0.17 kPA/L/s ($p<0.01$), 6MWD of +45.29 meters ($p=0.02$), **Rex5 of -0.09kPA/L/s ($p=0.03$), Xex5 of +0.25 kPa/L/s ($p<0.01$), Xin5-Xex5 of -0.28 kPa/L/s ($p<0.01$), AX of -1.06 ($p=0.01$), AXexp of -2.48 ($p<0.01$), Fres total of -3.12 ($p<0.01$), and Fres peripheral of -0.16 ($p=0.02$)**. (Table 4.2).

Small airways physiology delta correlations

Focusing on those small airways metrics that were significantly changed at 3 months: Δ**Xex5** was negatively related to Δ PCO_2 (r=-0.60; p=0.04); Δ **Xin5-Xex5** was positively correlated with Δ TLC (r=0.69; p=0.01); Δ**AX** was negatively related to ΔIC/TLC (r=-0.57; p=0.04) and positively correlated with Δ PCO_2 (r=0.69; p=0.02); Δ **Fres-total** was positively correlated with Δ PCO_2 (r=0.85; p<0.01). (Figure 4.1 and Appendix B: Table S4.1).

Predictors of volume reduction

14 of 15 subjects (93%) achieved a ≥10% RV reduction (Table 4.3): binomial logistic regression did not identify any baseline predictors and multivariable modelling was limited by small numbers.

Overall impact of LVRS on small airways function

At 3 months, IOS expiratory airways resistance at 5Hz, expiratory and within-breath reactance at 5 Hz, and peripheral resonant frequency were significantly improved. This was accompanied by a reduction in residual volume of 1.26 ± 0.58 litres (p<0.01) together with gains in spirometry, exercise capacity, total and functional gas trapping on CT, the BODE index, and quality of life. The changes in Xin5-Xex5 positively correlated with those in TLC and AX negatively with IC/TLC, highlighting the intimate relationships of these IOS indices with lung volume. Furthermore, a reduction in Fres-total correlated with a fall in PCO_2 inferring a benefit to gas exchange. These findings suggest improved peripheral airways function as a consequence of surgical resection of emphysematous tissue.

		LVRS	Valve	Coil	Group comparison
Demographics					*p-value*
Number		15	29	28	
Age, years		58.47 ± 12.13	64.86 ± 8.75	66.89 ± 8.21	0.05
Gender (male), %:		60.00	58.62	42.86	0.40†
BMI, kg/m^2		23.10 ± 3.40	24.63 ± 4.34	23.88 ± 3.77	0.44
Active co-morbidities		1 (0, 2)	2 (1, 3)	2 (1, 3)	0.35‡
Pack years		33.75 (25.00, 48.00)	45.00 (32.50, 53.00)	42.00 (33.38, 53.00)	0.49‡
Exacerbations (last year)		2 (0, 3)	1 (0, 3)	2 (0, 3)	0.90‡
GOLD grade, %	II	13	0	0	0.80‡
	III	27	43	36	
	IV	60	57	64	
Heterogeneous, %		53.84	46.43	44.00	0.84†
Baseline medications					
LABA, %		86.67	93.10	100.00	0.18†
LAMA, %		86.67	96.55	100.00	0.11†
ICS, %		100	89.66	89.29	0.42†
Oxygen, %		33.33	72.41	17.86	0.49†
Symptoms					
mMRC		3 (2, 3)	3 (2, 3)	3 (2, 3)	0.80‡
SGRQ	*total*	57.41 ± 10.94	59.98 ± 18.47	52.57 ± 10.78	0.16
	symptoms	57.90 ± 18.63	52.79 ± 21.88	51.78 ± 18.54	0.62
	impacts	43.98 ± 12.27	48.83 ± 24.35	36.93 ± 12.84	0.74
	activity	80.28 ± 16.12	82.62 ± 15.02	79.84 ± 11.54	0.06
Routine lung function					
FEV_1, L		0.93 ± 0.41	0.79 ± 0.23	0.71 ± 0.22	0.06
FEV_1, %		31.64 ± 11.85	29.28 ± 7.80	29.56 ± 7.73	0.68
FVC, L		3.20 ± 1.01	3.06 ± 0.65	2.83 ± 0.93	0.35
FVC, %		87.54 ± 19.57	89.57 ± 12.42	92.21 ± 16.85	0.64
FEV1/FVC, %		28.78 ± 8.03	24.94 ± 4.99	25.22 ± 5.90	0.12
MEF25-75%, L/s		0.28 ± 0.20	0.20 ± 0.06	0.19 ± 0.05	**0.04**
RV, L		5.51 ± 1.71	5.15 ± 0.96	5.14 ± 1.10	0.58
RV, %		253.10 ± 59.90	231.00 ± 41.93	232.70 ± 33.35	0.24
TLC, L		8.71 ± 2.09	8.29 ± 1.20	8.01 ± 1.81	0.42
TLC, %		140.50 ± 18.77	139.90 ± 12.57	142.30 ± 11.11	0.79
RV/TLC, %		62.79 ± 10.89	62.12 ± 6.32	64.46 ± 5.39	0.46
IC, L		2.01 ± 0.64	2.06 ± 0.55	1.90 ± 0.58	0.59

	LVRS	Valve	Coil	Group comparison
IC/TLC, %	23.34 ± 6.13	25.16 ± 5.01	23.67 ± 4.60	0.44
R_{aw}, kPA/L/s	0.88 ± 0.44	1.05 ± 0.54	1.09 ± 0.64	0.50
G_{aw}, kPA/L/s	0.27 ± 0.20	0.27 ± 0.15	0.23 ± 0.08	0.45
TLCOc, mmol/min/kPA	3.13 ± 1.01	2.83 ± 0.98	2.62 ± 0.88	0.30
TLCOc, %	33.93 ± 7.94	33.85 ± 10.31	33.03 ± 9.26	0.94
KCOc, mmol/min/kPA	0.68 ± 0.14	0.63 ± 0.18	0.60 ± 0.17	0.39
KCOc, %	44.33 ± 9.46	43.28 ± 12.75	40.47 ± 10.37	0.54
pH	7.44 ± 0.02	7.44 ± 0.02	7.44 ± 0.03	0.75
PCO_2	4.94 ± 0.54	5.05 ± 0.61	5.08 ± 0.73	0.81
PO_2	9.76 ± 1.14	9.04 ± 1.04	9.35 ± 1.44	0.22
HCO_3	24.34 ± 2.34	25.29 ± 2.68	25.10 ± 2.75	0.55
Static compliance, L/cm H_20	3.10 ± 1.56	3.76 ± 2.88	3.30 ± 2.97	0.76
Impulse oscillometry				
R5, kPa/L/s	0.71 ± 0.16	0.71 ± 0.18	0.73 ± 0.25	0.93
R20, kPa/L/s	0.39 ± 0.10	0.39 ± 0.07	0.39 ± 0.14	0.97
R5-20, kPa/L/s	0.31 ± 0.09	0.32 ± 0.13	0.34 ± 0.16	0.77
Rin5, kPa/L/s	0.48 ± 0.08	0.48 ± 0.11	0.50 ± 0.15	0.76
Rex5, kPa/L/s	0.86 ± 0.37	0.79 ± 0.23	0.83 ± 0.32	0.73
X5, kPa/L/s	-0.40 ± 0.25	-0.50 ± 0.20	-0.50 ± 0.21	0.28
Xin5, kPa/L/s	-0.18 ± 0.10	-0.21 ± 0.10	-0.22 ± 0.08	0.31
Xex5, kPa/L/s	-0.81 ± 0.39	-0.81 ± 0.38	-0.83 ± 0.39	0.98
Xin5-Xex5, kPa/L/s	0.68 ± 0.37	0.61 ± 0.34	0.61 ± 0.35	0.51
AX	4.63 ± 1.79	4.71 ± 2.27	4.76 ± 2.74	0.99
Axinsp	1.66 ± 0.74	1.92 ± 1.11	2.12 ± 1.39	0.46
Axexp	7.84 ± 5.02	7.12 ± 3.73	7.16 ± 3.80	0.84
Fres total	30.09 ± 4.61	29.48 ± 5.53	28.91 ± 4.59	0.76
Fres central	0.30 ± 0.06	0.30 ± 0.05	0.31 ± 0.08	0.93
Fres peripheral	0.86 ± 0.25	0.88 ± 0.26	0.93 ± 0.29	0.65
Exercise capacity				
6MWD, meters	343.70 ± 107.60	324.00 ± 114.10	338.90 ± 101.50	0.81
CT metrics				
Total Lung Vol_{insp}, ml	7401 ± 2146	6948 ± 1086	6432 ± 1500	0.23
Total Lung Vol_{exp}, ml	5915 ± 1828	5649 ± 1003	5072 ± 1437	0.22
Total Lung DS, % (-950insp)	41 (39, 47)	41 (34, 42)	33 (26, 39)	**<0.01**‡
Total Lung DS, % (-856exp)	77 (74, 84)	74 (65, 80)	76 (70, 78)	0.28‡
fGT, %	42 (39, 46)	43 (37, 45)	46 (42, 53)	**0.02**‡
Total Lung Vessel Vol, ml	188 (165, 245)	199 (170, 227)	151 (117, 183)	**<0.01**‡

	LVRS	Valve	Coil	Group comparison
PA ratio	0.79 (0.70, 0.92)	0.85 (0.78, 0.88)	0.78 (0.71, 0.83)	0.15‡
Mortality Score				
BODE Index	5 (4, 6)	6 (4, 7)	5 (4, 7)	0.83
Inflammatory marker				
White cell count, 10^9/L	8.33 ± 2.18	7.84 ± 2.01	8.48 ± 2.27	0.52
Fibrinogen, mg/dL	3.30 ± 0.26	3.45 ± 0.73	3.76 ± 0.62	0.14
C-reactive protein, mg/dL	2.64 ± 2.06	3.60 ± 4.98	5.39 ± 7.91	0.33

Categorical data are presented as a frequency (%) and compared using a Chi-square test† (nominal) or Kruskal-Wallis test‡ (ordinal). Parametric continuous data are presented as mean ± SD and compared using a one-way ANOVA unless otherwise stated. Non-parametric continuous data are presented as median (IQR) and compared using a Kruskal-Wallis test‡. AX, area under reactance; BMI, Body Mass Index; BODE index = Body mass index, airflow Obstruction, Dyspnoea, and Exercise capacity; c, corrected for haemoglobin concentration; DS, Destruction Score; ex, expiratory; FEV_1, Forced Expiratory Volume in 1 second; fGT, functional gas trapping; Fres, resonant frequency; FVC, Forced Vital Capacity; GOLD, Global Initiative for Obstructive Lung Disease; HCO_3, bicarbonate; G_{aw}, airways conductance; IC, Inspiratory Capacity; ICS, inhaled corticosteroid; in, inspiratory; K_{CO}, carbon monoxide diffusing capacity per unit alveolar volume; LABA, long-acting beta agonist; LAMA, long-acting muscarinic antagonist; LVRS, lung volume reduction surgery; mMRC, modified Medical Research Council dyspnoea scale; PCO_2, PA ratio, pulmonary artery to aorta ratio; Partial pressure for carbon dioxide; PO_2, Partial pressure for oxygen; R5, airways resistance at 5Hz; R20, airways resistance at 20Hz; R_{aw}, airways resistance; RV, Residual Volume; SGRQ, St George's Respiratory Questionnaire; TLC, Total Lung Capacity; TL_{CO}, Transfer factor for carbon monoxide; Vol, Volume; X5, reactance at 5Hz; 6MWD, Six-Minute Walk Distance.

Table 4.1. Baseline characteristics of patients.

		LVRS difference	*p-value*	Valve difference	*p-value*	Coil difference	*p-value*	Group comparison *p-value*
Symptoms								
∆mMRC		-1	**<0.01**†	-1	**<0.01**†	0	**0.01**†	0.18‡
∆SGRQ	*Total score*	-17.57 ± 12.82 (95% CI: -24.67, -10.47)	**<0.01**	-9.41 ± 15.60 (95% CI: -15.34, -3.48)	**<0.01**	-5.82 ± 16.54 (95% CI: -12.50, 0.86)	0.08	0.07
	Symptoms	-17.80 ± 18.12 (95% CI: -27.83, -7.77)	**<0.01**	-1.17 ± 25.05 (95% CI: -10.70, 8.36)	0.80	0.55 ± 22.79 (95% CI: -8.65, 9.76)	0.90	0.09
	Activity	-15.61 ± 18.71 (95% CI: -25.97, -5.25)	**<0.01**	-10.26 ± 16.65 (95% CI: -16.59, -3.92)	**<0.01**	-8.41 ± 14.69 (95% CI: -14.34, -2.47)	**<0.01**	0.40
	Impacts	-18.32 ± 14.19 (95% CI: -26.18, -10.46)	**<0.01**	-11.18 ± 17.47 (95% CI: -17.82, -4.53)	**<0.01**	-6.08 ± 19.69 (95% CI: -14.03, 1.88)	0.13	0.11
Routine lung function								
∆FEV_1, L		0.26 ± 0.24 (95% CI: 0.13, 0.39)	**<0.01**	0.19 ± 0.20 (95% CI: 0.11, 0.26)	**<0.01**	0.04 ± 0.14 (95% CI: -0.02, 0.10)	0.19	**<0.01**
∆FEV_1, %		8.59 ± 7.17 (95% CI: 4.62, 12.56)	**<0.01**	7.59 ± 7.20 (95% CI: 4.80, 10.38	**<0.01**	1.85 ± 6.02 (95% CI: -0.58, 4.29)	0.13	**<0.01**
∆FVC, L		0.19 ± 0.43 (95% CI -0.05, 0.43)	0.10	0.33 ± 0.52 (95% CI: 0.12, 0.53)	**<0.01**	0.09 ± 0.35 (95% CI: -0.05, 0.24)	0.18	0.17
∆FVC, %		6.09 ± 13.02 (95% CI: -1.12, 13.30)	0.09	11.74 ± 15.23 (95% CI: 5.84, 17.65)	**<0.01**	2.62 ± 12.46 (95% CI: -2.41, 7.65)	0.29	0.06
∆FEV1/FVC, %		5.26 ± 8.56 (95% CI: 0.52, 10.00)	**0.03**	3.03 ± 3.79 (95% CI: 1.56, 4.50)	**<0.01**	0.38 ± 4.07 (95% CI: -1.27, 2.02)	0.64	**0.02**
∆MEF25-75%, L/s		0.15 ± 0.28 (95% CI: -0.01, 0.30)	0.06	0.05 ± 0.07 (95% CI: 0.02, 0.09)	**<0.01**	0.02 ± 0.08 (95% CI: -0.01, 0.06)	0.17	0.05
∆RV, L		-1.26 ± 0.58 (95% CI: -1.58, -0.94)	**<0.01**	-0.91 ± 0.66 (95% CI: -1.17, -0.66)	**<0.01**	-0.31 ± 0.60 (95% CI: -0.55, -0.07)	**0.01**	**<0.01**
∆RV, %		-59.39 ± 25.39 (95% CI: -73.46, -45.33)	**<0.01**	-40.66 ± 28.33 (95% CI: -51.43, -29.88)	**<0.01**	-15.12 ± 29.26 (95% CI: -26.94, -3.30)	**0.01**	**<0.01**
∆TLC, L		-1.02 ± 0.36 (95% CI: -1.22, -0.82)	**<0.01**	-0.61 ± 0.48 (95% CI: -0.80, 0.43)	**<0.01**	-0.18 ± 0.40 (95% CI: -0.34, -0.02)	**0.03**	**<0.01**
∆TLC, %		-16.87 ± 7.09 (95% CI: -20.80, -12.95)	**<0.01**	-9.81 ± 6.95 (95% CI: -12.45, -7.16	**<0.01**	-3.67 ± 9.26 (95% CI: -7.41, 0.07)	0.05	**<0.01**
∆RV/TLC, %		-7.93 ± 5.15 (95% CI: -10.78, -5.08)	**<0.01**	-7.04 ± 6.99 (95% CI: -9.70, -4.38)	**<0.01**	-2.58 ± 5.53 (95% CI: -482, -0.35)	**0.03**	**<0.01**
∆IC, L		0.13 ± 0.27 (95% CI: -0.01, 0.28)	0.07	0.16 ± 0.40 (95% CI: -0.00, 0.31)	0.05	-0.00 ± 0.28 (95% CI: -0.11, 0.11)	0.99	0.20
∆IC/TLC, %		4.89 ± 3.72	**<0.01**	4.13 ± 4.82	**<0.01**	0.68 ± 4.03	0.40	**<0.01**

	LVRS difference	*p-value*	Valve difference	*p-value*	Coil difference	*p-value*	Group comparison *p-value*
	(95% CI: 2.83, 6.95)		(95% CI: 2.22, 6.04)		(95% CI: -0.95, 2.30)		
∆R_{aw}, kPA/L/s	-0.17 ± 0.37	0.09	-0.19 ± 0.46	**0.04**	-0.04 ± 0.41	0.61	0.41
	(95% CI: -0.38, 0.03)		(95% CI: -0.37, -0.01)		(95% CI: -0.21, 0.12)		
∆G_{aw}, kPA/L/s	0.17 ± 0.19	**<0.01**	0.03 ± 0.10	0.18	0.02 ± 0.10	0.25	**<0.01**
	(95% CI: 0.06, 0.27)		(95% CI: -0.01, 0.06)		(95% CI: -0.02, 0.06)		
∆TLCOc, mmol/min/kPA	0.28 ± 0.65	0.13	0.17 ± 0.49	0.09	-0.18 ± 0.39	0.06	**<0.01**
	(95% CI: -0.09, 0.66)		(95% CI: -0.03, 0.36)		(95% CI: -0.37, 0.01)		
∆TLCOc, %	3.07 ± 6.53	0.10	2.22 ± 5.71	0.05	-1.98 ± 4.94	0.10	**0.03**
	(95% CI: -0.70, 6.84)		(95% CI: -0.04, 4.48		(95% CI: -436, 0.40)		
∆KCOc, mmol/min/kPA	0.02 ± 0.16	0.67	0.00 ± 0.07	0.89	-0.06 ± 0.08	**<0.01**	**<0.01**
	(95% CI: -0.07, 0.11)		(95% CI: -0.02, 0.03)		(95% CI: -0.10, -0.02)		
∆KCOc, %	1.04 ± 8.86	0.67	0.78 ± 4.89	0.41	-3.67 ± 4.71	**<0.01**	**0.03**
	(95% CI: -4.08, 6.15)		(95% CI: -1.16, 2.72		(95% CI: -5.94, -1.40)		
∆pH	0.00 ± 0.03	0.92	-0.00 ± 0.03	0.94	0.00 ± 0.04	0.92	0.99
	(95% CI: -0.02, 0.02)		(95% CI: -0.01, 0.01)		(95% CI: -0.02, 0.01)		
∆PCO_2	-0.13 ± 0.48	0.34	-0.15 ± 0.44	0.09	0.16 ± 0.50	0.13	0.05
	(95% CI: -0.40, 0.15)		(95% CI: -0.33, 0.02)		(95% CI: -0.05, 0.36)		
∆PO_2	0.44 ± 1.12	0.16	-0.27 ± 0.91	0.15	-0.44 ± 1.25	0.09	0.05
	(95% CI: -0.21, 1.09)		(95% CI: -0.63, 0.10)		(95% CI: -0.96, 0.07)		
∆HCO_3	-0.52 ± 2.54	0.46	-0.92 ± 1.52	**0.04**	0.94 ± 1.80	**0.02**	**<0.01**
	(95% CI: -1.99, 0.95)		(95% CI: -1.54, -0.31)		(95% CI: 0.20, 1.68)		
∆Static compliance, L/cm H_20	1.91 ± 1.66	0.18	0.01 ± 3.01	0.99	0.28 ± 3.33	0.71	0.49
	(95% CI: -2.22, 6.04)		(95% CI: -1.40, 1.42)		(95% CI: -1.28, 1.83)		
Impulse oscillometry							
∆R5, kPa/L/s	-0.04 ± 0.09	0.11	-0.02 ± 0.12	0.31	-0.05 ± 0.14	0.06	0.68
	(95% CI: -0.10, 0.01)		(95% CI: -0.07, 0.02)		(95% CI: -0.11, 0.00)		
∆R20, kPa/L/s	-0.02 ± 0.06	0.30	0.00 ± 0.06	0.92	-0.02 ± 0.07	0.13	0.39
	(95% CI: -0.06, 0.02)		(95% CI: -0.02, 0.02)		(95% CI: -0.05, 0.01)		
∆R5-20, kPa/L/s	-0.03 ± 0.10	0.36	-0.03 ± 0.12	0.25	-0.03 ± 0.09	0.08	0.96
	(95% CI: -0.08, 0.03)		(95% CI: -0.07, 0.02)		(95% CI: -0.07, 0.00)		
∆Rin5, kPa/L/s	0.03 ± 0.06	0.07	0.03 ± 0.10	0.16	-0.01 ± 0.06	0.53	0.51
	(95% CI: -0.00, 0.07)		(95% CI: -0.01, 0.06)		(95% CI: -0.03, 0.02)		
∆Rex5, kPa/L/s	-0.09 ± 0.14	**0.03**	-0.07 ± 0.23	0.12	-0.06 ± 0.20	0.17	0.87
	(95% CI: -0.17, -0.01)		(95% CI: -0.16, 0.02)		(95% CI: -0.14, 0.03)		
∆X5, kPa/L/s	0.03 ± 0.29	0.68	0.05 ± 0.17	0.12	0.05 ± 0.18	0.20	0.97
	(95% CI: -0.14, 0.21)		(95% CI: -0.01, 0.12)		(95% CI: -0.03, 0.12)		

	LVRS difference	*p-value*	Valve difference	*p-value*	Coil difference	*p-value*	Group comparison *p-value*
ΔXin5, kPa/L/s	-0.03 ± 0.12 (95% CI: -0.11, 0.04)	0.35	-0.02 ± 0.08 (95% CI: -0.05, 0.01)	0.17	-0.00 ± 0.05 (95% CI: -0.02, 0.01)	0.63	0.54
ΔXex5, kPa/L/s	0.25 ± 0.23 (95% CI: 0.11, 0.39)	**<0.01**	0.16 ± 0.34 (95% CI: 0.03, 0.29)	**0.02**	0.11 ± 0.35 (95% CI: -0.03, 0.25)	0.13	0.43
ΔXin5-Xex5, kPa/L/s	-0.28 ± 0.18 (95% CI: -0.40, -0.17)	**<0.01**	-0.18 ± 0.31 (95% CI: -0.30, -0.06)	**<0.01**	-0.11 ± 0.32 (95% CI: -0.24, 0.02)	0.09	0.24
ΔAX	-1.06 ± 1.12 (95% CI: -1.73, -0.38)	**0.01**	-0.53 ± 1.58 (95% CI: -1.15, 0.08)	0.09	-0.63 ± 1.87 (95% CI: -1.39, 0.12)	0.10	0.50
ΔAXinsp	0.27 ± 0.55 (95% CI: -0.07, 0.60)	0.11	-0.03 ± 0.86 (95% CI: -0.36, 0.31)	0.88	0.05 ± 0.69 (95% CI: -0.24, 0.33)	0.73	0.52
ΔAXexp	-2.48 ± 2.08 (95% CI: -3.73, 1.22)	**<0.01**	-1.11 ± 2.65 (95% CI: -2.14, -0.08)	**0.03**	-1.08 ± 2.62 (95% CI: -2.14, -0.03)	**0.04**	0.22
ΔFres total	-3.12 ± 2.77 (95% CI: -4.79, -1.45)	**<0.01**	-0.97 ± 3.67 (95% CI: -2.40, 0.45)	0.17	-1.29 ± 4.28 (95% CI: -3.02, 0.44)	0.14	0.23
ΔFres central	0.02 ± 0.08 (95% CI: -0.03, 0.07)	0.48	0.01 ± 0.07 (95% CI: -0.02, 0.03)	0.67	-0.00 ± 0.05 (95% CI: -0.02, 0.02)	0.63	0.60
ΔFres peripheral	-0.16 ± 0.22 (95% CI: -0.29, -0.03)	**0.02**	-0.04 ± 0.34 (95% CI: -0.18, 0.09)	0.50	-0.08 ± 0.25 (95% CI: -0.18, 0.02)	0.13	0.50
Exercise capacity							
Δ6MWD, m	45.29 ± 63.19 (95% CI: 8.80, 81.77)	**0.02**	44.28 ± 63.06 (95% CI: 20.29, 68.26)	**<0.01**	4.04 ± 43.16 (95% CI: -13.39, 21.47)	0.64	**0.02**
CT metrics							
Δ Total Lung Vol_{insp}, ml	-873.80 ± 428.3 (95% CI: -1133, -615)	**<0.01**	-577.00 ± 769.30 (95% CI: -875, 279)	**<0.01**	-140.60 ± 298.80 (95% CI: -261, -20)	**0.02**	**<0.01**
Δ Total Lung Vol_{exp}, ml	-1297.00 ± 981.10 (95% CI: -1998, -595)	**<0.01**	-576.10 ± 529.40 (95% CI: -848, -304)	**<0.01**	-34.60 ± 909.90 (95% CI: -410, 341)	0.85	**<0.01**
ΔTotal Lung DS, % (-950insp)	-2.00	0.15†	-1.00	0.21†	-1.00	0.79†	0.35‡
ΔTotal Lung DS, % (-856exp)	-8.00	**<0.01**†	-5.61	**0.04**†	-1.00	0.89†	**<0.01**‡
Δ fGT, %	-6.00	**<0.01**†	-4.61	0.10†	0.00	0.94†	**0.02**‡
ΔTotal Lung Vessel Vol, ml	-3.00	0.64†	6.00	0.09†	16.50	**<0.01**†	**<0.01**‡
ΔPA ratio	0.01	0.85†	0.01	0.20†	0.02	0.38†	0.81‡
Mortality Score							
ΔBODE Index	-2.00	**<0.01**†	-1.00	**<0.01**†	-0.50	**<0.01**†	**0.02**‡
Inflammatory marker							
ΔWCC, 10^9/L	-0.96 ± 1.54 (95% CI: -1.86, -0.07)	0.04	0.32 ± 1.86 (95% CI: -0.43, 1.07)	0.39	-0.42 ± 2.01 (95% CI: -1.24, 0.39)	0.29	0.10

	LVRS difference	*p-value*	Valve difference	*p-value*	Coil difference	*p-value*	Group comparison *p-value*
△Fibrinogen, mg/dL	-0.08 ± 0.61 (95% CI: -1.04, 0.89)	0.82	-0.06 ± 0.51 (95% CI: -0.30, 0.19)	0.63	-0.05 ± 0.62 (95% CI: -0.31, 0.21)	0.69	0.93
△CRP, mg/dL	3.50 ± 9.48 (95% CI: -1.97, 9.97)	0.19	7.22 ± 29.48 (95% CI: -5.53, 19.97	0.25	2.73 ± 23.98 (95% CI: -6.96, 12.42)	0.57	0.13

Paired categorical (ordinal) and non-parametric continuous data are compared using a Wilcoxon signed-rank test†, presented as a median of differences, and between three groups using a Kruskal-Wallis test‡. Paired parametric continuous data are compared using a t-test, presented as mean ± SD (95% CI), and between three groups using a one-way ANOVA unless otherwise stated. AX, area under reactance; c, corrected for haemoglobin concentration; DS, Destruction Score; ex, expiratory; FEV_1, Forced Expiratory Volume in 1 second; fGT, functional gas trapping; Fres, resonant frequency; FVC, Forced Vital Capacity; HCO_3, bicarbonate; G_{aw}, airways conductance; IC, Inspiratory Capacity; in, inspiratory; K_{CO}, carbon monoxide diffusing capacity per unit alveolar volume; LVRS, lung volume reduction surgery; mMRC, modified Medical Research Council dyspnoea scale; PCO_2, PA ratio, pulmonary artery to aorta ratio; Partial pressure for carbon dioxide; PO_2, Partial pressure for oxygen; R5, airways resistance at 5Hz; R20, airways resistance at 20Hz; R_{aw}, airways resistance; RV, Residual Volume; SGRQ, St George's Respiratory Questionnaire; TLC, Total Lung Capacity; TL_{CO}, Transfer factor for carbon monoxide; Vol, Volume; X5, reactance at 5Hz; 6MWD, Six-Minute Walk Distance.

Table 4.2. Changes in clinical characteristics over 3-months.

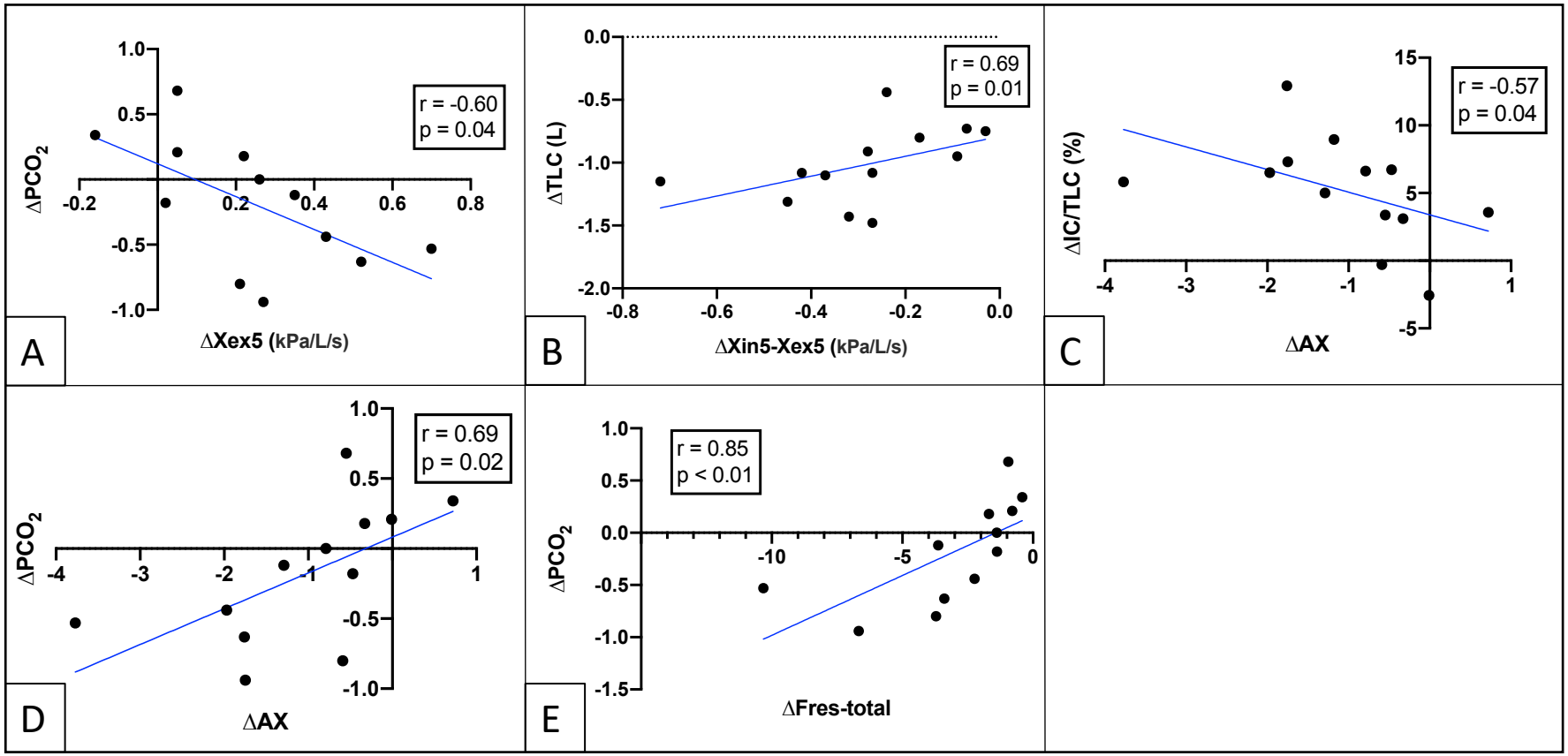

Figure 4.1. Delta correlations – surgery cohort.

Xex5 with PCO_2 (**A**); Xin5-Xex5 with TLC (**B**), AX with IC/TLC (**C**); AX with PCO_2 (**D**); Fres-total with PCO_2 (**E**).

		LVRS responder	LVRS non-responder	*p-value*
Demographics				
Number		14	1	
Age, years		59.86 ± 11.28	39	
Gender (male), %:		57.14	100	
BMI, kg/m^2		23.21 ± 3.51	21.70	
Active co-morbidities		2 (1, 2)	0	
Pack years		36.38 (25.75, 49.25)	23.75	
Exacerbations (last year)		2 (0, 3)	2	
GOLD grade, %	II	7	100	
	III	29	0	
	IV	64	0	
Heterogeneous, %		50	100	
Baseline medications				
LABA, %		93.00	0	
LAMA, %		86.00	100	
ICS, %		100	100	
Oxygen, %		35.71	0	
Symptoms				
mMRC		3 (2, 3)	2	
SGRQ	*total*	58.13 ± 10.97	47.32	
	symptoms	60.94 ± 15.00	15.43	
	impacts	43.62 ± 12.65	49.01	
	activity	81.77 ± 15.62	59.46	
Routine lung function				
FEV_1, L		0.83 ± 0.19	2.25	
FEV_1, %		29.46 ± 8.66	62.10	
FVC, L		3.10 ± 0.96	4.69	
FVC, %		86.20 ± 19.58	106.30	
FEV1/FVC, %		27.45 ± 6.40	47.35	
MEF25-75%, L/s		0.23 ± 0.06	0.98	
FRC, L		7.06 ± 1.86	4.39	
FRC, %		215.50 ± 33.41	142.30	
RV, L		5.75 ± 1.47	2.07	
RV, %		262.80 ± 48.37	117.10	
TLC, L		8.85 ± 2.09	6.82	
TLC, %		142.90 ± 16.79	106.10	
RV/TLC		65.11 ± 6.36	30.27	
IC, L		1.98 ± 0.65	2.43	
IC/TLC, %		22.47 ± 5.30	35.63	
R_{aw}, kPA/L/s		0.78 ± 0.32	0.24	
G_{aw}, kPA/L/s		0.26 ± 0.09	1.13	
TLCOc, mmol/min/kPA		3.10 ± 1.05	3.48	
TLCOc, %		34.15 ± 8.22	31.10	
KCOc, mmol/min/kPA		0.69 ± 0.14	0.55	
KCOc, %		45.50 ± 8.73	29.10	
pH		7.44 ± 0.02	7.42	
PCO_2		5.01 ± 0.50	4.11	
PO_2		9.83 ± 1.16	8.86	
HCO_3		24.70 ± 2.00	19.70	
Static compliance, L/cm H_20		3.10 ± 1.56	-	
Impulse oscillometry				
R5, kPa/L/s		0.72 ± 0.16	0.55	
R20, kPa/L/s		0.40 ± 0.11	0.34	

	LVRS responder	LVRS non-responder	*p-value*
R5-20, kPa/L/s	0.32 ± 0.09	0.21	
Rin5, kPa/L/s	0.49 ± 0.08	0.39	
Rex5, kPa/L/s	0.87 ± 0.38	0.68	
X5, kPa/L/s	-0.41 ± 0.25	-0.22	
Xin5, kPa/L/s	-0.18 ± 0.11	-0.16	
Xex5, kPa/L/s	-0.85 ± 0.37	-0.27	
Xin5-Xex5, kPa/L/s	0.73 ± 0.34	0.11	
AX	4.81 ± 1.71	2.17	
AXinsp	1.71 ± 0.75	0.97	
AXexp	8.17 ± 5.04	3.21	
Fres total	30.51 ± 4.47	24.1	
Fres central	0.30 ± 0.06	0.31	
Fres peripheral	0.89 ± 0.23	0.43	
Exercise capacity			
6MWD, meters	335.90 ± 107.10	453.00	
CT metrics			
Total Lung Vol_{insp}, ml	7531 ± 2187	5842	
Total Lung Vol_{exp}, ml	6016 ± 1909	5008	
Total Lung DS, % (-950insp)	41.0 (38.5, 43.8)	50.0	
Total Lung DS, % (-856exp)	77.0 (73.0, 84.0)	74.0	
fGT, %	42.0 (40.5, 46.5)	30.0	
Total Lung Vessel Vol, ml	187.0 (162.0, 234.5)	254.0	
PA raio	0.81 ± 0.12	0.83	
Mortality Score			
BODE Index	5 (4, 6)	2	
Inflammatory marker			
White cell count, 10^9/L	8.24 ± 2.24	9.50	
Fibrinogen, mg/dL	3.30 ± 0.29	3.30	
C-reactive protein, mg/dL	2.46 ± 2.03	5.00	

Categorical data are presented as a frequency (%). Parametric continuous data are presented as mean ± SD. Non-parametric continuous data are presented as median (IQR). AX, area under reactance; BMI, Body Mass Index; BODE index = Body mass index, airflow Obstruction, Dyspnoea, and Exercise capacity; c, corrected for haemoglobin concentration; DS, Destruction Score; ex, expiratory; FEV_1, Forced Expiratory Volume in 1 second; fGT, functional gas trapping; Fres, resonant frequency; FVC, Forced Vital Capacity; GOLD, Global Initiative for Obstructive Lung Disease; HCO3, bicarbonate; G_{aw}, airways conductance; IC, Inspiratory Capacity; ICS, inhaled corticosteroid; in, inspiratory; K_{CO}, carbon monoxide diffusing capacity per unit alveolar volume; LABA, long-acting beta agonist; LAMA, long-acting muscarinic antagonist; LVRS, lung volume reduction surgery; mMRC, modified Medical Research Council dyspnoea scale; PCO_2, PA ratio, pulmonary artery to aorta ratio; Partial pressure for carbon dioxide; PO_2, Partial pressure for oxygen; R5, airways resistance at 5Hz; R20, airways resistance at 20Hz; R_{aw}, airways resistance; RV, Residual Volume; SGRQ, St George's Respiratory Questionnaire; TLC, Total Lung Capacity; TL_{CO}, Transfer factor for carbon monoxide; Vol, Volume; X5, reactance at 5Hz; 6MWD, Six-Minute Walk Distance.

Table 4.3. Baseline characteristics of responders versus non-responders – surgery cohort.

[Responders were defined as those who achieved a RV reduction of ≥10% at 3 months].

Endobronchial valve (EBV)

Baseline characteristics

29 patients were enrolled: mean age 64.9 ± 8.8 years, 59% male, 45 pack year smoking history, and one exacerbation in the preceding 12 months. 43% were classified as GOLD grade III, 57% IV. Questionnaires recorded a mMRC of 3 (2, 3) and SGRQ-total of 59.98 ± 18.47 points. The cohort demonstrated severe airflow obstruction, FEV1 29.3 ± 7.8%, and hyperinflation, RV 231.0 ± 41.9%. Lung function, exercise capacity and quantitative CT parameters are detailed in Table 4.1.

Changes in characteristics at 3-months

At 3-months, reductions in mMRC of 1 ($p<0.01$), SGRQ-total of 9.41 points (<0.01) and in the BODE index of -1 ($p<0.01$) were recorded. qCT revealed decreases in total lung volume of 577.0 ± 769.3mls ($p<0.01$) and total gas trapping of 5.61% ($p=0.04$).

Functional improvements were measured in FEV1 of +7.59% ($p<0.01$), FEV1/FVC of +3.03% ($p<0.01$), $MEF_{25-75\%}$ of 0.05 ($p<0.01$), RV of -40.66% ($p<0.01$), TLC of -9.81% ($p<0.01$), RV/TLC of -7.04% ($p<0.01$), $R_{AW-total}$ of -0.19 kPA/L/s ($p=0.04$), HCO_3 of -0.92 ($p=0.04$), 6MWD of +44.28 meters ($p<0.01$), **Xex5 of +0.16kPa/L/s (p=0.02), Xin5-Xex5 of -0.18 kPa/L/s (p<0.01), and AXex of -1.11 (p=0.03).** (Table 4.2).

Small airways physiology delta correlations

Focusing on those small airways metrics that were significantly changed at 3 months: Δ**Xex5** was positively correlated with ΔMEF25-75% ($r=0.63$; $p<0.01$) and negatively related to ΔCT-PA ratio ($r=-0.43$; $p=0.02$); Δ**Xin5-Xex5** was negatively related to ΔMEF25-75% ($r=-0.48$; $p=0.04$); Δ**AXex** was negatively related to ΔMEF25-75% ($r=-0.56$; $p=0.01$). (Figure 4.2 and Appendix B: Table S4.2).

Predictors of volume reduction

18 of 29 subjects (62%) achieved a ≥10% reduction in RV. Responders were characterised at baseline by a lower gas transfer ($p=0.02$) and higher hyperinflation (IC/TLC) and emphysema destruction scores ($p=0.04$). (Table 4.4). Binomial logistic regression did not identify any baseline predictors of a ≥10% reduction in RV.

Overall impact of EBV implantation on small airways function

At 3 months, expiratory and within-breath breath reactance at 5Hz were significantly improved. This was accompanied by a reduction in residual volume of 0.91 ± 0.66 litres ($p<0.01$) together with gains in spirometry, exercise capacity, total gas trapping on CT, the BODE index, and quality of life. The changes in reactance correlated with those of MEF25-75%. Collectively, these findings suggest enhanced peripheral airways function from deflation of emphysematous lung.

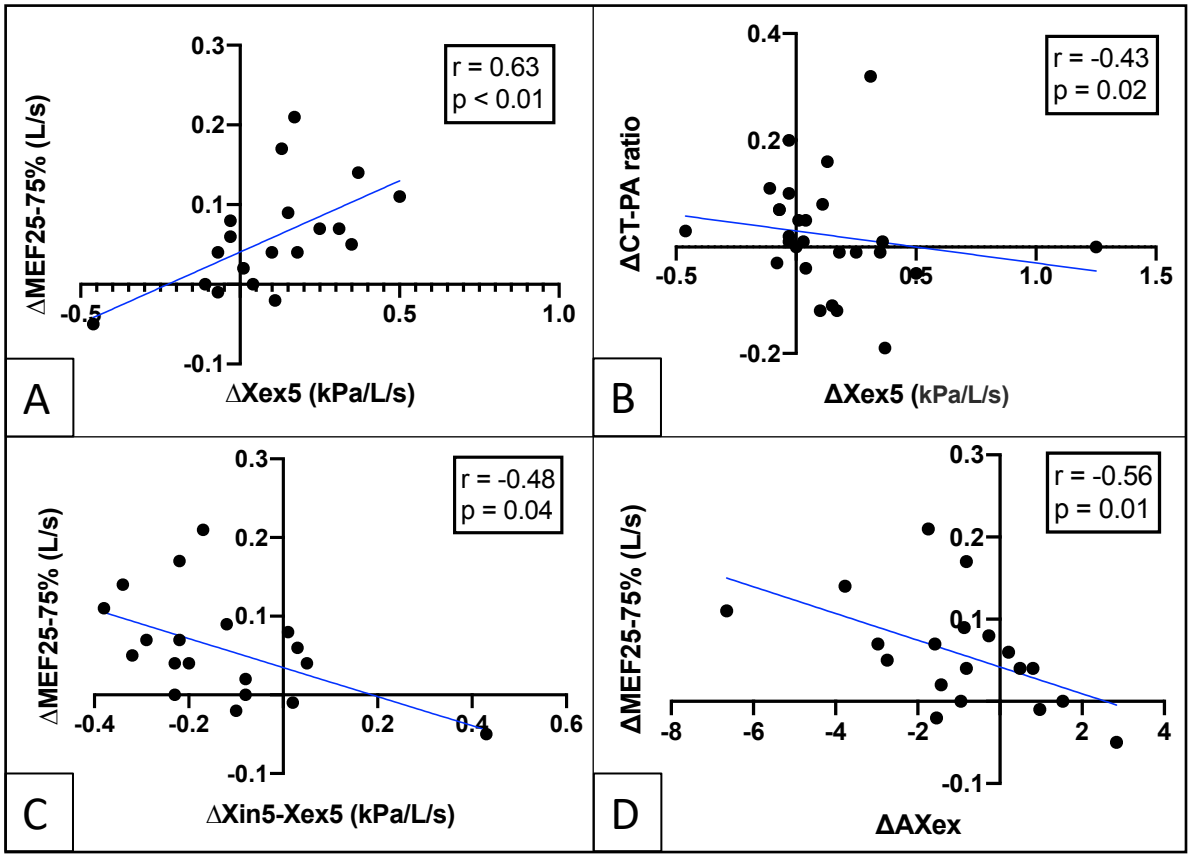

Figure 4.2. Delta correlations – valve cohort.

Xex5 with MEF25-75% (**A**) and CT-PA (**B**); Xin5-Xex5 with MEF25-75% (**C**); AXex with MEF25-75% (**D**).

		Valve responder	Valve non-responder	*p-value*	Coil responder	Coil non-responder	*p-value*
Demographics							*p-value*
Number		18	11		9	17	
Age, years		65.33 ± 8.10	64.09 ± 10.09	0.73	65.89 ± 12.62	67.00 ± 5.58	0.81
Gender (male), %:		61.11	54.54	1.00†	44.44	35.29	0.65†
BMI, kg/m^2		23.99 ± 4.04	25.69 ± 4.79	0.34	24.06 ± 3.94	24.31 ± 3.63	0.88
Active co-morbidities		2 (1, 3)	3 (1, 3)	0.39‡	1 (1, 2)	2 (1, 3)	0.45‡
Pack years		44.50 (30.50, 53.25)	46.00 (32.00, 54.00)	0.40‡	39.00 (15.30, 53.00)	42.00 (37.50, 54.75)	0.18‡
Exacerbations (last year)		3 (0, 3)	1 (1, 1)	0.15‡	1 (1, 2)	2 (0, 3)	0.50‡
GOLD grade, %	II	0	0	0.70‡	0	0	0.05‡
	III	39	50		66.67	23.53	
	IV	61	50		33.33	76.47	
Heterogeneous, %		52.94	36.36	0.39†	28.57	47.06	0.28†
Baseline medications							
LABA, %		94.44	90.91	1.00†	100.00	100.00	1.00†
LAMA, %		94.44	100.00	1.00†	100.00	100.00	1.00†
ICS, %		88.89	90.91	1.00†	88.89	88.24	0.96†
Oxygen, %		22.22	36.36	0.43†	11.11	17.65	0.66†
Symptoms							
mMRC		3 (2, 3)	2 (2, 3)	0.36‡	2 (2, 3)	3 (2, 3)	0.68‡
SGRQ	*total*	60.81 ± 21.08	58.61 ± 14.02	0.74	50.55 ± 11.14	51.91 ± 9.86	0.76
	symptoms	49.91 ± 23.32	57.50 ± 19.40	0.35	57.97 ± 19.90	49.01 ± 18.21	0.28
	impacts	51.00 ± 27.53	45.28 ± 18.71	0.51	34.29 ± 10.35	35.61 ± 12.13	0.77
	activity	82.91 ± 15.31	82.14 ± 15.24	0.90	74.44 ± 15.12	81.53 ± 8.11	0.22
Routine lung function							
FEV_1, L		0.76 ± 0.23	0.86 ± 0.24	0.28	0.83 ± 0.28	0.67 ± 0.17	0.13
FEV_1, %		28.18 ± 7.90	31.25 ± 7.61	0.33	35.27 ± 8.79	27.58 ± 5.46	**0.04**
FVC, L		2.97 ± 0.57	3.23 ± 0.77	0.37	2.77 ± 0.74	2.88 ± 1.05	0.75
FVC, %		88.01 ± 11.44	92.39 ± 14.20	0.42	92.98 ± 13.47	94.33 ± 17.48	0.83
FEV1/FVC, %		24.62 ± 5.78	25.52 ± 3.30	0.61	28.88 ± 5.50	23.58 ± 5.54	**0.03**
MEF25-75%, L/s		0.20 ± 0.06	0.22 ± 0.08	0.58	0.22 ± 0.06	0.17 ± 0.04	**0.02**
FRC, L		6.44 ± 0.96	6.02 ± 1.12	0.31	5.72 ± 1.21	6.09 ± 1.40	0.50
FRC, %		201.90 ± 26.07	190.4 ± 20.55	0.20	189.30 ± 18.18	202.40 ± 29.31	0.17
RV, L		5.35 ± 0.94	4.84 ± 0.97	0.18	4.98 ± 1.00	5.01 ± 1.04	0.95
RV, %		238.80 ± 46.24	218.10 ± 31.56	0.16	232.20 ± 33.85	228.70 ± 33.00	0.80

	Valve responder	Valve non-responder	*p-value*	Coil responder	Coil non-responder	*p-value*
TLC, L	8.36 ± 1.08	8.16 ± 1.43	0.69	7.73 ± 1.62	7.93 ± 1.88	0.78
TLC, %	141.10 ± 13.24	138.00 ± 11.74	0.52	141.30 ± 7.08	142.00 ± 13.16	0.86
RV/TLC	63.85 ± 6.18	59.30 ± 5.72	0.06	64.66 ± 3.89	63.74 ± 6.06	0.64
IC, L	1.98 ± 0.58	2.19 ± 0.49	0.32	2.02 ± 0.60	1.84 ± 0.62	0.48
IC/TLC, %	23.81 ± 5.49	27.44 ± 3.14	**0.04**	26.07 ± 4.54	23.02 ± 4.24	0.12
R_{aw}, kPA/L/s	0.94 ± 0.44	0.78 ± 0.35	0.29	0.73 ± 0.24	0.96 ± 0.46	0.10
G_{aw}, kPA/L/s	0.24 ± 0.15	0.27 ± 0.11	0.52	0.33 ± 0.11	0.24 ± 0.08	0.07
TLCOc, mmol/min/kPA	2.48 ± 0.74	3.45 ± 1.09	**0.03**	2.71 ± 1.17	2.61 ± 0.71	0.81
TLCOc, %	30.17 ± 8.24	40.47 ±10.73	**0.02**	35.09 ± 10.82	32.33 ± 8.31	0.53
KCOc, mmol/min/kPA	0.58 ± 0.13	0.73 ± 0.23	0.06	0.66 ± 0.15	0.57 ± 0.19	0.22
KCOc, %	39.61 ±9.99	49.89 ± 14.96	0.07	45.34 ± 9.41	37.13 ± 10.07	0.07
pH	7.44 ± 0.03	7.45 ± 0.02	0.09	7.45 ± 0.03	7.44 ± 0.03	0.56
PCO_2	5.11 ± 0.61	4.94 ± 0.62	0.51	4.69 ± 0.56	5.28 ± 0.78	**0.04**
PO_2	8.99 ± 1.06	9.14 ± 1.06	0.74	9.54 ± 0.80	9.24 ± 1.73	0.56
HCO_3	25.36 ± 2.53	25.14 ± 3.10	0.86	23.68 ± 2.45	25.98 ± 2.77	**0.04**
Static compliance, L/cm H_20	3.88 ± 3.27	3.59 ± 2.44	0.82	3.01 ± 2.05	3.59 ± 3.49	0.92
Impulse oscillometry						
R5, kPa/L/s	0.71 ± 0.20	0.72 ± 0.14	0.86	0.70 ± 0.19	0.76 ± 0.29	0.55
R20, kPa/L/s	0.38 ± 0.08	0.39 ± 0.06	0.67	0.38 ± 0.10	0.40 ± 0.16	0.70
R5-20, kPa/L/s	0.33 ± 0.15	0.32 ± 0.11	0.83	0.32 ± 0.10	0.36 ± 0.19	0.52
Rin5, kPa/L/s	0.47 ± 0.11	0.49 ± 0.10	0.62	0.46 ± 0.10	0.53 ± 0.17	0.18
Rex5, kPa/L/s	0.79 ± 0.26	0.78 ± 0.17	0.84	0.84 ± 0.25	0.86 ± 0.37	0.87
X5, kPa/L/s	-0.49 ± 0.22	-0.52 ± 0.18	0.74	-0.43 ± 0.13	-0.54 ± 0.25	0.15
Xin5, kPa/L/s	-0.21 ± 0.07	-0.20 ± 0.13	0.71	-0.18 ± 0.09	-0.24 ± 0.07	0.10
Xex5, kPa/L/s	-0.82 ± 0.42	-0.80 ± 0.32	0.86	-0.76 ± 0.26	-0.88 ± 0.46	0.38
Xin5-Xex5, kPa/L/s	0.61 ± 0.37	0.62 ± 0.30	0.94	0.57 ± 0.23	0.64 ± 0.42	0.60
AX	4.62 ± 2.31	4.86 ± 2.30	0.79	4.29 ± 1.50	5.17 ± 3.30	0.36
AXinsp	1.92 ± 1.22	1.93 ± 0.97	0.97	1.55 ± 0.80	2.44 ± 1.57	0.07
AXexp	7.23 ± 4.08	6.94 ± 3.24	0.83	6.76 ± 2.22	7.63 ± 4.57	0.52
Fres total	29.30 ± 5.16	29.76 ± 6.34	0.84	29.08 ± 4.31	29.13 ± 4.86	0.98
Fres central	0.30 ± 0.05	0.32 ± 0.05	0.23	0.30 ± 0.06	0.31 ± 0.10	0.90
Fres peripheral	0.88 ± 0.32	0.89 ± 0.13	0.86	0.82 ± 0.14	1.00 ± 0.34	0.08
Exercise capacity						
6MWD, meters	300.00 ± 114.60	363.40 ± 106.70	0.15	340.30 ± 107.30	341.90 ± 93.48	0.97
CT metrics						
Total Lung Vol_{insp}, ml	7020 ± 963	6837 ± 1296	0.69	6239 ± 1400	6504 ± 1623	0.67

	Valve responder	Valve non-responder	*p-value*	Coil responder	Coil non-responder	*p-value*
Total Lung Vol_{exp}, ml	5570 ± 927	5767 ± 1163	0.69	4845 ± 1165	5185 ± 1622	0.55
Total Lung DS, % (-950insp)	42.0 (35.5, 42.0)	35.0 (29.0, 41.0)	**0.04**‡	39.0 (21.5, 42.0)	31.0 (24.5, 38.5)	0.26‡
Total Lung DS, % (-856exp)	77.0 (65.0, 81.0)	71.0 (62.3, 76.3)	0.26‡	77.0 (67.0, 78.5)	74.0 (69.5, 78.5)	0.80‡
fGT, %	43.0 (37.0, 46.0)	42.5 (36.3, 44.8)	0.79‡	44.0 (41.0, 52.5)	46.0 (42.5, 53.5)	0.59‡
Total Lung Vessel Vol, ml	194.0 (163.0, 224.5)	206.0 (188.0, 228.0)	0.65‡	149.0 (114.5, 201.5)	160.0 (130.5, 190.0)	0.45‡
PA ratio	0.85 (0.81, 0.88)	0.84 (0.72, 0.88)	0.55‡	0.74 (0.71, 0.80)	0.79 (0.73, 0.91)	0.19‡
Mortality Score						
BODE Index	6 (5, 7)	5 (4, 6)	0.10‡	4 (4, 7)	5 (5, 7)	0.30‡
Inflammatory marker						
White cell count, 10^9/L	8.32 ± 2.04	7.08 ± 1.80	0.10	7.99 ± 1.50	8.59 ± 2.05	0.40
Fibrinogen, mg/dL	3.42 ± 0.36	3.49 ± 1.11	0.86	3.39 ± 0.53	3.94 ± 0.60	**0.03**
C-reactive protein, mg/dL	3.07 ± 3.08	4.40 ± 7.07	0.59	3.22 ± 3.15	6.94 ± 9.69	0.16

Categorical data are presented as a frequency (%) and compared using a Fisher's exact test † (nominal) or Mann-Whitney test‡ (ordinal). Parametric continuous data are presented as mean ± SD and compared using an independent t-test unless otherwise stated. Non-parametric continuous data are presented as median (IQR) and compared using a Mann-Whitney test‡. AX, area under reactance; BMI, Body Mass Index; BODE index = Body mass index, airflow Obstruction, Dyspnoea, and Exercise capacity; c, corrected for haemoglobin concentration; DS, Destruction Score; ex, expiratory; FEV_1, Forced Expiratory Volume in 1 second; fGT, functional gas trapping; Fres, resonant frequency; FVC, Forced Vital Capacity; GOLD, Global Initiative for Obstructive Lung Disease; HCO3, bicarbonate; G_{aw}, airways conductance; IC, Inspiratory Capacity; ICS, inhaled corticosteroid; in, inspiratory; K_{CO}, carbon monoxide diffusing capacity per unit alveolar volume; LABA, long-acting beta agonist; LAMA, long-acting muscarinic antagonist; mMRC, modified Medical Research Council dyspnoea scale; PCO_2, PA ratio, pulmonary artery to aorta ratio; Partial pressure for carbon dioxide; PO_2, Partial pressure for oxygen; R5, airways resistance at 5Hz; R20, airways resistance at 20Hz; R_{aw}, airways resistance; RV, Residual Volume; SGRQ, St George's Respiratory Questionnaire; TLC, Total Lung Capacity; TL_{CO}, Transfer factor for carbon monoxide; Vol, Volume; X5, reactance at 5Hz; 6MWD, Six-Minute Walk Distance.

Table 4.4. Baseline characteristics of responders versus non-responders – valve & coil cohorts.

[Responders were defined as those who achieved a RV reduction of ≥10% at 3 months].

Endobronchial coil (EBC)

Baseline characteristics

28 patients were enrolled: mean age 66.9 ± 8.2 years, 43% male, 42 pack year smoking history, and two exacerbations in the preceding 12 months. 36% were classified as GOLD grade III, 64% IV. Questionnaires recorded a mMRC of 3 (2, 3) and SGRQ-total of 52.6 ± 10.8 points. The cohort demonstrated severe airflow obstruction, FEV1 29.6 ± 7.7%, and hyperinflation, RV 232.7 ± 33.4%. Lung function, exercise capacity and quantitative CT parameters are detailed in Table 4.1.

Changes in characteristics at 3-months

At 3-months, reductions in SGRQ-activity of -8.41 points (<0.01) and in the BODE index of -0.5 (p<0.01) were recorded. qCT revealed a small median increase in total lung vessel volume of 16.5mls (p<0.01). Functional improvements were measured in RV of -15.12% (p=0.01), RV/TLC of -2.58% (p=0.03), and **AXex of -1.08 (p=0.04).** However, individuals experienced a fall in KCO of -3.67% (p<0.01). (Table 4.2).

Small airways physiology delta correlations

Focusing on those small airways metrics that were significantly changed at 3 months: Δ**Axex** was positively correlated with RV/TLC (r=0.45, p=0.03) and negatively related to FEV1 (r=-0.41, p=0.04), IC (r=-0.49, p=0.01), IC/TLC (r=-0.51, p=0.01), and 6MWD (r=-0.45, p=0.02). (Figure 4.3 and Appendix B: Table S4.3).

Predictors

9 of 26 subjects achieved a ≥10% reduction in RV. Responders were characterised by higher baseline FEV1% (p=0.04), FEV1/FVC% (p=0.03), MEF25-75% (p=0.02), and lower pCO_2 (p=0.04), HCO_3 (p=0.04), and fibrinogen (p=0.03) levels. (Table 4.4). Binomial logistic regression did not identify any baseline predictors of a ≥10% reduction in RV.

Overall impact of EBC implantation on small airways function

At 3 months, the area under reactance during expiration was significantly improved. This was accompanied by a modest reduction in residual volume of -0.31 ± 0.60L (p=0.01) together with small

gains in the BODE index and in quality of life. The changes in AXex positively correlated with worsening airflow limitation, hyperinflation, and exercise intolerance. The comparatively minor volume reduction achieved (and fall in gas transfer) using this technique may explain the lack of impact on peripheral airways function.

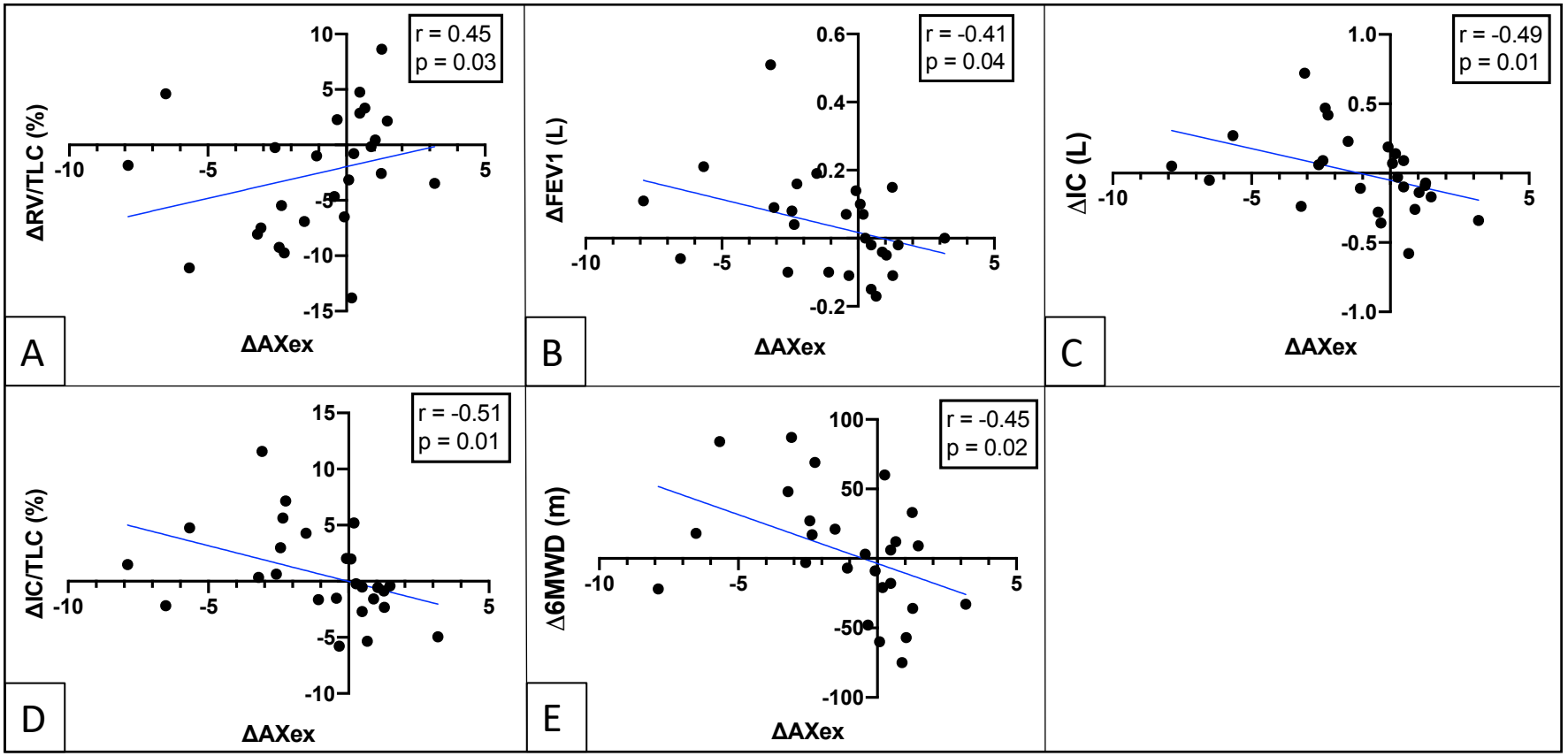

Figure 4.3. Delta correlations – coil cohort.

AXex with RV/TLC (**A**), FEV1 (**B**), IC (**C**), IC/TLC (**D**), and 6MWD (**E**).

Group comparisons

Baseline characteristics

There were no significant differences between surgery and valve cohorts. (Tables 4.1 and 4.5).

The surgery cohort had higher baseline values compared to the coil cohort for $MEF_{25-75\%}$ (0.28 versus 0.19 L/s; p=0.03), total lung emphysema score (41 versus 33%; p<0.01), and vessel volume (188 versus 151mls; p=0.01).

The valve cohort had higher SGRQ-impact score (48.83 versus 36.93points; p=0.04) and vessel volume (188 versus 151mls; p<0.01) but lower baseline fGT (42 versus 46%; p=0.03) compared to the coil cohort.

Changes in characteristics at 3-months

The surgery cohort achieved mean improvements greater than the valve cohort in TLC% (-7.07; p=0.02) and $G_{AW\text{-}total}$ (+0.14; p<0.01). (Tables 4.2 and 4.6).

The surgery cohort experienced gains in excess of those of the coil cohort in SGRQ-symptoms (-18.35; p=0.04), FEV1% (+6.73; p<0.01), FEV1/FVC (+4.88; p=0.02), $MEF_{25-75\%}$ (+0.12; p=0.04), RV% (-44.27; p<0.01), TLC% (-13.20; p<0.01), $G_{AW\text{-}total}$ (+0.03: ; p<0.01), TLCO (+0.73; p<0.01), BODE index (-17.32; p=0.02), CT-total lung $volume_{insp}$ (-733.2mls; p<0.01), CT-air trapping (-18.26; p<0.01), and CT-vessel volume (-19.53; p<0.01).

The valve cohort achieved greater mean improvements than the coil cohort in FEV1% (+5.74; p<0.01), RV% (-25.54; p<0.01), TLC% (-6.13; p=0.02), RV/TLC (-4.46; p=0.02), TLCO% (+5.22; p=0.03), KCO% (+4.45; p=0.04), HCO_3 (-1.86; p<0.01), 6MWD (+40.24 meters; p=0.03), and CT-total lung $volume_{insp}$ (-436.4mls; p=0.03).

		Group *p-value*	LVRS versus Valve difference	*p-value*	LVRS versus Coil difference	*p-value*	Valve versus Coil difference	*p-value*
Demographics								
Age, years		0.05	-6.40 (95% CI: -16.58, 3.79)	0.22	-8.43 (95% CI: -18.56, 1.71)	0.07	-2.03 (95% CI: -8.17, 4.11)	0.75
Gender (male), %		0.40†						
BMI, kg/m^2		0.44	-1.53 (95% CI: -4.85, 1.80)	0.50	-0.78 (95% CI: -3.96, 2.40)	0.87	0.75 (95% CI: -2.19, 3.69)	0.86
Active co-morbidities		0.35‡	-8.93	0.50	-3.69	1.00	5.24	1.00
Pack years		0.49‡	-7.72	0.74	-6.49	1.00	1.23	1.00
Exacerbations		0.90‡	-1.73	1.00	-3.01	1.00	-1.28	1.00
GOLD grade, %		0.80‡	-0.88	1.00	-3.35	1.00	-2.64	1.00
Heterogeneous, %		0.84‡						
Baseline medications								
LABA, %		0.18†						
LAMA, %		0.11†						
ICS, %		0.42†						
Oxygen, %		0.49†						
Symptoms								
mMRC		0.80‡	0.18	1.00	3.16	1.00	2.98	1.00
SGRQ	*Total Score*	0.16	-2.57 (95% CI: -13.56, 8.42)	0.84	4.84 (95% CI: -6.22, 15.90)	0.55	7.42 (95% CI: -1.74, 16.57)	0.14
	Symptoms	0.62	5.11 (95% CI: -10.11, 20.33)	0.70	6.12 (95% CI: -9.19, 21.43)	0.61	1.01 (95% CI: -11.67, 13.68)	0.98
	Activity	0.74	-2.34 (95% CI: -13.01, 8.34)	0.86	0.44 (95% CI: -10.30, 11.18)	0.99	2.78 (95% CI: -6.12, 11.67)	0.74
	Impacts	0.06	-4.86 (95% CI: -18.82, 9.10)	0.68	7.05 (95% CI: -7.00, 21.09)	0.46	11.90 (95% CI: 0.28, 23.53)	**0.04**
Routine lung function								
FEV_1, L		0.06	0.13 (95% CI: -0.07, 0.34)	0.28	0.21 (95% CI: 0.00, 0.42)	0.05	0.08 (95% CI: -0.10, 0.25)	0.54
FEV_1, %		0.68	2.37 (95% CI: -4.35, 9.08)	0.68	2.08 (95% CI: -4.64, 8.80)	0.74	-0.28 (95% CI: -5.89, 5.33)	0.99
FVC, L		0.35	0.14 (95% CI -0.51, 0.79)	0.86	0.38 (95% CI: -0.28, 1.03)	0.36	0.23 (95% CI: -0.31, 0.78)	0.56
FVC, %		0.64	-2.03 (95% CI: -14.22, 10.16)	0.92	-4.67 (95% CI: -16.87, 7.52)	0.63	-2.64 (95% CI: -12.83, 7.54)	0.81
FEV1/FVC, %		0.12	3.84 (95% CI: -0.82, 8.50)	0.13	3.56 (95% CI: -1.10, 8.22)	0.17	-0.28 (95% CI: -4.17, 3.62)	0.98
MEF25-75%, L/s		**0.04**	0.07 (95% CI: -0.02, 0.16)	0.15	0.09 (95% CI: 0.01, 0.17)	**0.03**	0.02 (95% CI: -0.06, 0.10)	0.83
RV, L		0.58	0.35 (95% CI: -0.56, 1.27)	0.62	0.37 (95% CI: -0.55, 1.29)	0.60	0.02 (95% CI: -0.74, 0.78)	1.00
RV, %		0.24	22.13 (95% CI: -10.88, 55.13)	0.25	20.39 (95% CI: -12.81, 53.60)	0.31	-1.74 (95% CI: -29.23, 25.76)	0.99
TLC, L		0.42	0.43 (95% CI: -0.83, 1.69)	0.70	0.71 (95% CI: -0.57, 1.98)	0.38	0.28 (95% CI: -0.77, 1.33)	0.80
TLC, %		0.79	0.53 (95% CI: -9.80, 10.86)	0.99	-1.88 (95% CI: -12.27, 8.52)	0.90	-2.40 (95% CI: -11.01, 6.20)	0.78
RV/TLC, %		0.46	0.66 (95% CI: -4.81, 6.14)	0.95	-1.67 (95% CI: -7.18, 3.83)	0.75	-2.34 (95% CI: -6.90, 2.23)	0.44
IC, L		0.59	-0.05 (95% CI: -0.50, 0.40)	0.96	0.11 (95% CI: -0.34, 0.55)	0.84	0.16 (95% CI: -0.22, 0.53)	0.57

	Group *p-value*	LVRS versus Valve difference	*p-value*	LVRS versus Coil difference	*p-value*	Valve versus Coil difference	*p-value*
IC/TLC, %	0.44	-1.81 (95% CI: -5.76, 2.13)	0.52	-0.33 (95% CI: -4.25, 3.59)	0.98	1.48 (95% CI: -1.82, 4.79	0.53
R_{aw}, kPA/L/s	0.50	-0.17 (95% CI: -0.60, 0.26)	0.60	-0.21 (95% CI: -0.64, 0.23)	0.49	-0.03 (95% CI: -0.39, 0.33)	0.98
G_{aw}, kPA/L/s	0.45	-0.00 (95% CI: -0.11, 0.11)	1.00	0.04 (95% CI: -0.07, 0.15)	0.63	0.05 (95% CI: -0.05, 0.14)	0.46
TLCOc, mmol/min/kPA	0.30	0.30 (95% CI: -0.45, 1.05)	0.60	0.51 (95% CI: -0.27, 1.28)	0.26	0.21 (95% CI: -0.44, 0.85)	0.72
TLCOc, %	0.94	0.08 (95% CI: -7.38, 7.53)	1.00	0.90 (95% CI: -6.82, 8.62)	0.96	0.82 (95% CI: -5.58, 7.23)	0.95
KCOc, mmol/min/kPA	0.39	0.04 (95% CI: -0.09, 0.18)	0.71	0.08 (95% CI: -0.06, 0.22)	0.36	0.04 (95% CI: -0.08, 0.15)	0.75
KCOc, %	0.54	1.05 (95% CI: -7.84, 9.94)	0.96	3.86 (95% CI: -5.34, 13.06)	0.58	2.81 (95% CI: -4.83, 10.45)	0.65
pH	0.75	-0.01 (95% CI: -0.03, 0.02)	0.76	-0.00 (95% CI: -0.02, 0.02)	0.96	0.00 (95% CI: -0.01, 0.02)	0.85
PCO_2	0.81	-0.11 (95% CI: -0.62, 0.41)	0.87	-0.14 (95% CI: -0.64, 0.37)	0.80	-0.03 (95% CI: -0.45, 0.40)	0.99
PO_2	0.22	0.72 (95% CI: -0.26, 1.70)	0.19	0.41 (95% CI: -0.56, 1.38)	0.57	-0.31 (95% CI: -1.12, 0.50)	0.63
HCO_3	0.55	-0.95 (95% CI: -3.05, 1.16)	0.53	-0.76 (95% CI: -2.84, 1.32)	0.66	0.19 (95% CI: -1.54, 1.92)	0.96
Static compliance, L/cm H_20	0.76	-0.65 (95% CI: -3.59, 2.28)	0.86	-0.20 ((95% CI: -3.06, 2.67)	1.00	0.45 (95% CI: -1.89, 2.80)	0.93
Impulse oscillometry							
R5, kPa/L/s	0.93	-0.01 (95% CI: -0.17, 0.15)	0.99	-0.02 (95% CI: -0.18, 0.14)	0.94	-0.02 (95% CI: -0.15, 0.12)	0.95
R20, kPa/L/s	0.97	0.01 (-0.07, 0.09)	0.97	0.01 (95% CI: -0.08, 0.09)	0.98	-0.00 (95% CI: -0.07, 0.07)	1.00
R5-20, kPa/L/s	0.77	-0.01 (95% CI: -0.12, 0.10)	0.96	-0.03 (95% CI: -0.14, 0.08)	0.78	-0.02 (95% CI: -0.11, 0.07)	0.86
Rin5, kPa/L/s	0.76	-0.00 (95% CI: -0.09, 0.09)	1.00	-0.02 (95% CI: -0.12, 0.07)	0.83	-0.02 (95% CI: -0.10, 0.06)	0.78
Rex5, kPa/L/s	0.73	0.07 (95% CI: -0.16, 0.30)	0.73	0.03 (95% CI: -0.20, 0.26)	0.95	-0.04 (95% CI: -0.23, 0.15)	0.84
X5, kPa/L/s	0.28	0.10 (95% CI: -0.06, 0.27)	0.29	0.10 (95% CI: -0.07, 0.26)	0.34	-0.01 (95% CI: -0.14, 0.13)	0.99
Xin5, kPa/L/s	0.31	0.03 (95% CI: -0.04, 0.10)	0.52	0.05 (95% CI: -0.02, 0.12)	0.28	0.01 (95% CI-0.04, 0.07)	0.84
Xex5, kPa/L/s	0.98	0.00 (95% CI: -0.29, 0.29)	1.00	0.02 (95% CI: -0.28, 0.31)	0.99	0.02 (95% CI: -0.23, 0.26)	0.99
Xin5-Xex5, kPa/L/s	0.51	-0.03 (95% CI: -0.29, 0.23)	0.95	-0.11 (95% CI: -0.38, 0.15)	0.56	-0.08 (95% CI: -0.29, 0.13)	0.64
AX	0.99	-0.07 (95% CI: -1.89, 1.74)	0.99	-0.13 (95% CI: -1.95, 1.69)	0.98	-0.06 (95% CI: -1.57, 1.45)	1.00
AXinsp	0.46	-0.26 (95% CI: -1.15, 0.62)	0.76	-0.47 (95% CI: -1.36, 0.43)	0.43	-0.20 (95% CI: -0.95, 0.55)	0.80
AXexp	0.84	0.72 (95% CI: -2.37, 3.80)	0.84	0.68 (-2.42, 3.79)	0.86	-0.04 (95% CI: -2.61, 2.53)	1.00
Fres total	0.76	0.61 (95% CI: -3.20, 4.42)	0.92	1.17 (95% CI: -2.66, 5.01)	0.74	0.57 (95% CI: -2.61, 3.74)	0.90
Fres central	0.93	-0.01 (95% CI: -0.06, 0.04)	0.94	-0.01 (95% CI: -0.06, 0.04)	0.93	-0.00 (95% CI: -0.04, 0.04)	1.00
Fres peripheral	0.65	-0.03 (95% CI: -0.23, 0.18)	0.95	-0.08 (95% CI: -0.28, 0.13)	0.66	-0.05 (95% CI: -0.22, 0.12)	0.77
Exercise capacity							
6MWD, m	0.81	19.70 (95% CI: -62.56, 102.0)	0.83	4.81 (95% CI: -77.95, 87.56)	0.99	-14.89 (95% CI: -83.42, 53.63)	0.86
CT metrics							
Total Lung Vol_{insp}, ml	0.23	453.0 (95% CI: -1448, 2354)	0.85	969.3 (95% CI: 981.6, 2920)	0.40	516.3 (95% CI: -457.4, 1490)	0.38
Total Lung Vol_{exp}, ml	0.22	266.2 (95% CI: -1674, 2206)	0.96	842.7 (95% CI: -1135, 2820)	0.49	576.5 (95% CI: -403.9, 1557)	0.30
Total Lung DS, % (-950insp)	**<0.01**‡	9.01	0.52	22.34	**<0.01**	13.33	0.04
Total Lung DS, % (-856exp)	0.28‡	9.42	0.41	8.82	0.43	-0.60	1.00
fGT, %	**0.02**‡	1.70	1.00	-11.15	0.19	-12.85	**0.03**

	Group *p-value*	LVRS versus Valve difference	*p-value*	LVRS versus Coil difference	*p-value*	Valve versus Coil difference	*p-value*
Total Lung Ves Vol, ml	**<0.01**‡	2.18	1.00	19.24	**0.01**	17.06	**<0.01**
PA ratio	0.15‡	-6.91	0.89	3.30	1.00	10.21	0.17
Mortality Score							
BODE Index	0.83‡	-3.73	1.00	-1.34	1.00	2.39	1.00
Inflammatory marker							
WCC, 10^9/L	0.52	0.49 (95% CI: -1.20, 2.18)	0.76	-0.15 (95% CI: -1.84, 1.53)	0.97	-0.64 (95% CI: -2.03, 0.73)	0.50
Fibrinogen, mg/dL	0.14	-0.15 (95% CI: -0.92, 0.62)	0.89	-0.46 (95% CI: -1.22, 0.30)	0.31	-0.32 (95% CI: -0.76, 0.13)	0.21
CRP, mg/dL	0.33	-0.96 (95% CI: -5.80, 3.88)	0.88	-2.75 (95% CI: -7.50, 2.00)	0.35	-1.79 (95% CI: -5.78, 2.20)	0.53

Group comparisons of categorial data are made using a Chi-square test† (nominal) or Kruskal-Wallis test‡ (ordinal). Parametric continuous data are compared using a one-way ANOVA unless otherwise stated: Tukey's multiple comparisons test is presented as mean difference (95% confidence interval, CI). Non-parametric continuous data are compared using a Kruskal-Wallis test‡: Dunn's multiple comparisons test is presented as mean rank difference. AX, area under reactance; c, corrected for haemoglobin concentration; DS, Destruction Score; ex, expiratory; FEV_1, Forced Expiratory Volume in 1 second; fGT, functional gas trapping; Fres, resonant frequency; FVC, Forced Vital Capacity; HCO_3, bicarbonate; G_{aw}, airways conductance; IC, Inspiratory Capacity; in, inspiratory; K_{CO}, carbon monoxide diffusing capacity per unit alveolar volume; LVRS, lung volume reduction surgery; mMRC, modified Medical Research Council dyspnoea scale; PCO_2, PA ratio, pulmonary artery to aorta ratio; Partial pressure for carbon dioxide; PO_2, Partial pressure for oxygen; R5, airways resistance at 5Hz; R20, airways resistance at 20Hz; R_{aw}, airways resistance; RV, Residual Volume; SGRQ, St George's Respiratory Questionnaire; TLC, Total Lung Capacity; TL_{CO}, Transfer factor for carbon monoxide; Vol, Volume; X5, reactance at 5Hz; 6MWD, Six-Minute Walk Distance.

Table 4.5. Group comparisons at baseline.

		Group *p-value*	LVRS versus Valve difference	*p-value*	LVRS versus Coil difference	*p-value*	Valve versus Coil difference	*p-value*
Symptoms								
∆mMRC		0.18‡	-7.93	0.57	-11.35	0.20	-3.42	1.00
∆SGRQ	*Total Score*	0.07	-8.11 (95% CI: -19.87, 3.64)	0.23	-11.70 (95% CI: -23.69, 0.28)	0.06	-3.59 (95% CI: -13.57, 6.39)	0.67
	Symptoms	0.09	-16.62 (95% CI: -34.08, 0.83)	0.07	-18.35 (95% CI: -36.15, -0.55)	**0.04**	-1.73 (95% CI: -16.55, 13.10)	0.96
	Activity	0.40	-5.35 (95% CI: -17.86, 7.16)	0.56	-7.20 (95% CI: -19.96, 5.56)	0.37	-1.85 (95% CI: -12.48, 8.78)	0.91
	Impacts	0.11	-7.14 (95% CI: -20.66, 6.37)	0.42	-12.25 (95% CI: -26.02, 1.53)	0.09	-5.10 (95% CI: -16.58, 6.38)	0.54
Routine lung function								
∆FEV_1, L		**<0.01**	0.07 (95% CI: -0.07, 0.22)	0.44	0.22 (95% CI: 0.07, 0.37)	**<0.01**	0.15 (95% CI: 0.02, 0.27)	**0.02**
∆FEV_1, %		**<0.01**	0.99 (95% CI: -4.20, 6.19)	0.89	6.73 (95% CI:1.47, 12.00)	**<0.01**	5.74 (95% CI: 1.32, 10.16)	**<0.01**
∆FVC, L		0.17	-0.13 (95% CI -0.47, 0.21)	0.62	0.10 (95% CI: -0.25, 0.44)	0.78	0.23 (95% CI: -0.06, 0.52)	0.15
∆FVC, %		0.06	-5.66 (95% CI: -16.22, 4.91)	0.41	3.47 (95% CI: -7.24, 14.17)	0.72	9.12 (95% CI: 0.13, 18.12)	0.05
∆FEV1/FVC, %		**0.02**	2.23 (95% CI: -1.81, 6.26)	0.39	4.88 (95% CI: 0.79, 8.97)	**0.02**	2.66 (95% CI: -0.78, 6.09)	0.16
∆MEF25-75%, L/s		0.05	0.09 (95% CI: -0.03, 0.22)	0.18	0.12 (95% CI: 0.00, 0.25)	**0.04**	0.03 (95% CI: -0.08, 0.14)	0.78
∆RV, L		**<0.01**	-0.35 (95% CI: -0.82, 0.13)	0.19	-0.95 (95% CI: -1.44, -0.47)	**<0.01**	-0.61 (95% CI: -1.01, -0.20)	**<0.01**
∆RV, %		**<0.01**	-18.73 (95% CI: -40.15, 2.69)	0.10	-44.27 (95% CI: -66.11, -22.43)	**<0.01**	-25.54 (95% CI: -43.72, -7.35)	**<0.01**
∆TLC, L		**<0.01**	-0.41 (95% CI: -0.73, -0.08)	**0.01**	-0.84 (95% CI: -1.17, 0.51)	**<0.01**	-0.44 (95% CI: -0.71, -0.16)	**<0.01**
∆TLC, %		**<0.01**	-7.07 (95% CI: -13.10, -1.03)	**0.02**	-13.20 (95% CI: -19.36, -7.05)	**<0.01**	-6.13 (95% CI: -11.26, -1.01)	**0.02**
∆RV/TLC		**<0.01**	-0.89 (95% CI: -5.55, 3.77)	0.89	-5.35 (95% CI: -10.10, -0.60)	**0.02**	-4.46 (95% CI: -8.42, -0.50)	**0.02**
∆IC, L		0.20	-0.02 (95% CI: -0.28, 0.23)	0.97	0.13 (95% CI: -0.12, 0.39)	0.43	0.16 (95% CI: -0.06, 0.37)	0.20
∆IC/TLC, %		**<0.01**	0.76 (95% CI: -2.56, 4.09)	0.85	4.21 (95% CI: 0.87, 7.56)	**0.01**	3.45 (95% CI: 0.62, 6.29)	**0.01**
∆R_{aw}, kPA/L/s		0.41	0.01 (95% CI: -0.31, 0.34)	0.99	-0.13 (95% CI: -0.46, 0.20)	0.60	-0.15 (95% CI: -0.43, 0.13)	0.41
∆G_{aw}, kPA/L/s		**<0.01**	0.14 (95% CI: 0.05, 0.24)	**<0.01**	0.03 (95% CI: -0.01, 0.06)	**<0.01**	0.00 (95% CI: -0.08, 0.08)	1.00
∆TLCOc, mmol/min/kPA		**<0.01**	0.04 (95% CI: -0.50, 0.58)	0.98	0.73 (95% CI: 0.16, 1.29)	**<0.01**	0.69 (95% CI: 0.21, 1.16)	**<0.01**
∆TLCOc, %		**0.03**	-0.16 (95% CI: -5.45, 5.13)	1.00	5.05 (95% CI: -0.64, 10.74)	0.09	5.22 (95% CI: 0.41, 10.02)	**0.03**
∆KCOc, mmol/min/kPA		**<0.01**	0.02 (95% CI: -0.09, 0.13)	0.93	0.14 (95% CI: 0.03, 0.25)	0.01	0.13 (95% CI: 0.03, 0.22)	**<0.01**
∆KCOc, %		**0.03**	0.25 (95% CI: -4.49, 5.00)	0.99	4.70 (95% CI: -0.37, 9.78)	0.07	4.45 (95% CI: 0.14, 8.76)	**0.04**
∆pH		0.99	0.00 (95% CI: -0.03, 0.03)	0.99	-0.00 (95% CI: -0.03, 0.03)	1.00	-0.00 (95% CI: -0.03, 0.02)	0.99
∆PCO_2		0.05	0.03 (95% CI: -0.35, 0.40)	0.98	-0.29 (95% CI: -0.66, 0.09)	0.18	-0.31 (95% CI: -0.63, 0.00)	0.06
∆PO_2		0.05	0.71 (95% CI: -0.16, 1.58)	0.13	0.88 (95% CI: 0.01, 1.76)	0.05	0.18 (95% CI: -0.56, 0.91)	0.83
∆HCO_3		**<0.01**	0.40 (95% CI: -1.10, 1.90)	0.80	-1.46 (95% CI: -2.97, 0.05)	0.06	-1.86 (95% CI: -3.13, -0.60)	**<0.01**
∆Cstat, L/cm H_20		0.49	1.90 (95% CI: -2.79, 6.59)	0.59	1.63 (95% CI: -3.06, 6.32)	0.68	-0.27 (95% CI: -2.66, 2.13)	0.96
Exercise capacity								
∆6MWD, m		**0.02**	1.01 (95% CI: -42.99, 45.01)	1.00	41.25 (95% CI: -3.57, 86.06)	0.08	40.24 (95% CI: 3.72, 76.75)	**0.03**
Impulse oscillometry								
∆R5, kPa/L/s		0.68	-0.02 (95% CI: -0.12, 0.08)	0.89	0.01 (95% CI: -0.09, 0.11)	0.97	0.03 (95% CI: -0.05, 0.11)	0.66
∆R20, kPa/L/s		0.39	-0.02 (95% CI: -0.07, 0.03)	0.62	0.00 (95% CI: -0.05, 0.05)	0.99	0.02 (95% CI: -0.02, 0.06)	0.40
∆R5-20, kPa/L/s		0.96	0.00 (95% CI: -0.08, 0.08)	1.00	0.01 (95% CI: -0.08, 0.09)	0.97	0.01 (95% CI: -0.06, 0.07)	0.96

ΔRin5, kPa/L/s	0.51	2.42 (95% CI: -4.22, 9.05)	0.66	0.04 (95% CI: -6.67, 6.76)	1.00	-2.38 (95% CI: -7.76, 3.01)	0.54
ΔRex5, kPa/L/s	0.87	-0.02 (95% CI: -0.19, 0.14)	0.94	-0.04 (95% CI: -0.20, 0.13)	0.86	-0.01 (95% CI: -0.15, 0.12)	0.97
ΔX5, kPa/L/s	0.97	-0.02 (95% CI: -0.18, 0.14)	0.96	-0.01 (95% CI: -0.18, 0.15)	0.98	0.01 (95% CI: -0.13, 0.14)	0.99
ΔXin5, kPa/L/s	0.54	-0.01 (95% CI: -0.08, 0.05)	0.90	-0.03 (95% CI: -0.10, 0.04)	0.55	-0.02 (95% CI: -0.0, 0.04)	0.71
ΔXex5, kPa/L/s	0.43	0.09 (95% CI: -0.17, 0.35)	0.68	0.14 (95% CI: -0.12, 0.41)	0.40	0.05 (95% CI: -0.16, 0.26)	0.82
ΔXin5-Xex5, kPa/L/s	0.24	-0.10 (95% CI: -0.34, 0.14)	0.56	-0.17 (95% CI: -0.42, 0.07)	0.21	-0.07 (95% CI: -0.26, 0.12)	0.66
ΔAX	0.50	-0.52 (95% CI: -1.84, 0.79)	0.60	-0.42 (95% CI: -1.75, 0.91)	0.73	0.10 (95% CI: -0.96, 1.17)	0.97
ΔAXinsp	0.52	0.29 (95% CI: -0.33, 0.91)	0.50	0.15 (95% CI: -0.47, 0.78)	0.83	-0.14 (95% CI: -0.64, 0.37)	0.79
ΔAXexp	0.22	-1.36 (95% CI: -3.41, 0.68)	0.25	-1.39 (95% CI: -3.46, 0.68)	0.25	-0.03 (95% CI: -1.69, 1.63)	1.00
ΔFres total	0.23	-2.15 (95% CI: -5.19, 0.90)	0.22	-1.83 (95% CI: -4.92, 1.25)	0.33	0.31 (95% CI: -2.16, 2.79)	0.95
ΔFres central	0.60	0.01 (95% CI: -0.04, 0.06)	0.85	0.02 (95% CI: -0.03, 0.07)	0.58	0.01 (95% CI: -0.03, 0.05)	0.83
ΔFres peripheral	0.50	-0.11 (95% CI: -0.35, 0.12)	0.47	-0.08 (95% CI: -0.32, 0.15)	0.68	0.03 (95% CI: -0.16, 0.22)	0.91
CT metrics							
ΔTotal Lung Vol_{insp}, ml	**<0.01**	-296.7 (95% CI: -818.8, 225.3)	0.32	-733.2 (95% CI: -1124, -342.5)	**<0.01**	-436.4 (95% CI: -873.7, 0.85)	**0.03**
ΔTotal Lung Vol_{exp}, ml	**<0.01**	-369.7 (95% CI: -1746, 1007)	0.83	-1262.0 (95% CI: -2338, -185.6)	**<0.01**	-892.2 (95% CI: -2072, 287.9)	0.11
ΔTotal Lung DS, % (-950insp)	0.35‡	-7.76	0.70	-9.29	0.47	-1.53	1.00
ΔTotal Lung DS, % (-856exp)	**<0.01**‡	-8.08	0.57	-18.26	**<0.01**	-10.18	0.10
Δ fGT, %	0.02‡	-6.00	0.99	-14.73	0.03	-8.72	0.21
ΔTotal Lung Ves Vol, ml	**<0.01**‡	-9.18	0.48	-19.53	**<0.01**	-10.35	0.14
ΔPA ratio	0.81‡	-4.07	1.00	-1.96	1.00	2.11	1.00
Mortality Score							
ΔBODE Index	**0.02**‡	-7.25	0.74	-17.32	**0.02**	-10.07	0.16
Inflammatory marker							
ΔWCC, 10^9/L	0.10	-1.28 (95% CI: -2.77, 0.20)	0.10	-0.54 (95% CI: -2.02, 0.94)	0.66	0.74 (95% CI: -0.50, 1.98)	0.33
ΔFibrinogen, mg/dL	0.93	-0.19 (95% CI: -1.42, 1.05)	0.93	-0.18 (95% CI: -1.40, 1.04)	0.93	0.00 (95% CI: -0.68, 0.68)	0.93
ΔCRP, mg/dL	0.13	2.21 (95% CI: -4.48, 8.91)	0.71	5.41 (95% CI: -1.17, 11.99)	0.13	3.20 (95% CI: -2.66, 9.06)	0.39

Parametric continuous data are compared using a one-way ANOVA unless otherwise stated: Tukey's multiple comparisons test is presented as mean difference (95% confidence interval, CI). Non-parametric continuous data are compared using a Kruskal-Wallis test‡: Dunn's multiple comparisons test is presented as mean rank difference. AX, area under reactance; c, corrected for haemoglobin concentration; cStat, static compliance, DS, Destruction Score; ex, expiratory; FEV_1, Forced Expiratory Volume in 1 second; fGT, functional gas trapping; Fres, resonant frequency; FVC, Forced Vital Capacity; HCO_3, bicarbonate; G_{aw}, airways conductance; IC, Inspiratory Capacity; in, inspiratory; K_{CO}, carbon monoxide diffusing capacity per unit alveolar volume; LVRS, lung volume reduction surgery; mMRC, modified Medical Research Council dyspnoea scale; PCO_2, PA ratio, pulmonary artery to aorta ratio; Partial pressure for carbon dioxide; PO_2, Partial pressure for oxygen; R5, airways resistance at 5Hz; R20, airways resistance at 20Hz; R_{aw}, airways resistance; RV, Residual Volume; SGRQ, St George's Respiratory Questionnaire; TLC, Total Lung Capacity; TL_{CO}, Transfer factor for carbon monoxide; Vol, Volume; X5, reactance at 5Hz; 6MWD, Six-Minute Walk Distance.

Table 4.6. Group comparisons at 3-months.

Multiple breath nitrogen washout

The majority of nitrogen washout traces were, unfortunately, unusable owing to a leak from one of the Douglas bags detected after review by an international authority on MBNW (Dr Sylvia Verbanck). The following data have been salvaged for endobronchial valve recipients.

Endobronchial valves (EBV)

Baseline characteristics

12 patients were enrolled: median age 68 (57 to 71) years, 58% male, 46 pack year smoking history, and one exacerbation in the preceding 12 months. 33% were classified as GOLD grade III, 67% IV. Questionnaires recorded a mMRC of 2.5 (2, 3) and SGRQ-total of 50.85 (43.05 to 65.73) points. The cohort demonstrated severe airflow obstruction, FEV1 27.55% (22.10 to 31.50), and hyperinflation, RV 225.10% (196.20 to 283.50). Lung function, exercise capacity and quantitative CT parameters are detailed in Table 4.7.

Changes in characteristics at 3-months

At 3-months, median reductions in SGRQ-activity of -6.28 points (p=0.04) and in the BODE index of -1 (p=0.03) were recorded. qCT revealed median decreases in CT-total lung volume$_{INSP}$ of -730mls (p<0.01) and in CT-emphysema score at -950HU of -1.5% (p=0.04).

Median functional improvements were measured in FEV1 of +7.8% (p<0.01), FVC of +12.5% (p=0.01), FEV1/FVC of +3.13% (p<0.01), FRC$_{PLETH}$ of -29.75% (p<0.01), RV of -40.95% (p<0.01), TLC of -8.80% (p<0.01), RV/TLC of -5.13% (p<0.01), 6MWD of +66meters (p=0.02), X5 of +0.11kPa/L/s (p=0.01), Xex5 of +0.12 (p=0.01), Xin5-Xex5 of -0.20 kPa/L/s (p=0.01), **FRC$_{MBNW}$ of -638mls (p<0.01), LCI of -1.4 (p=0.01), AME +5% (p<0.01), and in Sacin of -0.24 L^{-1}, with a trend towards statistical significance (p=0.05).** (Table 4.7). Delta correlations and baseline predictors were not calculated owing to the small cohort size.

Overall impact of EBV implantation on small airways function

At 3 months, LCI, AME and Sacin were improved. There was a reduction in residual volume of 0.92 (-1.67, -0.33) litres ($p<0.01$) accompanied by gains in spirometry, IOS reactance, exercise capacity, total gas trapping on CT, the BODE index, and quality of life. These findings suggest enhanced peripheral airways function resulting from deflation of emphysematous lung.

		Baseline	3 months	Median of differences	*p-value*
Demographics					
Number		12			
Age, years		67.50 (57.00, 71.25)			
Gender (male), %:		58.33			
BMI, kg/m^2		24.42 (21.70, 27.95)	24.93 (23.02, 28.37)	0.41 (-0.87, 0.97)	0.577
Active co-morbidities		1.00 (1.00, 2.75)			
Pack years		45.50 (27.25, 50.75)			
Exacerbations (last year)		1.00 (0.00, 2.75)			
GOLD grade, %	III	33.33			
	IV	66.67			
Heterogeneous, %		41.67			
Baseline medications					
LABA, %		100			
LAMA, %		100			
ICS, %		100			
Oxygen, %		33.33%			
Symptoms					
mMRC		2.50 (2.00, 3.00)	2.00 (1.00, 2.75)	-1.00 (-1.00, 0.00)	0.217
SGRQ	total	50.85 (43.05, 65.73)	42.40 (24.98, 69.41)	-5.81 (-23.39, 5.35)	0.204
	symptoms	57.32 (28.87, 73.02)	51.46 (33.52, 69.80)	0.12 (-23.82, 19.29)	0.791
	impacts	35.30 (24.38, 55.22)	19.94 (14.35, 53.12)	-7.06 (-19.56, 6.29)	0.233
	activity	82.86 (67.97, 92.51)	69.65 (43.23, 90.84)	-6.28 (-30.72, 0.00)	**0.039**
Routine lung function					
FEV_1, L		0.71 (0.57, 0.89)	0.86 (0.75, 1.29)	0.19 (0.08, 0.52)	**0.002**
FEV_1, %		27.55 (22.10, 31.50)	32.60 (28.28, 44.30)	7.80 (3.20, 16.20)	**0.001**
FVC, L		2.89 (2.45, 3.63)	3.53 (2.64, 4.11)	0.34 (-0.09, 0.84)	**0.036**
FVC, %		85.90 (79.40, 96.63)	98.10 (89.63, 114.10)	12.50 (1.70, 27.90)	**0.005**
FEV1/FVC, %		24.01 (21.03, 25.80)	25.87 (24.24, 34.15)	3.13 (0.29, 6.24)	**0.003**
MEF25-75%, L/s		0.18 (0.14, 0.21)	0.24 (0.22, 0.35)	0.06 (-0.02, 0.17)	0.156
FRC, L		6.31 (5.66, 7.17)	5.45 (4.69, 6.10)	-1.07 (-1.40, -0.29)	**0.001**
FRC, %		193.20 (172.90, 226.40)	160.50 (142.50, 207.00)	-29.75 (-38.00, -12.00)	**0.001**
RV, L		5.03 (4.64, 6.07)	4.15 (3.22, 5.12)	-0.92 (-1.67, -0.33)	**0.001**
RV, %		225.10 (196.20, 283.50)	191.60 (141.30, 232.60)	-40.95 (-67.10, -16.00)	**0.001**
TLC, L		8.40 (7.22, 9.70)	7.60 (6.87, 8.25)	-0.50 (-0.94, -0.30)	**0.001**

	Baseline	3 months	Median of differences	*p-value*
TLC, %	137.40 (126.90, 150.80)	123.90 (116.30, 147.90)	-8.80 (-13.80, -5.40)	**0.001**
RV/TLC, %	60.98 (56.49, 69.38)	55.02 (46.01, 63.31)	-5.13 (-15.09, -2.40)	**0.001**
IC, L	1.91 (1.57, 2.54)	2.34 (1.85, 2.58)	0.26 (-0.16, 0.84)	0.123
R_{aw}, kPA/L/s	1.17 (0.70, 1.65)	0.80 (0.64, 1.01)	-0.11 (-0.76, 0.11)	0.127
G_{aw}, kPA/L/s	0.22 (0.12, 0.38)	0.25 (0.20, 0.39)	0.02 (-0.02, 0.14)	0.229
TLCOc, mmol/min/kPA	2.97 (2.33, 3.44)	3.31 (2.60, 3.79)	0.24 (-0.24, 0.37)	0.204
TLCOc, %	34.85 (27.50, 44.65)	39.40 (30.90, 43.65)	2.85 (-2.00, 4.80)	0.197
KCOc, mmol/min/kPA	0.68 (0.50, 0.81)	0.66 (0.53, 0.84)	-0.02 (-0.04, 0.06)	0.593
KCOc, %	43.65 (35.63, 54.68)	46.35 (38.40, 51.75)	1.55 (-2.70, 5.90)	0.274
pH	7.44 (7.41, 7.45)	7.43 (7.42, 7.44)	0.00 (-0.02, 0.05)	0.398
PCO_2	5.06 (4.62, 5.63)	4.83 (4.60, 5.11)	-0.21 (-0.89, 0.16)	0.131
PO_2	8.92 (7.46, 9.62)	8.94 (7.92, 9.66)	-0.34 (-1.04, 0.55)	0.322
HCO_3	25.30 (23.28, 26.40)	23.70 (21.90, 26.33)	-0.65 (-2.60, 1.00)	0.232
Static compliance, L/cm H_20	2.13 (1.58, 2.86)	2.27 (1.74, 3.07)	0.05 (-0.74, 1.10)	0.465
Impulse oscillometry				
R5, kPa/L/s	0.72 (0.53, 0.96)	0.68 (0.64, 0.85)	-0.02 (-0.14, 0.11)	0.7
R20, kPa/L/s	0.40 (0.33, 0.44)	0.42 (0.37, 0.48)	0.03 (-0.05, 0.10)	0.3
R5-20, kPa/L/s	0.34 (0.20, 0.49)	0.30 (0.23, 0.36)	-0.05 (-0.12, 0.06)	0.3
Rin5, kPa/L/s	0.52 (0.39, 0.60)	0.51 (0.48, 0.64)	0.03 (-0.03, 0.12)	0.1
Rex5, kPa/L/s	0.82 (0.60, 0.99)	0.78 (0.68, 0.89)	0.03 (-0.12, 0.12)	0.9
X5, kPa/L/s	-0.56 (-0.72, -0.32)	-0.38 (-0.57, -0.30)	0.11 (-0.01, 0.18)	**0.013**
Xin5, kPa/L/s	-0.25 (-0.32, -0.20)	-0.24 (-0.30, -0.20)	-0.01 (-0.05, 0.04)	0.9
Xex5, kPa/L/s	-0.88 (-1.27, -0.51)	-0.55 (-0.96, -0.34)	0.12 (0.00, 0.37)	**0.010**
Xin5-Xex5, kPa/L/s	0.63 (0.34, 1.03)	0.34 (0.08, 0.78)	-0.20 (-0.37, -0.01)	**0.010**
AX	5.12 (2.62, 7.28)	3.75 (2.87, 4.95)	-0.46 (-2.34, 0.71)	0.15
AXinsp	2.20 (0.95, 2.86)	1.70 (1.34, 2.37)	0.20 (-0.53, 0.31)	0.68
AXexp	7.93 (4.48, 11.96)	6.07 (4.71, 7.43)	-0.23 (-3.63, 0.97)	0.38
Fres total	32.19 (25.51, 36.18)	28.51 (27.41, 31.05)	0.05 (-5.53, 1.69(	0.57
Fres central	0.31 (0.28, 0.35)	0.34 (0.30, 0.36)	0.01 (-0.04, 0.07)	0.31
Fres peripheral	0.97 (0.70, 1.00)	0.80 (0.69, 0.97)	-0.06 (-0.19, 0.00)	0.20
Multiple breath nitrogen washout				
FRC, mls	4804 (3586, 5269)	3761 (3529, 4443)	-638 (-1143, -133)	**0.001**
VDF, mls	235.50 (206.50, 279.30)	247.00 (216.50, 253.80)	0.50 (-26.00, 46.00)	0.898
LCI	12.00 (11.25, 13.00)	10.70 (9.83, 12.83)	-1.40 (-1.80, 0.20)	**0.006**
AME, %	58.00 (55.25, 60.75)	63.50 (57.75, 73.00)	5.00 (2.00, 15.00)	**0.001**

	Baseline	3 months	Median of differences	*p-value*
Sacin, L^{-1}	1.36 (1.24, 1.65)	1.24 (0.86, 1.43)	-0.24 (-0.55, 0.14)	0.052
Scond, L^{-1}	0.06 (0.03, 0.08)	0.05 (0.03, 0.07)	0.00 (-0.02, 0.02)	1.000
FRC_{PLETH}-FRC_{MBW}, L	1.4 (0.6, 2.7)	1.5 (1.2, 2.8)	0.2 (-0.3, 0.7)	0.3
Exercise capacity				
6MWD, meters	348.00 (291.30, 401.30)	423.00 (305.30, 466.50)	66.00 (-9.00, 93.00)	**0.020**
CT metrics				
Total Lung Vol_{insp}, ml	7188 (6426, 7853)	6441 (5636, 6700)	-730 (-1023, -202)	**<0.01**
Total Lung Vol_{exp}, ml	5866 (5192, 6493)	4850 (4497, 5260)	-581 (-911, -196)	0.25
Total Lung DS, % (-950insp)	35.00 (31.50, 42.00)	35.50 (28.25, 40.75)	-1.50 (-6.00, 0.00)	**0.043**
Total Lung DS, % (-856exp)	67.00 (61.25, 72.75)	58.00 (31.00, 65.50)	-5.00 (-41.00, 6.00)	0.75
fGT, %	44.00 (38.50, 46.50)	31.00 (6.75, 56.00)	-6.00 (-35.00, 18.00)	0.75
Total Lung Vessel Vol, ml	203.50 (175.50, 234.00)	222.00 (163.00, 247.00)	5.00 (-29.00, 33.00)	0.413
PA ratio	0.86 (0.82, 0.89)	0.87 (0.81, 1.01)	0.01 (-0.03, 0.08)	0.324
Mortality Score				
BODE Index	5.00 (4.00, 6.00)	4.00 (3.00, 5.00)	-1.00 (-2.00, -1.00)	**0.030**
Inflammatory marker				
White cell count, 10^9/L	8.00 (6.60, 10.40)	7.85 (7.43, 9.80)	-0.10 (-0.60, 0.90)	0.973
Fibrinogen, mg/dL	3.60 (3.30, 4.15)	4.10 (3.35, 4.53)	0.20 (-0.50, 0.40)	0.984
C-reactive protein, mg/dL	3.00 (2.50, 4.50)	4.50 (1.75, 7.25)	0.50 (-4.00, 5.00)	0.750

Categorical data are presented as a percentage (%). Numeric data are presented as median (IQR) and compared using the Wilcoxon test: median of differences is reported using 96.14% confidence intervals unless stated otherwise. AME, alveolar mixing efficiency; AX, area of reactance; BMI, body mass index; BODE index = Body mass index, airflow Obstruction, Dyspnoea, and Exercise capacity; c, corrected for haemoglobin concentration; DS, destruction score; FEV_1, forced expiratory volume in 1 second; FRC, functional residual capacity; Fres, resonant frequency; FVC, forced vital capacity; GOLD, Global initiative for chronic obstructive lung disease; HCO3, bicarbonate; G_{aw}, airways conductance; IC, inspiratory capacity; ICS, inhaled corticosteroid; KCO, carbon monoxide diffusing capacity per unit alveolar volume; LABA, long acting beta-agonist; LAMA, long acting muscarinic antagonist; LCI, lung clearance index; MEF25-75%, mid-expiratory flow 25-75%; mMRC, modified Medical Research Council dyspnoea scale; PCO_2, partial pressure for carbon dioxide; PO_2, partial pressure for oxygen; R_{aw}, airways resistance; RV, residual volume; Rex5-20, resistance at 5 and 20 Hertz during expiration; Sacin, ventilation heterogeneity in the acinar airway zone; Scond, ventilation heterogeneity in the conducting airway zone; SGRQ, St George's respiratory questionnaire; TLC, total lung capacity; TLCO, transfer factor for carbon monoxide; VDF, Fowler dead space; Vol, volume; X5, reactance at 5 Hertz; Xex5, reactance at 5 Hertz during expiration; Xin5, reactance at 5 Hertz during inspiration; 6MWD, Six-minute walk distance.

Table 4.7. Clinical characteristics at baseline and 3 months – valve cohort

Discussion

The diagnosis and classification of COPD are based on a spirometry necessarily entailing a forced manoeuvre to measure expiratory flow and dynamic lung volumes that can be challenging for breathless individuals[340]. The test yields little analysis of the small airways, the principal site of airflow obstruction[20]. IOS and MBNW are less taxing tidal breathing techniques and are more informative, improving understanding of the course of the disease and the response to therapeutic interventions in the peripheral airways compartment[341]. In the individual with emphysema and hyperinflation, the loss of parenchymal structures responsible for passive elastic recoil in the lung during expiration impacts on the alveoli diminishing the transmural pressure or drive resulting in a reduced calibre of the small bronchioles and increased resistance[149], compounded by small airways inflammation and remodelling[85]. For the population studied, we will now discuss the impact of lung volume reduction on small airways function employing these investigative modalities.

Impulse oscillometry (IOS)

Resistance

Hsu et al studied nine patients with severe COPD and hyperinflation undergoing bronchoscopic lung volume reduction with valves and showed a reduced airways resistance at 5Hz (R5) in four of those whose procedure was followed by complete atelectasis of the treated lobe[342]. Khattab et al evaluated 23 patients with heterogeneous emphysema or emphysematous bullae undergoing biological (histoacryl gel) bronchoscopic lung volume reduction and demonstrated a decrease in R5 and R20, but without a statistically significant change in X5 – surprisingly, no mention of the impact on lung volume was made in this trial[343].

In our study, airway resistances at 5Hz were high compared to others' reports in the literature[248, 252, 256], likely reflecting the severe burden of disease. Expiratory airways resistance at 5Hz, corresponding to total airways resistance, was reduced in the surgery cohort only, and whilst this may be seen only with substantial tissue resection, the absence of a signal in patients who achieved similar

physiological outcomes using endobronchial valves suggests that deflation or removal of emphysematous tissue is the principal driver of benefit improving chest wall asynchrony[172] and diaphragmatic movement[176].

Reactance

Studies by Hsu[342] and Khattab[343] showed minimal change in reactance at 5Hz following bronchoscopic lung volume reduction using valves and histoacryl gel, respectively.

In our study, baseline values for reactance at 5Hz and area under the reactance curve (AX) were high compared to previous reports[248, 252, 256], again most likely attributable to the severe physiological compromise of the cohort. Following both surgery and endobronchial valve implantation, expiratory airways reactance and within-breath reactance at 5Hz were significantly improved. Measurement of reactance is considered more sensitive to expiratory airflow limitation than airways resistance metrics[248, 344, 345], in particular within-breath reactance (Xin5-Xex5)[346], and is thought to reflect changes in pulmonary compliance[344]. Furthermore, a reduction in within-breath reactance may result in improved exercise performance (as suggested in our study), lower frequency of exacerbations and hospitalisations[347].

The change in expiratory AX (AXex) was the only IOS metric to be significantly improved in all three arms: surgery > valves and coils, and correlated with airflow limitation (FEV1, MEF25-75%), hyperinflation, and exercise intolerance. AX represents low frequency reactance in smaller airways with increased values reflecting reduced lung compliance[340].

Resonant frequency

Resonant frequency (Fres) is the oscillation at which the lung tissue moves from passive distension to active stretch (i.e. when reactance equals zero)[348]. In our study, baseline values were high compared to previous reports in the literature[248, 252, 256]. Similar to expiratory airways resistance at 5Hz, Fres was reduced in the surgery cohort only, and probably reflects the effects of lung tissue resection with greater volume reduction compared to the other interventions studied.

Multiple breath nitrogen washout (MBNW)

Travaline et al employed xenon washout scintigraphic imaging in 29 patients with severe emphysema in an elegant demonstration of improved small airways ventilation following bilateral lung volume reduction surgery that was independent of the area resected, implying a global enhancement of lung function[349].

We chose MBNW to evaluate the impact of lung volume reduction using endobronchial valves on overall lung physiology. Increased ventilation heterogeneity of the acinar airways is associated with worsening severity of COPD and is weakly related to IOS resistance and reactance parameters[270]. In our study, baseline values for S_{acin} were significantly higher compared to a previous report in the literature[270], again probably reflecting the severity of the cohort. Following valve implantation, modest improvements to alveolar gas mixing (AME) and small airways function (S_{acin}) were observed. Our data corroborates the findings of Travaline et al[349] and provides further mechanistic insight into the impact of LVR interventions on the peripheral airways compartment. Reference ranges for MBNW parameters in COPD are however yet to be validated.

Impact of individual lung volume reduction therapies

Surgery achieved the most volume reduction and the MCID was attained in more than 90% of recipients. It was the only intervention to be accompanied by improvements in IOS expiratory airways resistance, reactance, and peripheral resonant frequency, which together with reduced functional gas trapping on CT, infer improvement in small airways function. Emphysema with hyperinflation is the end-stage of the COPD spectrum with substantial loss of terminal bronchioles, destruction of the elastic scaffold maintaining patency of airways and facilitating passive recoil, and compromised tissue with functional potential[335]. The mechanically disadvantaged ventilatory pump is disencumbered by volume reduction, resurrecting functionally preserved tissue, and re-tensioning the remaining airway network[335]. This is conceptually attractive to explain the functional impact of surgery on the small airways network.

Valve implantations accomplished a smaller reduction in IOS expiratory reactance at 5Hz without an accompanying signal in resistance, resonant frequency, or functional gas trapping on CT. Modest improvements to alveolar gas mixing (AME) and small airways function (S_{acin}) were recorded using MBNW in a subset of patients. These data suggest the impact of valves on the peripheral airway compartment was less pronounced than with surgery and predominantly due to deflation of emphysematous lung tissue and relief of the mechanical pump, although diaphragmatic and chest wall function were not formally assessed in this study. The ultimate objective of surgery and of valve implantation is the same – and the three-month physiological outcomes were not overly dissimilar to surgery. One might speculate that the two techniques impact lung physiology via different mechanisms, but a 28% greater reduction in residual volume (RV) with surgery is a convincing alternative explanation. Only 62% of EBV recipients attained the MCID of ≥10% RV reduction.

Coil implantations resulted in partial volume reduction, rather less than in previous trials such as RESET[207], and may be consequence of a more infirm cohort, burden of airway sampling using bronchoalveolar lavage (two lobes versus one), or employment of smaller size coils with less tensioning effects. Only 35% of subjects achieved the MCID of ≥10% RV reduction and 3-month physiological outcomes were similarly disappointing with IOS detected improvement limited to the area under reactance during expiration (AXex).

Role of IOS and MBNW as biomarkers for lung volume reduction

Volume reduction is undoubtedly the crucial objective[214] and the majority of studies have adopted conventional lung function testing as the means of assessment not attempting to differentiate the contributions of the large and small airway compartments. In this study we have availed ourselves of the opportunity to do so with IOS and MBNW which may contribute to understanding the disparity in outcomes of the techniques. To facilitate comparison, a reduction of at least 10% of RV has been adopted as the MCID – a percentage threshold was considered better tailored to the individual.

IOS is a validated technique for measuring respiratory impedance that is safe, well-tolerated, and can be performed within a few minutes. In contrast to spirometry, measurement is made during quiet

tidal breathing obviating the need for forced manoeuvres, relevant for a breathless and physiologically compromised cohort of patients with COPD. It is increasingly employed as part of the diagnostic evaluation and surveillance of lung function in obstructive airways disease. Our data supports its potential utility both as a biomarker of disease severity and as a functional endpoint in individuals undergoing lung volume reduction that is complementary to conventional testing. However, its predictive value for therapeutic response is not established from this small dataset.

MBNW testing is well established in cystic fibrosis research and has shown promise as a means of assessing early airways disease in individuals with COPD[350]. In our study, changes in LCI, AME and S_{acin} indices have provided valuable insight into the impact of lung volume reduction on lung mechanics. However, each test run lasted on average 15 to 20 minutes and this proved particularly challenging for the majority of individuals with severe emphysema and hyperinflation while maintaining an adequate mouthpiece seal. Furthermore, the accuracy of commercial MBNW machines measuring FRC has been questioned[350] and reference ranges have yet to be validated. For these reasons, the clinical value of MBNW as a biomarker and functional endpoint in this niche population of individuals remains unclear.

Limitations

The study was small, and the target volume reduction was not universally achieved, particularly with endobronchial coils. Patient cooperation is paramount and MBNW testing is time consuming and exhausting for the population studied: Evaluation was limited to endobronchial valve recipients. Validation of reference ranges and minimal clinically important differences is required in larger cohorts for both modalities.

Conclusions

In conclusion, IOS and MBNW have provided insight into the impact of lung volume reduction on large and small airways function, which are proportionately affected by increasing degrees of volume reductions achieved. IOS is likely to prove complementary to disease phenotyping using conventional

lung function measures and is a safe, well-tolerated, and quick to perform non-invasive test with which to characterise COPD both as a biomarker of disease severity and as an objective endpoint for assessing interventional outcomes, however, its predictive value for therapeutic response is not established from this small dataset and further research in larger trials is needed.

CHAPTER 5: Impact of Lung Volume Reduction on Airways Inflammation

This chapter evaluates the inflammatory microenvironment before and after volume reductions achieved with each of the three validated procedures, surgical excision and deflation with endobronchial valves and with coils.

Abstract

Rationale – COPD is recognised as a chronic inflammatory disease but a robust biomarker to predict its course and response to therapy has proved elusive. Microvesicles are currently attracting interest as candidates for therapeutically modifiable components of the inflammatory process. The objective of this study was two-fold: 1) To perform a systematic characterisation of microvesicle populations in airway and in blood samples to establish correlations with conventional measures; 2) To investigate the hypothesis that lung volume reduction would be accompanied by measurable changes in microvesicle populations.

Methods – A preliminary validation study was undertaken in a cohort of 62 consecutive individuals representative of a range of COPD disease severities (GOLD I to IV) to identify microvesicle subtypes in airway and blood samples and their baseline correlations, followed by recruitment of subjects scheduled for endobronchial lung volume reductions – 16 valve and 16 coil emplacements, and testing before and 3 months after the interventions. All underwent detailed clinical phenotyping comprising demographic, symptom score, lung function, exercise capacity, and CT imaging measurements during exacerbation-free periods from 4th July 2016 to 13th August 2019.

Results – A variety of microvesicle (MV) populations in bronchoalveolar lavage fluid (BALF) and plasma of patients with mild to very severe COPD were identified. Of these, polymorphonuclear (neutrophil)-derived MVs were found to be substantially increased in BALF and their numbers correlated with

airflow limitation, reduced exercise capacity, impairment of quality of life, and BODE index. Furthermore, BALF neutrophil-derived MVs correlated with BALF neutrophil cell numbers but not with circulating neutrophil MV numbers, implying local alveolar release rather than translocation from the circulation.

Mean volume reduction in the coil recipients was exceeded threefold by that of the valve beneficiaries. Unexpectedly there was no statistically significant change in MV numbers at three months in the valve arm. Possible explanations include contamination from more proximal airway sampling / spill over from the ipsilateral lobe(s) or induction of a localised inflammatory response to biofilm formation overlying the nitinol-silicone implants. In contrast, a statistically significant fall in MV numbers was observed in the coil cohort in the absence of clinically meaningful volume reduction. It must however be borne in mind that despite the thin profile of the nitinol endobronchial coil, the surface area of the airway epithelium exposed to sampling is reduced. Lastly, there were no inflammatory predictors of volume reduction identified.

Conclusions – We suggest BALF neutrophil-derived MV observations are a potentially useful contributor to disease phenotyping alongside lung function tests and qCT imaging. However, a role as a biomarker to predict and to evaluate therapeutic response in individuals with COPD requires further research in larger trials including the evaluation of control lobes (i.e., those without implants).

Introduction

COPD is recognised as a chronic inflammatory disease[277] but a robust biomarker to predict its course and response to therapy has proved elusive[279]. Here we explore the blood and airway derivatives currently attracting interest as candidates for therapeutically modifiable components of the inflammatory process.

Microvesicles (MVs) have recently been proposed as potential biomarkers[125] and as mediators of intra-alveolar inflammation in another inflammatory disease, acute respiratory distress syndrome (ARDS)[351]. They are fragments of cell membrane, 0.1 to 2µm in diameter shed by most eukaryotic cells[125]. They have been observed to exert pro-inflammatory effects by virtue both of surface expressed proteins and their internal 'cargo'[126]. In COPD, circulating endothelial-derived MVs are elevated[127, 128], peak during acute exacerbations[129], and are predictive of rapid decline in FEV1[130]. Remarkably, a recent publication showed the neutrophil-derived exosome, a smaller member of the extracellular vesicle family, bypasses the antiprotease barrier and promotes extracellular matrix degradation in individuals with COPD, a phenotype which can also be transferred to animal models[132]. However, there is a paucity of data on airway-derived MVs[131]. The appeal of MVs as a potential biomarker is their inherent properties: 1) they are stable in their environment; 2) their cell lineage can be easily determined using surface marker analysis; 3) intra-vesicular molecules including cytokines, chemokines and miRNA can be interrogated for their mechanistic role in driving disease pathogenesis[352].

The hyperinflated lungs characteristic of advanced COPD are the consequence of irreversible expiratory airflow limitation caused by a combination of small airways disease and parenchymal destruction[1]. To the burden of resistance to airflow is added the constraints imposed on the mechanism of the respiratory pump[308]. Surgical excision and bronchoscopic deflation of diseased lung are radical solutions with proven benefit[214]. Volume reduction has been the principal focus of attention optimising the interventions. In the pursuit of dependable predictors of outcome to guide selection of patient and of procedure, a robust biomarker is lacking[279] and an easily acquired and

interpreted inflammatory metric would be welcome. The aim of this study is to explore the airway microenvironment: inflammatory cytokine and microvesicle levels, pre- and post-lung volume reduction for a possible predictive biomarker of disease severity and of therapeutic response.

Study objective

To investigate the hypothesis that lung volume reduction will be accompanied by measurable changes in inflammatory mediators obtained from the airways that can be correlated with changes to the conventional clinical parameters. Furthermore, reliable inflammatory signatures at baseline predicting therapeutic response (reduction of residual volume of at least 10%[206]), will be identified.

Methods

Ethics

This study was undertaken in accordance with the Declaration of Helsinki and is based on airway and blood samples acquired prospectively from an observational trial performed at the Royal Brompton Hospital and Chelsea & Westminster Hospital:

1) Studying the Airway Microenvironment in Patients Undergoing Surgical and Bronchoscopic Interventions for COPD (COPD-ENVIRON: REC reference 17/LO/0136, IRAS 217587, NCT03010592).

Written informed consent was obtained from all patients who had a confirmed diagnosis of COPD and were over the age of 18 years.

Study subjects

Validation cohort

A preliminary characterisation of microvesicle subpopulations to establish baseline correlations with conventional measures was undertaken in a cohort of 62 consecutive individuals with a range of COPD disease severity (GOLD I to IV).

Lung volume reduction cohort

32 subjects scheduled for lung volume reductions were recruited: Endobronchial valve – 16, Endobronchial coil – 16. All underwent detailed clinical phenotyping comprising demographic, symptom score, lung function, exercise capacity, and CT imaging measurements during an exacerbation-free period from 4th July 2016 to 13th August 2019. Inclusion and exclusion criteria are detailed in Table 5.1.

Inclusion criteria
• A diagnosis of COPD
• A smoking history ≥ 10 pack years but patients must have stopped for > 6 months
• All patients were taking guideline appropriate medical therapy
• Post bronchodilator $FEV_1/FVC \leq 70\%$
• $PaCO_2$ of ≤ 7.3 kPa and PaO2 ≥ 6.0 kPa on room air
• A minimum exercise tolerance of 140 metres on 6-minute walk test.
Exclusion criteria
• Exacerbation of COPD within 6 weeks of bronchoscopy
• Asthma
• Clinically significant bronchiectasis
• Giant bullae
• Previous lung volume reduction surgery
• Immunomodulatory therapy to treat a chronic inflammatory autoimmune disorder
• Antiplatelet or anticoagulant therapy that could not be stopped prior to bronchoscopy
• Known sensitivities to drugs required to perform bronchoscopy
• Any other disease or condition that would increase the risk of bronchoscopy.

Table 5.1. Inclusion and exclusion criteria.

Symptom scores

The modified Medical Research Council (mMRC) dyspnea scale[282] was used to evaluate disability associated with breathlessness due to COPD[292]. A minimum clinically important difference (MCID) of 1 post-intervention, was considered meaningful[294].

The St George's Respiratory Questionnaire (SGRQ) is a 50-item multidimensional instrument to measure quality of life in patients with airways obstruction and to quantify changes after therapy[295, 296]. Scores were calculated for three domains: Symptoms (frequency and severity), Activities (that cause or are limited by breathlessness), and Impacts (psycho-social disturbance resulting from airways

disease), that were combined to generate a total score. Scores range from 0 to 100, with higher scores indicating more severe limitation. An MCID of -4 was considered clinically meaningful[298].

Computed tomography

A Somatom Sensation 64 computed tomography scanner (Siemens, Erlangen, Germany) was used to acquire high resolution radiographic images of thin slices (1mm) of the lungs at maximal inspiration (corresponding to total lung capacity, TLC, measured using body plethysmography) and in expiration (corresponding to residual volume, RV). Supine subjects were scanned from lung apices to bases employing a peak voltage of 120 kilo volts peak (kVp) and tube current modulation range of 30 to 140 mA. Images were reconstructed using a high spatial frequency B40F kernel to axial, coronal and sagittal formats. Isolation of selected structures ranked by radiographic density using the Hounslow Unit scale was achieved with dedicated in-house software (see LungSeg Toolbox). (To minimise radiation exposure, pre-enrolment CT scans performed by a referring centre and adopting a similar imaging protocol were not repeated in a small number of patients).

The LungSeg Toolbox software package developed in the Hamlyn Centre (Imperial College London) in collaboration with the Royal Brompton Hospital[216] operates in MATLAB (by MathWorks), a multi-paradigm computing environment, and analyses CT acquired DICOM images. The user interface displays images in three planes (axial, coronal, and sagittal). Image optimization employs gaussian smoothing for noise reduction and histogram equalization for contrast enhancement. A variety of functions enable interrogation of the structure of the lung:

- Segmentation and calculation of total lung volume on maximal inspiration and expiration.
- Characterisation of parenchyma at -950 HU on inspiration and -856 HU on expiration.
- Extraction of intra-pulmonary vessels and calculation of vessel volume.
- Measurement of pulmonary artery to aorta ratio.

Routine lung function and exercise capacity

The Jaeger Master Lab (Cardinal Health, Hoechberg, Germany) comprises two pieces of equipment, a constant volume body plethysmograph (MasterScreen™ Body) and a single breath gas transfer unit (MasterScreen™ PFT). Each has an integral pneumotachograph accessed with FreeFlow™ mouthpiece (Carefusion, UK) and single-use bacterial filter, to perform spirometry. Prior to use, both machines were calibrated for ambient conditions (temperature in °C, relative humidity in %, and barometric pressure in kPA) and for volume using a 3-litre syringe. Anthropometric measurements including age, height, and weight were input to allow comparison with the European Community for Steel and Coal (ECSC) reference values. All measurements were made post-inhalation of 400mcg of salbutamol and at least three reproducible readouts were recorded[300]. An earlobe capillary blood sample was analysed on an ABL90 FLEX PLUS (Radiometer, UK) for pH, PCO_2 (kPA), PO_2 (kPA), and HCO_3 (mEq/L) and on HemoCue for haemoglobin. Six-minute walk test was performed to evaluate exercise capacity.

Impulse Oscillometry System (IOS)

The IOS (Cardinal Health, Hoechberg, Germany) was calibrated for ambient conditions (temperature in °C, relative humidity in %, and barometric pressure in mmHg), flow-volume using a 3-litre syringe, and resistance using a reference impedance device (resistance should measure 0.20 kPA between 5 – 35Hz). All test measurements were made post-bronchodilation using 400mcg of salbutamol. At least three reproducible readouts were recorded[246].

Blood sampling

Blood was obtained for full blood count (1 x 4ml Purple BD Vacutainer® K2 EDTA tube), coagulation (1 x 4.5ml Blue BD Vacutainer® Sodium Citrate tube), biochemistry (1 x 5ml Gold BD Vacutainer® Serum Separator Tube II Advance) and MV enumeration using methodology as previously described in the literature[353]. For MV analysis, 2 x 4ml green BD Vacutainer® Lithium Heparin tubes were used[354]. Full blood count, coagulation and biochemistry profiles were analysed in the Royal Brompton Hospital's clinical laboratory whilst the heparin tubes were transferred on wet ice to the Chelsea &

Westminster research laboratory within 3 hours of sample acquisition. Samples were handled with care to minimise artefactual generation of MVs. The MV-containing blood was centrifuged at 200g for 10 minutes to obtain platelet-rich plasma (PRP) which was aspirated into cryotubes and stored anonymously at -80°C for subsequent batch analysis – freeze-thawing has not been shown to have a measurable effect on MV counts[355]. MV numbers were measured in PRP, not platelet poor plasma (PPP) owing to a dramatic drop in yield following centrifugation.

Bronchoalveolar lavage sampling

Bronchoscopy was performed under sedation or general anaesthesia in accordance with BTS guidelines by Dr Justin L Garner, Dr Samuel V Kemp, and Professor Pallav L Shah[356]. Bronchoalveolar lavage fluid (BALF) was obtained by instilling 50mls of normal saline into the target lobe (the primary treatment site) and manually aspirating followed by entrained suction. The BAL was divided into two aliquots: several millilitres were sent for standard microbiology microscopy and culture; the remainder was transferred on wet ice to the research laboratory within 3 hours of acquisition. This was centrifuged at 200g for 5 minutes at 4°C and the pellet analysed for cell counts. The remaining cell free supernatant was passed through a 100µl strainer to remove any debris and centrifuged again at 200g for 5 minutes at 4°C to remove residual debris or larger particles. The refined MV-rich sample was stored anonymously in cryotubes at -80°C.

BALF cell analysis

BALF was analysed for neutrophil and alveolar macrophage counts. Cell pellets were isolated by centrifugation as described above and incubated for 30 minutes at 4°C with fluorescence-conjugated antibodies: 0.5µg/ml of CD45 (clone 30-F11; Biolegend), 0.5µg/ml of CD11b (M1/70; BD Biosciences, San Jose, CA) and 0.5µg/ml CD66b (G10F5; Biolegend) for neutrophils and CD45, 0.5µg/ml of CD11c (N418; Biolegend) and 0.5µg/ml of F4/80 (BM8; Biolegend) to identify alveolar macrophages.

Microvesicle analysis

Stored BALF and plasma samples underwent blind analysis. We identified MVs using flow cytometry as plasma membrane-derived particles that were: 1) less than 1µm in size; 2) staining positive for surface markers pertaining to their precursor cell; and 3) sensitivity to 0.1% Triton X-100 detergent to discriminate from antibody complexes.

Samples were thawed and combined with fluorophore-conjugated monoclonal antibodies to identify cell lineage. Samples were incubated in the dark at 4^{o}C for 30 minutes before dilution in 1ml of filtered phosphate buffered solution (PBS). Accucheck counting beads (Invitrogen, Paisley, UK) were added to determine absolute MV counts acquired using a CyAn ADP flow cytometer. Forward scatter-and side scatter (trigger threshold 0.01) were used to characterise a 1µm gate that was delineated using sizing beads (upper size 1.3µm, Polysciences Inc, Hamburg, Germany) (Figure 5.1 A and B). Stained MV samples were treated with 0.1% triton detergent (Figure 5.1C) to discriminate MVs from non-vesicular antibody-bound events[357] – detergent-insensitive events were subtracted from total MV counts. Unstained samples were also examined to exclude auto-fluorescence phenomena (Figure 5.1D). Data were analysed using FlowJo software. The methodology for centrifugation and flow cytometry to isolate and characterise MVs in this study has been validated using electron microscopy[358]. Freeze-thawing has no measurable effect on MV counts[353, 355].

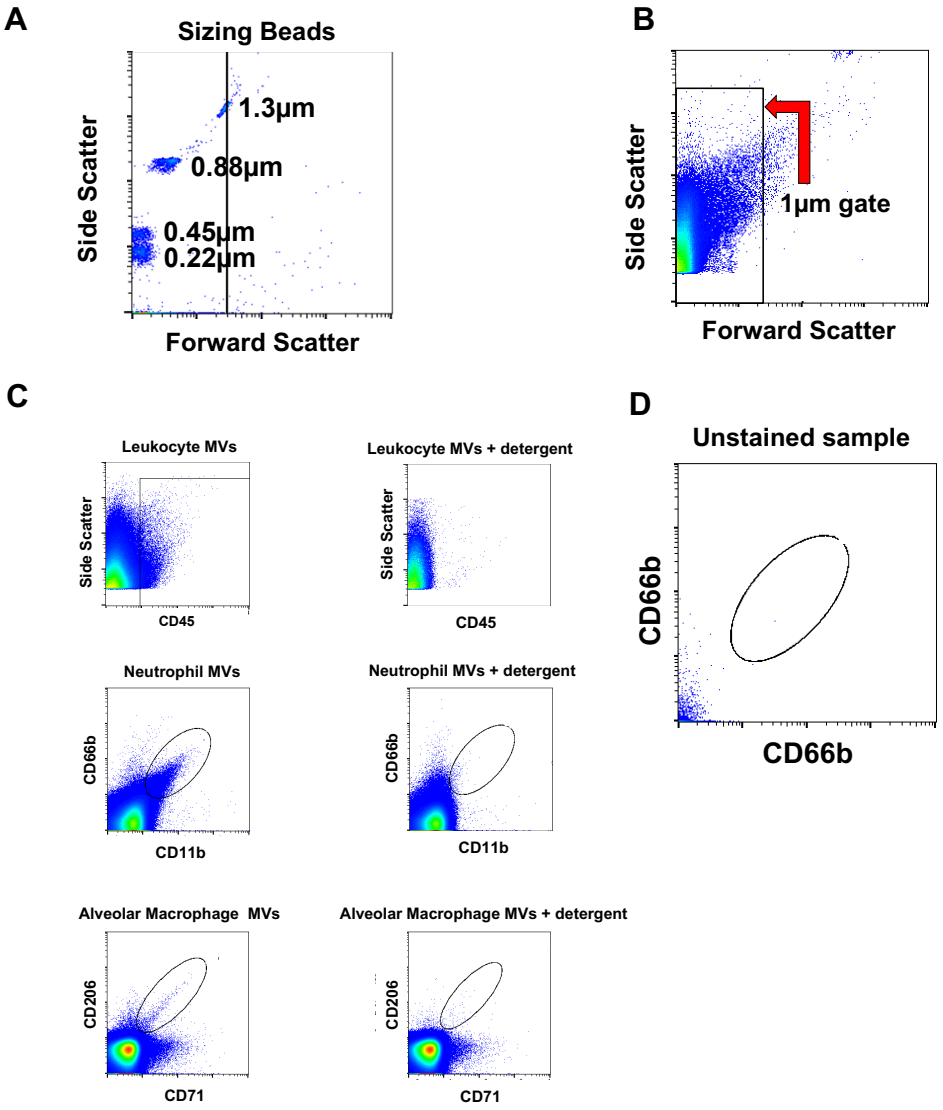

Figure 5.1. Flow cytometry plots.

Flow plots demonstrating fluorescent sizing beads (**A**), gating strategy used to identify events under 1µm in size (**B**), discrimination of positive events using 0.1% Titron detergent(**C**), and an unstained sample to rule out auto-fluorescence phenomena (**D**).

Cytokine Analysis

Sandwich ELISAs were used to measure TNF-α/IL-1β/IL-6/CXCL8 (R&D Systems, Abingdon, UK). Detectable ranges were TNF-α 15.6 to 1000pg/ml (DY210); IL-1β 3.9 to 250pg/ml (DY201); IL-6 9.4 to 600pg/ml (DY206); CXCL8 31.2 to 2000pg/ml (DY208).

Statistics

Categorical data are presented as percentages (%) and comparisons made using the Chi-squared or Fisher's exact test for two or more categorical variables. Parametric continuous data are presented as mean ± SD or 95% confidence intervals and non-parametric continuous data as median (interquartile range, IQR). Comparisons of two matched groups were made using a paired t test or the Wilcoxon test for parametric and non-parametric distributions, respectively; two unmatched groups, an unpaired t test or Mann-Whitney test; three matched groups, repeated measures ANOVA or Friedman test; and three unmatched groups, a one-way ANOVA or Kruskal-Wallis test (Tukey's and Dunn's tests applied, respectively, for multiple comparisons). Quantifying the association between two variables was measured using Pearson or Spearman correlations for parametric and non-parametric distributions, respectively. The strength of the correlation for the absolute value of *r* was described as follows: 0.00–0.19, 'very weak'; 0.20 – 0.39, 'weak'; 0.40 – 0.59, 'moderate'; 0.60–0.79, 'strong'; 0.80–1.0', 'very strong'. Binary logistic regression was undertaken to determine predictors of response, defined as a reduction in residual volume of ≥10%. All tests were 2 tailed and significance was set at $p < 0.05$. Statistical analysis was performed using SPSS version 24.0 (IBM, Chicago, IL, USA) and presented using GraphPad Prism version 8 (San Diego, CA).

Results

We first present the results of the validation cohort: baseline characteristics, microvesicle subpopulations identified, and their correlations as part of a preliminary validation enquiry. We then focus on individual lung volume reduction therapies and their impact on airways inflammation comparing clinical characteristics at baseline and at 3 months, △ correlations with microvesicle levels, and evaluating for inflammatory predictors of a ≥10% RV reduction to identify potential mechanisms of action. Finally, the cohorts are compared.

Validation cohort

Baseline characteristics

Sixty-two patients with mild to very severe COPD (FEV1% 16.40% to 84.60%) were recruited. Their demographics are described in Table 5.2. All were taking guideline appropriate medical therapy and were exacerbation-free for at least six weeks prior to enrolment.

Demographics		
Number		62
Age, years		65.90 ± 7.68
Gender (male), %:		51
BMI, kg/m^2		24.37 ± 3.80
Active co-morbidities		2 (1, 3)
Pack years		44 (33, 54)
Exacerbations (last year)		1 (0, 3)
GOLD grade, %	I	2 (1/62)
	II	10 (6/62)
	III	45 (28/62)
	IV	43 (27/62)
Symptoms		
mMRC		2 (2, 3)
SGRQ	*total*	56.59 ± 16.98
Lung function		
FEV_1, %		34.76 ± 12.49
RV, %		212.38 ± 44.57
TLC, %		136.50 ± 13.42
RV/TLC		60.02 ± 9.73
IC		2.13 ± 0.74
IC/TLC, %		26.42 ± 7.53
TLCOc, %		37.35 ± 13.48

KCOc, %	44.24 ± 13.34
pH	7.44 ± 0.03
PCO_2	4.93 ± 0.67
PO_2	9.43 ± 1.30
HCO_3	24.72 ± 2.74
Exercise capacity	
6MWD, meters	348.31 ± 118.92
Mortality Score	
BODE Index	5 (4, 7)
Inflammatory marker	
White cell count, 10^9/L	7.58 ± 2.06
Neutrophils, 10^9/L	4.59 ± 1.79
Fibrinogen, mg/dL	3.46 ± 0.61
C-reactive protein, mg/dL	4.47 ± 4.17

Categorical data are presented as a frequency (%). Parametric continuous data are presented as mean ± SD. Non-parametric continuous data are presented as median (IQR). BMI, Body Mass Index; BODE index = Body mass index, airflow Obstruction, Dyspnoea, and Exercise capacity; c, corrected for haemoglobin concentration; FEV_1, Forced Expiratory Volume in 1 second; GOLD, Global Initiative for Obstructive Lung Disease; HCO_3, Bicarbonate; IC, Inspiratory Capacity; KCO, carbon monoxide diffusing capacity per unit alveolar volume; mMRC, modified Medical Research Council dyspnoea scale; PCO_2, Partial pressure for carbon dioxide; PO_2, Partial pressure for oxygen; RV, Residual Volume; SGRQ, St George's Respiratory Questionnaire; TLC, Total Lung Capacity; TLCO, Transfer factor for carbon monoxide; 6MWD, Six-Minute Walk Distance.

Table 5.2. Baseline characteristics of Validation Cohort.

Microvesicle characterisation in BALF and plasma

We identified a variety of MV populations in BALF (Figure 5.2) including those derived from leukocyte (CD45+), polymorphonuclear (CD66b+/CD11b+), and monocyte (CD45+/CD14+) lineages, as previously described[353, 359, 360]. Alveolar macrophage MVs were characterised by expression of mannose (CD206) and transferrin (CD71) – their presence has not previously been reported in human samples. Epithelial (T1alpha+ or EpCAM+) and platelet (CD42b+/CD31) MV populations were also observed, however the latter speculated to be a consequence of mucosal traumatisation during BALF acquisition. The predominant MV population was leucocyte, specifically polymorphonuclear (i.e. neutrophil) in origin.

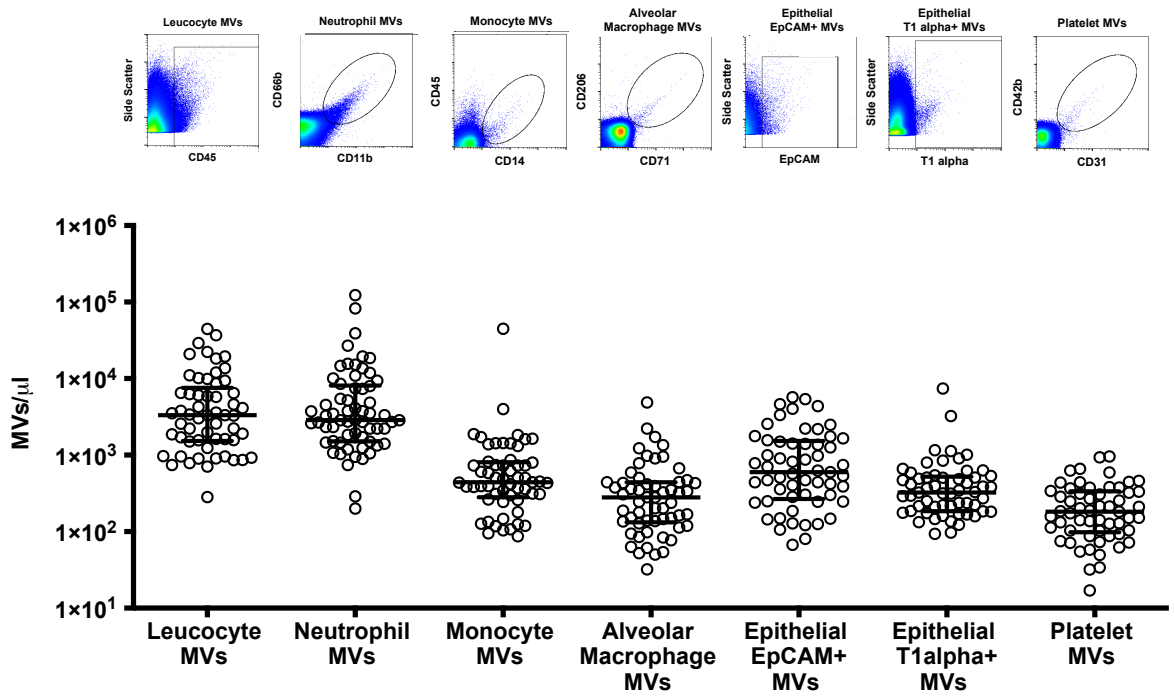

BALF MV population	MV Number/µL
Leukocyte MVs, median (IQR)	3322 (1534-7562)
Neutrophil MVs, median (IQR)	2865 (1517-8112)
Monocyte MVs, median (IQR)	442 (281-809)
Alveolar Macrophage MVs, median (IQR)	280 (132-443)
Epithelial EpCAM+ MVs, median (IQR)	598 (268-1532)
Epithelial T1alpha+ MVs, median (IQR)	324 (185-521)
Platelet MVs, median (IQR)	182 (98-336)

Figure 5.2. Microvesicle numbers in BALF.

Circulating MVs surveyed in platelet-rich plasma included leukocyte (CD45+), polymorphonuclear (CD66b+/CD11b+), monocyte (CD45+/CD14+), and endothelial (CD144+, CD146+ or CD62E+) populations (figure 5.3). The largest groups detected included polymorphonuclear and endothelial families.

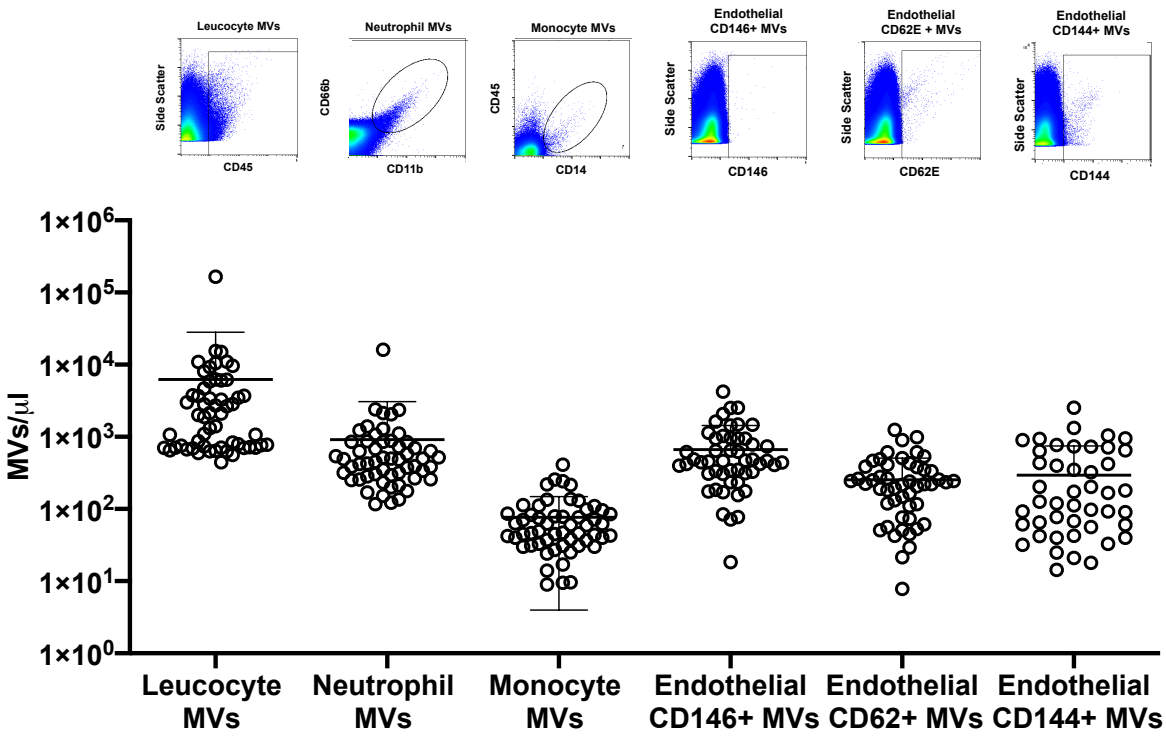

BLOOD MV population	MV Number/µL
Leukocyte MVs, median (IQR)	1941 (712-4441)
Neutrophil MVs, median (IQR)	483 (283-853)
Monocyte MVs, median (IQR)	49 (33-86)
Endothelial CD146+ MVs, median (IQR)	441 (185-942)
Endothelial CD62E+ MVs, median (IQR)	215 (56-350)
Endothelial CD144+ MVs, median (IQR)	92 (25-422)

Figure 5.3. Circulating microvesicle numbers in plasma.

BALF neutrophil-derived microvesicles correlate with COPD severity

We next tested the relationships of BALF MV numbers with the clinical variables measured in the validation cohort. PMN (neutrophil-derived) MVs alone were found to correlate with the BODE index ($r=0.38$, $p<0.01$) and this relationship persisted after excluding those patients in whom a bacterial growth was subsequently isolated on routine laboratory culture ($r=0.43$, $p<0.01$). (Figure 5.4).

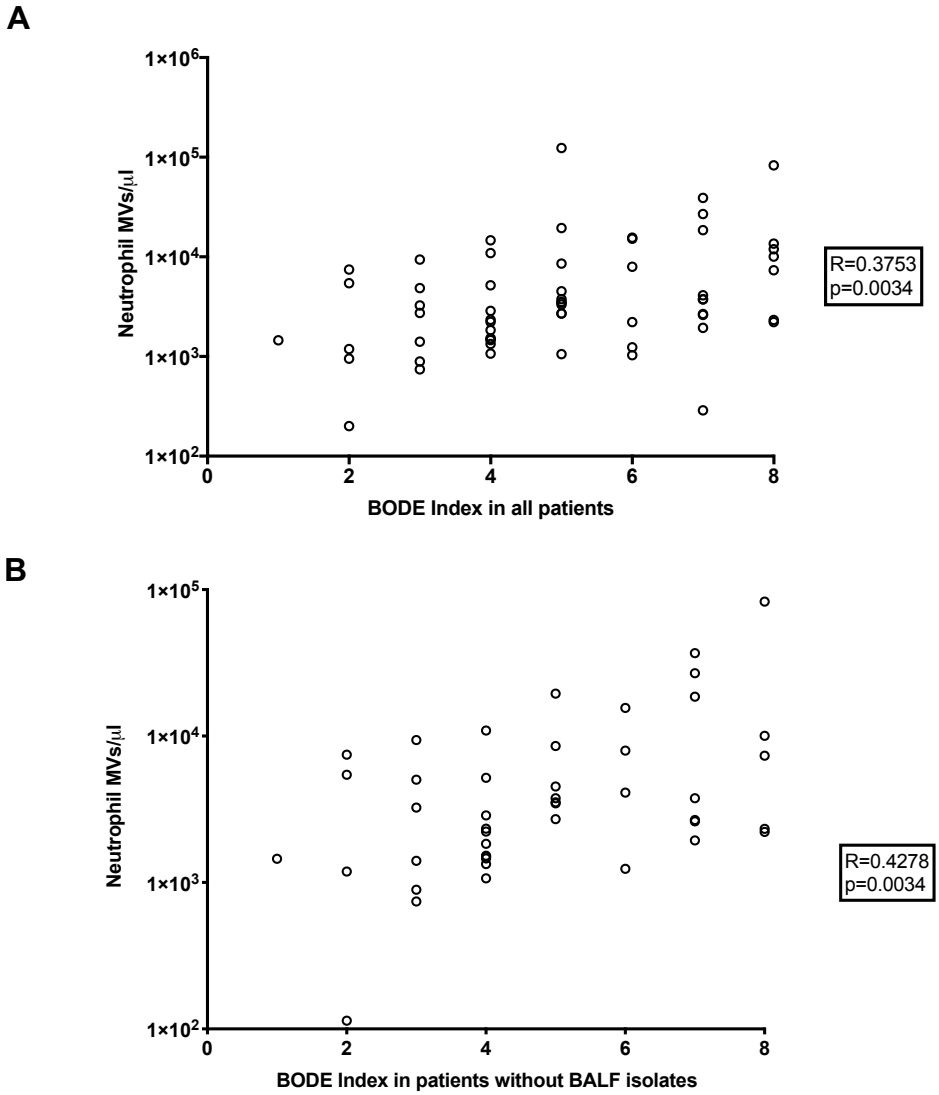

Figure 5.4. Relationship of neutrophil derived MVs to the BODE index.

Before (**A**) and after (**B**) excluding individuals with a BALF microbial isolate.

BALF neutrophil derived MVs were also shown to correlate with a number of indices of COPD severity including mMRC (r=0.32, p=0.01), FEV1% (r=-0.26, p=0.04), RV/TLC% (r=0.28, p=0.03), IC/TLC% (r=-0.28, p=0.03), TLCOc% (r=-0.30, p=0.04), and 6MWD (r=-0.27, p=0.04). (Figure 5.5).

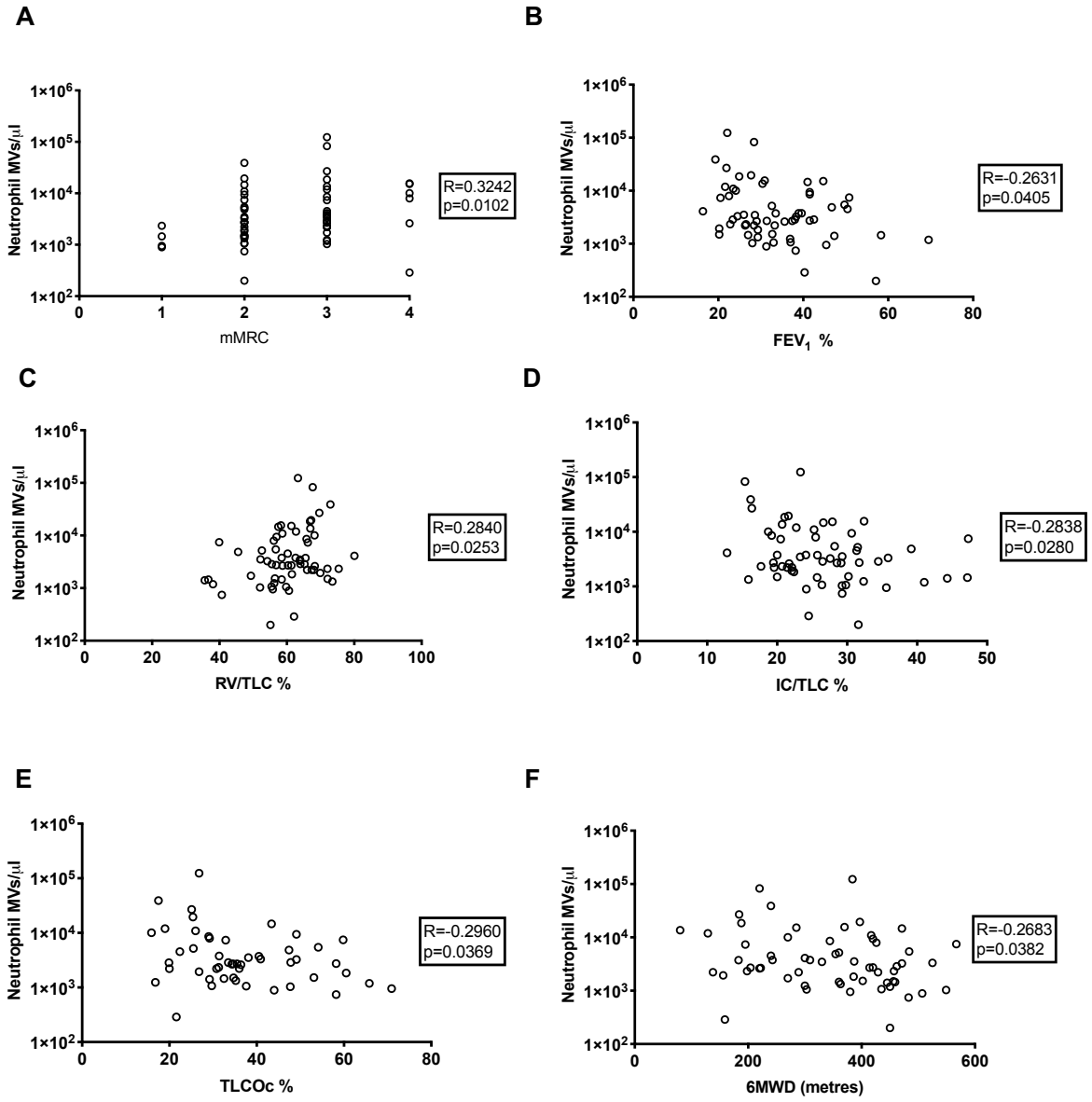

Figure 5.5. Correlations of BALF neutrophil-derived MVs.

Correlations with symptom score (**A**), airways obstruction (**B**), hyperinflation (**C-D**), gas transfer (**E**), and six-minute walk distance (**F**).

There were no correlations of the other BALF MV populations with any of these clinical parameters including the BODE index. However, the association of BALF EpCAM+ epithelial cell derived MVs and the frequency of exacerbations in the preceding 12 months approached statistical significance (r=0.26, p=0.05). (Table 5.3).

	Pack years		Co-morbidities		Exacerbations in 12m		mMRC		SGRQ-total	
MV population	**r**	**p**	**r**	**P**	**r**	**p**	**r**	**p**	**r**	**p**
Leukocyte MVs	0.1104	0.4051	0.2181	0.0971	0.2660	0.0843	0.1172	0.3769	0.0355	0.7898
Neutrophil MVs	-0.0049	0.9705	0.1518	0.2512	0.2215	0.0836	**0.3242**	**0.0102**	0.1019	0.4384
Monocyte MVs	0.0706	0.5955	0.1456	0.2712	-0.0353	0.7908	-0.0769	0.5625	0.0542	0.6838
Alveolar Macrophage MVs	0.2334	0.0752	0.1532	0.2466	0.0940	0.4789	-0.1704	0.1970	-0.1144	0.3883
Epithelial EpCAM+ MVs	0.1273	0.3368	0.0777	0.5584	**0.2570**	**0.0494**	0.1391	0.2932	0.0900	0.4981
Epithelial T1alpha+ MVs	0.0225	0.0871	-0.0080	0.9523	0.1670	0.2061	-0.0148	0.9113	0.0252	0.8498
Platelet MVs	0.0782	0.5559	-0.0342	0.7969	0.2390	0.0683	-0.0332	0.8028	0.1034	0.4359
	FEV1 (%)		**TLC (%)**		**RV (%)**		**RV/TLC (%)**		**IC/TLC (%)**	
MV population	**r**	**p**	**r**	**P**	**r**	**p**	**r**	**p**	**r**	**p**
Leukocyte MVs	-0.1246	0.3472	-0.0052	0.9686	0.0239	0.8574	0.1297	0.3274	-0.2002	0.1285
Neutrophil MVs	**-0.2631**	**0.0405**	0.1287	0.3190	0.1517	0.2392	**0.2840**	**0.0253**	**-0.2838**	**0.0280**
Monocyte MVs	-0.0774	0.5602	0.1126	0.3960	0.1606	0.2242	0.1899	0.1497	-0.1308	0.3235
Alveolar Macrophage MVs	-0.0229	0.8632	-0.1326	0.3166	-0.1507	0.2545	0.0902	0.4967	-0.1151	0.3852
Epithelial EpCAM+ MVs	0.0452	0.7338	0.0525	0.6930	-0.1143	0.3887	-0.0615	0.6436	-0.0280	0.8331
Epithelial T1alpha+ MVs	0.0880	0.5076	0.0719	0.5886	-0.0237	0.8588	-0.0548	0.6804	-0.0755	0.5699
Platelet MVs	-0.0343	0.7962	0.1027	0.4388	-0.0590	0.6573	0.0413	0.7560	-0.1725	0.1913
	TLCOc (mmol/min/kPA)		**PO_2**		**PCO_2**		**6MWD**		**BODE index**	
MV population	**r**	**p**	**r**	**p**	**r**	**p**	**r**	**p**	**r**	**p**
Leukocyte MVs	-0.1998	0.1734	-0.1806	0.1749	0.0749	0.5765	-0.1839	0.1633	0.1360	0.3045
Neutrophil MVs	**-0.2960**	**0.0369**	-0.1247	0.3382	0.0822	0.5288	**-0.2683**	**0.0382**	**0.3753**	**0.0034**
Monocyte MVs	0.0055	0.9702	0.1090	0.4155	0.0190	0.8876	-0.1128	0.3950	0.0268	0.8405
Alveolar Macrophage MVs	0.1270	0.3896	-0.1070	0.4241	0.1183	0.3765	0.0701	0.5979	-0.1913	0.1467
Epithelial EpCAM+ MVs	-0.1731	0.2393	0.0545	0.6843	-0.2040	0.1246	-0.1877	0.1545	0.0886	0.5046
Epithelial T1alpha+ MVs	-0.2544	0.0810	-0.1959	0.1406	0.0749	0.5765	0.0081	0.9517	-0.0324	0.8077
Platelet MVs	-0.0529	0.7212	0.0377	0.7788	-0.0094	0.9441	-0.0695	0.6011	0.0123	0.9262
	BODE index (no isolates)		**GOLD Stage**							
MV population	**r**	**p**	**r**	**p**						

Leukocyte MVs	0.1864	0.2203	0.1083	0.4143						
Neutrophil MVs	**0.4278**	**0.0034**	0.2368	0.0661						
Monocyte MVs	0.1615	0.2891	0.0842	0.5263						
Alveolar Macrophage MVs	-0.1458	0.3391	0.0943	0.4682						
Epithelial EpCAM+ MVs	0.0321	0.8341	-0.0782	0.5560						
Epithelial T1alpha+ MVs	-0.0873	0.5683	-0.1180	0.3735						
Platelet MVs	-0.0427	0.7804	0.0958	0.4703						

Table 5.3. Correlations of BALF MVs with clinical parameters.

BODE index = Body mass index, airflow Obstruction, Dyspnoea, and Exercise capacity; c, corrected for haemoglobin concentration; FEV_1, Forced Expiratory Volume in 1 second; GOLD, Global Initiative for Chronic Obstructive Lung Disease; IC, Inspiratory Capacity; m, months; mMRC, modified Medical Research Council dyspnoea scale; MVs, microvesicles; PCO_2, Partial pressure for carbon dioxide; PO_2, Partial pressure for oxygen; RV, Residual Volume; SGRQ-total, St George's Respiratory Questionnaire total score; TLC, Total Lung Capacity; TLCO, Transfer factor for carbon monoxide; 6MWD, Six-Minute Walk Distance.

Circulating microvesicles and COPD severity

No correlations were observed between circulating neutrophil derived MVs and any of the recorded clinical parameters. Monocyte MVs correlated with TLCO (r=0.38, p=0.01) and with the BODE index when excluding individuals with bacterial growth isolated from the BALF (r=-0.34, p=0.03) only. (Table 5.4).

Cytokines and COPD severity

We surveyed BALF for cytokines which have been implicated in the orchestration of COPD inflammation: IL-1β, IL-6, CXCL8 and TNF-α,[124] and found no correlation with any of the clinical parameters including the BODE index (Figure 5.6). However, we did observe correlations with several MV populations. (Table 5.5).

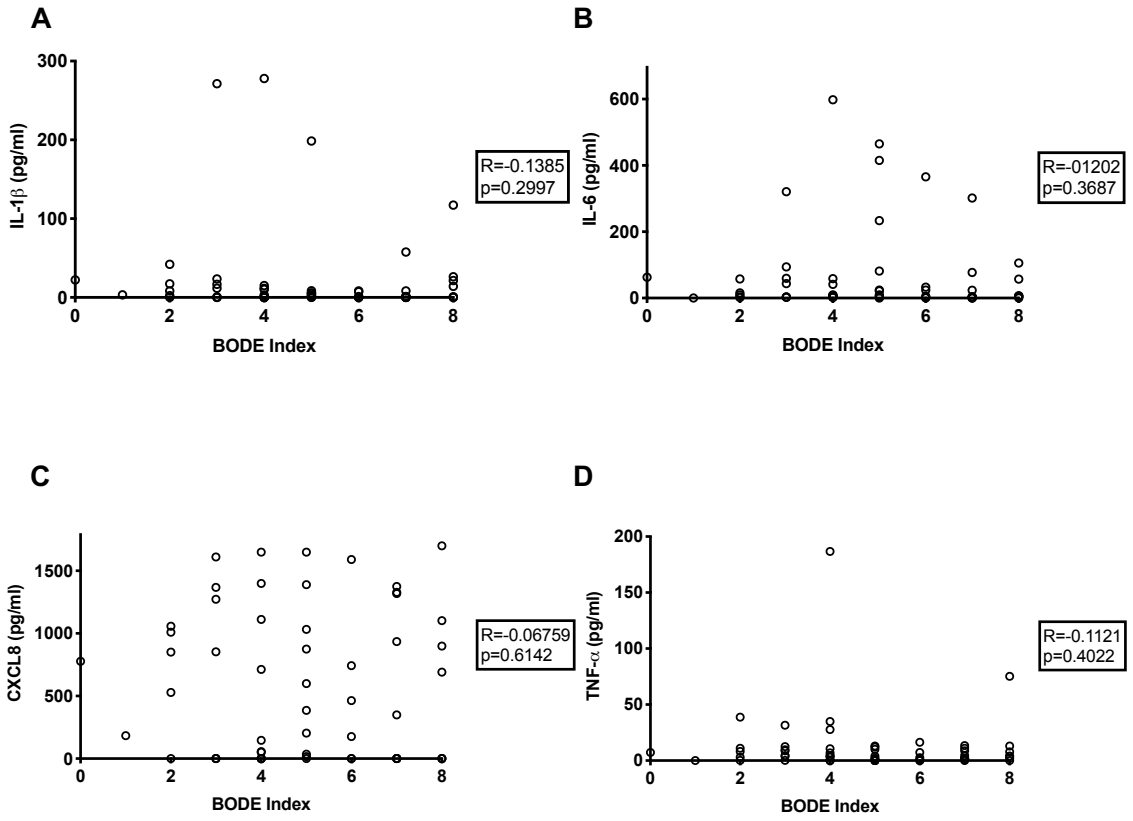

Figure 5.6. Correlations of BALF cytokines with the BODE index.

IL-1β (**A**), IL-6 (**B**), CXCL8 (**C**), TNF-α (**D**).

	Pack years		Co-morbidities		Exacerbations in 12m		mMRC		SGRQ-total	
MV population	**r**	**p**	**r**	**p**	**r**	**p**	**r**	**p**	**r**	**p**
Leukocyte MVs	0.0497	0.7163	-0.1270	0.3509	0.0112	0.9346	0.0316	0.8172	-0.0167	0.9031
Neutrophil MVs	-0.0155	0.9107	0.1012	0.4621	0.0705	0.6092	0.1538	0.2623	0.1732	0.2061
Monocyte MVs	0.0658	0.6330	-0.2453	0.0711	0.0107	0.4372	-0.1725	0.2078	-0.0231	0.8670
Endothelial CD62E+ MVs	0.0276	0.8415	0.0038	0.9779	0.0897	0.5150	0.0520	0.7060	-0.1238	0.3680
Endothelial CD144+ MVs	0.0707	0.6080	0.0816	0.5536	0.1918	0.1607	0.1032	0.4532	0.1296	0.3455
Endothelial CD146+ MVs	0.2131	0.1183	0.0772	0.5756	0.0998	0.4684	0.0683	0.6204	-0.1523	0.2671
	FEV1 (%)		**TLC (%)**		**RV (%)**		**RV/TLC (%)**		**IC/TLC (%)**	
MV population	**r**	**p**	**r**	**p**	**r**	**p**	**r**	**p**	**r**	**p**
Leukocyte MVs	-0.0383	0.7793	0.0798	0.5586	0.0664	0.6269	0.1577	0.2458	-0.1351	0.3207
Neutrophil MVs	-0.2336	0.0860	0.0103	0.9408	-0.0124	0.9286	0.0171	0.9014	-0.1099	0.4246
Monocyte MVs	0.1857	0.1746	-0.0867	0.5289	-0.2152	0.1146	-0.1871	0.1715	0.0747	0.5879
Endothelial CD62E+ MVs	0.0860	0.5324	-0.0175	0.8991	-0.0997	0.4677	-0.1604	0.2421	0.1967	0.1501
Endothelial CD144+ MVs	0.1057	0.4424	0.0527	0.7027	-0.0929	0.5001	-0.1171	0.3947	0.0635	0.6452
Endothelial CD146+ MVs	0.0978	0.4775	-0.1012	0.4623	-0.1692	0.2168	-0.2520	0.0635	0.2101	0.1236
	TLCOc (mmol/min/kPA)		**PO2**		**PCO2**		**6MWD**		**BODE index**	
MV population	**r**	**p**	**r**	**p**	**r**	**p**	**r**	**p**	**r**	**p**
Leukocyte MVs	0.0112	0.9410	0.1341	0.3289	0.1372	0.3180	0.0020	0.9882	0.0859	0.5291
Neutrophil MVs	-0.1149	0.4523	0.1067	0.4425	-0.2148	0.1189	0.0362	0.7933	0.0503	0.7154
Monocyte MVs	**0.3808**	**0.0099**	0.2515	0.0665	-0.1363	0.3258	0.2219	0.1035	-0.2029	0.1374
Endothelial CD62E+ MVs	0.1635	0.2833	0.1268	0.3608	-0.1855	0.1793	0.0558	0.6860	-0.1087	0.4296
Endothelial CD144+ MVs	-0.0365	0.8118	0.0234	0.8665	-0.2032	0.1406	-0.0256	0.8528	0.0049	0.9717
Endothelial CD146+ MVs	0.1292	0.3976	0.0920	0.5081	-0.1216	0.3811	0.0939	0.4952	-0.1281	0.3514
	BODE index (no isolates)		**GOLD Stage**							
MV population	**r**	**p**	**r**	**p**						
Leukocyte MVs	0.1041	0.5118	0.0620	0.6500						
Neutrophil MVs	-0.0655	0.6843	0.1912	0.1621						
Monocyte MVs	**-0.3446**	**0.0273**	-0.1506	0.2723						

Endothelial CD62E+ MVs	-0.2506	0.1140	-0.1502	0.2737						
Endothelial CD144+ MVs	-0.0827	0.6070	-0.1091	0.4279						
Endothelial CD146+ MVs	-0.1876	0.2401	-0.1343	0.3284						

Table 5.4. Correlations of circulating MVs with clinical parameters.

BODE index = Body mass index, airflow Obstruction, Dyspnoea, and Exercise capacity; c, corrected for haemoglobin concentration; FEV_1, Forced Expiratory Volume in 1 second; GOLD, Global Initiative for Chronic Obstructive Lung Disease; IC, Inspiratory Capacity; m, months; mMRC, modified Medical Research Council dyspnoea scale; MVs, microvesicles; PCO_2, Partial pressure for carbon dioxide; PO_2, Partial pressure for oxygen; RV, Residual Volume; SGRQ-total, St George's Respiratory Questionnaire total score; TLC, Total Lung Capacity; TLCO, Transfer factor for carbon monoxide; 6MWD, Six-Minute Walk Distance.

	Pack years		Co-morbidities		Exacerbations in 12m		mMRC		SGRQ-total	
Cytokine	**r**	**p**	**r**	**p**	**r**	**p**	**r**	**p**	**r**	**p**
IL-1β	-0.0500	0.7093	0.2052	0.1224	0.0076	0.9546	-0.2118	0.1105	-0.2146	0.1057
IL-6	0.0966	0.4665	0.2525	0.0537	0.0858	0.5181	-0.1356	0.3060	-0.1762	0.1819
CXCL8	0.2415	0.0654	0.2109	0.1089	0.1378	0.2979	-0.0502	0.7056	-0.1447	0.2743
TNFα	0.2128	0.1056	0.1153	0.3846	0.0666	0.6165	-0.1473	0.2655	-0.1515	0.2520
	FEV1 (%)		**TLC (%)**		**RV (%)**		**RV/TLC (%)**		**IC/TLC (%)**	
Cytokine	**r**	**p**	**r**	**p**	**r**	**p**	**r**	**p**	**r**	**p**
IL-1β	0.0141	0.9166	-0.0424	0.7523	0.0012	0.9929	-0.1596	0.2315	0.0502	0.7082
IL-6	-0.0552	0.6810	0.0255	0.8482	0.0170	0.8982	-0.0940	0.4787	0.0452	0.7364
CXCL8	0.0658	0.6236	-0.0455	0.7320	-0.0987	0.4570	-0.1124	0.3968	0.0820	0.5406
TNFα	0.1310	0.3270	-0.0253	0.8492	-0.0604	0.6495	-0.0410	0.7581	-0.0775	0.5632
	TLCOc (mmol/min/kPA)		**PO_2**		**PCO_2**		**6MWD**		**BODE index**	
Cytokine	**r**	**p**	**r**	**p**	**r**	**p**	**r**	**p**	**r**	**p**
IL-1β	0.2142	0.1482	-0.1465	0.2769	0.1550	0.2497	0.1226	0.3592	-0.1385	0.2997
IL-6	0.1147	0.4426	-0.1621	0.2240	0.1897	0.1538	0.0839	0.5278	-0.1202	0.3687
CXCL8	0.1512	0.3104	-0.1508	0.2587	0.1385	0.2998	0.0143	0.9145	-0.0676	0.6142
TNFα	0.1480	0.3209	0.1003	0.4539	-0.1838	0.1673	0.0079	0.9525	-0.1121	0.4022
	BODE index (no isolates)		**GOLD Stage**							
Cytokine	**r**	**p**	**r**	**p**						
IL-1β	-0.0997	0.5198	0.0890	0.5066						
IL-6	0.0500	0.7472	0.1418	0.2882						
CXCL8	-0.0290	0.8516	0.0162	0.9037						
TNFα	-0.0787	0.6115	-0.1515	0.2562						
	Leukocyte MVs		**Neutrophil MVs**		**Monocyte MVs**		**Alveolar macrophage MVs**		**Epithelial EpCAM+ MVs**	
Cytokine	**r**	**p**	**r**	**p**	**r**	**p**	**r**	**p**	**r**	**p**
IL-1β	**0.3545**	**0.0073**	**0.3896**	**0.0027**	0.0756	0.5797	0.2600	0.0530	0.2627	0.0505
IL-6	**0.3141**	**0.0184**	**0.4129**	**0.0013**	0.1271	0.3507	**0.3953**	**0.0026**	0.1739	0.1998
CXCL8	**0.4516**	**<0.001**	**0.5794**	**<0.001**	0.1448	0.2871	**0.3525**	**0.0077**	**0.4180**	**0.0013**

TNFα	**0.2900**	**0.0301**	0.0890	0.5096	0.1407	0.3010	**0.3230**	**0.0152**	**0.4484**	**<0.001**
	Epithelial T1alpha+ve MVs		**Platelet MVs**							
Cytokine	**r**	**p**	**r**	**p**						
IL-1β	0.0823	0.5466	**0.2976**	**0.0259**						
IL-6	0.1105	0.4174	**0.2924**	**0.0288**						
CXCL8	0.2012	0.1371	**0.2772**	**0.0386**						
TNFα	**0.3310**	**0.0127**	0.1536	0.2583						

Table 5.5. Correlations of BALF cytokines with clinical parameters and BALF microvesicles.

BODE index = Body mass index, airflow Obstruction, Dyspnoea, and Exercise capacity; c, corrected for haemoglobin concentration; FEV_1, Forced Expiratory Volume in 1 second; GOLD, Global Initiative for Chronic Obstructive Lung Disease; IC, Inspiratory Capacity; m, months; mMRC, modified Medical Research Council dyspnoea scale; MVs, microvesicles; PCO_2, Partial pressure for carbon dioxide; PO_2, Partial pressure for oxygen; RV, Residual Volume; SGRQ-total, St George's Respiratory Questionnaire total score; TLC, Total Lung Capacity; TLCO, Transfer factor for carbon monoxide; 6MWD, Six-Minute Walk Distance.

Origins of neutrophil-derived microvesicles

BALF neutrophil MVs correlated with BALF neutrophil cell numbers but not with circulating neutrophil MV numbers (Figure 5.7: A and B, respectively), implying local alveolar release rather than translocation from the circulatory compartment. Interestingly, there was no relationship between BALF neutrophil cell numbers and the BODE index (Figure 5.7: C), suggesting BALF neutrophil MVs are a better indicator of disease severity and of neutrophil activation status.

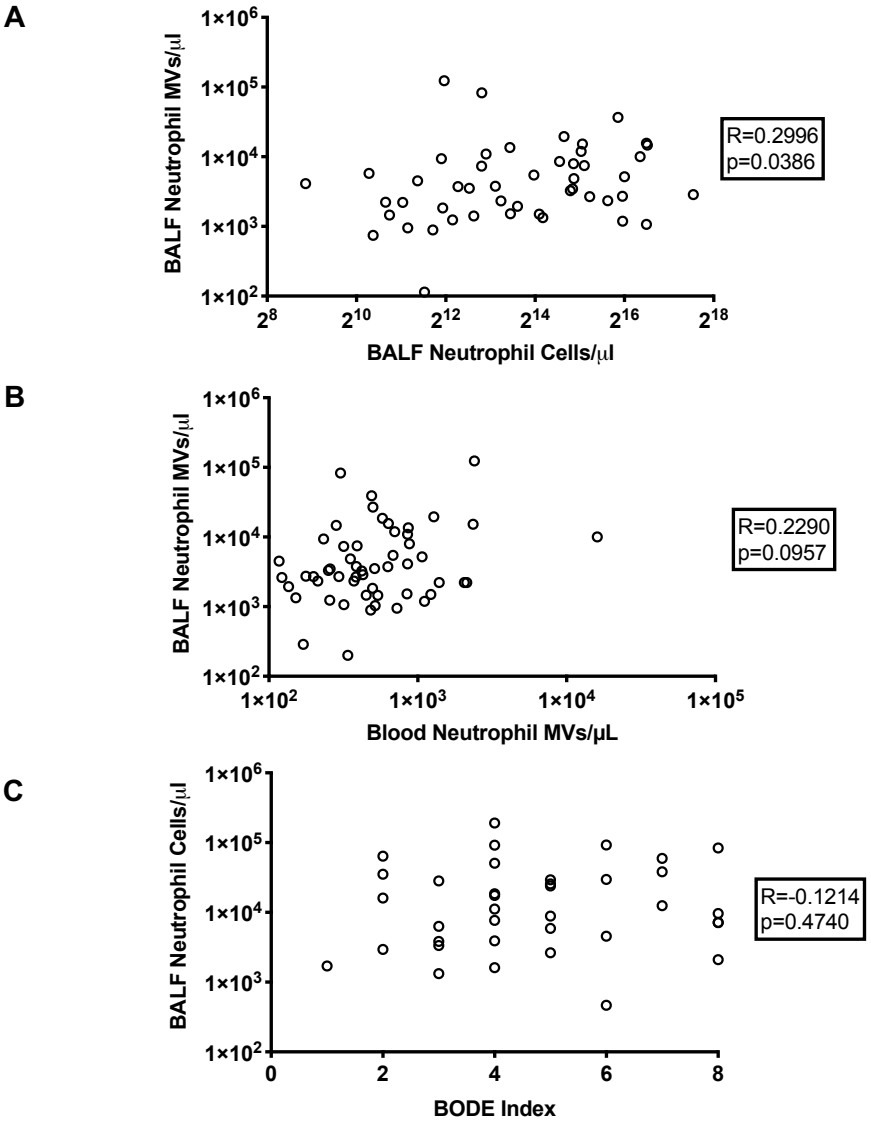

Figure 5.7. Origins of BALF neutrophil derived MVs.

Correlations between BALF neutrophil MVs and neutrophil cell count (**A**); correlations between BALF neutrophil MVs and circulating neutrophil cell MVs (**B**); correlation between BALF neutrophil cell count and the BODE index (**C**).

Endobronchial valve (EBV)

Baseline characteristics

16 patients were enrolled: mean age 66.1 ± 7.6 years, 62.5% male, BMI 23.9 ± 4.0, a median of two active comorbidities, 46 pack year smoking history, and one exacerbation in the preceding 12 months. 37.5% were classified as GOLD grade III and 56.3% IV (one patient missed baseline spirometry). Questionnaires recorded a median mMRC of 3 and mean SGRQ-total of 61.1 ± 18.4 points. Patients exhibited severe airflow obstruction, FEV1 29.9 ± 8.5%, and hyperinflation, RV 226.9 ± 33.0%. Baseline characteristics including BALF neutrophil-derived microvesicle levels are detailed in Table 5.6.

Changes in characteristics at 3-months

At 3-months, reductions in mMRC of 1 (p=0.02) and in SGRQ-impacts of 10.1 points (p=0.01) were observed. Improvements in FEV1 of +6.35% (p<0.01), FVC of +10.35% (p=0.03), FEV1/FVC of +2.34% (p=0.02), $MEF_{25-75\%}$ of 0.05L/s (p=0.03), RV of -38.66% (p<0.01), TLC of -10.56% (p<0.01), RV/TLC of -5.98% (p=0.01), $G_{AW-total}$ of +0.10 kPA/L/s (p<0.01), HCO_3 of -0.95 (p=0.04), $R5_{EX}$ of -0.07 (p=0.03), R20 of -0.02 kPA/L/s (p=0.03), 6MWD of +34.94 meters (p<0.01), CT-total lung $volume_{INSP}$ of -447.1mls (p<0.01), CT-total lung $volume_{EXP}$ of -618.4mls (p<0.01) and BODE index of -1 (p<0.01) were measured. There was however no statistically significant change in BALF neutrophil-derived microvesicle levels. (Table 5.7).

BALF neutrophil-derived microvesicle delta correlations

ΔBALF neutrophil-derived microvesicle counts were positively correlated with ΔCRP (r=0.69, p=0.01). (Figure 5.8 and Table 5.8).

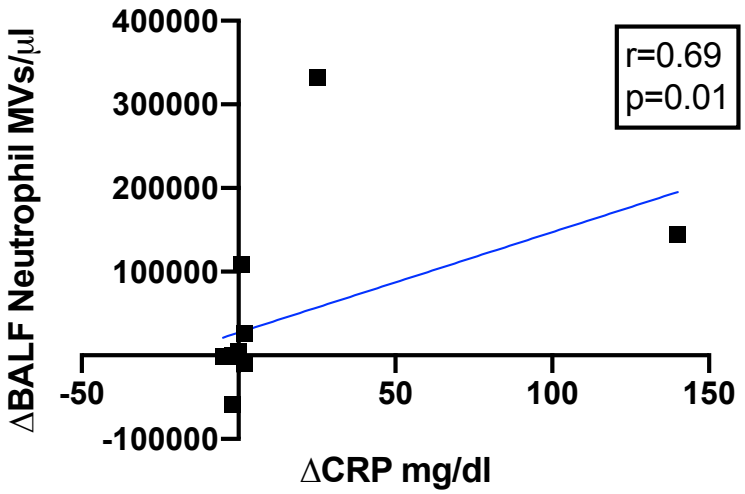

Figure 5.8. Change in BALF Neutrophil MVs versus change in CRP – valve cohort.

Predictors of volume reduction

10 of 16 subjects (62.5%), termed responders, achieved a ≥10% reduction in RV. They were characterised by a lower baseline FEV1 (0.73 versus 1.01L; p=0.04), FVC (2.81 versus 3.66L; p=0.03), and higher FRC (204.60 versus 185.70%; p=0.03), RV (241.20 versus 203.10%; p=0.01), RV/TLC (64.82 versus 57.10; p=0.01) (Table 5.9). Binomial logistic regression did not identify baseline BALF neutrophil-derived microvesicle counts as a predictor of ≥10% reduction in RV.

		Valve	Coil	Group comparison
Demographics				*p-value*
Number		16	16	
Age, years		66.06 ± 7.58	67.00 ± 9.56	0.76
Gender (male), %:		62.50	37.50	0.16†
BMI, kg/m^2		23.91 ± 3.96	24.39 ± 3.38	0.71
Active co-morbidities		2 (1, 3)	2 (1, 2)	0.20‡
Pack years		45.50 (32.25, 53.50)	41.00 (31.50, 53.75)	0.92‡
Exacerbations (last year)		1 (0, 3)	2 (1, 2)	0.67‡
GOLD grade, %	II	0	0	1.00‡
	III	37.50	43.75	
	IV	56.25	56.25	
Heterogeneous, %		50.00	43.75	0.72†
Baseline medications				
LABA, %		87.50	100.00	0.14†
LAMA, %		93.75	100.00	0.31†
ICS, %		81.25	87.50	0.63†
Oxygen, %		25.00	12.50	0.37†
Symptoms				
mMRC		3 (2, 4)	2 (2, 3)	0.34‡
SGRQ	*total*	61.14 ± 18.36	52.43 ± 9.16	0.10
	symptoms	52.25 ± 19.48	55.41 ± 20.12	0.65
	impacts	51.52 ± 24.83	35.68 ± 8.43	**0.03**
	activity	81.86 ± 16.60	76.69 ± 11.53	0.67
Lung function				
FEV_1, L		0.82 ± 0.27	0.75 ± 0.24	0.45
FEV_1, %		29.94 ± 8.47	30.81 ± 7.15	0.76
FVC, L		3.09 ± 0.66	2.94 ± 0.98	0.62
FVC, %		89.67 ± 11.72	96.19 ± 15.89	0.20
FEV1/FVC, %		25.43 ± 5.97	25.01 ± 5.81	0.84
MEF25-75%, L/s		0.22 ± 0.07	0.19 ± 0.06	0.24
RV, L		5.14 ± 0.81	4.85 ± 0.86	0.34
RV, %		226.90 ± 32.96	222.20 ± 28.70	0.67
TLC, L		8.31 ± 1.09	7.83 ± 1.63	0.34
TLC, %		139.40 ± 11.00	140.60 ± 8.88	0.73
RV/TLC, %		61.93 ± 5.94	62.37 ± 5.22	0.82

	Valve	Coil	Group comparison
IC, L	2.10 ± 0.57	1.94 ± 0.64	0.48
IC/TLC, %	25.29 ± 5.26	24.41 ± 3.96	0.60
R_{aw}, kPA/L/s	0.83 ± 0.32	0.79 ± 0.20	0.67
G_{aw}, kPA/L/s	0.23 ± 0.09	0.27 ± 0.06	0.12
TLCOc, mmol/min/kPA	2.65 ± 0.96	2.78 ± 1.03	0.71
TLCOc, %	31.50 ± 9.27	35.34 ± 9.98	0.29
KCOc, mmol/min/kPA	0.56 ± 0.13	0.65 ± 0.18	0.18
KCOc, %	39.63 ± 9.87	43.26 ± 11.00	0.36
pH	7.44 ± 0.02	7.44 ± 0.03	0.60
PCO_2	5.07 ± 0.58	5.01 ± 0.78	0.79
PO_2	9.17 ± 0.96	9.44 ± 1.65	0.58
HCO_3	25.68 ± 2.91	23.46 ± 2.89	0.49
Static compliance, L/cm H_20	5.03 ± 3.80	3.79 ± 3.52	0.44
Impulse oscillometry			
R5, kPa/L/s	0.69 ± 0.14	0.71 ± 0.20	0.77
R20, kPa/L/s	0.37 ± 0.06	0.40 ± 0.15	0.55
R5-20, kPa/L/s	0.31 ± 0.10	0.31 ± 0.12	0.98
Rin5, kPa/L/s	0.46 ± 0.07	0.50 ± 0.12	0.32
Rex5, kPa/L/s	0.78 ± 0.22	0.81 ± 0.25	0.80
X5, kPa/L/s	-0.46 ± 0.15	-0.45 ± 0.16	0.91
Xin5, kPa/L/s	-0.19 ± 0.11	-0.20 ± 0.07	0.63
Xex5, kPa/L/s	-0.73 ± 0.30	-0.75 ± 0.32	0.88
Xin5-Xex5, kPa/L/s	0.55 ± 0.27	0.54 ± 0.31	0.94
AX	4.48 ± 1.96	4.28 ± 1.95	0.78
AXinsp	1.89 ± 1.05	1.82 ± 0.86	0.83
AXexp	6.55 ± 3.20	6.43 ± 2.85	0.91
Fres total	29.25 ± 4.99	28.38 ± 4.12	0.60
Fres central	0.30 ± 0.03	0.31 ± 0.09	0.64
Fres peripheral	0.82 ± 0.16	0.87 ± 0.24	0.53
Exercise capacity			
6MWD, meters	315.20 ± 131.10	360.20 ± 101.10	0.29
CT metrics			
Total Lung Vol_{insp}, ml	6840 ± 989.20	6309 ± 1424	0.23
Total Lung Vol_{exp}, ml	5555 ± 1061	4955 ± 1382	0.18
Total Lung DS, % (-950insp)	41 (35, 42)	31 (24, 39)	**0.02**‡
Total Lung DS, % (-856exp)	75 (69, 81)	75 (69, 79)	0.72‡

	Valve	Coil	Group comparison
fGT, %	43 (36, 46)	47 (41, 55)	**0.04**‡
Total Lung Vessel Vol, ml	197 (160, 220)	157 (120, 183)	**0.01**‡
PA ratio	0.85 (0.76, 0.92)	0.79 (0.74, 0.87)	0.40‡
Mortality Score			
BODE Index	6 (4, 7)	5 (4, 6)	0.18‡
Inflammatory marker			
White cell count, 10^9/L	7.49 ± 1.90	8.28 ± 2.02	0.26
Neutrophil count, *10^9/L*	4.94 ± 2.16	5.54 ± 1.85	0.40
Fibrinogen, mg/dL	3.21 ± 0.63	3.78 ± 0.71	**0.03**
C-reactive protein, mg/dL	2.87 ± 3.16	7.44 ± 10.02	0.10
BALF neutrophil MVs/µl	3517 (1982, 7809)	3284 (2218, 16266)	0.75‡

Categorical data are presented as a frequency (%) and compared using a Fisher's exact test† (nominal) or Mann Whitney test‡ (ordinal). Parametric continuous data are presented as mean ± SD and compared using an independent t-test unless otherwise stated. Non-parametric continuous data are presented as median (IQR) and compared using a Mann Whitney test‡. AX, area of reactance; BALF, bronchoalveolar lavage fluid; BMI, Body Mass Index; BODE index = Body mass index, airflow Obstruction, Dyspnoea, and Exercise capacity; c, corrected for haemoglobin concentration; DS, Density Score; FEV_1, ex, expiratory phase; Forced Expiratory Volume in 1 second; FVC, Forced Vital Capacity; Fres, resonant frequency; fGT, functional gas trapping; G_{aw}, airways conductance; GOLD, Global Initiative for Obstructive Lung Disease; HCO3, Bicarbonate; IC, Inspiratory Capacity; in, inspiratory phase; ICS, inhaled corticosteroid; LABA, long acting beta-agonist; LAMA, long acting muscarinic antagonist; K_{CO}, carbon monoxide diffusing capacity per unit alveolar volume; MEF25-75%, mid-expiratory flow rate between 25 and 75%; mMRC, modified Medical Research Council dyspnoea scale; MVs, microvesicles; PA ratio, pulmonary artery to aorta ration; PCO_2, Partial pressure for carbon dioxide; PO_2, Partial pressure for oxygen; R5, resistance at 5 Hz; R20, resistance at 20 Hz; R_{aw}, airways resistance; RV, Residual Volume; SGRQ, St George's Respiratory Questionnaire; TLC, Total Lung Capacity; TL_{CO}, Transfer factor for carbon monoxide; Vol, Volume; X5, reactance at 5 Hz; 6MWD, Six-Minute Walk Distance.

Table 5.6. Baseline characteristics of patients.

		Valve difference	*p-value*	Coil difference	*p-value*	Group comparison *p-value*
Symptoms						
∆mMRC		-1 (95% CI: -1, 0)	**0.02**†	0 (95% CI: -1, 0)	0.08†	0.57‡
∆SGRQ	*Total score*	-6.99 ± 13.09 (95% CI: -13.96, -0.01)	0.05	-5.92 ± 17.71 (95% CI: -15.36, 3.51)	0.20	0.85
	Symptoms	1.65 ± 22.40 (95% CI: -10.29, 13.58)	0.77	-1.79 ± 26.35 (95% CI: -15.83, 12.26)	0.79	0.69
	Activity	-5.45 ± 12.63 (95% CI: -12.18, -1.28)	0.10	-8.13 ± 16.64 (95% CI: -17.00, 0.74)	0.07	0.61
	Impacts	-10.05 ± 13.86 (95% CI: -17.43, -2.66)	**0.01**	-5.84 ± 19.97 (95% CI: -16.47, 4.80)	0.26	0.49
Lung function						
∆FEV_1, L		0.14 ± 0.17 (95% CI: 0.04, 0.23)	**0.01**	0.03 ± 0.13 (95% CI: -0.04, 0.10)	0.38	**0.04**
∆FEV_1, %		6.35 ± 7.24 (95% CI: 2.35, 10.36)	**<0.01**	1.49 ± 5.38 (95% CI: -1.37, 4.36)	0.28	**0.04**
∆FVC, L		0.25 ± 0.58 (95% CI: -0.08, 0.57)	0.12	0.12 ± 0.41 (95% CI: -0.10, 0.34)	0.25	0.51
∆FVC, %		10.35 ± 17.12 (95% CI: 0.87, 19.83)	**0.03**	5.08 ± 14.01 (95% CI: -2.38, 12.55)	0.17	0.36
∆FEV1/FVC, %		2.34 ± 3.59 (95% CI: 0.36, 4.33)	**0.02**	-0.38 ± 3.00 (95% CI: -1.98, 1.21)	0.62	**0.03**
∆MEF25-75%, L/s		0.05 ± 0.07 (95% CI: 0.01, 0.09)	**0.03**	0.01 ± 0.03 (95% CI: -0.01, 0.02)	0.54	0.05
∆RV, L		-0.86 ± 0.70 (95% CI: -1.23, -0.49)	**<0.01**	-0.29 ± 0.60 (95% CI: -0.61, -0.03)	0.08	**0.02**
∆RV, %		-38.66 ± 31.11 (95% CI: -55.24, -22.09)	**<0.01**	-13.38 ± 30.26 (95% CI: -29.50, 2.75)	0.10	**0.03**
∆TLC, L		-0.67 ± 0.36 (95% CI: -0.86, 0.47)	**<0.01**	-0.17 ± 0.37 (95% CI: -0.36, 0.03)	0.10	**<0.01**
∆TLC, %		-10.56 ± 6.01 (95% CI: -13.76, -7.36	**<0.01**	-2.01 ± 7.38 (95% CI: -5.94, 1.93)	0.29	**<0.01**
∆RV/TLC, %		-5.98 ± 7.71 (95% CI: -10.08, -1.87)	**0.01**	-2.52 ± 6.28 (95% CI: -5.86, 0.83)	0.13	0.17
∆IC, L		0.07 ± 0.37	0.49	0.04 ± 0.30	0.62	0.82

	Valve difference	*p-value*	Coil difference	*p-value*	Group comparison *p-value*
	(95% CI: -0.14, 0.27)		(95% CI: -0.12, 0.20)		
∆IC/TLC, %	3.02 ± 4.72	**0.03**	1.32 ± 4.33	0.24	0.31
	(95% CI: 0.40, 5.63)		(95% CI: -0.99, 3.63)		
∆R_{aw}, kPA/L/s	-0.06 ± 0.24	0.39	0.05 ± 0.27	0.52	0.29
	(95% CI: -0.19, 0.08)		(95% CI: -0.10, 0.19)		
∆G_{aw}, kPA/L/s	0.10 ± 0.08	**<0.01**	0.02 ± 0.10	0.48	**0.01**
	(95% CI: 0.06, 0.14)		(95% CI: -0.03, 0.07)		
∆TLCOc, mmol/min/kPA	0.09 ± 0.49	0.50	-0.19 ± 0.40	0.12	0.12
	(95% CI: -0.19, 0.37)		(95% CI: -0.43, 0.05)		
∆TLCOc, %	1.41 ± 5.84	0.38	-2.14 ± 5.09	0.16	0.10
	(95% CI: -1.97, 4.78		(95% CI: -5.21, 0.94)		
∆KCOc, mmol/min/kPA	0.00 ± 0.07	1.00	-0.06 ± 0.08	**0.02**	0.05
	(95% CI: -0.04, 0.04)		(95% CI: -0.11, -0.01)		
∆KCOc, %	0.29 ± 4.98	0.83	-4.02 ± 5.32	**0.02**	**0.04**
	(95% CI: -2.58, 3.17)		(95% CI: -7.23, -0.80)		
∆pH	-0.01 ± 0.03	0.52	-0.00 ± 0.04	0.92	0.72
	(95% CI: -0.02, 0.01)		(95% CI: -0.02, 0.02)		
∆PCO_2	-0.11 ± 0.43	0.36	0.17 ± 0.50	0.20	0.12
	(95% CI: -0.34, 0.13)		(95% CI: -0.10, 0.43)		
∆PO_2	-0.14 ± 0.98	0.60	-0.33 ± 1.33	0.33	0.64
	(95% CI: -0.68, 0.41)		(95% CI: -1.05, 0.38)		
∆HCO_3	-0.95 ± 1.67	**0.04**	1.11 ± 1.49	**0.01**	**<0.01**
	(95% CI: -1.88, -0.03)		(95% CI: 0.31, 1.90)		
∆Static compliance, L/cm H_20	-0.87 ± 2.00	0.26	-0.29 ± 3.92	0.80	0.67
	(95% CI: -2.54, 0.80)		(95% CI: -2.78, 2.20)		
Impulse oscillometry					
∆R5, kPa/L/s	-0.04 ± 0.12	0.23	-0.03 ± 0.13	0.40	0.79
	(95% CI: -0.11, 0.03)		(95% CI: -0.10, 0.04)		
∆R20, kPa/L/s	-0.02 ± 0.03	**0.03**	-0.02 ± 0.07	0.34	1.00
	(95% CI: -0.03, -0.00)		(95% CI: -0.06, 0.02)		
∆R5-20, kPa/L/s	-0.02 ± 0.12	0.49	-0.01 ± 0.07	0.62	0.74
	(95% CI: -0.09, 0.04)		(95% CI: -0.05, 0.03)		
∆Rin5, kPa/L/s	0.02 ± 0.12	0.62	-0.00 ± 0.07	0.82	0.33
	(95% CI: -0.05, 0.08)		(95% CI: -0.04, 0.03)		
∆Rex5, kPa/L/s	-0.07 ± 0.11	**0.03**	-0.02 ± 0.19	0.64	0.42

	Valve difference	*p-value*	Coil difference	*p-value*	Group comparison *p-value*
	(95% CI: -0.13, -0.01)		(95% CI: -0.13, 0.08)		
∆X5, kPa/L/s	0.01 ± 0.14	0.76	-0.01 ± 0.10	0.65	0.61
	(95% CI: -0.07, 0.09)		(95% CI: -0.06, 0.04)		
∆Xin5, kPa/L/s	-0.03 ± 0.09	0.25	-0.01 ± 0.04	0.31	0.51
	(95% CI: -0.08, 0.02)		(95% CI: -0.03, 0.01)		
∆Xex5, kPa/L/s	0.07 ± 0.22	0.25	-0.02 ± 0.13	0.50	0.18
	(95% CI: -0.05, 0.19)		(95% CI: -0.09, 0.05)		
∆Xin5-Xex5, kPa/L/s	-0.10 ± 0.20	0.08	0.01 ± 0.13	0.72	0.09
	(95% CI: -0.20, 0.01)		(95% CI: -0.06, 0.08)		
∆AX	-0.43 ± 1.61	0.32	-0.19 ± 1.38	0.59	0.67
	(95% CI: -1.32, 0.47)		(95% CI: -0.92, 0.54)		
∆Axinsp	0.01 ± 0.79	0.97	0.19 ± 0.66	0.29	0.32
	0.02 (95% CI: -0.43, 0.44)		(95% CI: -0.18, 0.56)		
∆AXexp	-0.97 ± 1.85	0.06	-0.37 ± 1.94	0.46	0.39
	(95% CI: -2.00, 0.06)		(95% CI: -1.40, 0.66)		
∆Fres total	-1.15 ± 3.08	0.17	-0.99 ± 4.55	0.40	0.91
	(95% CI: -1.15, 3.08)		(95% CI: -3.41, 1.44)		
∆Fres central	-0.02 ± 0.04	0.07	-0.01 ± 0.04	0.55	0.38
	(95% CI: -0.04, 0.00)		(95% CI: -0.03, 0.02)		
∆Fres peripheral	0.03 ± 0.31	0.80	0.01 ± 0.11	0.63	0.92
	0.04 (95% CI: -0.15, 0.20)		(95% CI: -0.04, 0.07)		
Exercise capacity					
∆6MWD, m	34.94 ± 40.72	**<0.01**	2.38 ± 48.82	0.85	0.05
	(95% CI: 13.24, 56.64)		(95% CI: -23.64, 28.39)		
CT metrics					
∆Total Lung Vol_{insp}, ml	-447.10 ± 490.40	**<0.01**	-61.44 ± 291.20	0.41	**0.01**
	(95% CI: -708.40, 185.70)		(95% CI: -216.60, 93.74)		
∆Total Lung Vol_{exp}, ml	-618.40 ± 573.00	**<0.01**	-64.47 ± 974.10	0.80	0.07
	(95% CI: -949.20, 287.60)		(95% CI: -603.90, 475.00)		
∆Total Lung DS, % (-950insp)	0.00	0.50†	0.00	0.70†	0.87‡
	(95% CI: -2.00, 2.00)		(95% CI: -3.00, 4.00)		
∆Total Lung DS, % (-856exp)	-5.31	0.07†	-2.00	0.70†	0.16‡

	Valve difference	*p-value*	Coil difference	*p-value*	Group comparison *p-value*
	(95% CI: -12.00, 3.00)		(95% CI: -4.00, 5.00)		
∆fGT, %	3.00	0.07†	-0.50	0.45†	0.06‡
	(95% CI: -4.00, 17.00)		(95% CI: -8.00, 2.00)		
∆Total Lung Vessel Vol, ml	9.00	0.12†	18.00	**<0.01**†	0.21‡
	(95% CI: -4.00, 36.00)		(95% CI: 11.00, 23.00)		
∆PA ratio	0.03	0.35†	0.02	0.27†	0.82‡
	(95% CI: -0.04, 0.10)		(95% CI: -0.03, 0.05)		
Mortality Score					
∆BODE Index	-1.00	**<0.01**†	-0.50	**0.04**†	0.24‡
	(95% CI: -2.00, 0.00)		(95% CI: -2.00, 0.00)		
Inflammatory marker					
∆White cell count, 10^9/L	0.57 ± 2.33	0.34	-0.54 ± 1.38	0.14	0.12
	(95% CI: -0.67, 1.81)		(95% CI: -1.27, 0.20)		
∆Neutrophils, 10^9/L	0.41 ± 2.76	0.56	-0.63 ± 1.43	0.10	0.20
	(95% CI: -1.06, 1.89)		(95% CI: -1.39, 0.14)		
∆Fibrinogen, mg/dL	-0.06 ± 0.58	0.75	-0.06 ± 0.60	0.70	1.00
	(95% CI: -0.47, 0.35)		(95% CI: -0.39, 0.27)		
∆C-reactive protein, mg/dL	10.93 ± 36.33	0.26	-2.63 ± 10.47	0.32	0.18
	(95% CI: -9.19, 31.05)		(95% CI: -8.21, 2.96)		
∆BALF neutrophil MVs, per µl	245.00	0.46†	-855.00	**0.01**†	0.09
	(95% CI: -4461, 108920)		(95% CI: -606990, 208533)		

Non-parametric continuous data are compared using a Wilcoxon signed-rank test† (paired) or Mann-Whitney test‡ (unpaired) and presented as a median of differences (95% CI). Parametric continuous data are compared using a paired samples t-test or independent samples t-test (unpaired) and presented as mean ± SD (95% CI) unless otherwise specified. AX, area of reactance; BALF, bronchoalveolar lavage fluid; BMI, Body Mass Index; BODE index = Body mass index, airflow Obstruction, Dyspnoea, and Exercise capacity; c, corrected for haemoglobin concentration; DS, Density Score; FEV_1, ex, expiratory phase; Forced Expiratory Volume in 1 second; FVC, Forced Vital Capacity; Fres, resonant frequency; fGT, functional gas trapping; G_{aw}, airways conductance; HCO3, Bicarbonate; IC, Inspiratory Capacity; in, inspiratory phase; K_{CO}, carbon monoxide diffusing capacity per unit alveolar volume; MEF25-75%, mid-expiratory flow rate between 25 and 75%; mMRC, modified Medical Research Council dyspnoea scale; MVs, microvesicles; PA ratio, pulmonary artery to aorta ration; PCO_2, Partial pressure for carbon dioxide; PO_2, Partial pressure for oxygen; R5, resistance at 5 Hz; R20, resistance at 20 Hz; R_{aw}, airways resistance; RV, Residual Volume; SGRQ, St George's Respiratory Questionnaire; TLC, Total Lung Capacity; TL_{CO}, Transfer factor for carbon monoxide; Vol, Volume; X5, reactance at 5 Hz; 6MWD, Six-Minute Walk Distance.

Table 5.7. Changes in clinical characteristics over 3-months.

	ΔBODE Index		ΔmMRC		ΔSGRQtot		ΔBMI		ΔFEV1		ΔFEV1%		ΔFVC		ΔFVC%	
Parameter	r	p	r	p	r	p	r	p	r	p	r	p	r	p	r	p
ΔBALF neutrophil MVs	0.30	0.30	0.46	0.10	-0.35	0.21	0.31	0.28	0.07	0.81	-0.03	0.92	0.21	0.46	0.14	0.64
	ΔFEV1/FVC		**ΔMEF25-75%**		**ΔRAWtot**		**ΔGAWtot**		**ΔFRC**		**ΔFRC%**		**ΔRV**		**ΔRV%**	
Parameter	r	p	r	p	r	p	r	p	r	p	r	p	r	p	r	p
ΔBALF neutrophil MVs	-0.26	0.37	0.37	0.24	0.41	0.17	0.25	0.42	0.38	0.19	0.31	0.29	0.01	0.98	0.03	0.91
	ΔTLC		**ΔTLC%**		**ΔRV/TLC**		**ΔIC**		**ΔIC/TLC**		**ΔTLCO**		**ΔTLCO%**		**ΔKCO**	
Parameter	r	p	r	p	r	p	r	p	r	p	r	p	r	p	r	p
ΔBALF neutrophil MVs	0.50	0.07	0.45	0.11	-0.19	0.51	0.24	0.44	-0.03	0.94	0.51	0.08	0.54	0.06	0.45	0.12
	ΔKCO%		**ΔpH**		**ΔPCO_2**		**ΔPO_2**		**ΔCompliance**		**Δ6MWD**		**ΔR5**		**ΔR20**	
Parameter	r	p	r	p	r	p	r	p	r	P	r	p	r	p	r	p
ΔBALF neutrophil MVs	0.49	0.09	0.05	0.87	-0.10	0.75	0.23	0.46	0.20	0.71	-0.19	0.50	-0.21	0.49	0.10	0.75
	ΔR5-20		**ΔRin5**		**ΔRex5**		**ΔX5**		**ΔXin5**		**ΔXex5**		**ΔXin5-Xex5**		**ΔAX**	
Parameter	r	p	r	p	r	p	r	p	r	P	r	p	r	p		
ΔBALF neutrophil MVs	-0.35	0.24	-0.36	0.23	-0.12	0.70	0.29	0.34	0.31	0.30	0.23	0.44	-0.33	0.27	-0.25	0.41
	ΔAxinsp		**ΔAXexp**		**ΔFres total**		**ΔFres central**		**ΔFres peri**		**Δ6MWD**		**ΔTLV_{insp}**		**ΔTLV_{exp}**	
Parameter	r	p	r	p	r	p	r	p	r	P	r	p	r	p	r	p
ΔBALF neutrophil MVs	-0.48	0.10	-0.23	0.44	-0.26	0.40	0.10	0.74	-0.13	0.67	-0.19	0.50	-0.30	0.30	-0.12	0.72
	Δ-950_{insp}		**Δ-856_{exp}**		**ΔfGT**		**Δvessel vol**		**ΔPA ratio**		**ΔWCC**		**ΔFibrinogen**		**ΔCRP**	
Parameter	r	p	r	p	r	P	r	p	r	p	r	p	r	p	r	p
ΔBALF neutrophil MVs	-0.31	0.28	-0.07	0.83	0.28	0.35	-0.24	0.41	-0.52	0.06	0.18	0.53	0.34	0.36	**0.69**	**0.01**

Table 5.8. Delta correlations: BALF Neut-MVs and clinically relevant parameters – valve cohort.

		Valve responder	Valve non-responder	*p-value*	Coil responder	Coil non-responder	*p-value*
Demographics							*p-value*
Number		10	6		6	10	
Age, years		65.60 ± 9.14	66.83 ± 4.54	0.72	65.33 ± 14.84	68. 00 ± 5.21	0.69
Gender (male), %:		60.00	66.67	1.00†	33.33	75.00	0.30†
BMI, kg/m^2		22.78 ±3.34	25.80 ± 4.49	0.19	24.45 ± 3.10	24.36 ± 3.70	0.96
Active co-morbidities		2 (2, 3)	3 (1, 3)	1.00‡	2 (0, 2)	2 (1, 3)	0.22‡
Pack years		39.50 (29.13, 53.25)	48.50 (30.25, 55.50)	0.69‡	32.50 (14.13, 67.25)	42.00 (38.25, 54.38)	0.32‡
Exacerbations (last year)		3 (0, 4)	1 (0, 1)	0.18‡	2 (1, 3)	2 (0, 2)	0.85‡
GOLD grade, %	II	0	0	0.33‡	0	0	0.80‡
	III	30	60		66.67	30.00	
	IV	70	40		33.33	70.00	
Heterogeneous, %		30.00	83.33	0.66†	33.33	50.00	0.52†
Baseline medications							
LABA, %		90.00	83.33	1.00†	100.00	100.00	1.00†
LAMA, %		90.00	100.00	1.00†	100.00	100.00	1.00†
ICS, %		80.00	83.33	1.00†	100.00	80.00	0.24†
Oxygen, %		10.00	50.00	0.12†	16.67	10.00	0.70†
Symptoms							
mMRC		3 (2, 4)	2 (2, 3)	0.22‡	3 (2, 3)	2 (2, 3)	1.00‡
SGRQ	*total*	65.58 ± 19.95	53.74 ± 13.75	0.18	55.23 ± 10.43	50.74 ± 8.44	0.40
	symptoms	56.19 ± 21.02	45.69 ± 16.15	0.28	68.51 ± 11.03	47.55 ± 20.60	**0.02**
	impacts	56.45 ± 27.44	43.30 ± 19.09	0.28	37.15 ± 10.18	34.80 ± 7.65	0.64
	activity	85.62 ± 15.49	75.60 ± 17.89	0.28	79.53 ± 15.79	79.78 ± 9.12	0.97
Lung function							
FEV_1, L		0.73 ± 0.26	1.01 ± 0.20	**0.04**	0.82 ± 0.31	0.71 ± 0.19	0.45
FEV_1, %		27.90 ± 8.72	34.02 ± 6.96	0.17	33.95 ± 8.57	28.92 ± 5.82	0.24
FVC, L		2.81 ± 0.50	3.66 ± 0.62	**0.03**	2.77 ± 0.81	3.05 ± 1.10	0.57
FVC, %		86.56 ± 11.12	95.88 ± 11.39	0.17	92.42 ± 14.32	98.45 ± 17.07	0.46
FEV1/FVC, %		24.96 ± 6.97	26.37 ± 3.74	0.62	28.44 ± 5.89	22.95 ± 4.95	0.09
MEF25-75%, L/s		0.21 ± 0.06	0.27 ± 0.07	0.23	0.24 ± 0.06	0.17 ± 0.04	**0.04**
FRC, L		6.43 ± 0.90	6.18 ± 1.03	0.64	5.76 ± 0.96	5.99 ± 1.24	0.68
FRC, %		204.60 ± 19.94	185.70 ± 10.83	**0.03**	193.90 ± 10.60	195.50 ± 19.21	0.84
RV, L		5.34 ± 0.84	4.80 ± 0.69	0.19	4.90 ± 0.79	4.82 ± 0.95	0.87
RV, %		241.20 ± 33.00	203.10 ± 14.57	**0.01**	232.60 ± 29.11	215.90 ± 28.03	0.29
TLC, L		8.22 ± 0.95	8.46 ± 1.37	0.72	7.62 ± 1.35	7.96 ± 1.84	0.67
TLC, %		142.50 ± 11.53	134.10 ± 8.41	0.12	141.10 ± 7.79	140.30 ± 9.88	0.88

	Valve responder	Valve non-responder	*p-value*	Coil responder	Coil non-responder	*p-value*
RV/TLC	64.82 ±5.04	57.10 ± 3.96	**0.01**	64.60 ± 4.78	61.04 ± 5.24	0.19
IC	1.91 ± 0.60	2.38 ± 0.43	0.10	1.89 ± 0.62	1.97 ± 0.68	0.80
R_{aw}, kPA/L/s	0.96 ± 0.30	0.64 ± 0.25	0.05	0.84 ± 0.16	0.76 ± 0.22	0.41
G_{aw}, kPA/L/s	0.20 ± 0.09	0.27 ± 0.08	0.14	0.26 ± 0.07	0.28 ± 0.06	0.57
TLCOc, mmol/min/kPA	2.40 ± 0.65	3.14 ± 1.33	0.29	3.00 ± 1.36	2.62 ± 0.77	0.56
TLCOc, %	29.97 ± 8.07	34.56 ± 11.69	0.46	38.17 ± 12.23	33.21 ± 8.13	0.41
KCOc, mmol/min/kPA	0.56 ± 0.13	0.58 ± 0.16	0.79	0.73 ± 0.13	0.59 ± 0.20	0.13
KCOc, %	38.47 ± 8.62	41.94 ± 12.80	0.60	49.40 ± 8.89	38.65 ± 10.56	0.06
pH	7.45 ± 0.02	7.45 ± 0.01	0.71	7.45 ± 0.03	7.44 ± 0.03	0.51
PCO_2	5.06 ± 0.64	5.09 ± 0.54	0.92	4.56 ± 0.54	5.28 ± 0.79	0.05
PO_2	9.30 ± 0.84	8.98 ± 1.17	0.58	9.67 ± 0.92	9.30 ± 2.00	0.62
HCO_3	25.71 ± 3.06	25.63 ± 2.96	0.96	23.22 ± 2.47	25.92 ± 3.25	0.08
Static compliance, L/cm H_20	5.26 ± 4.46	4.74 ± 3.42	0.85	3.48 ± 2.32	3.95 ± 4.10	0.78
Impulse oscillometry						
R5, kPa/L/s	0.68 ± 0.17	0.71 ± 0.07	0.56	0.77 ± 0.18	0.67 v 0.21	0.37
R20, kPa/L/s	0.37 ± 0.08	0.37 ± 0.04	0.92	0.42 ± 0.10	0.38 ± 0.18	0.64
R5-20, kPa/L/s	0.31 ± 0.12	0.33 ± 0.04	0.62	0.35 ± 0.10	0.29 ± 0.14	0.32
Rin5, kPa/L/s	0.44 ± 0.06	0.49 ± 0.07	0.18	0.49 ± 0.08	0.50 ± 0.14	0.74
Rex5, kPa/L/s	0.80 ± 0.27	0.77 ± 0.11	0.76	0.92 ± 0.24	0.74 ± 0.25	0.18
X5, kPa/L/s	-0.42 ± 0.14	-0.52 ± 0.16	0.23	-0.45 ± 0.14	-0.45 ± 0.18	0.98
Xin5, kPa/L/s	-0.20 ± 0.05	-0.17 ± 0.18	0.73	-0.18 ± 0.09	-0.22 ± 0.06	0.39
Xex5, kPa/L/s	-0.69 ± 0.33	-0.79 ± 0.26	0.52	-0.81 ± 0.30	-0.71 ± 0.35	0.55
Xin5-Xex5, kPa/L/s	0.50 ± 0.31	0.66 ± 0.17	0.21	0.63 ± 0.27	0.49 ± 0.33	0.38
AX	4.19 ± 2.19	4.95 ± 1.59	0.44	4.74 ± 1.52	4.00 ± 2.20	0.44
Axinsp	1.73 ± 1.06	2.16 ± 1.08	0.46	1.71 ± 0.55	1.87 ± 1.01	0.71
AXexp	6.37 ± 3.81	6.85 ± 2.11	0.75	7.45 ± 2.35	5.82 ± 3.05	0.25
Fres total	28.58 ± 5.58	30.35 ± 4.05	0.48	29.99 ± 5.14	27.41 ± 3.29	0.31
Fres central	0.30 ± 0.03	0.30 ± 0.04	0.81	0.32 ± 0.05	0.31 ± 0.11	0.76
Fres peripheral	0.79 ± 0.17	0.89 ± 0.13	0.21	0.84 ± 0.14	0.89 ± 0.30	0.70
6MWD, meters	280.50 ± 118.30	373.00 ± 141.40	0.21	319.50 ± 127.70	384.60 ± 78.90	0.30
CT metrics						
Total Lung Vol_{insp}, ml	6717 ± 866	7045 ± 1226	0.49	6098 ± 1126	6436 ± 1621	0.63
Total Lung Vol_{exp}, ml	5524 ± 879	5617 ± 1482	0.68	4751 ± 751	5077 ± 1681	0.60
Total Lung DS, % (-950insp)	41.5 (36.3, 42.0)	38.0 (28.8, 42.3)	0.41‡	39.0 (19.5, 42.0)	29.5 (22.5, 36.0)	0.38‡
Total Lung DS, % (-856exp)	77.5 (70.3, 82.3)	69.0 (64.0, 77.0)	0.24‡	76.5 (68.5, 78.0)	73.0 (66.8, 79.3)	0.62‡
fGT, %	43.5 (37.8, 46.3)	37.0 (35.5, 45.5)	0.57‡	46.0 (38.5, 60.3)	48.5 (41.0, 54.3)	0.90‡

	Valve responder	Valve non-responder	*p-value*	Coil responder	Coil non-responder	*p-value*
Total Lung Vessel Vol, ml	187.5 (154.3, 203.3)	210.5 (175.3, 242.3)	0.38‡	139.0 (115.8, 192.3)	163.5 (139.8, 186.5)	0.65‡
PA ratio	0.85 (0.77, 0.88)	0.81 (0.69, 1.00)	0.96‡	0.77 (0.70, 0.83)	0.80 (0.77, 0.90)	0.33‡
Mortality Score						
BODE Index	7 (5, 8)	4 (3, 7)	0.09‡	5 (4, 7)	5 (4, 5)	0.81‡
Inflammatory marker						
White cell count, 10^9/L	7.94 ± 2.18	6.73 ± 1.08	0.16	7.98 ± 1.60	8.46 ± 2.30	0.63
Neutrophils*, 10^9/L*	5.14 ± 2.55	4.60 ± 1.41	0.59	5.18 ± 2.04	5.75 ± 1.80	0.59
Fibrinogen, mg/dL	3.31 ± 0.39	3.04 ± 0.92	0.56	3.43 ± 0.64	4.01 ± 0.69	0.12
C-reactive protein, mg/dL	3.44 ± 3.97	2.00 ± 1.10	0.33	4.33 ± 3.39	9.30 ± 12.28	0.25
BALF neutrophil MVs/µl	3491 (2071, 8484)	3940 (1016, 7806)	0.71	2542 (1476, 772249)	3499 (2284, 18791)	0.26

Categorical data are presented as a frequency (%) and compared using a Chi-square test† (nominal) or Mann-Whitney test‡ (ordinal). Parametric continuous data are presented as mean ± SD and compared using a paired t-test unless otherwise stated. Non-parametric continuous data are presented as median (IQR) and compared using a Mann-Whitney test‡. AX, area of reactance; BALF, bronchoalveolar lavage fluid; BMI, Body Mass Index; BODE index = Body mass index, airflow Obstruction, Dyspnoea, and Exercise capacity; c, corrected for haemoglobin concentration; DS, Density Score; FEV_1, ex, expiratory phase; Forced Expiratory Volume in 1 second; FVC, Forced Vital Capacity; Fres, resonant frequency; fGT, functional gas trapping; G_{aw}, airways conductance; GOLD, Global Initiative for Obstructive Lung Disease; HCO3, Bicarbonate; IC, Inspiratory Capacity; in, inspiratory phase; ICS, inhaled corticosteroid; LABA, long acting beta-agonist; LAMA, long acting muscarinic antagonist; K_{CO}, carbon monoxide diffusing capacity per unit alveolar volume; MEF25-75%, mid-expiratory flow rate between 25 and 75%; mMRC, modified Medical Research Council dyspnoea scale; MVs, microvesicles; PA ratio, pulmonary artery to aorta ration; PCO_2, Partial pressure for carbon dioxide; PO_2, Partial pressure for oxygen; R5, resistance at 5 Hz; R20, resistance at 20 Hz; R_{aw}, airways resistance; RV, Residual Volume; SGRQ, St George's Respiratory Questionnaire; TLC, Total Lung Capacity; TL_{CO}, Transfer factor for carbon monoxide; Vol, Volume; X5, reactance at 5 Hz; 6MWD, Six-Minute Walk Distance.

Table 5.9. Baseline characteristics of responders versus non-responders – valve & coil cohorts.

[Responders were defined as those individuals achieving a RV reduction of ≥10% at 3 months].

Endobronchial coil (EBC)

Baseline characteristics

16 patients were enrolled: mean age 67.0 ± 9.6 years, 37.5% male, BMI 24.4 ± 3.4, a median of two active comorbidities, 41 pack year smoking history, and two exacerbations in the preceding 12 months. 43.8% were classified as GOLD grade III and 56.2% IV. Questionnaires recorded a median mMRC of 2 and mean SGRQ-total of 52.4 ± 9.2 points. Patients exhibited severe airflow obstruction, FEV1 30.8 ± 7.2%, and hyperinflation, RV 222.2 ± 28.7%. Baseline characteristics including neutrophil-derived microvesicle levels are detailed in Table 5.6.

Changes in characteristics at 3-months

At 3-months, modest improvements in KCO of -4.02% (p=0.02), HCO_3 of +1.11 (p=0.01), total vessel volume of +18mls (p<0.01) and BODE index of -0.5 points (p=0.04) were observed. These were accompanied by a statistically significant reduction in BALF neutrophil-derived microvesicle levels of -855/µl (p=0.01). (Table 5.7).

BALF neutrophil-derived microvesicle delta correlations

ΔBALF neutrophil-derived microvesicle counts were negatively related to ΔKCO% (r=-0.67, p=0.01). (Figure 5.9 and Table 5.10).

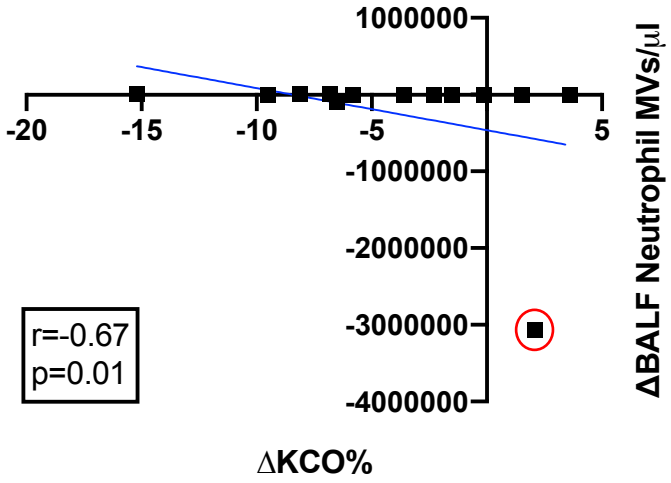

Figure 5.9. Change in BALF Neutrophil MVs and change in KCO% - coil cohort.

After exclusion of an outlier (indicated by the red circle), the correlation remained significant (r=-0.62; p=0.04).

Predictors

6 of 16 subjects achieved a ≥10% reduction in RV. Responders were characterised by a higher SGRQ-symptom score (68.51 versus 47.55 points; p=0.02) and MEF25-75% (0.24 versus 0.17L/s; p=0.04). (Table 5.9). Binomial logistic regression did not identify baseline BALF neutrophil-derived microvesicle levels as a predictor of ≥10% reduction in RV.

	ΔBODE Index		ΔmMRC		ΔSGRQtot		ΔBMI		ΔFEV1		ΔFEV1%		ΔFVC		ΔFVC%	
Parameter	r	p	r	p	r	p	r	p	r	p	r	p	r	p	r	p
ΔBALF neutrophil MVs	0.26	0.33	0.44	0.09	0.07	0.81	-0.11	0.69	-0.03	0.91	-0.05	0.84	-0.13	0.64	-0.22	0.42
	ΔFEV1/FVC		**ΔMEF25-75%**		**ΔRAWtot**		**ΔGAWtot**		**ΔFRC**		**ΔFRC%**		**ΔRV**		**ΔRV%**	
Parameter	r	p	r	p	r	p	r	p	r	p	r	p	r	p	r	p
ΔBALF neutrophil MVs	0.08	0.78	-0.08	0.76	-0.15	0.57	0.06	0.84	-0.20	0.45	-0.15	0.57	0.00	1.00	-0.05	0.87
	ΔTLC		**ΔTLC%**		**ΔRV/TLC**		**ΔIC**		**ΔIC/TLC**		**ΔTLCO**		**ΔTLCO%**		**ΔKCO**	
Parameter	r	p	r	p	r	p	r	p	r	p	r	p	r	p	r	p
ΔBALF neutrophil MVs	-0.21	0.43	-0.09	0.73	0.04	0.90	0.03	0.91	0.11	0.70	-0.36	0.22	-0.35	0.24	**-0.58**	**0.04**
	ΔKCO%		**ΔpH**		**ΔPCO_2**		**ΔPO_2**		**ΔCompliance**		**Δ6MWD**		**ΔR5**		**ΔR20**	
Parameter	r	p	r	p	r	p	r	p	r	P	r	p	r	p	r	p
ΔBALF neutrophil MVs	**-0.67**	**0.01**	0.13	0.62	-0.23	0.39	0.37	0.16	0.17	0.53	0.17	0.53	-0.04	0.90	-0.16	0.55
	ΔR5-20		**ΔRin5**		**ΔRex5**		**ΔX5**		**ΔXin5**		**ΔXex5**		**ΔXin5-Xex5**		**ΔAX**	
Parameter	r	p	r	p	r	p	r	p	r	p	r	p	r	p	r	p
ΔBALF neutrophil MVs	0.08	0.76	0.13	0.63	-0.26	0.33	-0.27	0.30	-0.22	0.41	-0.06	0.82	0.12	0.66	0.16	0.55
	ΔAxinsp		**ΔAXexp**		**ΔFres total**		**ΔFres central**		**ΔFres peri**		**Δ6MWD**		**ΔTLV_{insp}**		**ΔTLV_{exp}**	
Parameter	r	p	r	p	r	p	r	p	r	p	r	p	r	p	r	p
ΔBALF neutrophil MVs	0.26	0.34	0.13	0.64	0.09	0.74	-0.13	0.62	-0.04	0.87	0.17	0.53	-0.24	0.37	-0.31	0.26
	Δ-950_{insp}		**Δ-856_{exp}**		**ΔfGT**		**Δvessel vol**		**ΔPA ratio**		**ΔWCC**		**ΔFibrinogen**		**ΔCRP**	
Parameter	r	p	r	p	r	P	r	p	r	p	r	p	r	p	r	p
ΔBALF neutrophil MVs	-0.03	0.91	-0.03	0.93	0.04	0.87	0.28	0.29	0.32	0.23	-0.18	0.51	-0.29	0.29	-0.14	0.60

Table 5.10. Delta correlations: BALF Neut-MVs and clinically relevant parameters – coil cohort.

Group comparisons

Baseline

The valve cohort had higher baseline SGRQ-impacts (51.52 versus 35.68 points; p=0.03), CT-density score at -950HU (41 versus 31%; p=0.02), CT-intraparenchymal vessel volume (197 versus 157mls; p=0.01), and lower CT-fGT (43 versus 47%; p=0.04) compared to coil recipients (Table 5.6).

Changes at 3-months

The valve cohort achieved greater mean improvements than coil recipients in FEV1 (6.35 versus 1.49%; p=0.04), FEV1/FVC (2.34 versus -0.38; p=0.03), RV (-38.66 versus -13.38; p=0.03), TLC% (-10.56 versus -2.01; p<0.01), G_{AW} (0.10 versus 0.02 kPA/L/s; p=0.01), KCO (0.29 versus -4.02; p=0.04), HCO_3 (-0.95 versus 1.11; p<0.01), and CT-total lung $volume_{INSP}$ (-447.1 versus -61.4mls; p=0.01). (Table 5.7).

Discussion

The diagnosis of COPD is confirmed with spirometry, an assessment of function which alone is unable to determine the pathological processes in the small airways and the parenchyma. This is being addressed by radiological, physiological and molecular methods. BALF sampling of the airways surface microenvironment grants minimally invasive access to the inflammatory activity of the lungs and the responses to insult such as cigarette smoking and to therapeutic intervention (i.e., lung volume reduction) and the opportunity to appraise novel biomarkers such as microvesicles.

Validation cohort

This study has identified a variety of microvesicle (MV) populations in BALF and in plasma of patients with mild to very severe COPD. Of these, PMN (neutrophil)-derived MVs were found to be substantially increased in BALF and their numbers correlated with airflow limitation, reduced exercise capacity, impaired of quality of life, BODE index, the latter a composite score predicting risk of mortality[361] and COPD exacerbations[362].

BALF neutrophil-derived MVs are thought to have been produced locally rather than translocating from the circulation, a hypothesis challenging to confirm with currently available techniques but one which may be resolved employing immuno- or radiolabelling and electron microscopy (the latter for microparticle confirmation). BALF neutrophil cells are known to be the predominant population within the alveolar compartment. Intriguingly, we did not find a relationship between BALF neutrophil cell count and the aforementioned clinical indices and which may be accounted for by a number of possibilities. Firstly, this may reflect the limitations of bronchoalveolar lavage as activated or injured cells tend to aggregate, become adherent to the airway wall and are less effectively recovered[363]. Secondly, neutrophils produce MVs in response to inflammatory stimuli[364, 365] and hence their numbers may better reflect their activation status[366, 367].

Neutrophil-derived MVs may play a fundamental role in mediating neutrophilic inflammation and tissue damage, specifically hydrolysis of the alveolar extracellular matrix bed. Genschmer et al recently

showed that PMN-derived exosomes, a smaller subtype of extracellular vesicle, exist in clinical specimens from subjects with COPD but not healthy controls, and are capable of transmitting a COPD-like phenotype from humans to mice by way of surface-bound neutrophil elastase[132].

We also examined the MV populations in plasma. Previous reports have focused on endothelial MVs[127, 128], but we have found a variety of subtypes of which neutrophil-derived predominate. However, circulating neutrophil-derived MVs did not correlate with any of the clinical indices, supporting the theory that the alveolar microenvironment is perhaps, intuitively so, a more reliable barometer of airways inflammation and that a simple spill-over of inflammatory markers from the lung into the blood does not necessarily occur[368]. Interestingly, plasma monocyte MV numbers correlated with impairment of gas transfer, a marker of parenchymal damage, and with the BODE index after excluding individuals with BALF samples positive for microbial isolates. It is known that TNF-alpha production by circulating monocytes is elevated in individuals with COPD[369] and the collective secretions of these inflammatory molecules most likely reflects the activated cellular state. Moreover, monocyte recruitment to the lung is increased in COPD, giving rise to greater numbers of alveolar macrophages which are important players, together with the neutrophil, in orchestrating and perpetuating the inflammatory response[280]. However, we did not observe associations between circulating endothelial-derived MVs and hyperinflation[370] or frequency of exacerbations[128] as has been reported in cohorts more homogeneous (i.e. mild COPD patients) compared to our study population.

The potential role of cytokines in COPD was first reported by Keatings et al in 1996 who elegantly showed increased concentrations of TNF-α and CXCL8 (together with increased neutrophil numbers) in the sputum of patients with COPD compared with smoking and non-smoking control subjects[107]. Since then, over 50 cytokines have been identified in COPD, but their roles in what is now appreciated as complex pathophysiology remains unclear. Pro-inflammatory cytokines such as TNF-α, IL-1β, IL-6, and CXCL8 are increased in COPD and are thought to amplify inflammation via activation of the transcription factor, nuclear factor (NF)-κB[124]. Many cells including epithelial cells and macrophages

secrete TNF-α which has been implicated in cigarette-smoke induced emphysema in mice[371]. IL-1β is a potent activator of macrophages[372]. IL-6 is particularly stable in the circulation and is thought to be involved in the systemic manifestations of COPD[373] and exacerbations[374]. CXCL8 is important in neutrophil and monocyte recruitment and is associated with peripheral muscle weakness in COPD[375]. However, we found no correlations between TNF-alpha, IL-1β, IL-6, CXCL8 within BALF and any of the clinical indices and indeed reports in the literature are conflicting[376, 377]. A possible explanation for the variability of cytokine concentrations may relate to degradation within the alveolar space and their time-limited stability after sample collection[378]. We did find correlations with various MV subpopulations, specifically between IL-1β, IL-6, CXCL8 and neutrophil-derived MVs. Whilst this deserves further investigation, it is interesting to speculate this reflects cytokine-stimulated MV release[365][ref] or discharge of intravesicular cargo-containing cytokines[351].

These findings support the contention that BALF neutrophil-derived MVs are a clinically relevant biomarker of COPD severity. Interrogation of the intravesicular cargo may lend mechanistic insight into disease pathogenesis and reveal potentially novel targets which could be harnessed with therapeutic intent.

Impact of individual lung volume reduction therapies

Lung volume reduction following valve implantation surpassed almost three-fold those of the coil recipients and conferred meaningful clinical benefit. Seemingly paradoxically the depletion of BALF MVs observed in the coil group was not a feature of the valve cohort. One may speculate as to the reasons: It is in the nature of the interventions that the initially sampled sites are not readily accessible to resampling and this is particularly an issue for endobronchial valves where the aspirate obtained will inevitably be reflective of more proximal bronchial airways with potential contamination from the ipsilateral lobe(s) as it is not possible to wedge the bronchoscope as securely in the airway. Furthermore, it is unknown if there exists a gradient in MV levels with higher concentrations found in more proximal airways, however the ‘united airway disease’ hypothesis suggests otherwise[379]. The possibility that the nitinol-silicone valve might have induced a localised inflammatory reaction

secondary to the development of thick mucus biofilms that were frequently found to coat the implants is proffered for consideration in future trials. Analysis of a control lobe, either ipsilateral or contralateral, may mitigate these problems in lung volume reduction patients or those individuals receiving an endobronchial implant.

The peripheral airways are not thought to be obliterated by EBC implants but distorted by curling and therefore, still accessible to instrumentation. It must however be borne in mind that despite the thin profile of the endobronchial coil, the surface area of the airway epithelium exposed to sampling is reduced. Additionally, bronchoscopic removal of secretions is itself a therapeutic intervention and may have contributed to the lower MV levels.

Limitations

Our initial intention to use a bronchosorption sampling tool to capture epithelial lining fluid and avoid the problems of volume burden and dilution of bronchoalveolar lavage[380] had to be abandoned on account of the prohibitive expense. That the process of eluting MVs from the device was not as yet validated was also an issue. Instead we, as have others, adopted bronchoalveolar lavage as a means of sampling respiratory tract MVs but the technique is not standardised. The yield of fluid is but a fraction of that infused necessitating relatively large volumes to ensure adequate returns. Our COPD patients however were severely compromised and our prescribed 50mls necessarily conservative. We speculated, though, that the positive airways pressure in those intubated and ventilated might, in maintaining the patency of the airway, encourage return of the lavage. Troublesome tenacious secretions were repeatedly washed but retention of MVs could not be excluded.

Platelet-rich plasma was used to evaluate circulating MVs owing to a significant fall in MV yield during preparation of platelet-poor plasma[353]. This strategy prevented analysis of circulating platelet-derived MVs (as their size overlaps that of platelets at 1-3µm) – however, it was considered more valuable to focus on the accurate quantification of other MV subtypes. We employed a CyAn™ flow cytometer which, despite being designed primarily for cell analysis, is well established in the literature for microvesicle characterisation and quantification[358]. Although the resolution is lower compared

to newer flow cytometers, we believe the methodological approach using particle size, surface marker expression, and detergent sensitivity to detect MVs is both robust and reproducible[351]. Whilst this project has focused on microvesicles, there are other types of extracellular particle including exosomes and apoptotic bodies which would also be worthwhile evaluating in future research.

We have as yet not had the opportunity to asses MVs in healthy subjects. However, we found patients with mild COPD had lower levels of neutrophil-derived MVs compared to those with severe disease. Furthermore, it has been shown that untreated mice have lower numbers of BALF MVs (in particular neutrophil-derived MVs) compared to those with acute lung injury[351]. One may reasonably extrapolate from this data that non-COPD controls might have little or no neutrophil-derived MVs in BALF.

We demonstrated an association of neutrophil-derived MVs with clinical indices of COPD severity but not a causal relationship. The exosomal work by Genschmer et al[132] is fascinating and provides a tangible mechanistic link for extracellular particles inducing and perpetuating neutrophilic-predominant inflammation within the alveolar compartment. To substantiate our findings, we intend to interrogate the microvesicular cargo and evaluate their pro-inflammatory potential using cell culture. Lastly, our data are limited by lack of control lobe data and the unavoidable fact that bronchoscopy itself can be a therapeutic intervention with clearance of airway secretions.

Conclusions

BALF neutrophil-derived MV numbers may contribute to disease phenotyping using lung function and quantitative CT imaging. However, a role as a biomarker to predict and to evaluate therapeutic response in individuals with COPD requires further research in larger trials to fully realise their potential.

CHAPTER 6: Final Discussion

Overview and implications of findings

Impact of lung volume reduction on structure-function relationships

Surgery achieved the greatest degree of lung volume reduction and more than 90% of recipients met the minimal clinically important difference (MCID) of at least 10% residual volume (RV) reduction. It was the only intervention to be accompanied by improvements in functional gas trapping on computed tomography, IOS expiratory airways resistance at 5Hz, expiratory and within-breath reactance at 5Hz, and peripheral resonant frequency, collectively inferring improvement in small airways function. Emphysema with hyperinflation is the end-stage of the COPD spectrum with substantial loss of terminal bronchioles, destruction of the elastic scaffold maintaining patency of airways and facilitating passive recoil, and compromised tissue with functional potential[335]. The mechanically disadvantaged ventilatory pump is disencumbered by volume reduction, resurrecting functionally preserved tissue, and re-tensioning the remaining airway network[335]. This is conceptually attractive to explain the functional impact of surgery on the small airways network.

Valve implantations accomplished a smaller reduction in IOS expiratory and within-breath reactance at 5Hz without an accompanying signal in resistance, resonant frequency, or functional gas trapping on CT. Modest improvements to alveolar gas mixing (AME) and small airways function (Sacin) were measured with MBNW in a subset of patients. These data suggest the impact of valves on the peripheral airway compartment was less pronounced than with surgery and was predominantly due to deflation of emphysematous lung tissue and restoration of the mechanical pump, although diaphragmatic and chest wall function were not formally assessed in this study. The ultimate objective of surgery and of valve implantation is the same – and the three-month physiological outcomes were not overly dissimilar to surgery. One might speculate that the two techniques impact lung physiology via different mechanisms, but a 28% greater reduction in residual volume with surgery is a convincing

alternative explanation. Indeed, only 62% of EBV recipients attained the minimal clinically important difference (MCID) of ≥10% RV reduction.

Coil implantations resulted in limited volume reductions, rather less than in previous trials such as RESET[207], and this may be the consequence of a more infirm cohort, burden of airway sampling using bronchoalveolar lavage (two lobes versus one), or employment of smaller size coils with less tensioning effects. Only 35% of subjects achieved the MCID of ≥10% RV reduction and 3-month physiological outcomes were similarly disappointing with improvements limited to CT-intraparenchymal blood vessel volume (perhaps due to greater radial traction exerted by the coils on the surrounding parenchyma) and the area under reactance during expiration (AXex).

Extrapolation of these data are limited by the small size of the study and the lack of randomised controlled data. That said, the degree of volume reduction appears critical in determining favourable clinical outcomes[214] as does the impact of LVR on the small airways network, which not unexpectedly, is proportionally affected by increasing degrees of volume reduction achieved: surgery > endobronchial valve > endobronchial coil. It is likely the mechanical advantage regained from lobar resection / deflation is the principal driver of benefit – however, the finding that the small airways compartment can be modified by lung volume reduction is intriguing and may open avenues for the development of more peripherally targeted interventional therapies.

Impact of lung volume reduction on airways inflammation

The validation cohort study has identified a variety of microvesicle (MV) populations in BALF and in plasma of patients with mild to very severe COPD. Of these, PMN (neutrophil)-derived MVs were found to be substantially increased in BALF and their numbers correlated with airflow limitation, reduced exercise capacity, impaired of quality of life, BODE index, the latter a composite score predicting risk of mortality[361] and COPD exacerbations[362]. BALF neutrophil-derived MVs were shown to be a more robust biomarker of disease severity than BALF neutrophil cell and cytokine levels. Genschmer et al recently demonstrated PMN-derived exosomes, a smaller subtype of extracellular vesicle, exist in clinical specimens from subjects with COPD but not healthy controls, and are capable

of transmitting a COPD-like phenotype from humans to mice by way of surface-bound neutrophil elastase[132], raising the exciting possibility that BALF neutrophil-derived MVS may also be implicated in disease pathogenesis.

Lung volume reductions following valve implantation surpassed almost three-fold those of the coil recipients and conferred meaningful clinical benefit. Seemingly paradoxically the depletion of BALF MVs observed in the coil group was not a feature of the valve cohort. One may speculate as to the reasons: It is in the nature of the interventions that the initially sampled sites are not readily accessible to resampling and this is particularly an issue for the valves where the aspirate obtained will inevitably be reflective of more proximal bronchial airways with potential contamination from the ipsilateral lobe(s) as it is not possible to wedge the bronchoscope as securely in the airway. Furthermore, it is unknown if there exists a gradient in MV levels with higher concentrations found in more proximal airways, although this would be at variance with the 'united airway disease' hypothesis[379]. The possibility that the nitinol-silicone valve might have induced a localised inflammatory reaction secondary to the development of thick mucus biofilms that were frequently found to coat the implants is proffered for consideration in future trials. The peripheral airways are not thought to be obliterated by coil implants but distorted by curling and therefore, still accessible to instrumentation. It must however be borne in mind that despite the thin profile of the endobronchial coil, the surface area of the airway epithelium exposed to sampling is reduced. Additionally, bronchoscopic removal of secretions is itself a therapeutic intervention and may have contributed to the lower MV levels.

These findings support the contention that BALF neutrophil-derived MVs are a clinically relevant biomarker of COPD severity. Interrogation of the intravesicular 'cargo' may lend further insight into disease pathogenesis and reveal potentially novel targets which could be harnessed with therapeutic intent. However, analysis of a control lobe, either ipsilateral or contralateral, may resolve the aforementioned problems encountered in evaluating inflammatory outcomes in lung volume reduction patients or those individuals receiving an endobronchial implant.

Future directions

Investigative modalities

CT quantitative imaging analysis has increasingly been shown to be of value in COPD disease phenotyping and no less so in this study. Acknowledging the conflict of image resolution and radiation exposure, CT chest imaging is a widely available, relatively safe, and cost-effective modality with which to characterise COPD both as a biomarker and as an objective endpoint for assessing interventional outcomes. We anticipate the opportunity of further insights into the impact of lung volume reduction on the small airway and blood vessel compartments as the resolution of CT is improved. Four-dimensional computed tomography describes data correlated with patient respiratory phase, an assessment of real-time pulmonary mechanics[381-384] and which is likely to gain traction in years to come.

Similarly, IOS is a safe, well-tolerated, and quick to perform non-invasive test that permits discernment of pulmonary physiology that cannot be gleaned from conventional lung function measures, specifically changes affecting the peripheral airway compartment[385]. IOS is proving complementary to routine lung function testing and with the publication of detailed standardisation and technical guidelines[386], is likely to be more widely employed with establishment of robust reference ranges particularly for the COPD population. For those patients who are infirm and unable to perform forced respiratory manoeuvres, this will be a welcome alternative.

We suggest BALF neutrophil-derived MV observations are a potentially useful contributor to disease phenotyping alongside qCT imaging and lung function testing and may find a place as a biomarker and as an objective indicator of the outcomes of interventions in individuals with COPD. Our initial intention to use a bronchosorption sampling tool to capture epithelial lining fluid and avoid the problems of volume burden and dilution of bronchoalveolar lavage[380] had to be abandoned on account of the prohibitive expense. That the process of eluting MVs from the device was not as yet validated was also an issue. However, the potential usefulness of bronchosorption cannot be

underestimated and it would circumvent the challenges encountered with bronchoalveolar lavage and provide a blueprint of the inflammatory milieu whilst maximising the safety of our patients. Furthermore, it would be of interest to confirm that microvesicle populations are the same along the length of the nasal-tracheobronchial tree, as according to the unified hypothesis[379]. If this were proven to be the case, upper airway sampling would be a favoured alternative.

Study design

The employment of a randomised controlled trial design is considered the more robust means of minimising bias and establishing a cause-effect relationship between intervention and outcome which is crucial to clarifying the impact of these and of future interventional therapies on the small airways and establishing that modulation of this compartment is of therapeutic relevance in individuals with severe disease.

Conclusions

The degree of lung volume reduction achieved is critical in determining favourable clinical outcomes for patients with severe emphysema and hyperinflation. The structural and functional impacts of lung volume reduction on the small airways compartment, the principal site of airflow obstruction, are proportional to the degree of volume reduction achieved (surgery > valves > coils). The impact of these therapies on airways inflammation requires further scrutiny.

qCT and IOS are shown to be structural and functional biomarkers, respectively, for evaluating volume reduction – however, their predictive value for therapeutic response is not established from this small dataset. BALF neutrophil-derived MV observations are potentially useful contributors to disease phenotyping alongside lung function tests and qCT imaging – their role as biomarkers for predicting and assessing therapeutic response remains to be seen. Larger randomised controlled trial designs are recommended to further investigate these preliminary findings.

PUBLICATIONS

The following abstracts and manuscripts have been produced during this period of research:

Conference papers

Apps M, Walsted E, Pavitt M, Swanton L, Lewis A, Buttery S, et al. P138 Kinetics of intrathoracic pressure change following administration of cpap. Thorax. 2017;72:A158-A.

Garner J, Soni S, O'Dea K, Srikanthan K, Tenda E, Aboelhassan A, et al. Late Breaking Abstract - Intra-alveolar neutrophil-derived microvesicles: a biomarker of COPD severity. European Respiratory Journal. 2018;52(suppl 62):OA4921.

Garner S, Hardie R, Meireles I, Caneja C, Tenda ED, Srikanthan K, et al. Evaluation of a Low Cost, Re-Useable, Bronchoscopy Biosimulator with Ventilated Lungs: The Bronchoscopy BioSim. A35 INTERVENTIONAL PULMONOLOGY. p. A1405-A.

Dransfield M, Bhatt S, Slebos D-J, Klooster K, Sciurba F, Shah P, et al. Impact of endobronchial valves on patient reported outcomes in severe emphysema. European Respiratory Journal. 2019;54(suppl 63):RCT447.

Bon JM, Sue R, Wright S, Rivas-Perez H, Wiese TA, Gauhar UA, et al. Clinically Meaningful Reduction in Hyperinflation with Zephyr Endobronchial Valves (Zephyr Valve) Associated with Sustained Longitudinal Improvements in Lung Function, Exercise Tolerance, QoL and Dyspnea. A41 COPD: EPIDEMIOLOGY. p. A7308-A.

Apps M, Pavitt M, Lewis A, Orton C, Sadaka A, Garner J, et al. Increasing CPAP (Continuous Positive Airway Pressure) leads to increasing trans-pulmonary pressure with increased activity of the abdominal wall muscles to aid Expiration. European Respiratory Journal. 2019;54(suppl 63):PA3921.

Tenda ED, Aboelhassan AM, Kontogianni K, Rice A, Crichton S, Garner JL, et al. Endobronchial Ultrasound Transbronchial Needle Aspiration (EBUS-TBNA) versus Flexible 19G Endobronchial Ultrasound Transbronchial Needle (Flex 19G EBUS-TBNA) in the Assessment of Mediastinal and Hilar Lymphadenopathy: a Randomised Trial. European Respiratory Journal. 2019;54(suppl 63):PA324.

Garner J, Orton CM, Caneja C, Sin DD, Shaipanich T, Klooster K, et al. Safety and Feasibility of Metered CryoSpray (MCS) for Patients with Chronic Bronchitis in COPD: 9 Month Results. European Respiratory Journal. 2019;54(suppl 63):OA5172.

Hartman JE, Klooster K, Augustijn S, Van Geffen WH, Garner J, Shah PL, et al. Mechanisms of action of endobronchial coil treatment. European Respiratory Journal. 2019;54(suppl 63):PA3154.

Pison C, Shah PL, Slebos DJ, Ninane V, Janssens W, Perez T, et al. Safety of Denervation Following Targeted Lung Denervation (TLD) Therapy for COPD: Airflow-1 Three Year Outcomes. A24 EPIDEMIOLOGY, DIAGNOSIS, AND TREATMENT IN PLEURAL DISEASE AND IP. American Thoracic Society International Conference Abstracts: American Thoracic Society; 2020. p. A1119-A.

Original articles

Garner J, Kemp SV, Toma TP, Hansell DM, Polkey MI, Shah PL, et al. Survival after Endobronchial Valve Placement for Emphysema: A 10-Year Follow-up Study. American journal of respiratory and critical care medicine. 2016;194(4):519-21.

Garner J, Kemp SV. Interventional Bronchoscopy for COPD. Clinical Pulmonary Medicine. 2017;24(2):79-86.

Kemp SV, Slebos DJ, Kirk A, Kornaszewska M, Carron K, Ek L, et al. A Multicenter RCT of Zephyr(R) Endobronchial Valve Treatment in Heterogeneous Emphysema (TRANSFORM). American journal of respiratory and critical care medicine. 2017.

Wechalekar K, Garner J, Gregg S. Pre-surgical Evaluation of Lung Function. Seminars in nuclear medicine. 2018;49.

Slebos D-J, Cicenia J, Sciurba FC, Criner GJ, Hartman JE, Garner J, et al. Predictors of Response to Endobronchial Coil Therapy in Patients With Advanced Emphysema. Chest. 2019;155(5):928-37.

Conway F, Garner J, Orton C, Srikanthan K, Kemp S, Shah P. Contemporary Concise Review 2018: Lung cancer and pleural disease: Lung cancer and pleural disease. Respirology (Carlton, Vic). 2019;24.

Garner JL, Meireles I, Kemp SV, Shah PL. Fiducial marker implantation using convex probe EBUS and autologous blood. BMJ Case Reports. 2019;12.

Garner JL, Donovan J, Meireles I, Padley SPG, Cunningham D, Shah PL. A Golden Conundrum. American journal of respiratory and critical care medicine. 2019;200(5):631-2.

Garner J, Garner S, Hardie R, Molyneaux P, Singh S, Kemp S, et al. Evaluation of a re-useable bronchoscopy biosimulator with ventilated lungs. European Respiratory Journal. 2019;5.

Valipour A, Shah PL, Pison C, Ninane V, Janssens W, Perez T, et al. Safety and Dose Study of Targeted Lung Denervation in Moderate/Severe COPD Patients. Respiration. 2019;98(4):329-39.

Shen M, Tenda ED, McNulty W, Garner J, Robbie H, Luzzi V, et al. Quantitative Evaluation of Lobar Pulmonary Function of Emphysema Patients with Endobronchial Coils. Respiration. 2019;98(1):70-81.

Orton CM, Garner JL, Desai SR, Kemp SV, Shah PL. Aspergillus Cavitation Complicating Endobronchial Lung Volume Reduction Coil Placement. American journal of respiratory and critical care medicine. 2020;201(3):e8-e9.

Garner JL, Kemp SV, Srikanthan K, Caneja C, Zoumot Z, Roberts C, et al. 5-Year Survival after Endobronchial Coil Implantation: Secondary Analysis of the First Randomised Controlled Trial, RESET. Respiration. 2020;99(2):154-62.

Dransfield MT, Garner JL, Bhatt SP, Slebos D-J, Klooster K, Sciurba FC, et al. Effect of Zephyr Endobronchial Valves on Dyspnea, Activity Levels, and Quality of Life at One Year. Results from a Randomized Clinical Trial. Annals of the American Thoracic Society. 2020;17(7):829-38.

Garner JL, Shah PL. Lung Volume Reduction in Pulmonary Emphysema. Seminars in respiratory and critical care medicine. 2020.

Garner JL, Shaipanich T, Hartman JE, Orton CM, Caneja C, Klooster K, et al. A Prospective Safety and Feasibility Study of Metered CryoSpray (MCS) for Patients with Chronic Bronchitis in COPD. European Respiratory Journal. 2020:2000556.

Khalil K, Agbontaen K, McNally D, Love A, Mandalia S, Banya W, et al. Clinical characteristics and 28-day mortality of medical patients admitted with COVID-19 to a central London teaching hospital. Journal of Infection. 2020;81(3):e85-e9.

Garner JL, Shah PL. Challenges of evaluating lung function as part of cancer care during the COVID-19 pandemic. The European respiratory journal. 2020;56(2):2001621.

Soni S, Garner JL, O'Dea KP, Koh M, Tirlapur N, Srikanthan K, et al. Intra-alveolar neutrophil-derived microvesicles are associated with disease severity in COPD. Am J Physiol Lung Cell Mol Physiol. 2020 Nov 4. doi: 10.1152/ajplung.00099.2020. Online ahead of print.

Manuscripts under peer review

Garner JL, Biddiscombe M, Meah S, Lewis A, Buttery S, Hopkinson N, et al. Improved peripheral lung function post-endobronchial valves. AJRCCM (accepted).

Hartman J, Klooster K, Augustin SWS, Van Geffen WH, Garner JL, Shah PL, et al. Identifying responders and exploring mechanisms of action of the endobronchial coil treatment for emphysema. Respiration (accepted).

Hartman J, Garner JL, Shah PL, Slebos DJ. New bronchoscopic treatment modalities for patients with chronic bronchitis. ERJ (accepted).

APPENDICES

Appendix A

Figure 1.3. Schematic diagram of a secondary pulmonary nodule.
Frank Gaillard of Radiopedia.org, 2010. (Creative Commons attribution 4.0).

Figure 1.4. Pathology of small airways disease in COPD.
Adapted from Higham et al[85]. (Creative Commons attribution 4.0).

Figure 1.5. Pathological and radiological correlates for emphysema subtypes.
Frank Gaillard of Radiopedia.org, 2010. (Creative Commons attribution 4.0).

Appendix B

	ΔBODE Index		ΔmMRC		ΔSGRQtot		ΔBMI		ΔFEV1		ΔFEV1%		ΔFVC		ΔFVC%	
Parameter	R	p	r	p	r	p	r	p	r	p	r	p	r	p	r	p
ΔCT-lung volume$_{insp}$	0.34	0.28	0.11	0.72	-0.01	0.98	0.06	0.85	-0.09	0.76	0.06	0.85	0.13	0.67	0.37	0.21
ΔCT-lung volume$_{exp}$	0.67	0.06	0.55	0.11	0.31	0.39	0.13	0.73	-0.36	0.31	-0.27	0.44	0.45	0.19	0.37	0.30
ΔCT-950HU	0.57	0.06	**0.69**	**0.01**	0.00	1.00	0.04	0.91	-0.48	0.10	-0.30	0.32	0.47	0.10	0.56	0.05
ΔCT-856HU	0.62	0.08	**0.75**	**0.01**	-0.09	0.82	-0.07	0.86	-0.41	0.24	-0.39	0.26	0.44	0.20	0.30	0.40
ΔfGT%	0.17	0.65	0.30	0.40	0.10	0.78	-0.32	0.37	-0.31	0.38	-0.43	0.22	0.02	0.95	-0.16	0.65
ΔCT-vessel volume	0.21	0.52	0.17	0.61	-0.03	0.93	0.11	0.74	-0.14	0.65	-0.25	0.43	-0.11	0.73	-0.08	0.80
Δ CT-PA ratio	-0.42	0.17	-0.39	0.18	-0.22	0.47	0.55	0.05	0.48	0.10	0.39	0.18	0.49	0.09	0.51	0.08
	ΔFEV1/FVC		**ΔMEF25-75%**		**ΔRAWtot**		**ΔGAWtot**		**ΔFRC**		**ΔFRC%**		**ΔRV**		**ΔRV%**	
Parameter	r	p	r	p	r	p	r	p	r	p	r	p	r	p	r	p
ΔCT-lung volume$_{insp}$	-0.22	0.47	-0.12	0.70	0.28	0.36	-0.15	0.61	0.25	0.43	0.07	0.83	0.03	0.92	-0.05	0.88
ΔCT-lung volume$_{exp}$	-0.54	0.11	-0.32	0.36	0.17	0.64	-0.45	0.19	0.03	0.95	-0.05	0.91	-0.22	0.54	-0.30	0.41
ΔCT-950HU	**-0.65**	**0.02**	-0.52	0.07	0.17	0.57	**-0.68**	**0.01**	0.21	0.52	0.18	0.58	-0.26	0.39	-0.28	0.36
ΔCT-856HU	-0.64	0.05	-0.35	0.32	0.23	0.51	**-0.85**	**<0.01**	-0.39	0.29	-0.34	0.36	-0.63	0.06	-0.46	0.18
ΔfGT%	-0.21	0.56	-0.30	0.39	-0.04	0.92	-0.57	0.09	-0.61	0.09	-0.54	0.14	-0.46	0.18	-0.20	0.59
ΔCT-vessel volume	-0.02	0.94	0.05	0.87	-0.48	0.11	0.13	0.68	-0.21	0.53	-0.09	0.79	-0.06	0.86	0.10	0.75
Δ CT-PA ratio	0.26	0.39	0.70	0.05	-0.32	0.29	0.56	0.05	-0.04	0.91	0.01	0.99	-0.03	0.92	-0.14	0.66
	ΔTLC		**ΔTLC%**		**ΔRV/TLC**		**ΔIC**		**ΔIC/TLC**		**ΔTLCO**		**ΔTLCO%**		**ΔKCO**	
Parameter	r	p	r	p	r	p	r	p	r	p	r	p	r	p	r	p
ΔCT-lung volume$_{insp}$	0.15	0.61	-0.03	0.94	-0.15	0.62	-0.07	0.83	-0.13	0.68	0.34	0.29	0.33	0.30	0.27	0.39
ΔCT-lung volume$_{exp}$	-0.01	1.00	-0.24	0.51	-0.37	0.30	0.37	0.30	0.24	0.51	0.17	0.68	0.07	0.88	0.11	0.78
ΔCT-950HU	0.02	0.95	-0.10	0.75	-0.26	0.38	-0.03	0.92	-0.08	0.79	0.06	0.86	0.05	0.87	0.00	1.00
ΔCT-856HU	-0.46	0.19	-0.46	0.19	-0.14	0.70	0.41	0.24	0.42	0.23	-0.23	0.56	-0.22	0.57	-0.19	0.61
ΔfGT%	-0.40	0.26	-0.48	0.16	0.20	0.59	0.48	0.16	0.48	0.17	-0.52	0.16	-0.50	0.18	-0.41	0.28
ΔCT-vessel volume	-0.22	0.50	-0.09	0.79	0.07	0.84	0.14	0.66	0.07	0.82	**-0.68**	**0.02**	**-0.66**	**0.03**	-0.54	0.09
ΔCT-PA ratio	0.41	0.17	**0.57**	**0.04**	-0.52	0.07	0.14	0.65	-0.11	0.72	0.25	0.43	0.23	0.47	0.10	0.76

	ΔKCO%		ΔpH		ΔPCO2		ΔPO2		Δ6MWD							
Parameter	r	p	r	p	r	p	r	p	r	p						
ΔCT-lung volume$_{insp}$	0.16	0.62	**-0.68**	**0.02**	-0.03	0.94	-0.34	0.28	-0.35	0.27						
ΔCT-lung volume$_{exp}$	0.05	0.91	-0.54	0.14	-0.12	0.78	-0.23	0.55	-0.68	0.05						
ΔCT-950HU	-0.02	0.94	-0.27	0.40	-0.17	0.59	-0.20	0.53	**-0.66**	**0.02**						
ΔCT-856HU	-0.25	0.51	0.17	0.66	-0.17	0.67	0.11	0.78	-0.48	0.19						
ΔfGT%	-0.38	0.31	0.44	0.24	-0.21	0.59	0.24	0.52	0.03	0.94						
ΔCT-vessel volume	-0.56	0.08	0.29	0.38	0.47	0.14	0.12	0.72	0.04	0.92						
ΔCT-PA ratio	0.17	0.59	0.21	0.51	-0.43	0.16	0.06	0.86	0.28	0.37						

Appendix B: Table S3.1. Delta correlations: CT indices and clinically relevant parameters – surgery cohort.

	ΔBODE Index		ΔmMRC		ΔSGRQtot		ΔBMI		ΔFEV1		ΔFEV1%		ΔFVC		ΔFVC%	
Parameter	r	p	r	p	r	p	r	p	r	p	r	p	r	p	r	p
ΔCT-lung volume$_{insp}$	-0.16	0.42	-0.33	0.09	-0.06	0.76	0.07	0.71	-0.15	0.47	-0.04	0.83	0.08	0.69	0.18	0.38
ΔCT-lung volume$_{exp}$	0.17	0.51	0.16	0.54	0.13	0.60	0.16	0.53	-0.03	0.90	0.10	0.70	0.17	0.52	0.25	0.34
ΔCT-950HU	-0.15	0.46	-0.03	0.87	0.17	0.38	0.07	0.71	-0.29	0.14	-0.23	0.25	-0.13	0.52	-0.09	0.66
ΔCT-856HU	0.44	0.09	-0.04	0.87	0.25	0.32	-0.20	0.44	-0.35	0.18	-0.19	0.47	-0.25	0.34	-0.16	0.55
ΔfGT%	**0.52**	**0.04**	-0.03	0.91	0.18	0.49	-0.17	0.51	-0.34	0.20	-0.19	0.48	-0.23	0.39	-0.14	0.61
ΔCT-vessel volume	-0.31	0.12	0.00	0.98	0.11	0.59	-0.06	0.76	-0.07	0.72	-0.16	0.45	**-0.53**	**0.01**	**-0.55**	**<0.01**
ΔCT-PA ratio	0.12	0.56	-0.04	0.86	**0.40**	**0.03**	-0.02	0.91	-0.26	0.20	-0.22	0.26	**-0.42**	**0.03**	**-0.41**	**0.04**
	ΔFEV1/FVC		**ΔMEF25-75%**		**ΔRAWtot**		**ΔGAWtot**		**ΔFRC**		**ΔFRC%**		**ΔRV**		**ΔRV%**	
Parameter	r	p	r	p	r	p	r	p	r	p	r	p	r	p	r	p
ΔCT-lung volume$_{insp}$	-0.11	0.60	**-0.49**	**0.03**	0.03	0.88	0.05	0.80	0.23	0.23	0.04	0.84	0.08	0.69	-0.06	0.78
ΔCT-lung volume$_{exp}$	-0.10	0.71	-0.23	0.42	0.09	0.74	-0.38	0.14	0.12	0.64	-0.01	0.98	-0.06	0.83	-0.11	0.66
ΔCT-950HU	-0.12	0.55	-0.26	0.27	0.02	0.93	-0.04	0.84	0.23	0.25	0.12	0.54	0.23	0.24	0.22	0.26
ΔCT-856HU	-0.03	0.91	-0.15	0.61	-0.29	0.28	0.15	0.58	0.30	0.24	0.28	0.28	0.42	0.10	0.27	0.29
ΔfGT%	-0.10	0.71	-0.16	0.60	-0.24	0.36	0.19	0.49	0.35	0.16	0.31	0.23	0.44	0.08	0.26	0.31
ΔCT-vessel volume	0.20	0.32	0.33	0.15	-0.07	0.72	-0.29	0.16	-0.34	0.09	-0.20	0.32	-0.13	0.53	0.00	0.99
ΔCT-PA ratio	0.10	0.64	-0.35	0.13	0.36	0.06	-0.33	0.09	0.01	0.95	-0.01	0.95	0.33	0.09	0.27	0.17
	ΔTLC		**ΔTLC%**		**ΔRV/TLC**		**ΔIC**		**ΔIC/TLC**		**ΔTLCO**		**ΔTLCO%**		**ΔKCO**	
Parameter	r	p	r	p	r	p	r	p	r	p	r	p	r	p	r	p
ΔCT-lung volume$_{insp}$	**0.40**	**0.03**	0.28	0.15	-0.09	0.65	0.01	0.96	-0.18	0.39	0.03	0.87	-0.01	0.98	-0.13	0.53
ΔCT-lung volume$_{exp}$	0.01	0.98	-0.04	0.89	-0.17	0.49	0.31	0.25	0.29	0.28	0.20	0.43	0.20	0.44	-0.20	0.43
ΔCT-950HU	0.19	0.33	0.11	0.57	0.17	0.40	-0.12	0.56	-0.27	0.19	0.17	0.41	0.17	0.41	0.07	0.75
ΔCT-856HU	0.18	0.49	0.18	0.49	0.38	0.13	-0.07	0.80	0.01	0.98	**-0.56**	**0.02**	**-0.57**	**0.02**	-0.37	0.16
ΔfGT%	0.24	0.35	0.20	0.43	0.36	0.15	-0.01	0.97	0.05	0.87	**-0.51**	**0.04**	**-0.51**	**0.04**	-0.40	0.12
ΔCT-vessel volume	**-0.48**	**0.01**	**-0.47**	**0.01**	0.08	0.69	**-0.41**	**0.04**	-0.25	0.23	0.05	0.81	0.02	0.93	0.20	0.33
ΔCT-PA ratio	-0.07	0.72	-0.14	0.48	0.32	0.10	-0.14	0.49	-0.14	0.51	-0.28	0.15	-0.29	0.15	-0.13	0.51
	ΔKCO%		**ΔpH**		**ΔPCO2**		**ΔPO2**		**ΔCompliance**		**Δ6MWD**					
Parameter	r	p	r	p	r	p	r	p	r	p	r	p				
ΔCT- lung volume$_{insp}$	-0.19	0.35	-0.24	0.26	0.15	0.46	0.14	0.49	0.19	0.45	-0.08	0.67				

ΔCT-lung volume$_{exp}$	-0.23	0.38	-0.04	0.88	0.13	0.63	0.31	0.22	0.05	0.88	**-0.48**	**0.04**				
ΔCT-950HU	0.10	0.62	-0.14	0.52	0.01	0.95	0.15	0.48	-0.06	0.81	0.00	0.98				
ΔCT-856HU	-0.22	0.41	0.11	0.68	-0.14	0.61	0.18	0.49	0.21	0.55	**-0.55**	**0.02**				
ΔfGT%	-0.26	0.33	0.10	0.71	-0.07	0.79	0.15	0.58	0.31	0.38	**-0.63**	**0.01**				
ΔCT-vessel volume	0.19	0.36	-0.24	0.27	0.24	0.26	0.04	0.84	-0.28	0.25	0.33	0.09				
ΔCT-PA ratio	-0.21	0.30	-0.22	0.30	0.16	0.45	0.17	0.42	-0.26	0.29	0.18	0.37				

Appendix B: Table S3.2. Delta correlations: CT indices and clinically relevant parameters – valve cohort.

	ΔBODE Index		ΔmMRC		ΔSGRQ-tot		ΔBMI		ΔFEV1		ΔFEV1%		ΔFVC		ΔFVC%	
Parameter	r	p	r	p	r	p	r	p	r	p	r	p	r	p	r	p
ΔCT-lung volume$_{insp}$	0.11	0.58	-0.03	0.89	-0.08	0.70	-0.12	0.58	-0.17	0.42	-0.10	0.64	-0.21	0.31	-0.01	0.97
ΔCT-lung volume$_{exp}$	0.26	0.21	0.33	0.11	-0.02	0.93	-0.29	0.16	0.03	0.87	0.03	0.90	-0.05	0.82	-0.04	0.85
ΔCT-950HU	**0.44**	**0.02**	0.38	0.06	0.14	0.50	0.26	0.21	0.10	0.62	0.09	0.68	0.24	0.23	0.34	0.09
ΔCT-856HU	**0.54**	**<0.01**	0.37	0.06	0.10	0.62	-0.39	0.05	-0.14	0.51	-0.15	0.46	-0.37	0.07	**-0.40**	**0.04**
ΔfGT%	0.14	0.51	0.00	1.00	-0.02	0.93	**-0.46**	**0.02**	-0.23	0.26	-0.21	0.31	**-0.54**	**<0.01**	**-0.61**	**0.01**
ΔCT-vessel volume	-0.29	0.15	0.15	0.45	0.03	0.90	0.03	0.87	0.03	0.87	0.00	0.99	0.12	0.56	0.08	0.70
ΔCT-PA ratio	-0.04	0.86	-0.05	0.79	0.09	0.67	0.07	0.72	0.03	0.87	0.05	0.82	-0.15	0.47	-0.21	0.30
	ΔFEV1/FVC		**ΔMEF25-75%**		**ΔRAWtot**		**ΔGAWtot**		**ΔFRC**		**ΔFRC%**		**ΔRV**		**ΔRV%**	
Parameter	r	p	r	p	r	p	r	p	r	p	r	p	r	p	r	p
ΔCT-lung volume$_{insp}$	0.15	0.46	0.22	0.30	0.25	0.21	-0.18	0.39	0.09	0.68	0.25	0.23	0.18	0.37	0.29	0.15
ΔCT-lung volume$_{exp}$	0.10	0.62	-0.02	0.91	0.20	0.33	-0.30	0.14	0.09	0.68	0.12	0.57	0.02	0.91	0.07	0.75
ΔCT-950HU	-0.15	0.48	0.05	0.83	0.11	0.59	-0.08	0.69	0.00	0.99	0.07	0.73	0.06	0.75	0.12	0.56
ΔCT-856HU	0.24	0.24	-0.02	0.91	0.20	0.32	**-0.50**	**0.01**	0.31	0.12	0.28	0.17	0.30	0.14	0.29	0.14
ΔfGT%	0.35	0.08	0.00	0.99	0.10	0.64	-0.38	0.06	0.22	0.28	0.13	0.53	0.23	0.25	0.17	0.40
ΔCT-vessel volume	-0.09	0.67	-0.05	0.80	-0.25	0.21	0.38	0.05	-0.13	0.53	-0.11	0.61	-0.08	0.71	-0.07	0.72
ΔCT-PA ratio	0.33	0.10	-0.04	0.85	0.06	0.78	-0.20	0.32	-0.16	0.44	-0.21	0.29	-0.10	0.63	-0.12	0.56
	ΔTLC		**ΔTLC%**		**ΔRV/TLC**		**ΔIC**		**ΔIC/TLC**		**ΔTLCO**		**ΔTLCO%**		**ΔKCO**	
Parameter	r	p	r	p	r	p	r	p	r	p	r	p	r	p	r	p
ΔCT-lung volume$_{insp}$	0.15	0.46	0.37	0.07	0.20	0.32	-0.12	0.55	-0.17	0.41	0.17	0.48	0.15	0.53	0.20	0.42
ΔCT-lung volume$_{exp}$	0.13	0.53	0.11	0.60	0.01	0.97	0.08	0.70	-0.00	0.99	0.06	0.82	0.11	0.65	0.31	0.22
ΔCT-950HU	0.30	0.13	0.41	0.04	0.00	0.99	0.29	0.15	0.21	0.31	0.10	0.68	0.17	0.47	0.16	0.50
ΔCT-856HU	0.23	0.27	0.22	0.28	0.36	0.07	-0.09	0.65	-0.23	0.26	-0.15	0.54	-0.08	0.73	0.32	0.18
ΔfGT%	-0.05	0.81	-0.11	0.59	0.33	0.10	-0.25	0.23	-0.30	0.14	-0.22	0.38	-0.20	0.40	0.21	0.40
ΔCT-vessel volume	-0.03	0.90	-0.05	0.80	-0.13	0.54	0.09	0.65	0.07	0.72	0.22	0.36	0.17	0.50	-0.11	0.67
ΔCT-PA ratio	-0.35	0.08	-0.25	0.21	0.02	0.91	-0.08	0.68	0.03	0.87	-0.30	0.21	-0.33	0.16	-0.34	0.15
	ΔKCO%		**ΔpH**		**ΔPCO2**		**ΔPO2**		**ΔCompliance**		**Δ6MWD**					
Parameter	r	p	r	p	r	p	r	p	r	p	r	p				
ΔCT-lung volume$_{insp}$	0.14	0.57	-0.07	0.73	0.17	0.41	-0.18	0.40	-0.07	0.78	-0.26	0.20				

ΔCT-lung volume$_{exp}$	0.26	0.30	-0.23	0.29	0.01	0.96	0.00	1.00	0.35	0.13	-0.25	0.24				
ΔCT-950HU	0.19	0.44	-0.32	0.12	0.14	0.51	-0.13	0.54	-0.13	0.59	0.00	0.98				
ΔCT-856HU	0.37	0.12	-0.07	0.74	-0.02	0.93	0.03	0.89	0.25	0.28	-0.24	0.23				
ΔfGT%	0.24	0.33	0.20	0.33	-0.15	0.46	0.07	0.73	0.32	0.17	-0.17	0.42				
ΔCT-vessel volume	-0.16	0.52	0.10	0.64	-0.24	0.24	0.30	0.14	0.29	0.22	0.22	0.28				
ΔCT-PA ratio	-0.30	0.21	0.07	0.76	-0.14	0.51	0.03	0.89	0.00	0.99	-0.05	0.79				

Appendix B: Table S3.3. Delta correlations: CT indices and clinically relevant parameters – coil cohort.

	ΔBODE Index		ΔmMRC		ΔSGRQtot		ΔBMI		ΔFEV1		ΔFEV1%		ΔFVC		ΔFVC%	
Parameter	R	p	r	p	r	p	r	p	r	p	r	p	r	p	r	p
ΔR5	-0.23	0.46	-0.03	0.93	0.20	0.52	-0.32	0.28	-0.27	0.36	-0.20	0.51	0.21	0.48	0.17	0.57
ΔR20	-0.16	0.61	-0.00	1.00	-0.07	0.83	-0.22	0.46	-0.04	0.89	-0.01	0.97	-0.20	0.50	-0.25	0.40
ΔR5-20	-0.07	0.83	-0.07	0.82	0.21	0.49	-0.09	0.77	-0.15	0.62	-0.10	0.74	0.36	0.23	0.39	0.19
ΔRex5	-0.02	0.95	-0.06	0.85	-0.13	0.68	-0.14	0.65	-0.06	0.85	-0.02	0.95	0.24	0.44	0.18	0.55
ΔX5	0.09	0.78	-0.00	0.99	-0.22	0.47	0.45	0.12	0.31	0.30	0.16	0.60	-0.16	0.59	-0.05	0.87
ΔXex5	0.44	0.15	0.30	0.32	0.27	0.37	0.30	0.32	-0.03	0.93	-0.11	0.72	-0.25	0.40	-0.13	0.66
ΔXin5-Xex5	-0.36	0.24	-0.46	0.11	-0.23	0.45	-0.20	0.51	0.12	0.69	0.17	0.57	0.11	0.72	0.07	0.82
ΔAX	-0.39	0.21	-0.17	0.57	0.00	1.00	-0.38	0.20	-0.17	0.58	-0.10	0.73	0.26	0.39	0.12	0.70
ΔAXex	-0.30	0.34	-0.23	0.46	-0.30	0.32	-0.27	0.37	0.04	0.89	0.01	0.97	0.23	0.46	0.03	0.94
ΔFres total	-0.06	0.86	-0.04	0.91	-0.07	0.83	-0.23	0.46	-0.15	0.62	-0.09	0.78	0.34	0.26	0.15	0.63
ΔFres peripheral	0.34	0.28	0.25	0.40	0.21	0.49	-0.37	0.21	-0.36	0.23	-0.40	0.17	-0.22	0.47	-0.38	0.20
	ΔFEV1/FVC		**ΔMEF25-75%**		**ΔRAWtot**		**ΔGAWtot**		**ΔFRC**		**ΔFRC%**		**ΔRV**		**ΔRV%**	
Parameter	R	p	r	p	r	p	r	p	r	p	r	p	r	p	r	p
ΔR5	-0.33	0.28	-0.10	0.75	-0.16	0.60	0.37	0.21	0.03	0.93	0.09	0.78	-0.19	0.54	-0.22	0.47
ΔR20	0.12	0.70	0.17	0.57	-0.04	0.90	0.30	0.31	-0.15	0.62	-0.05	0.88	0.04	0.91	-0.10	0.74
ΔR5-20	-0.37	0.22	-0.33	0.26	-0.02	0.95	0.06	0.85	0.21	0.49	0.13	0.69	-0.20	0.51	-0.13	0.68
ΔRex5	-0.16	0.60	0.16	0.59	-0.30	0.32	0.36	0.23	-0.22	0.47	0.01	0.97	-0.19	0.53	-0.24	0.42
ΔX5	0.46	0.11	0.22	0.47	-0.42	0.16	-0.07	0.83	-0.34	0.25	-0.24	0.45	0.02	0.96	-0.07	0.82
ΔXex5	0.27	0.37	-0.13	0.67	-0.37	0.22	-0.13	0.67	-0.05	0.87	-0.19	0.56	0.07	0.82	0.01	0.98
ΔXin5-Xex5	-0.11	0.72	0.12	0.68	0.17	0.57	0.29	0.34	0.27	0.38	0.31	0.33	0.17	0.57	0.22	0.47
ΔAX	-0.41	0.16	-0.01	0.99	0.38	0.21	0.12	0.70	0.18	0.57	0.32	0.31	0.00	1.00	0.05	0.86
ΔAXex	-0.20	0.52	0.31	0.31	0.17	0.58	0.18	0.56	-0.25	0.42	0.06	0.85	-0.13	0.67	-0.08	0.79
ΔFres total	-0.43	0.14	0.15	0.62	0.42	0.16	0.15	0.61	-0.10	0.75	0.13	0.70	-0.18	0.57	-0.16	0.60
ΔFres peripheral	-0.32	0.28	-0.22	0.47	0.15	0.61	0.04	0.91	0.10	0.75	0.01	0.97	-0.08	0.79	0.05	0.88
	ΔTLC		**ΔTLC%**		**ΔRV/TLC**		**ΔIC**		**ΔIC/TLC**		**ΔTLCO**		**ΔTLCO%**		**ΔKCO**	
Parameter	R	p	r	p	r	p	r	p	r	p	r	p	r	p	r	p
ΔR5	0.00	0.99	0.04	0.89	-0.49	0.09	-0.44	0.13	-0.22	0.46	0.03	0.92	0.05	0.88	-0.22	0.49
ΔR20	**-0.57**	**0.04**	-0.35	0.24	-0.06	0.84	-0.47	0.11	-0.18	0.55	-0.17	0.59	-0.12	0.71	-0.10	0.75

ΔR5-20	**0.64**	**0.02**	0.48	0.10	-0.36	0.23	-0.01	0.99	-0.01	0.97	0.39	0.21	0.32	0.32	-0.02	0.94
ΔRex5	-0.09	0.77	0.06	0.85	-0.46	0.12	-0.41	0.17	-0.19	0.54	0.15	0.63	0.16	0.62	-0.06	0.85
ΔX5	-0.32	0.29	-0.20	0.50	0.11	0.71	0.36	0.23	0.35	0.24	-0.45	0.14	-0.41	0.18	-0.16	0.61
ΔXex5	-0.33	0.27	-0.44	0.13	0.17	0.57	0.49	0.09	0.48	0.10	-0.41	0.18	-0.41	0.19	-0.03	0.93
ΔXin5-Xex5	**0.69**	**0.01**	**0.64**	**0.02**	-0.04	0.90	-0.42	0.15	-0.47	0.10	0.43	0.16	0.40	0.20	0.01	0.98
ΔAX	0.39	0.19	0.42	0.16	-0.21	0.49	-0.50	0.09	**-0.57**	**0.04**	0.32	0.31	0.31	0.32	-0.05	0.88
ΔAXex	0.03	0.92	0.28	0.36	-0.25	0.42	-0.43	0.14	-0.43	0.14	0.22	0.50	0.23	0.47	-0.07	0.82
ΔFres total	0.07	0.82	0.22	0.47	-0.35	0.24	-0.39	0.19	-0.41	0.17	0.45	0.15	0.44	0.15	0.11	0.73
ΔFres peripheral	-0.09	0.76	-0.01	0.98	0.09	0.78	-0.08	0.79	0.00	1.00	0.09	0.78	0.03	0.92	-0.10	0.75
	ΔKCO%		**ΔpH**		**ΔPCO$_2$**		**ΔPO$_2$**		**Δ6MWD**		**ΔCT-VOL$_{INSP}$**		**ΔCT-VOL$_{EXP}$**		**ΔCT-950HU**	
Parameter	R	p	r	p	r	p	r	p	r	p						
ΔR5	-0.24	0.44	-0.07	0.82	0.40	0.19	-0.26	0.42	-0.09	0.77	-0.39	0.23	-0.29	0.45	-0.26	0.44
ΔR20	-0.11	0.73	0.47	0.13	0.38	0.22	-0.19	0.55	-0.01	0.98	-0.61	0.05	-0.53	0.15	-0.34	0.30
ΔR5-20	-0.04	0.91	-0.59	0.05	0.05	0.89	-0.11	0.73	0.00	1.00	0.26	0.43	-0.08	0.85	0.11	0.75
ΔRex5	-0.08	0.79	-0.02	0.96	0.11	0.75	-0.18	0.57	-0.17	0.59	-0.14	0.68	-0.17	0.67	-0.16	0.64
ΔX5	-0.14	0.65	0.39	0.20	**-0.76**	**0.01**	-0.11	0.74	0.04	0.90	0.08	0.81	0.18	0.63	-0.04	0.92
ΔXex5	0.01	0.98	0.25	0.43	**-0.60**	**0.04**	-0.23	0.47	-0.23	0.47	0.15	0.66	0.54	0.14	0.14	0.68
ΔXin5-Xex5	-0.02	0.94	-0.57	0.06	0.39	0.21	0.18	0.57	0.27	0.39	0.17	0.61	-0.42	0.27	-0.26	0.44
ΔAX	-0.08	0.80	-0.32	0.31	**0.69**	**0.02**	0.08	0.80	0.23	0.47	-0.13	0.71	-0.35	0.36	-0.10	0.77
ΔAXex	-0.11	0.74	-0.01	0.98	0.50	0.10	0.20	0.53	0.21	0.51	-0.31	0.36	-0.52	0.16	-0.28	0.40
ΔFres total	0.09	0.77	-0.26	0.42	**0.85**	**<0.01**	0.10	0.75	-0.05	0.89	-0.03	0.95	0.07	0.88	-0.09	0.80
ΔFres peripheral	-0.09	0.77	-0.04	0.90	0.51	0.09	0.25	0.43	0.01	0.97	-0.45	0.16	-0.33	0.39	-0.24	0.48
	ΔCT-856HU		**ΔfGT%**		**ΔCT-VES VOL**		**ΔCT-PA ratio**									
ΔR5	-0.36	0.34	-0.28	0.45	0.00	1.00	0.22	0.51								
ΔR20	-0.36	0.34	-0.20	0.61	0.22	0.52	-0.02	0.96								
ΔR5-20	-0.29	0.44	-0.23	0.54	-0.49	0.13	0.06	0.86								
ΔRex5	-0.39	0.29	-0.50	0.17	0.39	0.23	0.51	0.11								
ΔX5	0.06	0.88	0.10	0.80	**0.77**	**0.01**	0.42	0.19								
ΔXex5	0.31	0.41	0.24	0.52	0.48	0.14	0.04	0.92								
ΔXin5-Xex5	-0.60	0.09	-0.51	0.16	-0.40	0.22	0.15	0.65								

ΔAX	-0.32	0.40	-0.28	0.45	-0.45	0.17	0.00	0.99								
ΔAXex	-0.33	0.39	-0.28	0.45	0.10	0.78	0.38	0.25								
ΔFres total	-0.18	0.63	-0.59	0.10	-0.28	0.40	0.20	0.56								
ΔFres peripheral	-0.12	0.77	-0.09	0.82	-0.20	0.55	-0.39	0.23								

Appendix B: Table S4.1. Delta correlations: IOS indices and clinically relevant parameters – surgery cohort.

	ΔBODE Index		ΔmMRC		ΔSGRQtot		ΔBMI		ΔFEV1		ΔFEV1%		ΔFVC		ΔFVC%	
Parameter	r	p	r	p	r	p	r	p	r	p	r	p	r	p	r	p
ΔR5	0.08	0.70	0.15	0.45	0.20	0.31	-0.37	0.06	0.09	0.66	0.20	0.31	0.08	0.71	0.12	0.54
ΔR20	0.07	0.75	0.15	0.43	0.23	0.25	0.14	0.49	0.12	0.56	0.13	0.51	0.35	0.07	0.32	0.10
ΔR5-20	0.02	0.92	0.03	0.87	0.12	0.55	**-0.50**	**0.01**	0.11	0.58	0.22	0.26	0.04	0.86	0.10	0.64
ΔRex5	0.08	0.71	0.24	0.21	0.17	0.38	-0.33	0.09	0.03	0.88	0.07	0.73	0.14	0.50	0.15	0.45
ΔX5	-0.03	0.88	-0.03	0.88	-0.24	0.22	0.19	0.34	0.04	0.83	-0.06	0.76	0.13	0.53	0.11	0.59
ΔXex5	-0.36	0.07	-0.15	0.44	-0.38	0.05	0.21	0.28	-0.02	0.94	-0.10	0.60	0.08	0.70	0.06	0.76
ΔXin5-Xex5	0.29	0.14	0.15	0.46	0.27	0.17	-0.07	0.73	0.15	0.45	0.21	0.29	0.10	0.61	0.14	0.50
ΔAX	0.07	0.75	0.06	0.77	0.24	0.21	-0.24	0.22	0.12	0.56	0.22	0.26	0.00	0.99	0.02	0.93
ΔAXex	0.27	0.18	0.23	0.24	0.22	0.25	-0.28	0.15	0.04	0.86	0.13	0.51	-0.08	0.69	-0.07	0.72
ΔFres total	0.09	0.65	0.25	0.19	0.22	0.26	-0.14	0.47	0.01	0.94	0.10	0.61	-0.05	0.79	-0.03	0.88
ΔFres peripheral	0.24	0.22	0.08	0.69	0.15	0.46	-0.01	0.95	-0.13	0.50	-0.04	0.84	-0.14	0.50	-0.10	0.62
	ΔFEV1/FVC		**ΔMEF25-75%**		**ΔRAWtot**		**ΔGAWtot**		**ΔFRC**		**ΔFRC%**		**ΔRV**		**ΔRV%**	
Parameter	r	p	r	p	r	p	r	p	r	p	r	p	r	p	r	p
ΔR5	0.13	0.51	**-0.63**	**<0.01**	0.11	0.59	-0.06	0.78	0.25	0.20	0.14	0.48	0.11	0.59	0.01	0.98
ΔR20	-0.01	0.97	-0.21	0.38	0.18	0.38	-0.09	0.67	0.37	0.05	0.27	0.16	0.13	0.50	0.09	0.65
ΔR5-20	0.13	0.53	**-0.60**	**0.01**	0.02	0.93	0.01	0.96	0.07	0.72	-0.04	0.82	-0.02	0.92	-0.12	0.54
ΔRex5	-0.08	0.69	**-0.47**	**0.04**	0.13	0.52	-0.05	0.80	0.14	0.48	0.10	0.62	-0.04	0.82	-0.10	0.61
ΔX5	-0.09	0.64	**0.58**	**0.01**	-0.08	0.68	-0.05	0.81	-0.06	0.75	0.10	0.63	-0.20	0.30	-0.09	0.65
ΔXex5	-0.12	0.54	**0.63**	**<0.01**	-0.22	0.28	0.17	0.39	-0.14	0.48	-0.05	0.81	-0.25	0.19	-0.17	0.38
ΔXin5-Xex5	0.04	0.84	**-0.48**	**0.04**	0.26	0.18	-0.23	0.25	0.04	0.82	-0.06	0.75	0.10	0.61	0.02	0.92
ΔAX	0.18	0.37	**-0.57**	**0.01**	0.19	0.33	-0.05	0.80	0.13	0.50	-0.00	1.00	0.18	0.36	0.08	0.68
ΔAXex	0.16	0.43	**-0.56**	**0.01**	0.22	0.27	-0.15	0.45	0.14	0.47	0.10	0.63	0.14	0.47	0.09	0.66
ΔFres total	0.11	0.59	-0.41	0.08	**0.39**	**0.04**	-0.16	0.43	0.10	0.61	0.02	0.91	0.14	0.49	0.08	0.69
ΔFres peripheral	0.07	0.74	**-0.48**	**0.04**	0.04	0.83	0.05	0.82	0.07	0.72	-0.02	0.92	0.27	0.17	0.20	0.31
	ΔTLC		**ΔTLC%**		**ΔRV/TLC**		**ΔIC**		**ΔIC/TLC**		**ΔTLCO**		**ΔTLCO%**		**ΔKCO**	
Parameter	r	p	r	p	r	p	r	p	r	p	r	p	r	p	r	p
ΔR5	0.12	0.55	0.05	0.79	0.03	0.88	-0.09	0.68	0.01	0.96	-0.20	0.33	-0.21	0.31	-0.16	0.44
ΔR20	**0.41**	**0.03**	**0.39**	**0.04**	-0.05	0.80	0.32	0.11	0.23	0.27	0.07	0.73	0.11	0.61	-0.26	0.19

ΔR5-20	-0.04	0.82	-0.12	0.55	-0.04	0.85	-0.19	0.36	-0.03	0.90	-0.21	0.29	-0.23	0.25	-0.10	0.63
ΔRex5	0.03	0.89	-0.02	0.93	-0.10	0.61	-0.06	0.78	0.03	0.89	-0.14	0.50	-0.11	0.61	-0.31	0.12
ΔX5	0.05	0.82	0.18	0.37	-0.12	0.55	0.13	0.53	0.01	0.95	0.15	0.46	0.20	0.33	0.10	0.64
ΔXex5	0.01	0.96	0.08	0.69	-0.25	0.19	0.30	0.14	0.18	0.37	0.26	0.19	0.29	0.15	0.08	0.69
ΔXin5-Xex5	-0.08	0.69	-0.15	0.46	0.08	0.70	-0.18	0.39	-0.06	0.75	-0.22	0.28	-0.22	0.27	-0.16	0.42
ΔAX	-0.01	0.97	-0.08	0.68	0.07	0.74	-0.08	0.71	0.05	0.79	-0.18	0.38	-0.20	0.32	-0.15	0.47
ΔAXex	-0.05	0.78	-0.11	0.56	0.13	0.51	-0.30	0.14	-0.15	0.47	-0.28	0.17	-0.31	0.13	-0.21	0.30
ΔFres total	-0.07	0.72	-0.14	0.47	0.03	0.89	-0.08	0.69	0.03	0.88	-0.19	0.36	-0.19	0.36	-0.21	0.30
ΔFres peripheral	0.08	0.67	-0.01	0.98	0.26	0.17	-0.14	0.49	-0.11	0.58	-0.12	0.57	-0.15	0.48	0.07	0.73
	ΔKCO%		**ΔpH**		**ΔPCO_2**		**ΔPO_2**		**Δ6MWD**		**ΔCompliance**		**$\Delta CT\text{-}VOL_{INSP}$**		**$\Delta CT\text{-}VOL_{EXP}$**	
Parameter	r	p	r	p	r	p	r	p	r	p	r	p	r	p	r	p
ΔR5	-0.31	0.12	0.02	0.91	0.04	0.86	-0.23	0.28	-0.21	0.29	0.05	0.83	0.27	0.17	0.19	0.48
ΔR20	-0.13	0.53	0.05	0.82	-0.02	0.92	-0.07	0.75	-0.28	0.15	0.33	0.16	0.22	0.26	0.21	0.43
ΔR5-20	-0.26	0.19	-0.01	0.98	0.01	0.98	-0.22	0.30	-0.07	0.72	-0.13	0.60	0.23	0.25	0.10	0.71
ΔRex5	-0.32	0.11	-0.08	0.70	0.19	0.37	-0.13	0.53	-0.12	0.56	0.13	0.58	0.11	0.59	0.20	0.44
ΔX5	0.27	0.19	0.10	0.63	0.02	0.92	0.10	0.65	0.13	0.52	0.38	0.10	-0.29	0.15	0.18	0.51
ΔXex5	0.22	0.27	0.05	0.80	0.02	0.93	-0.06	0.78	0.25	0.19	0.31	0.19	-0.16	0.42	0.04	0.90
ΔXin5-Xex5	-0.28	0.16	-0.17	0.43	0.15	0.48	-0.09	0.66	-0.32	0.10	-0.35	0.14	0.18	0.36	0.04	0.87
ΔAX	-0.33	0.10	-0.10	0.62	0.05	0.81	-0.18	0.39	-0.15	0.44	-0.27	0.24	0.23	0.25	0.02	0.95
ΔAXex	-0.37	0.07	-0.11	0.61	0.13	0.54	-0.18	0.40	-0.27	0.16	-0.23	0.34	0.15	0.47	0.13	0.64
ΔFres total	**-0.40**	**0.04**	-0.11	0.60	0.16	0.44	-0.16	0.46	-0.07	0.74	-0.19	0.43	0.31	0.12	0.02	0.95
ΔFres peripheral	-0.09	0.67	0.10	0.64	-0.20	0.33	0.13	0.55	-0.13	0.52	-0.32	0.17	0.19	0.33	-0.29	0.27
	ΔCT-950HU		**ΔCT-856HU**		**ΔfGT%**		**ΔCT-VES VOL**		**ΔCT-PA ratio**							
ΔR5	-0.11	0.59	0.01	0.99	-0.05	0.85	**-0.48**	**0.01**	0.09	0.65						
ΔR20	0.21	0.28	-0.14	0.60	0.23	0.38	**-0.56**	**<0.01**	-0.04	0.85						
ΔR5-20	-0.18	0.38	-0.05	0.84	-0.09	0.74	-0.31	0.12	0.12	0.55						
ΔRex5	-0.09	0.67	0.00	0.99	-0.04	0.90	-0.25	0.22	-0.06	0.78						
ΔX5	-0.19	0.35	0.27	0.30	-0.03	0.90	0.17	0.42	**-0.47**	**0.01**						
ΔXex5	0.05	0.80	-0.01	0.97	0.20	0.46	0.32	0.11	**-0.43**	**0.02**						
ΔXin5-Xex5	-0.05	0.79	-0.22	0.41	0.01	0.96	-0.29	0.15	0.31	0.12						

ΔAX	-0.07	0.74	-0.22	0.41	0.06	0.83	-0.38	0.06	**0.47**	**0.01**						
ΔAXex	-0.24	0.22	-0.07	0.80	-0.09	0.73	-0.36	0.07	0.30	0.12						
ΔFres total	0.00	0.99	-0.41	0.11	0.22	0.41	-0.29	0.15	**0.53**	**<0.01**						
ΔFres peripheral	0.11	0.59	-0.15	0.59	-0.13	0.63	-0.27	0.19	0.33	0.10						

Appendix B: Table S4.2. Delta correlations: IOS indices and clinically relevant parameters – valve cohort.

	ΔBODE Index		ΔmMRC		ΔSGRQtot		ΔBMI		ΔFEV1		ΔFEV1%		ΔFVC		ΔFVC%	
Parameter	r	p	r	p	r	p	r	p	r	p	r	p	r	p	r	p
ΔR5	0.17	0.41	-0.08	0.70	**0.46**	**0.02**	-0.05	0.82	**-0.44**	**0.03**	-0.38	0.05	-0.39	0.05	-0.35	0.08
ΔR20	-0.55	0.33	-0.62	0.13	-0.26	0.46	-0.29	0.54	-0.52	0.43	-0.49	0.59	-0.51	0.49	-0.51	0.48
ΔR5-20	0.36	0.07	0.14	0.51	**0.53**	**<0.01**	-0.05	0.80	**-0.44**	**0.02**	**-0.42**	**0.03**	-0.36	0.07	-0.34	0.09
ΔRex5	0.08	0.71	-0.06	0.76	0.33	0.10	0.13	0.54	**-0.40**	**0.04**	**-0.40**	**0.04**	-0.21	0.31	-0.26	0.21
ΔX5	-0.23	0.25	0.00	0.99	-0.28	0.17	**0.49**	**0.01**	**0.46**	**0.02**	**0.44**	**0.02**	**0.47**	**0.02**	**0.44**	**0.03**
ΔXex5	-0.29	0.15	-0.06	0.76	-0.28	0.16	0.33	0.10	**0.40**	**0.04**	0.38	0.06	0.31	0.13	0.24	0.24
ΔXin5-Xex5	0.29	0.15	0.11	0.59	0.27	0.19	-0.23	0.26	-0.35	0.08	-0.34	0.09	-0.20	0.33	-0.16	0.44
ΔAX	0.29	0.16	-0.04	0.85	**0.41**	**0.04**	-0.28	0.17	**-0.50**	**0.01**	**-0.46**	**0.02**	**-0.48**	**0.01**	**-0.42**	**0.03**
ΔAXex	0.27	0.18	-0.00	0.98	0.29	0.15	-0.20	0.33	**-0.41**	**0.04**	**-0.41**	**0.04**	-0.30	0.13	-0.28	0.16
ΔFres total	0.26	0.19	-0.07	0.74	0.19	0.36	-0.08	0.71	**-0.43**	**0.03**	**-0.43**	**0.03**	-0.37	0.07	-0.32	0.11
ΔFres peripheral	0.18	0.38	-0.03	0.89	0.33	0.10	-0.17	0.41	**-0.59**	**<0.01**	**-0.56**	**<0.01**	-0.38	0.05	-0.29	0.15
	ΔFEV1/FVC		**ΔMEF25-75%**		**ΔRAWtot**		**ΔGAWtot**		**ΔFRC**		**ΔFRC%**		**ΔRV**		**ΔRV%**	
Parameter	r	p	r	p	r	p	r	p	r	p	r	p	r	p	r	p
ΔR5	-0.15	0.47	-0.13	0.52	0.17	0.40	-0.18	0.37	0.32	0.11	0.28	0.17	0.29	0.15	0.29	0.16
ΔR20	-0.43	0.83	-0.44	0.85	-0.35	0.81	-0.31	0.63	-0.40	1.00	-0.08	0.60	0.05	0.80	-0.01	0.95
ΔR5-20	-0.22	0.29	-0.15	0.49	0.22	0.28	-0.24	0.23	**0.41**	**0.04**	**0.41**	**0.04**	0.32	0.11	0.35	0.08
ΔRex5	-0.28	0.16	-0.23	0.26	0.07	0.73	-0.09	0.66	0.38	0.06	0.27	0.18	0.35	0.08	0.31	0.12
ΔX5	0.11	0.61	0.14	0.51	-0.29	0.15	0.31	0.13	-0.31	0.12	-0.32	0.12	-0.24	0.23	-0.26	0.19
ΔXex5	0.18	0.38	0.06	0.79	-0.32	0.11	0.29	0.15	-0.40	0.05	-0.39	0.05	-0.33	0.10	-0.35	0.08
ΔXin5-Xex5	-0.22	0.28	-0.05	0.80	0.28	016	-0.26	0.20	0.38	0.06	0.36	0.07	0.31	0.12	0.33	0.10
ΔAX	-0.12	0.55	-0.08	0.71	0.24	0.25	-0.28	0.17	0.37	0.06	0.36	0.07	0.30	0.14	0.31	0.12
ΔAXex	-0.12	0.55	-0.02	0.92	0.25	0.21	-0.28	0.16	0.39	0.05	0.36	0.07	0.32	0.11	0.33	0.10
ΔFres total	-0.17	0.40	-0.07	0.73	0.04	0.86	-0.14	0.48	0.31	0.12	0.27	0.18	0.29	0.15	0.29	0.16
ΔFres peripheral	**-0.40**	**0.04**	-0.10	0.63	0.1	0.37	-0.13	0.52	0.32	0.12	0.36	0.07	0.31	0.13	0.35	0.08
	ΔTLC		**ΔTLC%**		**ΔRV/TLC**		**ΔIC**		**ΔIC/TLC**		**ΔTLCO**		**ΔTLCO%**		**ΔKCO**	
Parameter	r	p	r	p	r	p	r	p	r	p	r	p	r	p	r	p
ΔR5	0.01	0.97	0.00	0.99	**0.44**	**0.02**	**-0.48**	**0.01**	**-0.45**	**0.02**	**-0.54**	**0.02**	**-0.52**	**0.02**	-0.22	0.37
ΔR20	-0.21	0.31	-0.27	0.19	0.13	0.54	-0.29	0.16	-0.15	0.48	-0.15	0.54	-0.14	0.55	-0.09	0.72

ΔR5-20	0.14	0.50	0.16	0.42	**0.47**	**0.02**	**-0.52**	**0.01**	**-0.52**	**0.01**	**-0.58**	**0.01**	**-0.54**	**0.02**	-0.27	0.27
ΔRex5	0.15	0.47	0.06	0.76	**0.42**	**0.03**	-0.38	0.06	-0.39	0.05	**-0.49**	**0.03**	**-0.49**	**0.03**	-0.21	0.38
ΔX5	-0.02	0.91	-0.02	0.91	**-0.40**	**0.04**	**0.45**	**0.02**	**0.49**	**0.01**	**0.61**	**0.01**	**0.62**	**<0.01**	00.27	0.26
ΔXex5	-0.12	0.57	-0.11	0.58	**-0.43**	**0.03**	**0.41**	**0.04**	**0.48**	**0.01**	0.43	0.07	0.41	0.08	0.20	0.42
ΔXin5-Xex5	0.12	0.56	0.11	0.61	0.39	0.05	-0.35	0.08	**-0.42**	**0.03**	-0.41	0.08	-0.39	0.10	-0.27	0.27
ΔAX	0.02	0.94	0.04	0.84	**0.47**	**0.02**	**-0.55**	**<0.01**	**-0.55**	**<0.01**	**-0.56**	**0.01**	**-0.55**	**0.02**	-0.17	0.49
ΔAXex	0.08	0.71	0.09	0.65	**0.45**	**0.03**	**-0.49**	**0.01**	**-0.51**	**0.01**	-0.42	0.07	-0.42	0.07	-0.20	0.42
ΔFres total	0.04	0.84	0.05	0.82	**0.41**	**0.04**	-0.36	0.07	-0.40	0.05	**-0.50**	**0.03**	**-0.51**	**0.03**	-0.23	0.34
ΔFres peripheral	0.09	0.66	0.15	0.45	**0.41**	**0.04**	-0.36	0.07	**-0.42**	**0.03**	**-0.66**	**<0.01**	**-0.67**	**<0.01**	-0.43	0.06
	ΔKCO%		**ΔpH**		**ΔPCO$_2$**		**ΔPO$_2$**		**Δ6MWD**		**ΔCompliance**		**ΔCT-VOL$_{INSP}$**		**ΔCT-VOL$_{EXP}$**	
Parameter	r	p	r	p	r	p	r	p	r	p						
ΔR5	-0.17	0.49	0.10	0.63	-0.18	0.39	0.13	0.53	**-0.53**	**<0.01**	-0.22	0.35	-0.00	0.99	0.05	0.80
ΔR20	-0.06	0.81	0.38	0.06	**-0.44**	**0.03**	0.25	0.22	-0.08	0.70	-0.13	0.57	-0.23	0.26	-0.09	0.68
ΔR5-20	-0.21	0.38	-0.08	0.70	-0.00	0.98	0.04	0.83	**-0.62**	**0.01**	-0.19	0.42	0.18	0.38	0.11	0.62
ΔRex5	-0.13	0.59	-0.00	0.99	0.03	0.88	0.09	0.67	-0.34	0.09	0.01	0.97	-0.10	0.62	-0.02	0.91
ΔX5	0.26	0.28	-0.01	0.95	0.00	1.00	0.05	0.81	**0.50**	**0.01**	0.24	0.30	-0.17	0.41	-0.16	0.44
ΔXex5	0.16	0.51	-0.03	0.88	-0.10	0.64	0.01	0.94	**0.58**	**<0.01**	0.16	0.50	-0.25	0.23	-0.10	0.62
ΔXin5-Xex5	-0.21	0.39	-0.01	0.95	0.14	0.52	-0.02	0.94	**-0.54**	**<0.01**	-0.13	0.60	0.17	0.41	0.06	0.78
ΔAX	-0.11	0.65	0.03	0.89	-0.08	0.72	0.01	0.97	**-0.57**	**<0.01**	-0.22	0.36	0.16	0.43	0.15	0.46
ΔAXex	-0.11	0.66	-0.04	0.86	0.14	0.50	-0.10	0.65	**-0.45**	**0.02**	-0.13	0.57	0.27	0.19	-0.02	0.92
ΔFres total	-0.14	0.58	-0.10	0.62	0.04	0.86	-0.18	0.39	**-0.47**	**0.02**	-0.25	0.28	0.12	0.56	0.01	0.96
ΔFres peripheral	-0.42	0.08	-0.13	0.55	0.04	0.85	-0.06	0.77	**-0.53**	**0.01**	-0.20	0.41	0.18	0.37	0.04	0.83
	ΔCT-950HU		**ΔCT-856HU**		**ΔfGT%**		**ΔCT-VES VOL**		**ΔCT-PA ratio**							
ΔR5	-0.23	0.26	0.14	0.50	0.50	0.05	0.03	0.87	0.14	0.49						
ΔR20	-0.29	0.15	-0.15	0.46	0.24	0.36	0.13	0.54	0.06	0.78						
ΔR5-20	0.00	1.00	0.22	0.29	0.31	0.24	0.01	0.97	0.04	0.83						
ΔRex5	-0.28	0.16	-0.01	0.97	0.42	0.11	0.08	0.70	0.18	0.38						
ΔX5	0.15	0.47	-0.28	0.17	**-0.60**	**0.02**	0.05	0.80	0.03	0.87						
ΔXex5	0.04	0.86	-0.18	0.37	-0.44	0.09	0.06	0.77	0.04	0.86						
ΔXin5-Xex5	-0.03	0.88	0.13	0.52	0.36	0.18	-0.04	0.86	0.04	0.84						

ΔAX	-0.12	0.56	0.31	0.12	**0.58**	**0.02**	-0.05	0.82	0.09	0.66						
ΔAXex	-0.02	0.91	0.16	0.44	0.40	0.12	-0.07	0.73	0.16	0.44						
ΔFres total	-0.17	0.41	0.21	0.31	**0.64**	**0.01**	-0.02	0.92	0.24	0.23						
ΔFres peripheral	-0.06	0.78	0.05	0.81	0.18	0.51	-0.07	0.72	-0.10	0.63						

Appendix B: Table S4.3. Delta correlations: IOS indices and clinically relevant parameters – coil cohort.

REFERENCES

1. *Global Strategy for the Diagnosis, Management and Prevention of Chronic Obstructive Pulmonary Disease 2019 Report*. 2019; Available from: https://goldcopd.org/wp-content/uploads/2018/11/GOLD-2019-v1.7-FINAL-14Nov2018-WMS.pdf.
2. Thurlbeck, W.M. and N.L. Muller, *Emphysema: definition, imaging, and quantification.* AJR Am J Roentgenol, 1994. **163**(5): p. 1017-25.
3. Coxson, H.O., *Computed tomography and monitoring of emphysema.* European Respiratory Journal, 2007. **29**(6): p. 1075-1077.
4. Gagnon, P., et al., *Pathogenesis of hyperinflation in chronic obstructive pulmonary disease.* Int J Chron Obstruct Pulmon Dis, 2014. **9**: p. 187-201.
5. Kim, V. and G.J. Criner, *Chronic bronchitis and chronic obstructive pulmonary disease.* Am J Respir Crit Care Med, 2013. **187**(3): p. 228-37.
6. Bonet, T., *Sepulchretum sive anatonia pructica ex Cadaveribus Morbo denatis, proponens Histoa's Observations omnium pené humani corporis affectuum, ipsarcomoue Causas recorditas revelans. Geneva.* . 1679.
7. Morgagni, G.B., *The seats and causes of disease. Investigated by anatomy; in fi ve books, containing a great variety of dissections, with remarks. Translated by Alexander B, Miller A, Caldwell T. London: Johnson and Payne.* 1769.
8. Ruysch, F., *Observationes anatomico-chirurgicae. Amsterdam.* Vol. 1. 1671.
9. Baillie, M., *The Morbid Anatomy of Some of the Most Important Parts of the Human Body. London: W Bulmer.* 1803.
10. McHenry, L.C., *Dr. Samuel Johnson's emphysema.* Arch Intern Med, 1967. **119**(1): p. 98-105.
11. Badham, C., *An Essay on Bronchitis: With a Supplement Containing Remarks on Simple Pulmonary Abscess, Etc. Callow.* 1814.
12. Laennec, R.T.H., Forbes, J., *A treatise on the diseases of the chest and on mediate auscultation : London : Thomas & George Underwood* 1829.
13. Gough, J., *The pathological diagnosis of emphysema.* Proceedings of the Royal Society of Medicine, 1952. **45**(9): p. 576-577.
14. McLean, K.H., *The pathology of acute bronchiolitis; a study of its evolution. I. The exudative phase.* Australas Ann Med, 1956. **5**(4): p. 254-67.
15. McLean, K.H., *The pathology of acute bronchiolitis; a study of its evolution. II. The repair phase.* Australas Ann Med, 1957. **6**(1): p. 29-43; concl.
16. McLean, K.H., *The histology of generalized pulmonary emphysema. I. The genesis of the early centrolobular lesion: focal emphysema.* Australas Ann Med, 1957. **6**(2): p. 124-40.
17. Mc, L.K., *The significance of pulmonary vascular changes in emphysema.* Australas Ann Med, 1958. **7**(1): p. 69-84.
18. Weibel, E.R., *Principles and Methods of Morphometry*, in *Morphometry of the Human Lung*. 1963, Springer Berlin Heidelberg: Berlin, Heidelberg. p. 9-39.
19. Macklem, P.T. and J. Mead, *Resistance of central and peripheral airways measured by a retrograde catheter.* J Appl Physiol, 1967. **22**(3): p. 395-401.
20. Hogg, J.C., P.T. Macklem, and W.M. Thurlbeck, *Site and nature of airway obstruction in chronic obstructive lung disease.* N Engl J Med, 1968. **278**(25): p. 1355-60.
21. Hogg, J.C., et al., *Age as a factor in the distribution of lower-airway conductance and in the pathologic anatomy of obstructive lung disease.* N Engl J Med, 1970. **282**(23): p. 1283-7.
22. Levine, G., et al., *Gas exchange abnormalities in mild bronchitis and asymptomatic asthma.* N Engl J Med, 1970. **282**(23): p. 1277-82.
23. Mead, J., *The Lung's Quiet Zone.* New England Journal of Medicine, 1970. **282**(23): p. 1318-1319.

24. Buist, A.S., et al., *The Burden of Obstructive Lung Disease Initiative (BOLD): rationale and design.* Copd, 2005. **2**(2): p. 277-83.
25. Adeloye, D., et al., *Global and regional estimates of COPD prevalence: Systematic review and meta-analysis.* J Glob Health, 2015. **5**(2): p. 020415.
26. *Global, regional, and national age-sex specific all-cause and cause-specific mortality for 240 causes of death, 1990-2013: a systematic analysis for the Global Burden of Disease Study 2013.* Lancet, 2015. **385**(9963): p. 117-71.
27. Lopez, A.D., et al., *Chronic obstructive pulmonary disease: current burden and future projections.* Eur Respir J, 2006. **27**(2): p. 397-412.
28. Mathers, C.D. and D. Loncar, *Projections of global mortality and burden of disease from 2002 to 2030.* PLoS Med, 2006. **3**(11): p. e442.
29. WHO. *Projections of mortality and causes of death, 2016 to 2060 (accessed 10th March 2019)*. Available from: https://www.who.int/healthinfo/global_burden_disease/projections/en/.
30. Divo, M.J., et al., *Chronic Obstructive Pulmonary Disease (COPD) as a disease of early aging: Evidence from the EpiChron Cohort.* PLoS One, 2018. **13**(2): p. e0193143.
31. Chen, W., et al., *Risk of cardiovascular comorbidity in patients with chronic obstructive pulmonary disease: a systematic review and meta-analysis.* Lancet Respir Med, 2015. **3**(8): p. 631-9.
32. Mannino, D.M., et al., *Economic Burden of COPD in the Presence of Comorbidities.* Chest, 2015. **148**(1): p. 138-150.
33. Lozano, R., et al., *Global and regional mortality from 235 causes of death for 20 age groups in 1990 and 2010: a systematic analysis for the Global Burden of Disease Study 2010.* Lancet, 2012. **380**(9859): p. 2095-128.
34. Sin, D.D., et al., *The impact of chronic obstructive pulmonary disease on work loss in the United States.* Am J Respir Crit Care Med, 2002. **165**(5): p. 704-7.
35. DiBonaventura, M., et al., *The impact of COPD on quality of life, productivity loss, and resource use among the elderly United States workforce.* Copd, 2012. **9**(1): p. 46-57.
36. Murray, C.J. and A.D. Lopez, *Alternative projections of mortality and disability by cause 1990-2020: Global Burden of Disease Study.* Lancet, 1997. **349**(9064): p. 1498-504.
37. Murray, C.J., et al., *Global, regional, and national disability-adjusted life years (DALYs) for 306 diseases and injuries and healthy life expectancy (HALE) for 188 countries, 1990-2013: quantifying the epidemiological transition.* Lancet, 2015. **386**(10009): p. 2145-91.
38. Fletcher, C., Peto, R., Tinker C., Speizer F.E., *The natural history of chronic bronchitis and emphysema: OUP.* 1976.
39. Eisner, M.D., et al., *An official American Thoracic Society public policy statement: Novel risk factors and the global burden of chronic obstructive pulmonary disease.* Am J Respir Crit Care Med, 2010. **182**(5): p. 693-718.
40. Lundback, B., et al., *Not 15 but 50% of smokers develop COPD?--Report from the Obstructive Lung Disease in Northern Sweden Studies.* Respir Med, 2003. **97**(2): p. 115-22.
41. Løkke, A., et al., *Developing COPD: a 25 year follow up study of the general population.* Thorax, 2006. **61**(11): p. 935.
42. Lundback, B., et al., *A 20-year follow-up of a population study-based COPD cohort-report from the obstructive lung disease in Northern Sweden studies.* Copd, 2009. **6**(4): p. 263-71.
43. Vestbo, J. and P. Lange, *Fletcher and Peto 40 Years On. A Tribute and Reflection.* American Journal of Respiratory and Critical Care Medicine, 2017. **195**(11): p. 1420-1422.
44. Agustí, A. and J.C. Hogg, *Update on the Pathogenesis of Chronic Obstructive Pulmonary Disease.* New England Journal of Medicine, 2019. **381**(13): p. 1248-1256.
45. Hunninghake, G.M., et al., *MMP12, lung function, and COPD in high-risk populations.* N Engl J Med, 2009. **361**(27): p. 2599-608.

46. Ding, Z., et al., *Association between glutathione S-transferase gene M1 and T1 polymorphisms and chronic obstructive pulmonary disease risk: A meta-analysis.* Clin Genet, 2019. **95**(1): p. 53-62.
47. Cho, M.H., et al., *Risk loci for chronic obstructive pulmonary disease: a genome-wide association study and meta-analysis.* Lancet Respir Med, 2014. **2**(3): p. 214-25.
48. Mercado, N., K. Ito, and P.J. Barnes, *Accelerated ageing of the lung in COPD: new concepts.* Thorax, 2015. **70**(5): p. 482-9.
49. Silverman, E.K., et al., *Gender-related differences in severe, early-onset chronic obstructive pulmonary disease.* Am J Respir Crit Care Med, 2000. **162**(6): p. 2152-8.
50. Martinez, F.J., et al., *Sex differences in severe pulmonary emphysema.* Am J Respir Crit Care Med, 2007. **176**(3): p. 243-52.
51. Lawlor, D.A., S. Ebrahim, and G. Davey Smith, *Association of birth weight with adult lung function: findings from the British Women's Heart and Health Study and a meta-analysis.* Thorax, 2005. **60**(10): p. 851-8.
52. Lange, P., et al., *Lung-Function Trajectories Leading to Chronic Obstructive Pulmonary Disease.* N Engl J Med, 2015. **373**(2): p. 111-22.
53. Allinson, J.P., et al., *Combined Impact of Smoking and Early-Life Exposures on Adult Lung Function Trajectories.* Am J Respir Crit Care Med, 2017. **196**(8): p. 1021-1030.
54. Kohansal, R., et al., *The natural history of chronic airflow obstruction revisited: an analysis of the Framingham offspring cohort.* Am J Respir Crit Care Med, 2009. **180**(1): p. 3-10.
55. Raad, D., et al., *Effects of water-pipe smoking on lung function: a systematic review and meta-analysis.* Chest, 2011. **139**(4): p. 764-774.
56. Hagstad, S., et al., *Passive smoking exposure is associated with increased risk of COPD in never smokers.* Chest, 2014. **145**(6): p. 1298-1304.
57. Hnizdo, E., et al., *Association between chronic obstructive pulmonary disease and employment by industry and occupation in the US population: a study of data from the Third National Health and Nutrition Examination Survey.* Am J Epidemiol, 2002. **156**(8): p. 738-46.
58. Balmes, J., et al., *American Thoracic Society Statement: Occupational contribution to the burden of airway disease.* Am J Respir Crit Care Med, 2003. **167**(5): p. 787-97.
59. Marchetti, N., et al., *Association between occupational exposure and lung function, respiratory symptoms, and high-resolution computed tomography imaging in COPDGene.* Am J Respir Crit Care Med, 2014. **190**(7): p. 756-62.
60. Sana, A., et al., *Chronic obstructive pulmonary disease associated with biomass fuel use in women: a systematic review and meta-analysis.* BMJ Open Respir Res, 2018. **5**(1): p. e000246.
61. Gauderman, W.J., et al., *The effect of air pollution on lung development from 10 to 18 years of age.* N Engl J Med, 2004. **351**(11): p. 1057-67.
62. Gauderman, W.J., et al., *Association of Improved Air Quality with Lung Development in Children.* New England Journal of Medicine, 2015. **372**(10): p. 905-913.
63. de Marco, R., et al., *Risk factors for chronic obstructive pulmonary disease in a European cohort of young adults.* Am J Respir Crit Care Med, 2011. **183**(7): p. 891-7.
64. Bigna, J.J., et al., *Prevalence of chronic obstructive pulmonary disease in the global population with HIV: a systematic review and meta-analysis.* Lancet Glob Health, 2018. **6**(2): p. e193-e202.
65. Byrne, A.L., et al., *Tuberculosis and chronic respiratory disease: a systematic review.* Int J Infect Dis, 2015. **32**: p. 138-46.
66. Sethi, S., *Infection as a comorbidity of COPD.* European Respiratory Journal, 2010. **35**(6): p. 1209-1215.
67. Lindberg, A., et al., *Seven-year cumulative incidence of COPD in an age-stratified general population sample.* Chest, 2006. **129**(4): p. 879-85.

68. de Marco, R., et al., *Incidence of chronic obstructive pulmonary disease in a cohort of young adults according to the presence of chronic cough and phlegm.* Am J Respir Crit Care Med, 2007. **175**(1): p. 32-9.
69. Allinson, J.P., et al., *The Presence of Chronic Mucus Hypersecretion across Adult Life in Relation to Chronic Obstructive Pulmonary Disease Development.* Am J Respir Crit Care Med, 2016. **193**(6): p. 662-72.
70. Townend, J., et al., *The association between chronic airflow obstruction and poverty in 12 sites of the multinational BOLD study.* Eur Respir J, 2017. **49**(6).
71. *Essentials of Clinical Pulmonology.*, ed. P. Shah, Herth, F., Lee, Y., Criner, G. . 2018: Boca Raton: CRC Press.
72. Weibel, *Morphometry of the Human Lung*. 1963: New York: Academic Press Inc.
73. Hogg, J.C., *State of the art. Bronchiolitis in chronic obstructive pulmonary disease.* Proc Am Thorac Soc, 2006. **3**(6): p. 489-93.
74. Hansen, J.E., et al., *Branching pattern of airways and air spaces of a single human terminal bronchiole.* J Appl Physiol, 1975. **38**(6): p. 983-9.
75. Haefeli-Bleuer, B. and E.R. Weibel, *Morphometry of the human pulmonary acinus.* Anat Rec, 1988. **220**(4): p. 401-14.
76. Berend, N., A.C. Rynell, and H.E. Ward, *Structure of a human pulmonary acinus.* Thorax, 1991. **46**(2): p. 117-21.
77. Ryan, S.F., *The structure of the primary lung lobule.* Ann Clin Lab Sci, 1973. **3**(3): p. 147-55.
78. Gurney, J.W., *Pathophysiology of obstructive airways disease.* Radiol Clin North Am, 1998. **36**(1): p. 15-27.
79. Bergin, C., et al., *The secondary pulmonary lobule: normal and abnormal CT appearances.* AJR Am J Roentgenol, 1988. **151**(1): p. 21-5.
80. Berg, K. and J.L. Wright, *The Pathology of Chronic Obstructive Pulmonary Disease: Progress in the 20th and 21st Centuries.* Arch Pathol Lab Med, 2016. **140**(12): p. 1423-1428.
81. Usmani, O.S., M.F. Biddiscombe, and P.J. Barnes, *Regional lung deposition and bronchodilator response as a function of beta2-agonist particle size.* Am J Respir Crit Care Med, 2005. **172**(12): p. 1497-504.
82. Hogg, J.C., *Pathophysiology of airflow limitation in chronic obstructive pulmonary disease.* Lancet, 2004. **364**(9435): p. 709-21.
83. Hogg, J.C., et al., *Survival after lung volume reduction in chronic obstructive pulmonary disease: insights from small airway pathology.* American journal of respiratory and critical care medicine, 2007. **176**(5): p. 454-459.
84. Hogg, J.C., et al., *The nature of small-airway obstruction in chronic obstructive pulmonary disease.* N Engl J Med, 2004. **350**(26): p. 2645-53.
85. Higham, A., et al., *The pathology of small airways disease in COPD: historical aspects and future directions.* Respiratory Research, 2019. **20**(1): p. 49.
86. Gohy, S.T., et al., *Imprinting of the COPD airway epithelium for dedifferentiation and mesenchymal transition.* Eur Respir J, 2015. **45**(5): p. 1258-72.
87. Heijink, I.H., et al., *Abnormalities in Airway Epithelial Junction Formation in Chronic Obstructive Pulmonary Disease.* American Journal of Respiratory and Critical Care Medicine, 2014. **189**(11): p. 1439-1442.
88. Polosukhin, V.V., et al., *Bronchial secretory immunoglobulin a deficiency correlates with airway inflammation and progression of chronic obstructive pulmonary disease.* Am J Respir Crit Care Med, 2011. **184**(3): p. 317-27.
89. Niewoehner, D.E., J. Kleinerman, and D.B. Rice, *Pathologic Changes in the Peripheral Airways of Young Cigarette Smokers.* New England Journal of Medicine, 1974. **291**(15): p. 755-758.
90. McDonough, J.E., et al., *Small-airway obstruction and emphysema in chronic obstructive pulmonary disease.* N Engl J Med, 2011. **365**(17): p. 1567-75.

91. Koo, H.K., et al., *Small airways disease in mild and moderate chronic obstructive pulmonary disease: a cross-sectional study.* Lancet Respir Med, 2018. **6**(8): p. 591-602.
92. Snider, G.L., et al., *The Definition of Emphysema.* American Review of Respiratory Disease, 1985. **132**(1): p. 182-185.
93. Stuart, B.O., *Deposition and clearance of inhaled particles.* Environ Health Perspect, 1984. **55**: p. 369-90.
94. Lynch, D.A., et al., *CT-Definable Subtypes of Chronic Obstructive Pulmonary Disease: A Statement of the Fleischner Society.* Radiology, 2015. **277**(1): p. 192-205.
95. Bhatt, S.P., et al., *Association between Functional Small Airway Disease and FEV1 Decline in Chronic Obstructive Pulmonary Disease.* Am J Respir Crit Care Med, 2016. **194**(2): p. 178-84.
96. Oswald-Mammosser, M., et al., *Prognostic factors in COPD patients receiving long-term oxygen therapy. Importance of pulmonary artery pressure.* Chest, 1995. **107**(5): p. 1193-8.
97. Chaouat, A., R. Naeije, and E. Weitzenblum, *Pulmonary hypertension in COPD.* European Respiratory Journal, 2008. **32**(5): p. 1371-1385.
98. Matsuoka, S., et al., *Pulmonary hypertension and computed tomography measurement of small pulmonary vessels in severe emphysema.* American journal of respiratory and critical care medicine, 2010. **181**(3): p. 218-225.
99. Talhout, R., et al., *Hazardous compounds in tobacco smoke.* International journal of environmental research and public health, 2011. **8**(2): p. 613-628.
100. Li, X., et al., *Characterization of particle size distribution of mainstream cigarette smoke generated by smoking machine with an electrical low pressure impactor.* Journal of Environmental Sciences, 2014. **26**(4): p. 827-833.
101. Summers, C., et al., *Neutrophil kinetics in health and disease.* Trends Immunol, 2010. **31**(8): p. 318-24.
102. Sapey, E. and R.A. Stockley, *Red, amber and green: the role of the lung in de-priming active systemic neutrophils.* Thorax, 2014. **69**(7): p. 606-608.
103. Borregaard, N. and J.B. Cowland, *Granules of the human neutrophilic polymorphonuclear leukocyte.* Blood, 1997. **89**(10): p. 3503-21.
104. Jasper, A., et al., *Understanding the role of neutrophils in chronic inflammatory airway disease [version 1; peer review: 2 approved].* F1000Research, 2019. **8**(557).
105. Thompson, A.B., et al., *Intraluminal airway inflammation in chronic bronchitis. Characterization and correlation with clinical parameters.* Am Rev Respir Dis, 1989. **140**(6): p. 1527-37.
106. Stanescu, D., et al., *Airways obstruction, chronic expectoration, and rapid decline of FEV1 in smokers are associated with increased levels of sputum neutrophils.* Thorax, 1996. **51**(3): p. 267-71.
107. Keatings, V.M., et al., *Differences in interleukin-8 and tumor necrosis factor-alpha in induced sputum from patients with chronic obstructive pulmonary disease or asthma.* Am J Respir Crit Care Med, 1996. **153**(2): p. 530-4.
108. Donaldson, G.C., et al., *Airway and systemic inflammation and decline in lung function in patients with COPD.* Chest, 2005. **128**(4): p. 1995-2004.
109. Parr, D.G., et al., *Inflammation in sputum relates to progression of disease in subjects with COPD: a prospective descriptive study.* Respir Res, 2006. **7**: p. 136.
110. O'Donnell, R.A., et al., *Relationship between peripheral airway dysfunction, airway obstruction, and neutrophilic inflammation in COPD.* Thorax, 2004. **59**(10): p. 837-42.
111. Pilette, C., et al., *Increased galectin-3 expression and intra-epithelial neutrophils in small airways in severe COPD.* Eur Respir J, 2007. **29**(5): p. 914-22.
112. Vaitkus, M., et al., *Reactive oxygen species in peripheral blood and sputum neutrophils during bacterial and nonbacterial acute exacerbation of chronic obstructive pulmonary disease.* Inflammation, 2013. **36**(6): p. 1485-93.

113. Thulborn, S.J., et al., *Neutrophil elastase as a biomarker for bacterial infection in COPD.* Respiratory research, 2019. **20**(1): p. 170-170.
114. Hoenderdos, K. and A. Condliffe, *The Neutrophil in Chronic Obstructive Pulmonary Disease. Too Little, Too Late or Too Much, Too Soon?* American Journal of Respiratory Cell and Molecular Biology, 2013. **48**(5): p. 531-539.
115. Subramanian, D.R., et al., *Assessment of Pulmonary Neutrophilic Inflammation in Emphysema by Quantitative Positron Emission Tomography.* American Journal of Respiratory and Critical Care Medicine, 2012. **186**(11): p. 1125-1132.
116. Tregay, N., et al., *Use of autologous (99m)Technetium-labelled neutrophils to quantify lung neutrophil clearance in COPD.* Thorax, 2019. **74**(7): p. 659-666.
117. Fujita, M. and Y. Nakanishi, *The pathogenesis of COPD: lessons learned from in vivo animal models.* Med Sci Monit, 2007. **13**(2): p. Ra19-24.
118. Demkow, U. and F.J. van Overveld, *Role of elastases in the pathogenesis of chronic obstructive pulmonary disease: implications for treatment.* European journal of medical research, 2010. **15 Suppl 2**(Suppl 2): p. 27-35.
119. Barnes, P.J., *Alveolar macrophages in chronic obstructive pulmonary disease (COPD).* Cell Mol Biol (Noisy-le-grand), 2004. **50 Online Pub**: p. Ol627-37.
120. Gadgil, A. and S.R. Duncan, *Role of T-lymphocytes and pro-inflammatory mediators in the pathogenesis of chronic obstructive pulmonary disease.* International journal of chronic obstructive pulmonary disease, 2008. **3**(4): p. 531-541.
121. Polverino, F., et al., *B cells in chronic obstructive pulmonary disease: moving to center stage.* Am J Physiol Lung Cell Mol Physiol, 2016. **311**(4): p. L687-l695.
122. Singh, D., et al., *Eosinophilic inflammation in COPD: prevalence and clinical characteristics.* European Respiratory Journal, 2014. **44**(6): p. 1697-1700.
123. Muñoz-Esquerre, M., et al., *Impact of acute exacerbations on platelet reactivity in chronic obstructive pulmonary disease patients.* International journal of chronic obstructive pulmonary disease, 2017. **13**: p. 141-148.
124. Barnes, P.J., *The Cytokine Network in Chronic Obstructive Pulmonary Disease.* American Journal of Respiratory Cell and Molecular Biology, 2009. **41**(6): p. 631-638.
125. Kubo, H., *Extracellular Vesicles in Lung Disease.* Chest, 2018. **153**(1): p. 210-216.
126. Wahlund, C.J.E., et al., *Pulmonary Extracellular Vesicles as Mediators of Local and Systemic Inflammation.* Front Cell Dev Biol, 2017. **5**: p. 39.
127. Gordon, C., et al., *Circulating endothelial microparticles as a measure of early lung destruction in cigarette smokers.* Am J Respir Crit Care Med, 2011. **184**(2): p. 224-32.
128. Takahashi, T., et al., *Increased circulating endothelial microparticles in COPD patients: a potential biomarker for COPD exacerbation susceptibility.* Thorax, 2012. **67**(12): p. 1067-74.
129. Eltom, S., et al., *Respiratory infections cause the release of extracellular vesicles: implications in exacerbation of asthma/COPD.* PLoS One, 2014. **9**(6): p. e101087.
130. Takahashi, T., et al., *Annual FEV1 changes and numbers of circulating endothelial microparticles in patients with COPD: a prospective study.* BMJ Open, 2014. **4**(3): p. e004571.
131. Lacedonia, D., et al., *Microparticles in sputum of COPD patients: a potential biomarker of the disease?* International Journal of Chronic Obstructive Pulmonary Disease, 2016. **11**: p. 527-533.
132. Genschmer, K.R., et al., *Activated PMN Exosomes: Pathogenic Entities Causing Matrix Destruction and Disease in the Lung.* Cell, 2019. **176**(1-2): p. 113-126.e15.
133. Abboud, R.T. and S. Vimalanathan, *Pathogenesis of COPD. Part I. The role of protease-antiprotease imbalance in emphysema.* Int J Tuberc Lung Dis, 2008. **12**(4): p. 361-7.
134. Barnes, P.J., *Senescence in COPD and Its Comorbidities.* Annu Rev Physiol, 2017. **79**: p. 517-539.

135. Antony, V.B. and V.J. Thannickal, *Cellular Senescence in Chronic Obstructive Pulmonary Disease: Multifaceted and Multifunctional.* American Journal of Respiratory Cell and Molecular Biology, 2018. **59**(2): p. 135-136.
136. Sze, M.A., et al., *Host Response to the Lung Microbiome in Chronic Obstructive Pulmonary Disease.* American Journal of Respiratory and Critical Care Medicine, 2015. **192**(4): p. 438-445.
137. Thomas, M., M. Decramer, and D.E. O'Donnell, *No room to breathe: the importance of lung hyperinflation in COPD.* Prim Care Respir J, 2013. **22**(1): p. 101-11.
138. Marin, J.M., et al., *Inspiratory capacity, dynamic hyperinflation, breathlessness, and exercise performance during the 6-minute-walk test in chronic obstructive pulmonary disease.* Am J Respir Crit Care Med, 2001. **163**(6): p. 1395-9.
139. O'Donnell, D.E., et al., *Decline of resting inspiratory capacity in COPD: the impact on breathing pattern, dyspnea, and ventilatory capacity during exercise.* Chest, 2012. **141**(3): p. 753-762.
140. O'Donnell, D.E., et al., *The Link between Reduced Inspiratory Capacity and Exercise Intolerance in Chronic Obstructive Pulmonary Disease.* Ann Am Thorac Soc, 2017.
141. Zaman, M., S. Mahmood, and A. Altayeh, *Low inspiratory capacity to total lung capacity ratio is a risk factor for chronic obstructive pulmonary disease exacerbation.* Am J Med Sci, 2010. **339**(5): p. 411-4.
142. Casanova, C., et al., *Inspiratory-to-total lung capacity ratio predicts mortality in patients with chronic obstructive pulmonary disease.* Am J Respir Crit Care Med, 2005. **171**(6): p. 591-7.
143. Tantucci, C., et al., *Inspiratory capacity predicts mortality in patients with chronic obstructive pulmonary disease.* Respir Med, 2008. **102**(4): p. 613-9.
144. Mead, J., et al., *Significance of the relationship between lung recoil and maximum expiratory flow.* J Appl Physiol, 1967. **22**(1): p. 95-108.
145. Dayman, H., *Mechanics of airflow in health and in emphysema.* J Clin Invest, 1951. **30**(11): p. 1175-90.
146. Colebatch, H.J., K.E. Finucane, and M.M. Smith, *Pulmonary conductance and elastic recoil relationships in asthma and emphysema.* J Appl Physiol, 1973. **34**(2): p. 143-53.
147. West JB, L.A., *West's Pulmonary Pathophysiology: The Essentials*. 9th Edition ed. 2017: West's Pulmonary Pathophysiology.
148. Hogg, J.C., P.D. Pare, and T.L. Hackett, *The Contribution of Small Airway Obstruction to the Pathogenesis of Chronic Obstructive Pulmonary Disease.* Physiol Rev, 2017. **97**(2): p. 529-552.
149. O'Donnell, D.E. and P. Laveneziana, *Physiology and consequences of lung hyperinflation in COPD.* European Respiratory Review, 2006. **15**(100): p. 61-67.
150. Stevenson, N.J., et al., *Lung mechanics and dyspnea during exacerbations of chronic obstructive pulmonary disease.* Am J Respir Crit Care Med, 2005. **172**(12): p. 1510-6.
151. Polkey, M.I., et al., *Diaphragm strength in chronic obstructive pulmonary disease.* Am J Respir Crit Care Med, 1996. **154**(5): p. 1310-7.
152. Cassart, M., et al., *Effect of chronic hyperinflation on diaphragm length and surface area.* Am J Respir Crit Care Med, 1997. **156**(2 Pt 1): p. 504-8.
153. Decramer, M., *Hyperinflation and respiratory muscle interaction.* Eur Respir J, 1997. **10**(4): p. 934-41.
154. Faisal, A., et al., *Common Mechanisms of Dyspnea in Chronic Interstitial and Obstructive Lung Disorders.* Am J Respir Crit Care Med, 2016. **193**(3): p. 299-309.
155. Wagner, P.D., et al., *Ventilation-perfusion inequality in chronic obstructive pulmonary disease.* J Clin Invest, 1977. **59**(2): p. 203-16.
156. Brantigan, O.C. and E. Mueller, *Surgical treatment of pulmonary emphysema.* Am Surg, 1957. **23**(9): p. 789-804.

157. Snider, G.L., *Reduction pneumoplasty for giant bullous emphysema. Implications for surgical treatment of nonbullous emphysema.* Chest, 1996. **109**(2): p. 540-8.
158. Cooper, J.D., et al., *Results of 150 consecutive bilateral lung volume reduction procedures in patients with severe emphysema.* J Thorac Cardiovasc Surg, 1996. **112**(5): p. 1319-29; discussion 1329-30.
159. Fishman, A., et al., *A randomized trial comparing lung-volume-reduction surgery with medical therapy for severe emphysema.* N Engl J Med, 2003. **348**(21): p. 2059-73.
160. Clark, S.J., et al., *Surgical approaches for lung volume reduction in emphysema.* Clin Med (Lond), 2014. **14**(2): p. 122-7.
161. Estenne, M., H.E. Fessler, and M.M. DeCamp, *Lung transplantation and lung volume reduction surgery.* Compr Physiol, 2011. **1**(3): p. 1437-71.
162. Gelb, A.F., et al., *Mechanism of short-term improvement in lung function after emphysema resection.* Am J Respir Crit Care Med, 1996. **154**(4 Pt 1): p. 945-51.
163. Sciurba, F.C., et al., *Improvement in pulmonary function and elastic recoil after lung-reduction surgery for diffuse emphysema.* N Engl J Med, 1996. **334**(17): p. 1095-9.
164. Ingenito, E.P., et al., *Physiological characterization of variability in response to lung volume reduction surgery.* J Appl Physiol (1985), 2003. **94**(1): p. 20-30.
165. Fessler, H.E. and S. Permutt, *Lung volume reduction surgery and airflow limitation.* Am J Respir Crit Care Med, 1998. **157**(3 Pt 1): p. 715-22.
166. Fessler, H.E., et al., *Physiologic basis for improved pulmonary function after lung volume reduction.* Proc Am Thorac Soc, 2008. **5**(4): p. 416-20.
167. Lammi, M.R., N. Marchetti, and G.J. Criner, *Reduced dynamic hyperinflation after LVRS is associated with improved exercise tolerance.* Respir Med, 2014. **108**(10): p. 1491-7.
168. Fessler, H.E., S.M. Scharf, and S. Permutt, *Improvement in spirometry following lung volume reduction surgery: application of a physiologic model.* Am J Respir Crit Care Med, 2002. **165**(1): p. 34-40.
169. Teschler, H., et al., *Effect of surgical lung volume reduction on respiratory muscle function in pulmonary emphysema.* Eur Respir J, 1996. **9**(9): p. 1779-84.
170. Martinez, F.J., et al., *Lung-volume reduction improves dyspnea, dynamic hyperinflation, and respiratory muscle function.* Am J Respir Crit Care Med, 1997. **155**(6): p. 1984-90.
171. Degano, B., et al., *Improvement after lung volume reduction surgery: a role for inspiratory muscle adaptation.* Respir Physiol Neurobiol, 2004. **139**(3): p. 293-301.
172. Zoumot, Z., et al., *Lung Volume Reduction in Emphysema Improves Chest Wall Asynchrony.* Chest, 2015. **148**(1): p. 185-195.
173. Cassart, M., et al., *Effects of lung volume reduction surgery for emphysema on diaphragm dimensions and configuration.* Am J Respir Crit Care Med, 2001. **163**(5): p. 1171-5.
174. Criner, G., et al., *Effect of lung volume reduction surgery on diaphragm strength.* Am J Respir Crit Care Med, 1998. **157**(5 Pt 1): p. 1578-85.
175. Laghi, F., et al., *Effect of lung volume reduction surgery on diaphragmatic neuromechanical coupling at 2 years.* Chest, 2004. **125**(6): p. 2188-95.
176. Hamnegard, C.H., et al., *Effect of lung volume reduction surgery for emphysema on diaphragm function.* Respir Physiol Neurobiol, 2006. **150**(2-3): p. 182-90.
177. Oswald-Mammosser, M., et al., *Effect of lung volume reduction surgery on gas exchange and pulmonary hemodynamics at rest and during exercise.* Am J Respir Crit Care Med, 1998. **158**(4): p. 1020-5.
178. Benditt, J.O., et al., *Lung volume reduction surgery improves maximal O2 consumption, maximal minute ventilation, O2 pulse, and dead space-to-tidal volume ratio during leg cycle ergometry.* Am J Respir Crit Care Med, 1997. **156**(2 Pt 1): p. 561-6.
179. Takayama, T., et al., *Effects of lung volume reduction surgery for emphysema on oxygen cost of breathing.* Chest, 2003. **123**(6): p. 1847-52.

180. Ferguson, G.T., et al., *Improved exercise performance following lung volume reduction surgery for emphysema.* Am J Respir Crit Care Med, 1998. **157**(4 Pt 1): p. 1195-203.
181. Ciccone, A.M., et al., *Long-term outcome of bilateral lung volume reduction in 250 consecutive patients with emphysema.* J Thorac Cardiovasc Surg, 2003. **125**(3): p. 513-25.
182. Meyers, B.F., et al., *Outcomes after unilateral lung volume reduction.* Ann Thorac Surg, 2008. **86**(1): p. 204-11; discussion 211-2.
183. Toma, T.P., et al., *Bronchoscopic volume reduction with valve implants in patients with severe emphysema.* Lancet, 2003. **361**(9361): p. 931-3.
184. Sciurba, F.C., et al., *A randomized study of endobronchial valves for advanced emphysema.* N Engl J Med, 2010. **363**(13): p. 1233-44.
185. Herth, F.J., et al., *Efficacy predictors of lung volume reduction with Zephyr valves in a European cohort.* Eur Respir J, 2012. **39**(6): p. 1334-42.
186. Davey, C., et al., *Bronchoscopic lung volume reduction with endobronchial valves for patients with heterogeneous emphysema and intact interlobar fissures (the BeLieVeR-HIFi study): a randomised controlled trial.* Lancet, 2015. **386**(9998): p. 1066-73.
187. Zoumot, Z., et al., *Endobronchial valves for patients with heterogeneous emphysema and without interlobar collateral ventilation: open label treatment following the BeLieVeR-HIFi study.* Thorax, 2017. **72**(3): p. 277-279.
188. Klooster, K., et al., *Endobronchial Valves for Emphysema without Interlobar Collateral Ventilation.* N Engl J Med, 2015. **373**(24): p. 2325-35.
189. Kemp, S.V., et al., *A Multicenter RCT of Zephyr(R) Endobronchial Valve Treatment in Heterogeneous Emphysema (TRANSFORM).* Am J Respir Crit Care Med, 2017.
190. Criner, G.J., et al., *A Multicenter Randomized Controlled Trial of Zephyr Endobronchial Valve Treatment in Heterogeneous Emphysema (LIBERATE).* Am J Respir Crit Care Med, 2018. **198**(9): p. 1151-1164.
191. Valipour, A., et al., *Endobronchial Valve Therapy in Patients with Homogeneous Emphysema: Results from the IMPACT Study.* Am J Respir Crit Care Med, 2016.
192. Hartman, J.E., et al., *Endobronchial valves for severe emphysema.* Eur Respir Rev, 2019. **28**(152).
193. Gompelmann, D., et al., *Predictors of pneumothorax following endoscopic valve therapy in patients with severe emphysema.* Int J Chron Obstruct Pulmon Dis, 2016. **11**: p. 1767-73.
194. van Geffen, W.H., et al., *Pleural Adhesion Assessment as a Predictor for Pneumothorax after Endobronchial Valve Treatment.* Respiration, 2017. **94**(2): p. 224-231.
195. Herth, F.J.F., et al., *Endoscopic Lung Volume Reduction: An Expert Panel Recommendation - Update 2019.* Respiration, 2019. **97**(6): p. 548-557.
196. Valipour, A., et al., *Expert statement: pneumothorax associated with endoscopic valve therapy for emphysema--potential mechanisms, treatment algorithm, and case examples.* Respiration, 2014. **87**(6): p. 513-21.
197. Gompelmann, D., et al., *Survival after Endoscopic Valve Therapy in Patients with Severe Emphysema.* Respiration, 2018: p. 1-8.
198. Gompelmann, D., et al., *Long-term follow up after endoscopic valve therapy in patients with severe emphysema.* Ther Adv Respir Dis, 2019. **13**: p. 1753466619866101.
199. Pietzsch, J.B., A. Garner, and F.J. Herth, *Cost-effectiveness of endobronchial valve therapy for severe emphysema: a model-based projection based on the VENT study.* Respiration, 2014. **88**(5): p. 389-98.
200. Hartman, J.E., et al., *Cost-effectiveness of endobronchial valve treatment in patients with severe emphysema compared to standard medical care.* Respirology, 2018.
201. Garner, J., et al., *Survival after Endobronchial Valve Placement for Emphysema: A 10-Year Follow-up Study.* Am J Respir Crit Care Med, 2016. **194**(4): p. 519-21.
202. Welling, J.B.A., et al., *Collateral ventilation measurement using Chartis: procedural sedation versus general anesthesia.* CHEST.

203. Herth, F.J., et al., *Bronchoscopic lung volume reduction with a dedicated coil: a clinical pilot study.* Ther Adv Respir Dis, 2010. **4**(4): p. 225-31.
204. Slebos, D.J., et al., *Endobronchial Coils for Endoscopic Lung Volume Reduction: Best Practice Recommendations from an Expert Panel.* Respiration, 2018. **96**(1): p. 1-11.
205. Palamidas, A.F., et al., *Putative Mechanisms of Action of Endobronchial Coils.* Am J Respir Crit Care Med, 2017. **196**(1): p. 109-115.
206. Slebos, D.J., et al., *Bronchoscopic lung volume reduction coil treatment of patients with severe heterogeneous emphysema.* Chest, 2012. **142**(3): p. 574-82.
207. Shah, P.L., et al., *Endobronchial coils for the treatment of severe emphysema with hyperinflation (RESET): a randomised controlled trial.* Lancet Respir Med, 2013. **1**(3): p. 233-40.
208. Zoumot, Z., et al., *Endobronchial coils for severe emphysema are effective up to 12 months following treatment: medium term and cross-over results from a randomised controlled trial.* PLoS One, 2015. **10**(4): p. e0122656.
209. Deslee, G., et al., *Lung Volume Reduction Coil Treatment vs Usual Care in Patients With Severe Emphysema: The REVOLENS Randomized Clinical Trial.* Jama, 2016. **315**(2): p. 175-84.
210. Deslee, G., et al., *Two-year follow-up after endobronchial coil treatment in emphysema: results from the REVOLENS study.* Eur Respir J, 2017. **50**(6).
211. Sciurba, F.C., et al., *Effect of Endobronchial Coils vs Usual Care on Exercise Tolerance in Patients With Severe Emphysema: The RENEW Randomized Clinical Trial.* Jama, 2016. **315**(20): p. 2178-89.
212. Slebos, D.J., et al., *Predictors of Response to Endobronchial Coil Therapy in Patients With Advanced Emphysema.* Chest, 2019. **155**(5): p. 928-937.
213. Hartman, J.E., et al., *Long-term follow-up after bronchoscopic lung volume reduction treatment with coils in patients with severe emphysema.* Respirology, 2015. **20**(2): p. 319-26.
214. van Geffen, W.H., et al., *Surgical and endoscopic interventions that reduce lung volume for emphysema: a systemic review and meta-analysis.* Lancet Respir Med, 2019. **7**(4): p. 313-324.
215. Garner, J.L., et al., *5-Year Survival after Endobronchial Coil Implantation: Secondary Analysis of the First Randomised Controlled Trial, RESET.* Respiration, 2020. **99**(2): p. 154-162.
216. Shen, M., et al., *Quantitative Evaluation of Lobar Pulmonary Function of Emphysema Patients with Endobronchial Coils.* Respiration, 2019. **98**(1): p. 70-81.
217. Gevenois, P.A., et al., *Comparison of computed density and macroscopic morphometry in pulmonary emphysema.* Am J Respir Crit Care Med, 1995. **152**(2): p. 653-7.
218. Gevenois, P.A., et al., *Comparison of computed density and microscopic morphometry in pulmonary emphysema.* Am J Respir Crit Care Med, 1996. **154**(1): p. 187-92.
219. Schroeder, J.D., et al., *Relationships between airflow obstruction and quantitative CT measurements of emphysema, air trapping, and airways in subjects with and without chronic obstructive pulmonary disease.* AJR Am J Roentgenol, 2013. **201**(3): p. W460-70.
220. Galban, C.J., et al., *Computed tomography-based biomarker provides unique signature for diagnosis of COPD phenotypes and disease progression.* Nat Med, 2012. **18**(11): p. 1711-5.
221. Labaki, W.W., et al., *Voxel-Wise Longitudinal Parametric Response Mapping Analysis of Chest Computed Tomography in Smokers.* Acad Radiol, 2018.
222. Hogg, J.C., et al., *Micro-computed tomography measurements of peripheral lung pathology in chronic obstructive pulmonary disease.* Proc Am Thorac Soc, 2009. **6**(6): p. 546-9.
223. Pompe, E., et al., *Parametric response mapping on chest computed tomography associates with clinical and functional parameters in chronic obstructive pulmonary disease.* Respir Med, 2017. **123**: p. 48-55.
224. Occhipinti, M., et al., *Emphysematous and Nonemphysematous Gas Trapping in Chronic Obstructive Pulmonary Disease: Quantitative CT Findings and Pulmonary Function.* Radiology, 2018. **287**(2): p. 683-692.

225. Iyer, A.S., et al., *CT scan-measured pulmonary artery to aorta ratio and echocardiography for detecting pulmonary hypertension in severe COPD.* Chest, 2014. **145**(4): p. 824-832.
226. Estepar, R.S., et al., *Computed tomographic measures of pulmonary vascular morphology in smokers and their clinical implications.* Am J Respir Crit Care Med, 2013. **188**(2): p. 231-9.
227. Quanjer, P.H., et al., *Lung volumes and forced ventilatory flows. Report Working Party Standardization of Lung Function Tests, European Community for Steel and Coal. Official Statement of the European Respiratory Society.* Eur Respir J Suppl, 1993. **16**: p. 5-40.
228. Pride, N.B., *Tests of forced expiration and inspiration.* Clin Chest Med, 2001. **22**(4): p. 599-622, vii.
229. Vestbo, J., et al., *Global strategy for the diagnosis, management, and prevention of chronic obstructive pulmonary disease: GOLD executive summary.* Am J Respir Crit Care Med, 2013. **187**(4): p. 347-65.
230. Kaplan, R.M., et al., *Measurement of health-related quality of life in the national emphysema treatment trial.* Chest, 2004. **126**(3): p. 781-9.
231. Foglio, K., et al., *Physiological and symptom determinants of exercise performance in patients with chronic airway obstruction.* Respir Med, 2000. **94**(3): p. 256-63.
232. McFadden, E.R., Jr. and D.A. Linden, *A reduction in maximum mid-expiratory flow rate. A spirographic manifestation of small airway disease.* Am J Med, 1972. **52**(6): p. 725-37.
233. Gelb, A.F., A.J. Williams, and N. Zamel, *Spirometry. FEV1 vs FEF25-75 percent.* Chest, 1983. **84**(4): p. 473-4.
234. Hansen, J.E., X.G. Sun, and K. Wasserman, *Discriminating measures and normal values for expiratory obstruction.* Chest, 2006. **129**(2): p. 369-77.
235. Yanai, M., et al., *Site of airway obstruction in pulmonary disease: direct measurement of intrabronchial pressure.* J Appl Physiol (1985), 1992. **72**(3): p. 1016-23.
236. Hogg, J.C., J.E. McDonough, and M. Suzuki, *Small airway obstruction in COPD: new insights based on micro-CT imaging and MRI imaging.* Chest, 2013. **143**(5): p. 1436-1443.
237. Leuallen, E.C. and W.S. Fowler, *Maximal midexpiratory flow.* Am Rev Tuberc, 1955. **72**(6): p. 783-800.
238. Stockley, J.A., et al., *Maximal mid-expiratory flow detects early lung disease in alpha1-antitrypsin deficiency.* Eur Respir J, 2017. **49**(3).
239. Mirsadraee, M., M.H. Boskabady, and D. Attaran, *Diagnosis of chronic obstructive pulmonary disease earlier than current Global Initiative for Obstructive Lung Disease guidelines using a feasible spirometry parameter (maximal-mid expiratory flow/forced vital capacity).* Chron Respir Dis, 2013. **10**(4): p. 191-6.
240. Topalovic, M., et al., *Computer quantification of airway collapse on forced expiration to predict the presence of emphysema.* Respir Res, 2013. **14**: p. 131.
241. Topalovic, M., et al., *Airways resistance and specific conductance for the diagnosis of obstructive airways diseases.* Respir Res, 2015. **16**: p. 88.
242. Gould, G.A., et al., *Lung CT density correlates with measurements of airflow limitation and the diffusing capacity.* Eur Respir J, 1991. **4**(2): p. 141-6.
243. Hoesein, F.M., et al., *Association of the transfer coefficient (Kco) with emphysema progression in heavy smokers.* European Respiratory Journal, 2011. **38**(Suppl 55): p. p3518.
244. Elbehairy, A.F., et al., *Pulmonary Gas Exchange Abnormalities in Mild Chronic Obstructive Pulmonary Disease. Implications for Dyspnea and Exercise Intolerance.* Am J Respir Crit Care Med, 2015. **191**(12): p. 1384-94.
245. Dubois, A.B., et al., *Oscillation mechanics of lungs and chest in man.* J Appl Physiol, 1956. **8**(6): p. 587-94.
246. Brashier, B. and S. Salvi, *Measuring lung function using sound waves: role of the forced oscillation technique and impulse oscillometry system.* Breathe (Sheff), 2015. **11**(1): p. 57-65.
247. Goldman, M.D., C. Saadeh, and D. Ross, *Clinical applications of forced oscillation to assess peripheral airway function.* Respir Physiol Neurobiol, 2005. **148**(1-2): p. 179-94.

248. Wei, X., et al., *Impulse oscillometry system as an alternative diagnostic method for chronic obstructive pulmonary disease.* Medicine, 2017. **96**(46): p. e8543.
249. Pisi, R., et al., *Small airway dysfunction and flow and volume bronchodilator responsiveness in patients with chronic obstructive pulmonary disease.* Int J Chron Obstruct Pulmon Dis, 2015. **10**: p. 1191-7.
250. Frantz, S., et al., *Impulse oscillometry may be of value in detecting early manifestations of COPD.* Respir Med, 2012. **106**(8): p. 1116-23.
251. Crisafulli, E., et al., *Prevalence of Small-Airway Dysfunction among COPD Patients with Different GOLD Stages and Its Role in the Impact of Disease.* Respiration, 2017. **93**(1): p. 32-41.
252. Crim, C., et al., *Respiratory system impedance with impulse oscillometry in healthy and COPD subjects: ECLIPSE baseline results.* Respir Med, 2011. **105**(7): p. 1069-78.
253. Liu, Z., L. Lin, and X. Liu, *Clinical application value of impulse oscillometry in geriatric patients with COPD.* Int J Chron Obstruct Pulmon Dis, 2017. **12**: p. 897-905.
254. Haruna, A., et al., *Relationship between peripheral airway function and patient-reported outcomes in COPD: a cross-sectional study.* BMC Pulm Med, 2010. **10**: p. 10.
255. Silva, K.K., et al., *Within-breath respiratory impedance and airway obstruction in patients with chronic obstructive pulmonary disease.* Clinics (Sao Paulo), 2015. **70**(7): p. 461-9.
256. Aarli, B.B., et al., *Variability of within-breath reactance in COPD patients and its association with dyspnoea.* Eur Respir J, 2015. **45**(3): p. 625-34.
257. Mineshita, M., et al., *The application of impulse oscillation system for the evaluation of treatment effects in patients with COPD.* Respir Physiol Neurobiol, 2014. **202**: p. 1-5.
258. Saadeh, C., et al., *Advantage of impulse oscillometry over spirometry to diagnose chronic obstructive pulmonary disease and monitor pulmonary responses to bronchodilators: An observational study.* SAGE Open Med, 2015. **3**: p. 2050312115578957.
259. Fowler, W.S., *Lung function studies; the respiratory dead space.* Am J Physiol, 1948. **154**(3): p. 405-16.
260. Robinson, P.D., M.D. Goldman, and P.M. Gustafsson, *Inert gas washout: theoretical background and clinical utility in respiratory disease.* Respiration, 2009. **78**(3): p. 339-55.
261. Robinson, P.D., et al., *Consensus statement for inert gas washout measurement using multiple- and single- breath tests.* Eur Respir J, 2013. **41**(3): p. 507-22.
262. Gennimata, S.A., et al., *Pathophysiology of evolution of small airways disease to overt COPD.* Copd, 2010. **7**(4): p. 269-75.
263. Mikamo, M., et al., *Predictors of phase III slope of nitrogen single-breath washout in COPD.* Respir Physiol Neurobiol, 2013. **189**(1): p. 42-6.
264. Lapperre, T.S., et al., *Small airways dysfunction and neutrophilic inflammation in bronchial biopsies and BAL in COPD.* Chest, 2007. **131**(1): p. 53-9.
265. Becklake, M.R., *A new index of the intrapulmonary mixture of inspired air.* Thorax, 1952. **7**(1): p. 111-6.
266. Horsley, A., *Lung clearance index in the assessment of airways disease.* Respir Med, 2009. **103**(6): p. 793-9.
267. Verbanck, S. and M. Paiva, *Gas mixing in the airways and airspaces.* Compr Physiol, 2011. **1**(2): p. 809-34.
268. Verbanck, S., et al., *Conductive and acinar lung-zone contributions to ventilation inhomogeneity in COPD.* Am J Respir Crit Care Med, 1998. **157**(5 Pt 1): p. 1573-7.
269. Timmins, S.C., et al., *Changes in oscillatory impedance and nitrogen washout with combination fluticasone/salmeterol therapy in COPD.* Respir Med, 2014. **108**(2): p. 344-50.
270. Jarenback, L., et al., *Acinar ventilation heterogeneity in COPD relates to diffusion capacity, resistance and reactance.* Respir Med, 2016. **110**: p. 28-33.
271. Timmins, S.C., et al., *The relationship between airflow obstruction, emphysema extent, and small airways function in COPD.* Chest, 2012. **142**(2): p. 312-319.

272. Santus, P., et al., *Faster reduction in hyperinflation and improvement in lung ventilation inhomogeneity promoted by aclidinium compared to glycopyrronium in severe stable COPD patients. A randomized crossover study.* Pulm Pharmacol Ther, 2015. **35**: p. 42-9.
273. Mineo, D., et al., *Variations of inflammatory mediators and alpha1-antitrypsin levels after lung volume reduction surgery for emphysema.* Am J Respir Crit Care Med, 2010. **181**(8): p. 806-14.
274. Suki, B., et al., *Emphysema and mechanical stress-induced lung remodeling.* Physiology (Bethesda, Md.), 2013. **28**(6): p. 404-413.
275. Agustí, A., et al., *Persistent Systemic Inflammation is Associated with Poor Clinical Outcomes in COPD: A Novel Phenotype.* PLOS ONE, 2012. **7**(5): p. e37483.
276. Leng, S.X., et al., *ELISA and multiplex technologies for cytokine measurement in inflammation and aging research.* The journals of gerontology. Series A, Biological sciences and medical sciences, 2008. **63**(8): p. 879-884.
277. Barnes, P.J., *Immunology of asthma and chronic obstructive pulmonary disease.* Nat Rev Immunol, 2008. **8**(3): p. 183-92.
278. Group, F.-N.B.W., in *BEST (Biomarkers, EndpointS, and other Tools) Resource*. 2016, Food and Drug Administration (US): Silver Spring (MD).
279. Mannino, D.M., *Biomarkers for chronic obstructive pulmonary disease diagnosis and progression: insights, disappointments and promise.* Curr Opin Pulm Med, 2019. **25**(2): p. 144-149.
280. Barnes, P.J., *Inflammatory mechanisms in patients with chronic obstructive pulmonary disease.* Journal of Allergy and Clinical Immunology, 2016. **138**(1): p. 16-27.
281. Shah, P.L., et al., *Lung volume reduction for emphysema.* Lancet Respir Med, 2017. **5**(2): p. 147-156.
282. Mahler, D.A. and C.K. Wells, *Evaluation of clinical methods for rating dyspnea.* Chest, 1988. **93**(3): p. 580-6.
283. Fletcher, C.M., *The clinical diagnosis of pulmonary emphysema; an experimental study.* Proc R Soc Med, 1952. **45**(9): p. 577-84.
284. Fletcher, C.M., et al., *The significance of respiratory symptoms and the diagnosis of chronic bronchitis in a working population.* British medical journal, 1959. **2**(5147): p. 257-266.
285. Hajiro, T., et al., *Analysis of clinical methods used to evaluate dyspnea in patients with chronic obstructive pulmonary disease.* Am J Respir Crit Care Med, 1998. **158**(4): p. 1185-9.
286. Chhabra, S.K., A.K. Gupta, and M.Z. Khuma, *Evaluation of three scales of dyspnea in chronic obstructive pulmonary disease.* Annals of thoracic medicine, 2009. **4**(3): p. 128-132.
287. Henoch, I., et al., *Health-related quality of life in a nationwide cohort of patients with COPD related to other characteristics.* European clinical respiratory journal, 2016. **3**: p. 31459-31459.
288. Cheng, S.L., et al., *Comparison between COPD Assessment Test (CAT) and modified Medical Research Council (mMRC) dyspnea scores for evaluation of clinical symptoms, comorbidities and medical resources utilization in COPD patients.* J Formos Med Assoc, 2019. **118**(1 Pt 3): p. 429-435.
289. Nishimura, K., et al., *Dyspnea is a better predictor of 5-year survival than airway obstruction in patients with COPD.* Chest, 2002. **121**(5): p. 1434-40.
290. Jones, P.W., et al., *Comparisons of health status scores with MRC grades in COPD: implications for the GOLD 2011 classification.* Eur Respir J, 2013. **42**(3): p. 647-54.
291. Stenton, C., *The MRC breathlessness scale.* Occup Med (Lond), 2008. **58**(3): p. 226-7.
292. Bestall, J.C., et al., *Usefulness of the Medical Research Council (MRC) dyspnoea scale as a measure of disability in patients with chronic obstructive pulmonary disease.* Thorax, 1999. **54**(7): p. 581-6.
293. Jones, P.W., et al., *Minimal clinically important differences in pharmacological trials.* Am J Respir Crit Care Med, 2014. **189**(3): p. 250-5.

294. Araújo Oliveira, A.L., L. Andrade, and A. Marques, *Minimal clinically important difference and predictive validity of the mMRC and mBorg in acute exacerbations of COPD.* European Respiratory Journal, 2017. **50**(suppl 61): p. PA4705.
295. Jones, P.W., F.H. Quirk, and C.M. Baveystock, *The St George's Respiratory Questionnaire.* Respir Med, 1991. **85 Suppl B**: p. 25-31; discussion 33-7.
296. Jones, P.W., et al., *A self-complete measure of health status for chronic airflow limitation. The St. George's Respiratory Questionnaire.* Am Rev Respir Dis, 1992. **145**(6): p. 1321-7.
297. Jones, P.W., *Interpreting thresholds for a clinically significant change in health status in asthma and COPD.* Eur Respir J, 2002. **19**(3): p. 398-404.
298. Jones, P.W., *St. George's Respiratory Questionnaire: MCID.* Copd, 2005. **2**(1): p. 75-9.
299. Jones, P.W., et al., *Responder Analyses for Treatment Effects in COPD Using the St George's Respiratory Questionnaire.* Chronic Obstr Pulm Dis, 2017. **4**(2): p. 124-131.
300. Miller, M.R., et al., *General considerations for lung function testing.* European Respiratory Journal, 2005. **26**(1): p. 153-161.
301. Wanger, J., et al., *Standardisation of the measurement of lung volumes.* Eur Respir J, 2005. **26**(3): p. 511-22.
302. Graham, B.L., et al., *2017 ERS/ATS standards for single-breath carbon monoxide uptake in the lung.* Eur Respir J, 2017. **49**(1).
303. Graham, B.L., et al., *Standardization of Spirometry 2019 Update. An Official American Thoracic Society and European Respiratory Society Technical Statement.* American Journal of Respiratory and Critical Care Medicine, 2019. **200**(8): p. e70-e88.
304. Verbanck, S., et al., *Ventilation distribution during histamine provocation.* Journal of Applied Physiology, 1997. **83**(6): p. 1907-1916.
305. Gibson, G.J. and N.B. Pride, *Lung distensibility. The static pressure-volume curve of the lungs and its use in clinical assessment.* Br J Dis Chest, 1976. **70**(3): p. 143-84.
306. Singh, S.J., et al., *An official systematic review of the European Respiratory Society/American Thoracic Society: measurement properties of field walking tests in chronic respiratory disease.* Eur Respir J, 2014. **44**(6): p. 1447-78.
307. Du Rand, I.A., et al., *Summary of the British Thoracic Society guidelines for advanced diagnostic and therapeutic flexible bronchoscopy in adults.* Thorax, 2011. **66**(11): p. 1014-5.
308. O'Donnell, D.E., et al., *Pathophysiology of Dyspnea in Chronic Obstructive Pulmonary Disease.* Proceedings of the American Thoracic Society, 2007. **4**(2): p. 145-168.
309. Kauczor, H.U., et al., *Computed Tomography Imaging for Novel Therapies of Chronic Obstructive Pulmonary Disease.* J Thorac Imaging, 2019. **34**(3): p. 202-213.
310. Scichilone, N., et al., *Bronchodilatory effect of deep inspiration is absent in subjects with mild COPD.* Chest, 2004. **125**(6): p. 2029-35.
311. Scichilone, N., et al., *Association between reduced bronchodilatory effect of deep inspiration and loss of alveolar attachments.* Respiratory research, 2005. **6**(1): p. 55-55.
312. Scichilone, N., et al., *The airway response to deep inspirations decreases with COPD severity and is associated with airway distensibility assessed by computed tomography.* J Appl Physiol (1985), 2008. **105**(3): p. 832-8.
313. Petty, T.L., G.W. Silvers, and R.E. Stanford, *Radial traction and small airways disease in excised human lungs.* Am Rev Respir Dis, 1986. **133**(1): p. 132-5.
314. Diaz, A.A., et al., *Association between airway caliber changes with lung inflation and emphysema assessed by volumetric CT scan in subjects with COPD.* Chest, 2012. **141**(3): p. 736-744.
315. Cerveri, I., et al., *Mechanisms for isolated volume response to a bronchodilator in patients with COPD.* J Appl Physiol (1985), 2000. **88**(6): p. 1989-95.
316. Tanabe, N., et al., *Associations of airway tree to lung volume ratio on computed tomography with lung function and symptoms in chronic obstructive pulmonary disease.* Respiratory Research, 2019. **20**(1): p. 77.

317. Watz, H., et al., *Micro-CT of the human lung: imaging of alveoli and virtual endoscopy of an alveolar duct in a normal lung and in a lung with centrilobular emphysema--initial observations.* Radiology, 2005. **236**(3): p. 1053-8.
318. Ostridge, K., et al., *Relationship of CT-quantified emphysema, small airways disease and bronchial wall dimensions with physiological, inflammatory and infective measures in COPD.* Respiratory Research, 2018. **19**(1): p. 31.
319. Wells, J.M., et al., *Pulmonary arterial enlargement and acute exacerbations of COPD.* N Engl J Med, 2012. **367**(10): p. 913-21.
320. *ATS statement: guidelines for the six-minute walk test.* Am J Respir Crit Care Med, 2002. **166**(1): p. 111-7.
321. Nakano, Y., et al., *Quantitative assessment of airway remodeling using high-resolution CT.* Chest, 2002. **122**(6 Suppl): p. 271s-275s.
322. Han, M.K., et al., *Chronic obstructive pulmonary disease exacerbations in the COPDGene study: associated radiologic phenotypes.* Radiology, 2011. **261**(1): p. 274-82.
323. Pare, P.D. and W. Mitzner, *Airway-parenchymal interdependence.* Compr Physiol, 2012. **2**(3): p. 1921-35.
324. Müller, N.L., et al., *"Density mask". An objective method to quantitate emphysema using computed tomography.* Chest, 1988. **94**(4): p. 782-7.
325. Coxson, H.O., et al., *A quantification of the lung surface area in emphysema using computed tomography.* Am J Respir Crit Care Med, 1999. **159**(3): p. 851-6.
326. Bankier, A.A., et al., *Pulmonary emphysema: subjective visual grading versus objective quantification with macroscopic morphometry and thin-section CT densitometry.* Radiology, 1999. **211**(3): p. 851-8.
327. Madani, A., et al., *Pulmonary emphysema: objective quantification at multi-detector row CT--comparison with macroscopic and microscopic morphometry.* Radiology, 2006. **238**(3): p. 1036-43.
328. Heussel, C.P., et al., *Fully automatic quantitative assessment of emphysema in computed tomography: comparison with pulmonary function testing and normal values.* Eur Radiol, 2009. **19**(10): p. 2391-402.
329. Washko, G.R., et al., *Computed tomographic-based quantification of emphysema and correlation to pulmonary function and mechanics.* Copd, 2008. **5**(3): p. 177-86.
330. Stoel, B.C., et al., *Volume correction in computed tomography densitometry for follow-up studies on pulmonary emphysema.* Proc Am Thorac Soc, 2008. **5**(9): p. 919-24.
331. Rahaghi, F.N., et al., *Morphologic Response of the Pulmonary Vasculature to Endoscopic Lung Volume Reduction.* Chronic obstructive pulmonary diseases (Miami, Fla.), 2015. **2**(3): p. 214-222.
332. Thurnheer, R., et al., *Effect of lung volume reduction surgery on pulmonary hemodynamics in severe pulmonary emphysema1.* European Journal of Cardio-Thoracic Surgery, 1998. **13**(3): p. 253-258.
333. Howell, J.B.L., et al., *Effect of inflation of the lung on different parts of pulmonary vascular bed.* Journal of Applied Physiology, 1961. **16**(1): p. 71-76.
334. Eberhardt, R., et al., *Effect of endoscopic lung volume reduction on established pulmonary hypertension in severe emphysema patients.* European Respiratory Journal, 2014. **44**(Suppl 58): p. P3711.
335. Garner, J.L. and P.L. Shah, *Lung Volume Reduction in Pulmonary Emphysema.* Semin Respir Crit Care Med, 2020.
336. Madani, A., A. Van Muylem, and P.A. Gevenois, *Pulmonary emphysema: effect of lung volume on objective quantification at thin-section CT.* Radiology, 2010. **257**(1): p. 260-8.
337. Madani, A., et al., *Pulmonary emphysema: radiation dose and section thickness at multidetector CT quantification--comparison with macroscopic and microscopic morphometry.* Radiology, 2007. **243**(1): p. 250-7.

338. Boedeker, K.L., et al., *Emphysema: effect of reconstruction algorithm on CT imaging measures.* Radiology, 2004. **232**(1): p. 295-301.
339. Bakker, M.E., et al., *Variability in densitometric assessment of pulmonary emphysema with computed tomography.* Invest Radiol, 2005. **40**(12): p. 777-83.
340. Lipworth, B.J. and S. Jabbal, *What can we learn about COPD from impulse oscillometry?* Respiratory Medicine, 2018. **139**: p. 106-109.
341. McNulty, W. and O.S. Usmani, *Techniques of assessing small airways dysfunction.* Eur Clin Respir J, 2014. **1**.
342. Hsu, K., et al., *Endoscopic lung volume reduction (ELVR) in COPD: Changes in lung mechanics with ELVR using the forced oscillation technique (FOT).* European Respiratory Journal, 2016. **48**(suppl 60): p. PA1863.
343. Khattab, A., et al., *Assessment of lung functions using impulse oscillometry before and after bronchoscopic lung volume reduction with histoacryl gel.* Egyptian Journal of Bronchology, 2019. **13**(1): p. 43-48.
344. Kolsum, U., et al., *Impulse oscillometry in COPD: identification of measurements related to airway obstruction, airway conductance and lung volumes.* Respir Med, 2009. **103**(1): p. 136-43.
345. Gong, S.G., et al., *Evaluation of respiratory impedance in patients with chronic obstructive pulmonary disease by an impulse oscillation system.* Mol Med Rep, 2014. **10**(5): p. 2694-2700.
346. Dellacà, R.L., et al., *Effect of bronchodilation on expiratory flow limitation and resting lung mechanics in COPD.* Eur Respir J, 2009. **33**(6): p. 1329-37.
347. Aarli, B.B., et al., *The association of tidal EFL with exercise performance, exacerbations, and death in COPD.* International journal of chronic obstructive pulmonary disease, 2017. **12**: p. 2179-2188.
348. Michaelson, E.D., E.D. Grassman, and W.R. Peters, *Pulmonary mechanics by spectral analysis of forced random noise.* J Clin Invest, 1975. **56**(5): p. 1210-30.
349. Travaline, J.M., et al., *Quantitation of regional ventilation during the washout phase of lung scintigraphy: measurement in patients with severe COPD before and after bilateral lung volume reduction surgery.* Chest, 2000. **118**(3): p. 721-7.
350. Bell, A.S., et al., *Feasibility and challenges of using multiple breath washout in COPD.* Int J Chron Obstruct Pulmon Dis, 2018. **13**: p. 2113-2119.
351. Soni, S., et al., *Alveolar macrophage-derived microvesicles mediate acute lung injury.* Thorax, 2016.
352. O'Farrell, H.E. and I.A. Yang, *Extracellular vesicles in chronic obstructive pulmonary disease (COPD).* Journal of thoracic disease, 2019. **11**(Suppl 17): p. S2141-S2154.
353. O'Dea, K.P., et al., *Circulating Microvesicles Are Elevated Acutely following Major Burns Injury and Associated with Clinical Severity.* PLOS ONE, 2016. **11**(12): p. e0167801.
354. Jayachandran, M., et al., *Methodology for isolation, identification and characterization of microvesicles in peripheral blood.* Journal of immunological methods, 2012. **375**(1-2): p. 207-214.
355. Jayachandran, M., et al., *Methodology for isolation, identification and characterization of microvesicles in peripheral blood.* J Immunol Methods, 2012. **375**(1-2): p. 207-14.
356. Du Rand, I.A., et al., *British Thoracic Society guideline for diagnostic flexible bronchoscopy in adults: accredited by NICE.* Thorax, 2013. **68 Suppl 1**: p. i1-i44.
357. Osteikoetxea, X., et al., *Differential detergent sensitivity of extracellular vesicle subpopulations.* Organic & Biomolecular Chemistry, 2015. **13**(38): p. 9775-9782.
358. Soni, S., et al., *ATP redirects cytokine trafficking and promotes novel membrane TNF signaling via microvesicles.* The FASEB Journal, 2019. **33**(5): p. 6442-6455.
359. Nieuwland, R., et al., *Cellular origin and procoagulant properties of microparticles in meningococcal sepsis.* Blood, 2000. **95**(3): p. 930-935.

360. Zhang, Y., et al., *CIRCULATING MICROPARTICLES, BLOOD CELLS, AND ENDOTHELIUM INDUCE PROCOAGULANT ACTIVITY IN SEPSIS THROUGH PHOSPHATIDYLSERINE EXPOSURE.* Shock, 2016. **45**(3): p. 299-307.
361. Martinez, F.J., et al., *Longitudinal change in the BODE index predicts mortality in severe emphysema.* Am J Respir Crit Care Med, 2008. **178**(5): p. 491-9.
362. Marin, J.M., et al., *Prediction of risk of COPD exacerbations by the BODE index.* Respir Med, 2009. **103**(3): p. 373-8.
363. Patel, B.V., et al., *In vivo compartmental analysis of leukocytes in mouse lungs.* American Journal of Physiology-Lung Cellular and Molecular Physiology, 2015. **309**(7): p. L639-L652.
364. Akuthota, P., et al., *Extracellular Microvesicle Production by Human Eosinophils Activated by "Inflammatory" Stimuli.* Frontiers in Cell and Developmental Biology, 2016. **4**(117).
365. Colombo, F., et al., *Cytokines Stimulate the Release of Microvesicles from Myeloid Cells Independently from the P2X7 Receptor/Acid Sphingomyelinase Pathway.* Frontiers in immunology, 2018. **9**: p. 204-204.
366. Dengler, V., et al., *Neutrophil Intercellular Communication in Acute Lung Injury. Emerging Roles of Microparticles and Gap Junctions.* American Journal of Respiratory Cell and Molecular Biology, 2013. **49**(1): p. 1-5.
367. Mayadas, T.N., X. Cullere, and C.A. Lowell, *The multifaceted functions of neutrophils.* Annual review of pathology, 2014. **9**: p. 181-218.
368. Röpcke, S., et al., *Repeatability of and Relationship between Potential COPD Biomarkers in Bronchoalveolar Lavage, Bronchial Biopsies, Serum, and Induced Sputum.* PLOS ONE, 2012. **7**(10): p. e46207.
369. de Godoy, I., et al., *Elevated TNF-alpha production by peripheral blood monocytes of weight-losing COPD patients.* Am J Respir Crit Care Med, 1996. **153**(2): p. 633-7.
370. Thomashow, M.A., et al., *Endothelial microparticles in mild chronic obstructive pulmonary disease and emphysema. The Multi-Ethnic Study of Atherosclerosis Chronic Obstructive Pulmonary Disease study.* Am J Respir Crit Care Med, 2013. **188**(1): p. 60-8.
371. Churg, A., et al., *Tumor Necrosis Factor-α Drives 70% of Cigarette Smoke–induced Emphysema in the Mouse.* American Journal of Respiratory and Critical Care Medicine, 2004. **170**(5): p. 492-498.
372. Culpitt, S.V., et al., *Impaired inhibition by dexamethasone of cytokine release by alveolar macrophages from patients with chronic obstructive pulmonary disease.* Am J Respir Crit Care Med, 2003. **167**(1): p. 24-31.
373. Barnes, P.J. and B.R. Celli, *Systemic manifestations and comorbidities of COPD.* European Respiratory Journal, 2009. **33**(5): p. 1165-1185.
374. Bhowmik, A., et al., *Relation of sputum inflammatory markers to symptoms and lung function changes in COPD exacerbations.* Thorax, 2000. **55**(2): p. 114-120.
375. Spruit, M.A., et al., *An official American Thoracic Society/European Respiratory Society statement: key concepts and advances in pulmonary rehabilitation.* Am J Respir Crit Care Med, 2013. **188**(8): p. e13-64.
376. Hollander, C., et al., *Serum and bronchial lavage fluid concentrations of IL-8, SLPI, sCD14 and sICAM-1 in patients with COPD and asthma.* Respir Med, 2007. **101**(9): p. 1947-53.
377. Sapey, E., et al., *Imbalances between interleukin-1 and tumor necrosis factor agonists and antagonists in stable COPD.* J Clin Immunol, 2009. **29**(4): p. 508-16.
378. Valaperti, A., et al., *Variability of cytokine concentration in whole blood serum and bronchoalveolar lavage over time.* Cytokine, 2019. **123**: p. 154768.
379. Hens, G., et al., *Sinonasal pathology in nonallergic asthma and COPD: 'united airway disease' beyond the scope of allergy.* Allergy, 2008. **63**(3): p. 261-7.
380. Leaker, B.R., et al., *Bronchoabsorption; a novel bronchoscopic technique to improve biomarker sampling of the airway.* Respir Res, 2015. **16**: p. 102.

381. Xu, Y., et al., *Hyperinflated lungs compress the heart during expiration in COPD patients: a new finding on dynamic-ventilation computed tomography.* Int J Chron Obstruct Pulmon Dis, 2017. **12**: p. 3123-3131.
382. Yamashiro, T., et al., *Asynchrony in respiratory movements between the pulmonary lobes in patients with COPD: continuous measurement of lung density by 4-dimensional dynamic-ventilation CT.* Int J Chron Obstruct Pulmon Dis, 2017. **12**: p. 2101-2109.
383. Nagatani, Y., et al., *Continuous quantitative measurement of the main bronchial dimensions and lung density in the lateral position by four-dimensional dynamic-ventilation CT in smokers and COPD patients.* Int J Chron Obstruct Pulmon Dis, 2018. **13**: p. 3845-3856.
384. Xu, Y., et al., *Strain measurement on four-dimensional dynamic-ventilation CT: quantitative analysis of abnormal respiratory deformation of the lung in COPD.* Int J Chron Obstruct Pulmon Dis, 2019. **14**: p. 65-72.
385. Calverley, P.M.A. and R. Farré, *Oscillometry: old physiology with a bright future.* European Respiratory Journal, 2020. **56**(3): p. 2001815.
386. King, G.G., et al., *Technical Standards for Respiratory Oscillometry.* European Respiratory Journal, 2019: p. 1900753.